Molecular Epidemiology and Physiology of Shiraz Disease with an Emphasis on Grapevine Virus A.

Qi Wu
M.Sc. (Plant Health and Biosecurity)

May, 2023

A thesis submitted to the University of Adelaide in fulfilment of the requirements for the degree of **Doctor of Philosophy**

The University of Adelaide
Faculty of Sciences, Engineering and Technology (SET)
School of Agriculture, Food and Wine

THE UNIVERSITY *of* ADELAIDE

Table of Contents

Table of Contents

Citation List of Included Publications

Wu, Q.; Habili, N.; Constable, F.; Al Rwahnih, M.; Goszczynski, D.E.; Wang, Y.; Pagay, V. Virus Pathogens in Australian Vineyards with an Emphasis on Shiraz Disease. Viruses 2020, 12, 818, doi:10.3390/v12080818.

Wu, Q.; Habili, N.; Kinoti, W.M.; Tyerman, S.D.; Rinaldo, A.; Zheng, L.; Constable, F.E. A Metagenomic Investigation of the Viruses Associated with Shiraz Disease in Australia. Viruses 2023, 15, 774, doi:10.3390/v15030774.

Wu, Q.; Kehoe, M.; Kinoti, W.M.; Wang, C.; Rinaldo, A.; Tyerman, S.; Habili, N.; Constable, F.E. First Report of Grapevine Rupestris Vein Feathering Virus in Grapevine in Australia. Plant Dis. 2020, 105, 515, doi:10.1094/PDIS-06-20-1240-PDN.

Molecular Epidemiology and Physiology of Shiraz Disease with an Emphasis on Grapevine Virus A.

Supervised by:

Primary Supervisor

Prof. Stephen Tyerman

Emeritus Professor, School of Agriculture, Food and Wine, The University of Adelaide

Co or External supervisor

Dr. Nuredin Habili

Visiting Fellow, the University of Adelaide

Honorary Fellow, the Australian Wine Research Institute

Dr. Fiona Constable

Research Leader – Microbiology, Microbial Sciences, Pests and Diseases, Agriculture Victoria Research, Department of Jobs, Precincts and Regions, AgriBio, Bundoora, Australia

School of Applied Systems Biology, La Trobe University, Bundoora, Victoria, Australia

Dr. Amy Rinaldo

Manager-Applied Biosciences, the Australian Wine Research Institute

Thesis submitted in fulfilment of the requirements for the degree of

Doctor of Philosophy

The University of Adelaide

Faculty of Sciences, Engineering and Technology (SET)

School of Agriculture, Food and Wine

Email: qi.wu@adelaide.edu.au

Abstract

Shiraz disease (SD) is one of the most virulent viral diseases of several SD-sensitive grapevine varieties including Shiraz, Merlot, Malbec, Gamay, Ruby Cabernet and Sumoll in Australia. The viromes of a large number of grapevines with SD, leafroll disease (LRD) symptoms, and asymptomatic grapevines (ASY) were assessed for grapevine virus A (GVA) and other viruses using endpoint reverse transcription polymerase chain reaction (RT-PCR) and metagenomic high throughput sequencing (Meta-HTS) approaches. A minimum of one GVA isolate from phylogenetic group II (GVA^{II}) was present in a SD grapevine. In contrast, phylogroups GVA^{I} and GVA^{III} were not associated with SD, since they were also present in LRD and ASY grapevines. These results support previous studies both in Australia and South Africa that demonstrated that GVA^{II} was strongly associated with SD symptoms. At least one grapevine leafroll-associated virus (GLRaV) species was also found in SD grapevines and might contribute to disease expression, however no association to a specific GLRaV species was found. Analysis of GVA quasispecies using the median-joining networks (MJNs) demonstrated the potential emergence of new GVA^{II} variants related to one or a few dominant variants within a population. When MJNs were constructed using all samples from different vineyards, variant groups were revealed, some of which were linked to the actual geographical locations of grapevine populations, demonstrating potential spread within a vineyard, and some which linked different vineyards indicating a spread through planting material. No single GVA^{II} variant was specifically linked to SD. A series of physiological parameters of SD, LRD and ASY grapevines were monitored in two South Australian vineyards, Willunga (WIL) and Langhorne Creek (LC), during 2018-19, and at WIL only in 2019-20, and 2020-21. Vine decline and dead arms symptoms were also observed at WIL that may be attributed to grapevine trunk diseases (GTDs). Plant area index (PAI) data in combination with a vine health score (VHS) system, which was developed for this study to measure the severity of decline and dead arms symptoms, showed that canopy vigor in SD/GTD affected grapevines was significantly reduced, as compared to LRD and ASY grapevines. PAI can be used to distinguish SD/GTD and ASY grapevines using kmeans clustering. Other parameters like leaf chlorophyll, photosynthesis, total non-structural carbohydrate in cane and trunk, leaf stomatal conductance and water potential were less affected or unaffected. Fresh berry mass (FBM), total soluble solids (TSS) and juice pH were also compared. According to the timewise berry development curves for the three growing seasons, berries of SD/GTD affected grapevines tend to have a lower TSS and pH but a higher FBM. This is likely due to delayed berry ripening which could be a consequence of delayed canopy growth associated with SD and/or GTDs. The yield of berries was significantly reduced compared to non-Shiraz disease (NSD) grapevines at the Willunga site which was related to the presence of the physiological disorder called bunch stem necrosis (BSN) which caused berries to drop before harvesting, especially the SD/GTD affected grapevines. Thus only 900g of berries from two SD/GTD affected grapevines could be used to make wines and asses impact of disease on wine quality. The preliminary wine data suggests that wine made from SD/GTD affected grapevines with GVA^{II} had lower ethanol, less colour and tannins compared to wines from NSD grapevines. The wines from SD/GTD affected grapevines may have more vegetal characters and less

flavour compounds that contribute to pleasant aromas than those from NSD grapevines. The differences between wines from SD/GTD and NSD grapevines need to be re-investigated to see if this could be due to a chemical metabolism resulting from the GVA^{II} infection or a direct consequence of delayed berry ripening. This study provides comprehensive insights into SD in Australia, encompassing virological, molecular, physiological, and oenological aspects, which may provide valuable guidance for future investigation of this disease.

Thesis Declaration

I certify that this work contains no material which has been accepted for the award of any other degree or diploma in my name, in any university or other tertiary institution and, to the best of my knowledge and belief, contains no material previously published or written by another person, except where due reference has been made in the text. In addition, I certify that no part of this work will, in the future, be used in a submission in my name, for any other degree or diploma in any university or other tertiary institution without the prior approval of the University of Adelaide and where applicable, any partner institution responsible for the joint award of this degree.

The author acknowledges that copyright of published works contained within the thesis resides with the copyright holder(s) of those works.

I give permission for the digital version of my thesis to be made available on the web, via the University's digital research repository, the Library Search and also through web search engines, unless permission has been granted by the University to restrict access for a period of time.

I acknowledge the support I have received for my research through the provision of an Australian Government Research Training Program Scholarship.

09/05/2023

…….

Qi Wu Date

Acknowledgments

Foremost, I'm so grateful that I have a strong supervisor panel that allows me to complete this multidisciplinary research. I would like to thank my principal supervisor, Professor Stephen Tyerman, who concepted the physiological experiments and carry on doing the field experiments for me while I was on maternity leave. He continuously and patiently provides his precious advice on grapevine physiology and data statistics which I did not have any experience before I started my Ph.D. I also would like to thank my co-supervisor Dr. Nuredin Habili who promotes this Ph.D. and always answers my questions regarding any virus experiment using his rich knowledge and experiences of grapevine virology. While I was in my early career, he conducted virus research together with me and guided me enter the world of grapevine virology. My external supervisor Dr. Fiona Constable not just contributed to the overall concept of the metagenomic and amplicon sequencing studies, but also provide sequencing facilities and absorbed partial costs of the sequencing experiment. She and her teams also provide full technical support to my sequencing experiments as well as providing the bioinformatics training to allow me to analyze complicated sequencing data. Thanks to my external supervisor Dr. Amy Rinaldo who always provide valuable thoughts and suggestions when I have trouble making difficult decisions while conducting research. She and her team fully supported the wine-making part of my study and gave advice on downstream wine data analysis.

I wish to take the chance to say thanks to all the people who helped me during my Ph.D. My supervisor's lab technician Wendy Sullivan managed the glasshouse, organized, and recorded some measurements of field experiments, and demonstrated lab experiments for me. My supervisor's research team, Dr. Cliff Kinoti and Dr. Linda Zheng, whom I appreciated their time and patience in helping me conduct the metagenomic experiments and advising me on the bioinformatic side of my study. My colleague Dr. Alan Little participated in my field trips and provided valuable suggestions to my research questions. My colleague Caroline Bartel helped me with the winemaking.

I am so thankful that the University of Adelaide that offered me the admission to the degree and the Australian Government Research and Training Program scholarship and massive facilities and resources including self-enrolled classes which are absolutely indispensable to my academic career and my life. I appreciated that the Australian Wine Research Institute (AWRI) hosted my Ph.D. study. I was permitted by AWRI to use any lab consumables and instruments, office space, and any shared facilities.

Thanks to the supplementary scholarship provided by the Wine Australia, I was able to have sufficient funding to conduct expensive sequencing experiments and have additional life expense support. I wish to thank the owners and managers of three Australian vineyards where I have undertaken my studies. I was allowed to sample their grapevines and grapes and take measurements in the vineyards as well as they provided all additional information I needed. Without their support, none of the field experiments would have been possible. The wine fermentation analysis was kindly supported by NCRIS funding from Bioplatforms Australia and the South Australian State Government to the South Australian node of Metabolomics Australia.

I would like to give my special thanks to my families who always support me during my Ph.D. My husband Gang Wang participated in most of the Viticanopy and berry harvesting experiments and financially support me towards the end of my candidature while the scholarship finished. My mother Guiqin Yan looked after my son for 18 months which allowed me to have more time to do my studies.

Thesis Format

A combination of conventional thesis chapters and publications was formatted for this Ph.D. thesis. Chapter 1 includes a review paper and additional general background sections which were not included in the review paper. The results chapters (Chapters 2–6) are arranged as independent articles with their own materials and methods, results, discussion, and conclusion since it is easier to relate the methods to each experiment. Chapter 2 explores the virome of the Shiraz disease (SD) grapevines, and Chapter 3 details a study of the intra-host diversity of the main viral pathogen associated with SD, grapevine virus A (GVA). The significance of SD infection in terms of grapevine field performance (Chapter 4) and wine composition (Chapter 5) were studied. In the metagenomic high-throughput sequencing (Meta-HTS) experiments, a virus that is new to Australia has been discovered and reported (Chapter 6). The findings of each study are discussed and summarized in Chapter 7.

List of Abbreviations

Part A: General

aa	amino acid
accession no.	GenBank accession number
Agro-mediated	Agrobacterium tumefaciens-mediated
amplicon-HTS	amplicon high throughput sequencing
ANOVA	analysis of variance
ASY	asymptomatic
AWRI	Australian Wine Research Institute
BI	biological indexing
bp	base pair
BSN	bunch stem necrosis
BV	Barossa Valley
Chl	leaf chlorophyll
C_i	internal CO_2 concentration
CP	coat protein
CV	Coombe's research vineyard
DAP	diammonium phosphate
ddNTPs	di-deoxynucleotides triphosphates
DNA	deoxyribonucleic acid
dNTPs	deoxynucleotide Triphosphates
dsRNA	double stranded ribonucleic acid
E	transpiration
ELISA	enzyme-linked immunosorbent assay
EM	electron microscopy
ETR	electron transport rate
FBM	fresh berry mass
g	gram
GDD	growing degree day
GHC	guanidine hydrochloride
g_s	stomatal conductance
GVA^{I}, GVA^{II}, GVA^{III}	grapevine virus A variants in the phylogenetic group I, II, III
ha	hectares
HPLC	high-performance liquid chromatography

HS-SPME-GC-MS	headspace solid-phase microextraction coupled with gas chromatography mass spectrometry
HSP70h	heat shock protein 70 homologue
HTS	high-throughput sequencing
ICTV	International Committee on Taxonomy of Viruses
IRGA	infrared gas analyser
ISEM	immunosorbent electron microscopy
kb	kilo base
kDa	kilodaltons
kg	kilogram
LAI	leaf area index
LAMP	loop-mediated isothermal amplification
LC	Langhorne Creek
LN2	liquid nitrogen
Meta-HTS	metagenomics high-throughput sequencing
mhl	million hectolitres
min	minute
MJNs	median joining networks
mL	milliliter
MP	movement protein
Mpa	Mega Pascal
N. benthamiana	*Nicotiana benthamiana*
NEB	New England Biolabs®
nM	nano molar
NSD	non-Shiraz disease
nt	nucleotide
nts	nucleotides
OIV	International organisation of vine and wine
ORF	open reading frame
PacBio	Pacific Biosciences
PAI	plant area indexing
PCA	principal Component Analysis
PCR	polymerase chain reaction
phylogroup	phylogenetic group
P_n	net photosynthesis

R2	R square value
RB	RNA binding
RDP5	Recombination detection program 5
RdRp	RNA dependent RNA polymerase
RNA	ribonucleic acid
rRNA	ribosomal ribonucleic acid
RSG	restricted spring growth
RT	reverse transcription
RT-PCR	reverse transcription polymerase chain reaction
RT-qPCR	quantitative reverse transcription PCR
SA	South Australia
SBB	sequencing by binding
SBS	sequencing by synthesis
SDev	standard deviations
SDT	sequence demarcation tool
SE	somatic embryogenesis
siRNA	small interfering RNAs
SMRT	single molecule real-time sequencing
TA	titratable acidity
TNA	total nucleic acid
TSS	total soluble solids
TWSS	total within sum of square
ULC	uneven lignification of canes
VG	variant group
VHS	vine health score
VPRI	Victorian plant pathogen reference collection
WA	Western Australia
WIL	Willunga
WUE_i	intrinsic water use efficiency
YPD	yeast extract peptone dextrose
ZMW	zero-mode waveguide
ZMW	zero-mode waveguide
μg	microgram
μl	microliter
μm	micrometer

°C	degrees celcius
Ψ_{leaf}	leaf water potential
Ψ_{stem}	stem water potential

Part B: Viruses and diseases

GRVFV	grapevine rupestris vein feathering virus
GPGV	grapevine Pinot Gris virus
GRLDaV	roditis leaf discoloration-associated virus
ApMV	apple mosaic virus
ArMV	arabis mosaic virus
BBLMV	blueberry leaf mottle virus
CLRV	cherry leafroll virus
ENMV	endive necrotic mosaic virus
GAMaV	grapevine asteroid mosaic associated virus
GARSV	grapevine Anatolian ringspot virus
GBLV	grapevine Bulgarian latent virus
GCMV	grapevine chrome mosaic virus
GCSV	grapevine Cabernet Sauvignon reovirus
GDefV	grapevine deformation virus
GFkV	grapevine fleck virus
GFLV	grapevine fanleaf virus
GGVA	grapevine geminivirus A
GINV	grapevine berry inner necrosis virus
GLRaV-1,2,3,4,7,13	grapevine leafroll-associated viruses 1,2,3,4,7,13
GLRaV-4/4, GLRaV-4/5, GLRaV-4/6, GLRaV-4/9, GLRaV-4/10	grapevine leafroll-associated viruses 4 strains 4, 5,6,9,10
GLRaVs	grapevine leafroll-associated viruses
GRBV	grapevine red blotch virus
GRD	Red blotch disease
GRGV	grapevine red globe virus
GRLDaV	grapevine roditis leaf discoloration-associated virus
GRSPaV	grapevine rupestris stem pitting-associated virus
GSV-1	grapevine Syrah virus 1
GTDs	grapevine trunk diseases

GTRV	grapevine Tunisian ringspot virus
GVA, GVB, GVD, GVE, GVF, GVG, GVH, GVI, GVJ, GVK, GVL, GVM, GVT	grapevine virus A, B, D, E, F, G, H, I, J, K, L, M, T
GVCV	grapevine vein clearing virus
KSG	Kober stem grooving
LRD	grapevine leafroll disease
PDV	Prune dwarf virus
PNRSV	Prunus necrotic ringspot virus
PRMV	peach rosette mosaic virus
RpRSV	raspberry ringspot virus
SD	Shiraz disease
SLRSV	strawberry latent ringspot virus
TBRV	tomato black ring virus
ToRSV	tomato ringspot virus
TRSV	tobacco ringspot virus
TYLCV	tomato yellow leaf curl virus

Chapter 1: Literature Review

1.1. Australian wine industry and importance of red grape varieties

Grapevines (*Vitis vinifera* L.) were introduced to Australia 230 years ago by Governor Arthur Phillip with the first British settlements in 1788 [1]. The cuttings were brought from Rio de Janeiro and the Cape of Good Hope and were firstly planted as a small plantation at Farm Cove, New South Wales. As grapevines were well adapted to some local areas of the Australian environment, the wine industry has subsequently flourished. In 2020, the surface area of Australian vineyards totaled 146,000 hectares (ha) and wine production totaled 14.2 million hectolitres (mhl) which is about 5.7% of the world total wine production [2]. In the last ten years, the Australian grape and wine sector has been steadily expanding. The wine production in 2021 increased by 30% compared to 2020, while it increased by 14% compared to the 2016-2020 average [3]. Australia produces top quality wines that are exported to many countries of the world. Internationally, Australia has become the fifth largest wine exporter with yearly export totaling 7.5 mhl [2].

Wine grapes are grown in all states of Australia, except the Northern Territory. South Australia (SA) with the largest growing area, contributes to 1.06 million tonnes, which is 52% of the Australian total [4].

Among all grapevine varieties grown in Australia, Shiraz (syn. Syrah) has been the most popular red variety with a record of 538,402 tonnes accounting for about 26.5% of the total crush (Wine Australia national vintage report 2021). Red varieties are getting more popular, with Shiraz, Cabernet Sauvignon, Merlot, Pinot Noir, and Petit Verdot experiencing an annual crush increase of 41%, 36%, 26%, 52%, and 19%, respectively, for the year 2021 compared to 2020 [4].

1.2. Wine production regions in South Australia

Early private vineyards in SA were first planted in 1836 by John Barton Hack and George Stevenson in North of Adelaide now known as the Barossa Valley [5]. The first plantation was moved to the Adelaide Hills region near Mount Barker in 1843 [5]. During the 1890s, the SA grape and wine industry entered a fast-growing period since it was promoted by viticulturist Arthur Perkins from the government and by increasing wine exports to the United Kingdom [6]. From 1840 to 1900, over 200 growers worked in the grape and wine industry in the Adelaide Hills [7]. Nowadays, four major wine zones (Barossa/Mt Lofty, Fleurieu, Limestone Coast and Lower Murray/Far North) and a total of 18 distinctive wine regions have been established in SA from the northmost of the Southern Flinders Ranges to the southernmost region of Mount Gambier [8].

1.3. Virus diseases of the grapevine

Ninety three viruses have been detected in the grapevine (*Vitis vinifera* L.) worldwide [9-11] of which 31 are considered as disease associated viruses [12]. Grapevine viruses mainly are associated with five types of disease: leafroll, degeneration and decline, fleck, rugose wood and red blotch disease (GRD), which will be briefly described in the following sections.

1.3.1. Grapevine leafroll disease (LRD)

Grapevine leafroll disease (LRD) which is known to be associated with grapevine leafroll-associated viruses (GLRaVs), is one of the most widespread diseases, appearing in every grape-growing country globally. Typical LRD symptoms and pathogens are discussed by Wu, *et al.* [13] which is presented later in this Chapter. GLRaVs are scattered across three genera, *Ampelovirus*, *Closterovirus* and *Velarivirus* within the family *Closteroviridae.* Grapevine leafroll-associated viruses 1, 3, 4 and 13 (GLRaV-1, 3, 4 and 13) are classified in the genus *Ampelovirus,* which are transmitted by mealybugs and scale insects [14-16]. GLRaV-2 and GLRaV-7 are assigned to the genera *Closterovirus* and *Velarivirus,* respectively, for which the vector species remains unknown [17-19].

1.3.2. Degenerative and decline disease

Fifteen viruses belonging to the family *Secoviridae* under the genus *Nepovirus,* including grapevine fanleaf virus (GFLV), are associated with degenerative decline diseases [12,20,21]. The progressive degeneration and decline of the entire plant associated with *Nepovirus* infection can be highly destructive since affected grapevines may eventually die [22]. Grapevines infected with GFLV and other nepoviruses display various symptoms including abnormal leaf morphology, typically fan shape leaves, leaf vein clearing [22]. In severe cases, GFLV infected vineyards can show patchy distribution of diseased grapevines related to the movement of the nematode vector *Xiphinema index* [23]. GFLV, was thought to have originated from North America and spread worldwide by human activities [12]. GFLV was known to be present in Australia but was declared absent in 2015 since there had been no detections since 1989 [24].

1.3.3. Grapevine fleck disease and associated diseases

There are four fleck or fleck-like viruses (fleck complex) within the family *Tymoviridae* including grapevine fleck virus (GFkV), grapevine rupestris vein feathering virus (GRVFV), grapevine red globe virus (GRGV), and grapevine asteroid mosaic associated virus (GAMaV) in genera *Maculavirus* and *Marafivirus* [12,25]. These viruses are known to be associated with fleck, asteroid mosaic and vein feathering diseases and grafting incompatibility [26-28]. GFkV, GRGV and GRVFV have a global distribution, but no vectors have been identified [29]. The economic impact of the associated diseases has not been comprehensively studied [30].

1.3.4. Rugose wood complex

Rupestris stem pitting, Kober stem grooving (KSG), corky bark, and LN33 stem grooving are all diseases of the rugose wood complex that are frequently associated with virus species in the genera *Foveavirus* and *Vitivirus* [31,32]. Grapevine rupestris stem pitting-associated virus (GRSPaV) associated with rupestris stem pitting disease [33,34], Grapevine virus B (GVB) is known to associated with corky bark [35,36]. Grapevine virus A (GVA), was originally known to be associated with the KSG syndrome [32,37]. When virus infected materials were grafted onto cv. Kober 5BB, the success rate was reduced and severe stem grooving symptoms developed after three years [38,39]. Later, GVA was found to be associated with SD in South Africa and Australia [40-42]. [see section 1.8]

1.3.5. Red blotch disease (GRD)

The importance of grapevine red blotch disease (GRD) caused by grapevine red blotch virus (GRBV) (genus *Grablovirus*, family *Geminiviridae*) has been raised in the last 10 years, since observing that fruit quality and berry ripening were substantially affected by the disease leading to a significant economic impact to the wine industry in the USA [43,44]. GRD was first reported in Cabernet Sauvignon grapevines from the Napa Valley, California. Symptoms were described as the progression from green to red leaves towards the middle and later part of the growing season [44]. The Koch's postulates of GRBV were achieved using *Agrobacterium tumefaciens*-mediated (Agro-mediated) methods in 2018 [45]. The three-cornered alfalfa hopper *(Spissistilus festinus*) is known to be the vector of GRBV [46,47] and *Stictocephala basalis* and *Stictocephala bisonia* were identified as potential vectors of GRBV [48]. Although GRBV was first reported from the USA [49], it has also been found in Canada [50], Mexico [51], Argentina [52], Brittain [53], India [54], and Korea [55], a germplasm collection in Italy [56] and most recently in three states of Australia (Western Australian, Victoria and South Australia) [57].

1.4. Diagnostic methods for grapevine virus disease

Diagnostic methods used for grapevine virus detection and identification include, but are not limited to, biological indexing, electron microscopy (EM), polymerase chain reaction (PCR), loop-mediated isothermal amplification (LAMP), enzyme linked immunosorbent assays (ELISA) and high-throughput sequencing (HTS) technologies.

1.4.1. Biological indexing

Biological indexing for grapevine viruses involves grafting a budwood from a grapevine variety suspected to be infected with a virus onto a virus sensitive indicator grapevine to identify the symptoms associated with the presence of one or more viruses. For studying the rugose wood complex, the commonly used indicator grapevines are *Vitis rupestris* (stem pitting), Kober 5BB (stem grooving) and LN 33 (corky bark) [32,35]. LRD detection has used *V. vinifera* cv. Cabernet Sauvignon, Cabernet franc and Pinot Noir and *V. riparia* cv. Gloire as indicators [58,59]. Although biological indexing is a helpful method to identify virus disease based on symptoms, it is a time-consuming process that may need several years for symptoms to develop on indicator grapevines and symptom expression can be impacted by bud-take, inefficient virus transmission and climate [60]. Also, it does not differentiate between virus species that might be associated with similar disease symptoms.

1.4.2. Electron Microscopy (EM)

EM can be used to detect virus particles in infected plants, including grapevines. Virus morphology, including the length and the structure of the virion provide useful guidance for virus identification of virus families or genera and, in combination with symptoms, this may indicate which genus is present. Transmission EM without concentrating the virus or capturing it may lead to false-negative results if the virus is in low titre. A serological-based method called immunosorbent electron microscopy (ISEM) allows observation of virus particles by capturing as well as the

identification between different viruses by coating the virus with virus-specific antibodies [61]. ISEM was first applied for plant virus diagnosis by Derrick and Brlansky [62] for the detection of barley yellow dwarf virus in crude extracts. Since the early 1980s, ISEM had been used for the specific detection and discovery of grapevine viruses including GVA, GVB and GLRaVs in extracts isolated from diseased grapevines [36,63-66]. Decoration of the virus coat protein with gold-labelled antibodies allows the distinction between target viruses and other viruses to which the antibodies do not bind [65]. Since the sensitivity and reliability of EM, ISEM and decoration are lower than PCR or ELISA-based methods, it cannot be used for routine virus detection [67].

1.4.3. Enzyme-linked immunosorbent assay (ELISA)

ELISA is a serological and semi-quantitative method to capture viruses using enzyme-labelled antibodies that target virus coat proteins. The presence or absence of a virus is indicated by the colour changes of the ELISA test. As early as 1977, ELISA was implemented in plant virus detection [68] and it fast became one of the most desirable and routine virus testing methods [69]. Virus-specific ELISA is still commonly employed in large-scale screening of grapevine viruses [70,71], due to its low cost, quick processing [72] and reliable results [73]. ELISA-based methods are generally less sensitive than PCR-based methods and may provide false negative results due to genetic diversity of virus strains that cause changes in the coat protein and poor antibody recognition. Therefore, they are being used less frequently for grapevine virus detection compared to more adaptable methods such as PCR [74-76].

1.4.4. Nucleic acid amplification methods

The principle of endpoint reverse transcription PCR (RT-PCR) virus detection is as follows: RNA is first reverse transcribed into cDNA by an RT enzyme; virus-specific primers bind and amplify a targeted virus fragment, then the fragment amplicons are visualized by gel electrophoresis to indicate the presence of a virus. The endpoint PCR has been well established and adapted worldwide since the early 1990s [33,76-80]. Additionally, since endpoint PCR can rapidly detect all known viruses with reasonable costs and higher sensitivity compared to ELISA [81], it is currently the most popular technique for grapevine virus detection in Australia. Later, more advanced PCR based methods named quantitative reverse transcription PCR (RT-qPCR) were introduced and developed for grapevine virus diagnostics [82-87]. In addition to enabling the real-time monitoring of target amplification and endpoint analysis, RT-qPCR is a quantitative PCR based method that can determine copy numbers of viral RNA in original extracts and has the potential to be more sensitive than endpoint RT-PCR. A fluorescence-based real-time LAMP assay has been developed to detect GRSPaV, GLRaV-3, GRBV, GVA and GFLV [88-92]. The advantages of LAMP assay compared to laboratory-based RT-qPCR are rapidity of the assay, higher sensitivity and specificity, fewer sample preparation steps and fewer equipment requirements [93-95]. LAMP has great potential as an in-field tool for grapevine virus diagnosis. However, LAMP assay requires internal PCR inhibition control, complicated primer design, and the use of non-specific dyes which may lead to false positive results [96,97]. Due to high specificity of LAMP associated with multiple primers, it may miss the

diversity of virus species when doing broader virus screens.

1.5. Sequencing technologies

The virus detection methods listed above lack the power of directly obtaining genetic information of a virus; therefore, sequencing is the final step in confirming the presence of a virus in a host plant. This can be done using several sequencing technologies that are discussed in this section. Except for Sanger sequencing, sequencing technologies that generate a large amount of data are generically called HTS.

1.5.1 Sanger sequencing

Sanger sequencing was invented by Fred Sanger and Alan R. Coulson in 1977 [98,99], stimulating molecular biology studies to develop rapidly. This method provides the possibility to sequence a complete gene or even a whole genome. From 1988 through to 2003, the human genome project, the world's first largest biology project, used Sanger sequencing and encouraged the development of more efficient large-scale sequencing technologies towards the finishing line [100,101]. To date, Sanger sequencing is still used on a regular basis in biology as a gold standard for comparing and validating HTS results in plant virus studies [102-104] .

1.5.2. Short read sequencing

In comparison to Sanger sequencing, which can only sequence one fragment at a time, HTS is capable of sequencing millions of DNA fragments in parallel [105]. The core technology of HTS is called sequencing by synthesis (SBS) and was developed in 2005 [106]. While DNA fragments are synthesized in a large number of micro wells using di-deoxynucleotides triphosphates (ddNTPs) (fluorescent labelled dNTPs), the sequencer reads and records the sequences according to the fluorescent emission of the di-deoxynucleotide simultaneously [107]. Illumina, Ion Torrent and 454 pyrosequencing come under this category. Illumina technology is one of the leading sequencing approaches in the world, as it has the highest throughput among all sequencing approaches [108], the lowest error rate (1 in 1000) high coverage [109] and supports massive protocols such as genomic sequencing, targeted sequencing, metagenomic sequencing, etc [110]. The read length of the Illumina platforms is up to 301 base pairs (bp) and the latest Novaseq system can generate a maximum of 20 billion reads per run. [111].

1.5.3. Long read HTS

In 2009, single molecule, real-time sequencing (SMRT) was introduced as an alternative sequencing technology. A single molecule is bound to a polymerase inside a nanostructure called a zero-mode waveguide (ZMW), while the ddNTPs are incorporated with the polymerase, fluorescence pulses corresponding to each nucleotide are captured and recoded by the sequencer in real-time [112]. Thousands of molecules are sequenced simultaneously in the ZMWs.

A representative of long read sequencing technology is the Pacific Biosciences (PacBio) instrument which offers SMRT sequencing up to 25 kilo bases (kb) read length and accuracy of 99.9% through a combination of HiFi sequencing and sequencing by binding (SBB) [113]. Long-read

sequencing could be used for genome assembly correction to polish and improve the quality of the reference genomes [114]. Although SMRT has less throughput than Illumina and Ion Torrent, it is beneficial for sequencing small genomes since it offers long read-length, high accuracy and uniform coverage [115].

As early as 1989, the concept of "a single strand of DNA being drawn through a membrane's nanoscopic pore by electrophoresis" was described by David Deamer [116]. After nearly three decades the nanopore technology was commercialised by Oxford nanopore in 2015 [117]. The principle of nanopore sequencing is that a DNA or RNA molecule is driven through a nanopore by a motor protein [118,119]. This functions similar to biological nanopores, where proteins embedded in membranes allow molecules to be transported between cells [120]. The motor protein drives the molecules at a certain speed that allows a sensitive ammeter to detect the digital signals of current changes while the molecule passes through the nanopore [116]. The nanopore reader identifies the sequence of each four nucleotides passing through the nanopore based on the characteristics of the digital signals. Although this method has a lower accuracy of 99% compared to other sequencing methods, it is still the most effective method in terms of obtaining the longest read length. Researchers have sequenced 2.3 million bases of a DNA fragment, and with an average sequence length of 10 to 30 kb using the nanopore technology [121].

1.5.4. Application of HTS technologies in plant virus diagnostics

HTS technologies are widely used in various fields of biological sciences. The main applications of HTS include whole genome sequencing, targeted sequencing, epigenetics, transcriptome, and siRNA sequencing [122-124]. Here, the application in grapevine virology is discussed.

1.5.4.1. Metagenomic high-throughput sequencing (Meta-HTS)

Meta-HTS, also known as whole metagenome shotgun sequencing, outputs untargeted environmental sequence information from samples containing nucleic acids of multiple organisms [125-127]. HTS was employed for plant virus detection as early as 2009 [128,129]. Since then, HTS has been widely used as a powerful tool to identify known and novel viruses in grapevines [10,130-132]. The major advantage of HTS for virus detection is that it does not require previous knowledge of the organisms in a sample, whereas both PCR-based, or ELISA-based approaches require the identification and characterization of the target organism to enable development of the specific diagnostic tool. Many new grapevine viruses have been discovered by Meta-HTS including grapevine roditis leaf discoloration-associated virus (GRLDaV), grapevine vein clearing virus (GVCV) and grapevine Pinot Gris virus (GPGV), to name a few [133-135]. The ever-increasing discovery of new and diverse viral species and strains across a broad range of life forms opened a discussion as to whether viral contigs assembled by Meta-HTS alone should be incorporated into official virus taxonomy. A panel of expert scientists from the International Committee on Taxonomy of Viruses (ICTV) finally consented to include viruses identified by Meta-HTS in the ICTV taxonomy [136]. Due to the advancement of sequencing technology in the past ten years, many viruses have been discovered by HTS. Since HTS often detects multiple

viruses in single grapevine samples, cause and effect of the viruses identified by HTS often remain poorly understood. These include grapevine leafroll-associated virus 13 in genus *Ampelovirus* (GLRaV-13) [130], grapevine nepovirus A (Al Rwahnih et al. 2021), grapevine virus T (GVT) in genus *foveavirus* (Yeonhwa Jo 2017) and ten grapevine infecting vitiviruses [131,137-149]. However meta-HTS has limitations: it may have less sensitivity compared to RT-qPCR when virus is in low titre [150,151] and sequencing depth of each organism is often insufficient to do any fine resolution quasispecies analysis.

1.5.4.2. Amplicon high throughput sequencing (amplicon-HTS)

Amplicon-HTS is a targeted sequencing approach that detects the genetic variations of a targeted gene region by sequencing PCR amplicons. The success of amplicon-HTS has been clearly demonstrated in cancer research [152-155], microbial diversity and activity studies [156-158] and plant virology studies. Amplicon-HTS was employed to study intra-host and between-host diversity of endive necrotic mosaic virus (ENMV) in various hosts [159], intra-host diversity of *Ilarvirus* in *Prunus* trees [160-162] and the detection of up to four viral species in legumes [163]. Amplicon-HTS is a powerful method to study the pathways of virus evolution and intra-host diversity within a virus population. However, the results are not always reproducible or quantitative since genome coverage is depended on the libraries captured of each experiment [155]. The data analysis of Amplicon-HTS is complicated and time consuming and it requires heavy bioinformatic skills. To the best of my knowledge, this method has not been used to study the diversity of grapevine viruses.

1.5.4.3. Small RNAs sequencing

Instead of using total nucleic acids as input (e.g., in Meta and amplicon-HTS), small RNA sequencing uses small interfering RNAs (siRNA) that are 20-30 nucleotides in length [164]. When host cells are infected with viral pathogens, they are attacked by host silencing machinery [165]. During viral infection, siRNA accumulate in order to regulate the expression of virus genes or genomes [164]. The applications of studying siRNA are as follows: this approach has been used to study the mechanisms of plant and virus interactions across different genera of grapevine viruses [166-169]; to identify the virome in grapevine host targeting seven viruses and two viroids for diagnostic purposes [170]; analyze virus evolutionary history and the origin of tomato yellow leaf curl virus (TYLCV) [171], discover novel viruses [135], and to identify an RNA silencing suppressor of GLRaV-3 [172]. This approach has been widely used since RNAi-related activities have been reported in almost all eukaryotic organisms and it is able to detect DNA, RNA viruses and viroids with a reasonably high sensitivity [173-176]. However, the bioinformatic process of assembled virus genomes using such short reads can be challenging especially for novel viruses [177].

1.5.4.4 The scope of high-throughput sequencing in routine diagnostics (HTS)

In Australia, HTS is not frequently used for routine plant virus detection due to its current higher cost and longer turnaround time associated with library preparation and data analysis as compared to endpoint PCR and ELISA technologies. Furthermore, HTS instruments

are expensive and so often small diagnostic laboratories require outsourcing to an external service provider to conduct the sequencing, thus the turnaround time may not be controllable. HTS methods have been well investigated in plant virus research [178], and was successfully used for the detection of viruses and viroids in the Australian post-entry quarantine facilities [179,180]. It could soon become a standard diagnostic method for plant viruses, especially for post-entry quarantine materials.

1.6. Shiraz disease and grapevine virus A (GVA)

1.6.1. Shiraz disease in Australia

Shiraz Disease (SD) has been reported as a very destructive virus associated disease that has resulted in significant economic damage to a number of Australian red varieties including Shiraz, Merlot, Malbec, Gamay, Ruby Cabernet and Sumoll, particularly in South Australia (Nuredin Habili, personal communication). GVA has been previously identified as the key pathogen of SD [40,181,182]. This section reviews the historical classification and the genome organization of GVA. A more detailed review of this disease and its symptoms on various varieties are included in Wu *et al.* [13] which is presented in the second part of this chapter.

1.6.2. Taxonomy history of GVA

GVA was initially classified as a *Closterovirus*-like virus until the name grapevine virus A was proposed by Milne, Conti, Lesemann, Stellmach, Tanne and Cohen [63]. Since the taxonomy of GVA remained unassigned, it was sometimes called closterovirus A [183]. After the genus *Trichovirus* had been classified [184], it was proposed to classify GVA [185] and GVB [186] as members of this genus. Since GVA and GVB were differentiated from true trichoviruses by the number of their open reading frames (ORFs), they were separated from *Trichovirus* and finally assigned to the genus *Vitivirus* [187,188].

1.6.3. Genome organization of GVA

The species GVA is a positive-sense single-stranded RNA virus that has been classified into the family *Betaflexiviridae* under the genus *Vitivirus* [189]. GVA particles are filamentous about 800 nm long. The first full-length genome of GVA (GenBank accession no. X75433) was obtained from the exemplar isolate, Is-151, which was maintained in the laboratory host *Nicotiana benthamiana* and was from Italy [190]. The genome is approximately 7.4 kb and is comprises of five open reading frames (ORFs) and a 3′ terminal polyadenylation [188]. The function of four ORFs (excluding ORF 2) have been clearly identified and well-studied. ORFs 1, 3 and 4, encode a 194 kilodalton (kDa) RNA-dependent RNA polymerase (RdRp), 31 kDa movement protein (MP) and 21.5 kDa coat protein (CP), respectively [185,191]. ORF 2 encodes a 19 kDa hypothetical protein with a homology only within the *Vitivirus* genus, and its function remains unknown [185]. ORF 5 encodes a 10 kDa polypeptide putatively involved in nucleic acid-binding functions suppressing RNA-silencing responses generally called RNA binding protein (RB) [185].

1.6.4. Genetic variants of GVA and its association with SD

Three phylogroups, I, II and III (GVA^{I}, GVA^{II} and GVA^{III}) based on the phylogenetic similarities of partial MP, entire CP and RB genes, were identified in GVA and could be linked to symptom variability in South Africa [40,181,192]. Based on the sensitivity of different grapevine varieties to SD, a few varieties, including Shiraz, Merlot, Malbec, Gamay, and Sumoll, were categorized into SD-susceptible varieties as they show severe SD symptoms when infected with certain phylogroups of GVA [181,193]. Grapevine varieties tolerant to GVA, including Cabernet Sauvignon, Grenache, and Nero d'Avola, never display SD symptoms while infected with GVA. The GVA isolates that express SD symptoms on SD sensitive grapevines were categorized as SD inducing isolates [13,194,195]. Those GVA isolates that did not induce SD symptoms, even on SD-susceptible varieties, were categorized as SD-negative isolates [40]. The severity of disease symptoms caused by GVA isolates in grapevines corresponded to their severity on the herbaceous host *N. benthamiana* following sap inoculation [186,192]. Furthermore, the severity of symptoms on herbaceous and grapevine hosts was also linked to the phylogroup of GVA [192]. Isolate GTR1-1 (accession no. DQ787959) and P163-1 (accession no. DQ855088), which were symptomatic on grapevines and induce mild clearing of leaf veins on *N. benthamiana* have been classified into GVA^{III}. The SD sensitive grapevines consistently showed severe types of symptoms when infected with GVA^{II} [40]. The nucleotide sequences of GVA isolates within the same phylogroup share 91.0–99.8% identity, whereas isolates within different phylogroups share 78.0–89.3% nucleotide identity based on the 3′ terminal part of the genome which includes partial MP, entire CP and RB, and a partial 3′ untranslated region [192]. Goszczynski and Jooste [196] developed a phylogroup-specific RT-PCR assay that was employed for the phylogroup identification of GVA used in this thesis.

1.6.5. GVA Infectious clones prepared by transcription reaction or agroinfiltration

Since GVA cannot be mechanically inoculated onto the grapevine host [187], researchers have mainly used two strategies to work towards Koch's postulates, i.e. using infectious RNA transcripts, or agrobacterium inoculation or infiltration of cDNAs onto healthy grapevines or model hosts. *In-vitro* synthesized cDNA of a virus has been shown to be infectious, however, it is normally unstable [197]. Galiakparov, *et al.* [198] described a method to study symptom expression of GVA in which full-length infectious RNAs were inoculated onto herbaceous hosts. The full-length cDNA was transcribed *in vitro* to obtain infectious RNAs using T7 polymerase. They claimed that there was no difference between symptom expression when using infectious RNA transcripts or grapevine extracts for inoculation [199]. Agroinoculation and infiltration methods were first developed for gene functional analysis [200] and later used for studying symptoms of viruses in grapevines, including GVA and GVB [201,202], GRSPaV [203], GPGV [204], GLRaV-3 [205] and GRBV [45]. So far, the symptoms of various GVA isolates on herbaceous species have been studied [197,202,206,207], but no success in transmitting GVA into grapevines has been achieved.

1.7. The effects of viruses on physiological performance, berry and juice composition

The impacts of GLRaV-1 and 3, GFLV, GFkV and GRBV on various grapevine varieties on vine performance, berry and juice compositions by several previous studies are summarised in Table 1. Generically, viral infection results in a reduction of vine vigor, yield, berry maturity, photosynthetic pigments, juice total soluble solids (TSS) and total anthocyanin. Viral infection sometimes resulted in increased titratable acidity (TA), flavanol, sugars and starch contents in leaves. The impacts are highly variable and depend on grapevine variety and rootstock, seasons, and the particular virus species and isolates studied [208,209].

Table 1. The effects of viruses on physiological performance, berry and juice compositions of different grapevine varieties and clones.

Virus[1] and abiotic stress	Cultivars	Effects			Reference	Additional findings
		Increased	Reduced	Unaffected		
GLRaV-3 and GVA	Nebbiolo	-	Vine vegetative vigor, flavonoids, anthocyanins, berry maturity, net photosynthesis (P_n)	Yield, total soluble solids (TSS), titratable acidity (TA),	[210].	-
GLRaV-3	Albariño	TA	Juice TSS, pH, P_n	Yield	[211]	-
GLRaV-1, 2 and 3, GVA, GRSPaV, GFkV	Chardonnay clones 75, 76, and 95	-	Vigor, yield, berry maturity, TA	TSS	[212]	GLRaV-2 was the most important species among all viruses studied
GLRaV-1 and GVA	Nebbiolo	TA	Vigor and yield	TSS and phenol contents	[213]	Virus depressed the function of proteins involves oxidative stress and cell structure metabolism in berries.
GLRaV-3	Dolcetto	-	Vine vigor, yield, leaf photosynthesis and pH	TSS	[214]	Minor impacts on wine sensory profiles
GLRaV-1 and 3	Touriga Nacional	-	Yield, P_n, photosynthetic pigments, soluble sugars, soluble proteins, and elements N, P, Ca, S and Fe in leaves	elements K,Mg,B, Cu, Zn and Mn	[215]	Lower yield due to lower berry cluster weight
GLRaV-3	Cabernet Franc	-	Vigor, yield, cane lignification, berry TSS, P_n, stomatal conductance (g_s), transpiration (E)	Phenolic and anthocyanin contents in berries	[216]	-
GFkV	Manto Negro	-	g_s, E, internal CO2 concentration (C_i)	Leaf pigments, P_n, electron transport rate (ETR)	[217]	-

GLRaV-3, drought	Malvasia de Banyalbufar and Giró Ros	-	P_n, g_s, maximum velocity of carboxylation and ETR	-	[218]	Most growth parameters were negatively affected under both stress
GLRaV-3, drought	Malvasia de Banyalbufar and Giró Ros	-	Whole-plant and leaf hydraulic conductance	-	[219]	-
GRBV	Zinfandel grafted onto Gammay	pH	Juice TSS, TA, anthocyanins	Yield	[220]	GRBV may originated from the USA
GLRaV-3	Merlot	Leaf carbohydrates	g_s, P_n	Leaf and stem water potentials	[221]	Susceptibility to drought and winter damage unaffected by GLRaV-3
GRBV	Cabernet Sauvignon, Merlot, and Chardonnay	TA, flavonol and proanthocyanidin	Total anthocyanin	TSS	[209]	GRBV affects primary metabolites
GRBV	Cabernet Franc	Juice pH and TA	Juice TSS, anthocyanin, yeast assimilable nitrogen, and tannins in berry, anthocyanin and alcohol, colour in wine	-	[222]	Incomplete or delay leaf fall, change wine sensory profile
GRBV	Merlot and Shiraz	Leaf carbohydrates	Juice TSS	Cell wall composition of canes	[223]	-
GRBV	Pinot noir	TA	Vigor, yield, P_n, berry weight, TSS,	-	[224]	Hight stem water potential (Ψ_{stem}) improves performance of virus infected grapevines
GFLV, drought	Schioppettino	-	Stem water potential (Ψ_{stem})	-	[225]	GFLV infection benefit grapevines with mild water stress

[1] GRSPaV = grapevine rupestris stem pitting-associated virus, GLRaV-1, -2, -3 = grapevine leafroll-associated virus 1, 2, and 3, GVA = grapevine virus A, GRBV= grapevine red blotch virus, GFLV = grapevine fanleaf virus, GFkV = grapevine fleck virus.

1.8. Viruses in Australian Vineyards: Virus Pathogens in Australian Vineyards with an Emphasis on Shiraz Disease

Wu, Q.; Habili, N.; Constable, F.; Al Rwahnih, M.; Goszczynski, D.E.; Wang, Y.; Pagay, V. Virus Pathogens in Australian Vineyards with an Emphasis on Shiraz Disease. Viruses 2020, 12, 818, doi:10.3390/v12080818.

Statement of Authorship

Title of Paper	Virus Pathogens in Australian Vineyards with an Emphasis on Shiraz Disease
Publication Status	☒ Published ☐ Accepted for Publication ☐ Submitted for Publication ☐ Unpublished and Unsubmitted work written in manuscript style
Publication Details	Journal MDPI virus Year 2020, volume 12, issue 8, page 818

Principal Author

Name of Principal Author (Candidate)	Qi Wu
Contribution to the Paper	original draft preparation, review and editing, data and photos
Overall percentage (%)	30%
Certification:	This paper reports on original research I conducted during the period of my Higher Degree by Research candidature and is not subject to any obligations or contractual agreements with a third party that would constrain its inclusion in this thesis. I am the primary author of this paper.
Signature	Date 16/01/2023

Co-Author Contributions

By signing the Statement of Authorship, each author certifies that:

i. the candidate's stated contribution to the publication is accurate (as detailed above);
ii. permission is granted for the candidate in include the publication in the thesis; and
iii. the sum of all co-author contributions is equal to 100% less the candidate's stated contribution.

Name of Co-Author	Nuredin Habili
Contribution to the Paper	original draft preparation, review and editing, data and photos
Signature	Date 11/1/2023

Name of Co-Author	Fiona Constable
Contribution to the Paper	original draft preparation, review and editing, data and photos
Signature	Date 21/10/2022

Name of Co-Author	Maher Al Rwahnih		
Contribution to the Paper	review and editing		
Signature	Maher Al Rwahnih	Date	11/3/2022

5/16/2023

Name of Co-Author	Darius E. Goszczynski		
Contribution to the Paper	review and editing		
Signature		Date	27/10/22

Name of Co-Author	Yeniu Wang		
Contribution to the Paper	data and photos		
Signature		Date	14/10/2022

Name of Co-Author	Vinay Pagay		
Contribution to the Paper	original draft preparation, review and editing, data and photos		
Signature		Date	24/10/2022

viruses

MDPI

Review

Virus Pathogens in Australian Vineyards with an Emphasis on Shiraz Disease †

Qi Wu [1,2,‡], Nuredin Habili [2,‡], Fiona Constable [3,‡], Maher Al Rwahnih [4], Darius E. Goszczynski [5], Yeniu Wang [1] and Vinay Pagay [1,*]

1 School of Agriculture, Food & Wine, University of Adelaide, Waite Precinct, PMB 1, Glen Osmond, Adelaide 5064, South Australia, Australia; qi.wu@adelaide.edu.au (Q.W.); yeniu.wang@adelaide.edu.au (Y.W.)
2 The Australian Wine Research Institute, PO Box 197, Glen Osmond, Adelaide 5064, South Australia, Australia; nuredin.habili@awri.com.au
3 Agriculture Victoria Research, Department of Economic Development, Jobs, Transport and Resources, AgriBio, Bundoora, Melbourne 3083, Victoria, Australia; fiona.constable@agriculture.vic.gov.au
4 Department of Plant Pathology, University of California, Davis, CA 95616, USA; malrwahnih@ucdavis.edu
5 Plant Protection Research Institute, Agricultural Research Council, Private Bag X134, Pretoria 0001, South Africa; goszczynskid@arc.agric.za
* Correspondence: vinay.pagay@adelaide.edu.au
† In memory of Professor Giovanni Martelli.
‡ These authors contributed equally to this manuscript.

Received: 24 June 2020; Accepted: 25 July 2020; Published: 28 July 2020

Abstract: Grapevine viruses are found throughout the viticultural world and have detrimental effects on vine productivity and grape and wine quality. This report provides a comprehensive and up-to-date review on grapevine viruses in Australia with a focus on "Shiraz Disease" (SD) and its two major associated viruses, grapevine virus A (GVA) and grapevine leafroll-associated virus 3 (GLRaV-3). Sensitive grapevine cultivars like Shiraz infected with GVA alone or with a co-infection of a leafroll virus, primarily GLRaV-3, show symptoms of SD leading to significant yield and quality reductions in Australia and in South Africa. Symptom descriptors for SD will be outlined and a phylogenetic tree will be presented indicating the SD-associated isolates of GVA in both countries belong to the same clade. Virus transmission, which occurs through infected propagation material, grafting, and naturally vectored by mealybugs and scale insects, will be discussed. Laboratory and field-based indexing will also be discussed along with management strategies including rogueing and replanting certified stock that decrease the incidence and spread of SD. Finally, we present several cases of SD incidence in South Australian vineyards and their effects on vine productivity. We conclude by offering strategies for virus detection and management that can be adopted by viticulturists. Novel technologies such as high throughput sequencing and remote sensing for virus detection will be outlined.

Keywords: grapevine; high throughput sequencing; vectors; rogueing; leafroll disease; scale insects; mealybugs

1. Introduction

Vitis vinifera, cv. Shiraz (syn. Syrah) is the most popular cultivar in Australia. In 2018, of the total of 135,133 ha under cultivation, Shiraz accounted for 39,893 ha (approximately 30% of total winegrape acreage in Australia) making it the most widely planted winegrape cultivar in Australia (www.wineaustralia.com/market-insights/australian-wine-sector-at-a-glance). Of 86 viruses detected in the grapevine to date [1], 35 have been reported to have negative effects on vine performance,

especially in red-berried cultivars [2]. Grapevine virus A (GVA), grapevine virus B (GVB), grapevine leafroll associated viruses (GLRaV-1, -2, -3, and -4), grapevine rupestris stem pitting associated virus (GRSPaV) and grapevine fleck virus (GFkV) have been found in Australian vineyards historically [3]. The most recent viruses reported from Australia are grapevine Pinot gris virus (GPGV) and grapevine rupestris vein feathering virus [4]. Grapevine fanleaf virus has been eradicated and it is now listed as quarantined [5].

Sensitivity of different grapevine cultivars to viruses is variable [6]. Among the red-berried cultivars, Shiraz is highly sensitive to infections by GVA; symptoms associated with GVA infections include retarded shoot growth, decreased sugar accumulation in the berries and, in some cases, even vine mortality [7,8]. The disease is called Shiraz Disease (SD), which is one of the most debilitating diseases of Shiraz in Australia and South Africa [9]. This disease was first reported in 1985 from South Africa without knowledge of its associated virus [10]. In 2003, it was reported that GVA was associated with the disease in both South Africa and Australia [11,12]. The first GVA infection in Australia was detected by our group in 1997 in symptomatic Shiraz vines in the Clare Valley, South Australia. SD is associated with either infection by GVA alone, or co-infection of GVA with one or more of leafroll viruses such as GLRaV-3, GLRaV-4 strain 9, or GLRaV-1 in sensitive red-berried cultivars like, Shiraz, Merlot, Malbec, and Sumoll. The virus associated disease occurs only in South Africa and Australia, and it appears to be different from Syrah decline in the USA and France, which may be a genetic disease [13,14].

In this review, we will refer to viruses affecting grapevines in Australia with an emphasis on those associated with SD. Information on the nature of the associated viruses, symptom expression, genomics, and detection will be provided. We then review the effects of SD on grapevine growth, physiological function, and fruit and wine composition. We conclude by sharing some recent observations of SD-affected vineyards in South Australia and proposing strategies for disease control.

2. Grapevine Viruses in Australian Vineyards

Viruses are widespread in vineyards worldwide. To date, few viruses have been detected in grapevines in Australia compared to globally (Table 1); this is partly attributed to strict biosecurity measures that have prevented the introduction of infected material into Australia as well as the lack of more efficient vectors [15–17]. The selection of material from productive clones and cultivars, virus-testing, in vitro virus eradication, and established certification programs have assisted in preventing some of the more serious diseases and pathogens of grapevine entering or dispersing within Australia. Nevertheless, some serious virus associated diseases, including leafroll disease and diseases of the rugose wood complex, occur and spread in Australian vineyards (Table 1).

Table 1. Common grapevine viruses in Australia, their associated disease, and vectors. Viruses indicated in bold text are the focus of this review.

Family/Genome	Genus	Species [1]	Associated Disease	Vector
Betaflexiviridae Monopartite linear ssRNA (+)	*Vitivirus*	**grapevine virus A** (GVA)	Shiraz Disease, Kober Stem Grooving	Mealybug/scale
		grapevine virus B (GVB)	Corky Bark	Mealybug/scale
	Foveavirus	grapevine rupestris stem pitting associated virus (GRSPaV)	Asymptomatic in most, stem pitting	Unknown
	Trichovirus	grapevine Pinot gris virus (GPGV)	Leaf mottling and deformation, symptomless	*Colomerus vitis*

Table 1. *Cont.*

Family/Genome	Genus	Species [1]	Associated Disease	Vector
Closteroviridae Monopartite linear ssRNA (+)	*Ampelovirus*—**Subgroup I**	grapevine leafroll associated virus **(GLRaV)-1** and **GLRaV-3**	Leafroll disease	Mealybug/scale
	Ampelovirus—Subgroup II	**GLRaV-4 and its strains: 5, 6, 9** [2]	Leafroll disease	Mealybug/scale
	Closterovirus	GLRaV-2	Leafroll disease, Graft incompatibility	Unknown
Secoviridae Bipartite, linear ssRNA (+)	*Nepovirus*	grapevine fanleaf virus (GFLV) [3]	Fanleaf, degeneration, decline, chlorosis	*Xiphinema index*; *X. diversicaudatum*
Tymoviridae Monopartite, linear ssRNA (+)	*Maculavirus*	grapevine fleck virus (GFkV)	Fleck on *V. rupestris*, Asymptomatic in other *Vitis* sp.	Unknown
	Marafivirus	grapevine rupestris vein feathering virus (GRVFV)	Asymptomatic	Unknown

[1] Viruses associated with Shiraz Disease are highlighted in bold. [2] GLRaV-4 strains; Pr^2, De^2 and Car^2 strains have not been detected. [3] GFLV has been eradicated [5].

3. Virus Transmission in Vineyards

Many of the commonly occurring grapevine viruses are specific to *Vitis* sp. so the likelihood of the virus infection spreading to or from another perennial or herbaceous plant is low. Spread of the major viruses, particularly GVA and GLRaV-1 and -3, in Australian vineyards occurs primarily through infected propagation material; there is no evidence to date of mechanical transmission, including pruning. In established vineyards, vector transmission is thought to be the dominant mode of virus transmission between vines.

3.1. Primary Transmission

Primary transmission is the introduction of a virus infection into a crop. This type of transmission often occurs in vineyards following establishment using propagation material sourced from infected mother vines, but it could also occur when a viruliferous vector is introduced to a vineyard from another area. Over centuries, primary transmission of viruses has inadvertently been practiced by humans using infected cuttings for propagating own-rooted and grafted plants and top working. Top-working—grafting by either chip bud, T-bud or cleft methods—new cultivars onto an existing virus-infected grapevine is a common practice by vignerons in Australia [12,18]. However, this practice is risky if the virus status of a grapevine to be top-worked is unknown and symptoms are not apparent. One example of this trend is top-working of the popular Australian cultivar Shiraz onto Chardonnay or Riesling. When infected with GVA, these white-berried cultivars do not show typical red-leaf symptoms as observed in red-berried cultivars, but rather appear "clean", i.e., asymptomatic or having a faint chlorotic appearance on leaves. However, GVA is associated with drastic symptoms in Shiraz, Malbec, and Merlot in Australia following grafting (see below). A random distribution of infected grapevines within a block is often indicative of primary spread into a vineyard and suggests that either infected material was planted randomly across the block or the viruliferous vectors were transported long distance by wind or other carriers.

3.2. Secondary Transmission

Once a primary infection is established in a vineyard, secondary infections or spread within a block can occur via vectors such as mealybugs and scale insects [19–23]. When secondary virus spread occurs, the pattern of infected vines is aggregated [24], because viruliferous mealybug nymphs (crawlers) transmit the virus to vines located at close proximity to the primary infection. Adjacent vines within a row and neighbouring vines in adjacent rows may become infected forming a cluster ("hot spot") around the primary infection within a vineyard. Gradients of infection can be observed when transmission occurs from infected vines located at the edge of vineyards [25]. Over the course of several seasons, entire vineyards can become infected. The rate of secondary spread is likely correlated with the abundance of vectors. For example, in a French vineyard, an increase in leafroll disease incidence from 5% to 86% over eight years was linked to a 74% incidence of *Phenacoccus aceris* during the same period [26]. A study in an Australian Pinot noir vineyard showed that the incidence of GLRaV-3 increased from 23% to 52% over a 10 year period, with no change in incidence until the last three years suggesting a change in ecology of the virus vectors [27]. The same study also found that the rate of spread was one-third of that observed in a NZ Cabernet Sauvignon vineyard; this might be attributed to differences in vector species and population dynamics between the two regions. Therefore, it is critical to understand vector populations and ecology so that efficient management strategies can be developed to control secondary virus spread.

The spread of phloem-limited grapevine viruses such as GVA and GLRaV-3 is mediated by mealybugs (Family: *Pseudococcidae*) and soft scales (Family: *Coccidae*) [25,28]. Co-infections of GVA with GLRaV-1, GLRaV-3, or GLRaV-4 strain 9 have been observed [7], and these viruses can be transmitted simultaneously. In adult mealybugs, *Pseudococcus viburni* (Signoret), isolated from the cultivar Shiraz infected with SD, both GLRaV-3 and GVA were detected, and further work is required to understand the role of this vector and other vectors in SD spread. Table 2 lists the mealybug vectors, and Table 3 lists the scale insect vectors of grapevine viruses, including those that occur in Australia.

Table 2. Common mealybug vectors of grapevine viruses.

Mealybugs	Common Name	Transmitted Viruses	Presence in Australia	References
Ferrisia gilli (Gullan)	Gill's mealybug	GLRaV-3,4	No	[29]
Heliococcus bohemicus	Bohemian mealybug	GLRaV-1,3; GVA	No	[30–33]
Phenacoccus aceris	Apple mealybug	GLRaV-1,3,4; GVA; GVB	No	[26,32,34]
Planococcus citri	Citrus mealybug	GLRaV-1,3; GVA	Yes	[31,35,36]
Planococcus ficus	Grapevine mealybug	GLRaV-1,3, 4; GVA	No	[19,31,37,38]
Pseudococcus viburni	Obscure mealybug, tuber mealybug	GLRaV-3; GVA; GVB	Yes	[39]
Pseudococcus comstocki	Comstock mealybug	GVE	No	[40]
Pseudococcus maritimus	Grape mealybug	GLRaV-1,3	No	[41]
Pseudococcus calceolariae	Citrophilus mealybug, scarlet mealybug	GLRaV-3	Yes	[42]
Pseudococcus longispinus	Long-tailed mealybug	GLRaV-1,3; GVA	Yes	[22,42,43]

Transmission of grapevine viruses by all mealybug and scale species is thought to be in a non-circulative, semipersistent manner: viruses may be acquired, but they do not replicate in the insect. Instead viruses are retained in the foregut and transmitted after hours or days [44,45]. Research suggests that there is no virus-vector specificity, and multiple mealybug species can transmit one virus species (Table 2). Conversely, a single mealybug species can transmit multiple GLRaV species and

some vitiviruses [46]. GLRaV-3 appears to be transmitted more efficiently by mealybugs than other viruses [25,47]. A recent study found that virus transmission by mealybugs was 22% more efficient for GLRaV-3 than GVA, and that GVA transmission was enhanced in the presence of GLRaV-3 [47]. First and second instars nymphs (crawlers) are more efficient at spreading the leafroll viruses and GVA because these viruses are easily dispersed within and between vineyards by crawlers, wind, and mechanical methods [48,49]. Certain mealybug species have been reported to have up to six generations per year [50]. Population size and number of generations of the insect in a single season are key factors influencing virus transmission rates, and high numbers can lead to rapid spread of viruses. Transmission of viruses within or between vineyards can be facilitated by movement of mealybug nymphs on vineyard equipment, ants, humans, and wind [51]. Evidence for the mode of spread can be found from the pattern of infection in the newly infected vineyard: clusters of virus infection may be observed near equipment entry points in the vineyard or along edges next to other infected vineyards. Mealybug crawlers, which are most efficient in virus transmission [52], are very light and can therefore be easily blown by wind from vineyard blocks as far as several kilometers away, depending on humidity and temperature [53]. In wind-borne transmission of the virus, the resulting distribution of associated disease in the vineyard may appear random, or edge effects might be observed [54].

Table 3. Common scale insect vectors of grapevine viruses.

Scale Insects	Common Name	Transmitted Viruses	Presence in Australia	References
Ceroplastes rusci	Fig wax scale	GLRaV-3,4 strains 5	Yes	[37]
Coccus hesperidium	Brown soft scale	GLRaV-3	Yes	[17]
Coccus longulus	Long brown scale	GLRaV-3	Yes	[20]
Parasaissetia nigra	Nigra scale	GLRaV-3	Yes	[20]
Parthenolecanium corni	Brown scale, European fruit lecanium scale	GLRaV-1,3; GVA	Yes	[32,34,48,54,55]
Parthenolecanium persicae	Grapevine scale	GLRaV-3; GVA	Yes	[56–59]
Parthenolecanium pruinosum	Frosted scale	Unknown	Yes	[57,58]
Pulvinaria vitis	Wooly vine scale	GLRaV-3	No	[60]
Neopulvinaria innumerabilis	Soft scale	GLRaV-1	No	[55]
Saissetia sp.	Soft scale	GLRaV-3	Yes	[20]

4. Symptomatology

The ability to detect virus infections based on symptoms is largely dependent on experience and the specific combination of virus species, grapevine cultivar, and geographical region (e.g., symptoms of GLRaV-3 on Shiraz cultivar in Thailand; N Habili, unpublished). The challenge with symptom-based identification is the fact that several viruses can be present in a host, altering symptom expression. Certain *Vitis vinifera* cultivars may be symptomless or show only minor leaf chlorosis, such as many white-berried cultivars (e.g., Sauvignon Blanc, Chardonnay, and Riesling) as well as *Vitis* rootstocks. The genetic variability of a virus species also influences symptom expression. Multiple genetic variants of specific viruses including GVA [62] and GRSPaV [63,64], both of which are found in Australian vineyards, have been observed to exist in an individual grapevine and are thought to have occurred via grafting, vectors, and/or pollination [63]. Virus infections in grapevines that are symptomatic can be mistaken with certain nutrient deficiencies or phytoplasma-associated diseases such as Australian grapevine yellows and flavescence dorée. Viruses can produce specific symptoms on the vine, and these

symptoms sometimes form part of the virus name. Below, we describe the symptoms of SD associated with GVA in conjunction with GLRaV infection [65] with special reference to Australia. Readers are referred to [66] and [6] for a detailed description of grapevine virus symptomatology.

4.1. Shiraz Disease

In GVA-infected *V. vinifera* cv. Shiraz (syn. Syrah), symptoms of primary bud necrosis (PBN) are often observed in buds during the dormant season (Figure 1a). A survey of GVA-positive Shiraz vines in a South Australian vineyard found that 41% of primary buds had PBN, while in GVA-negative Shiraz vines, only 11% had PBN.

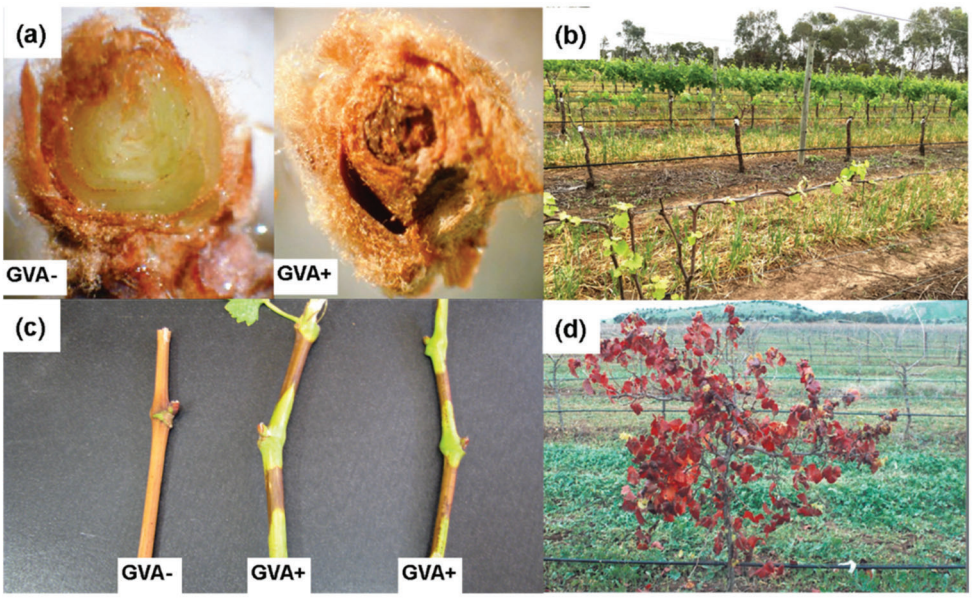

Figure 1. Symptomatology of grapevine virus A (GVA)-associated Shiraz Disease. (**a**) primary bud necrosis shown on right; (**b**) restricted spring growth (front row); (**c**) partial lignification showing islands of green immature canes; (**d**) retention of crimson coloured leaves on canopy in winter.

Early in the growing season, shoot growth of SD vines is retarded or restricted and is known as "restricted spring growth" [12] (Figure 1b). Following véraison (the onset of grape berry ripening and a change from green to red skin in red-berried cultivars), shoots display symptoms of delayed maturity (e.g., lack of lignification), and often exhibit green "islands" on the periderm (Figure 1c) [12]. Over time, the leaves transition to a bright crimson colour with either green veins or red veins (Figure 1d) and persist on the vine into the dormant season, i.e., have delayed senescence. The symptoms of GVA-associated SD have been observed in several grapevine cultivars including Shiraz, Malbec, and Merlot in South Africa and Australia [9,12]. To date, SD has not been reported in other viticultural regions of the world, where GVA is known to be associated with Kober stem grooving [67]. In warmer viticultural regions of Australia (e.g., Riverland, SA), vine decline has also been observed.

4.2. Leafroll Disease

In red-berried cultivars, visible symptoms of grapevine leafroll disease (GLD) typically appear around véraison. However, the virus can be detected using molecular techniques at the pre-véraison stage [68]. Basal leaves turn red, thick and have a marked cupped appearance with the leaf margins curled downwards towards the abaxial side of the leaf (Figure 2a).

Red grape cultivars are more sensitive to GLD and can develop dark red or purple colouration in the interveinal sections of the leaf, often with distinct green veins (Figure 2b), while leaves of white grape cultivars turn yellow or remain symptomless (Figure 2c). Mild symptoms are most observed in

grapevines infected with GLRaV-4 and its strains 5, 6, 9, Car, De, and Pr (Ampelovirus, subgroup II). The symptoms associated with GLRaV-4 strain 9 are more severe in Shiraz than in Cabernet Sauvignon, especially at later phenological stages of development (Figure 2d,e). It remains unknown why GLD symptoms develop at specific phenological stages. Naidu et al. [69] suggested that the degree of virus-host interaction may be based on the phenological stage of development resulting from the response of the host's cellular machinery to the virus.

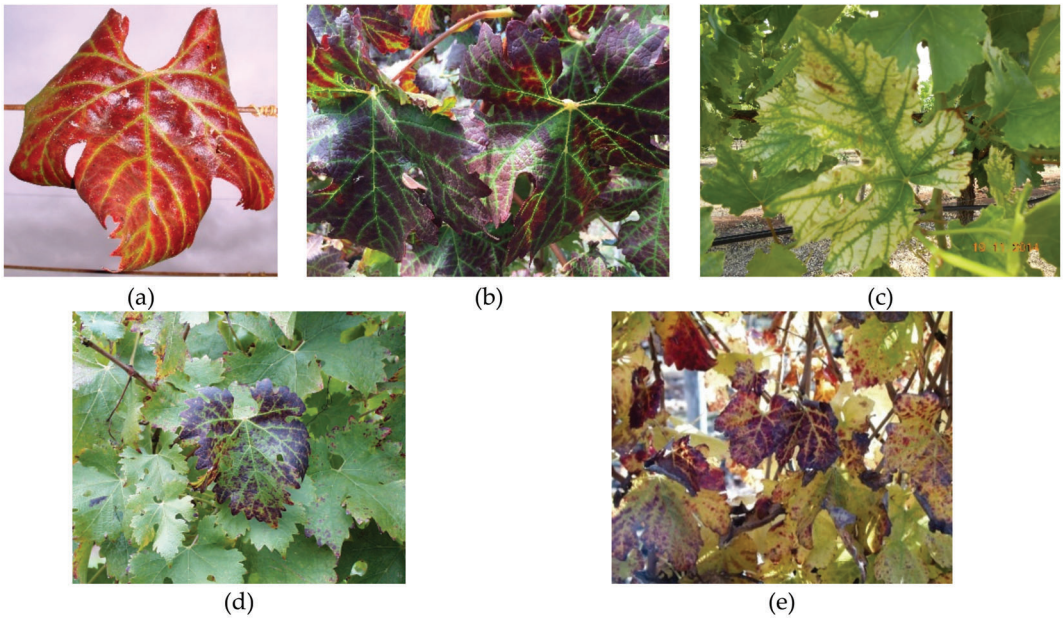

Figure 2. Symptomatology of grapevine leafroll disease. (**a**) leaf margins curled downwards towards the abaxial side of the leaf; (**b**) interveinal regions of leaf blades appear dark red or purple in colour with distinct green veins; (**c**) leaves of white cultivars sometimes appear slightly chlorotic, and the veins may remain green; (**d**) GLRaV-4 strain 9 symptoms on Cabernet Sauvignon; (**e**) GLRaV-4 strain 9 symptoms on Shiraz.

5. High Throughput Sequencing (HTS) and Phylogenetic Analysis of Viruses Associated with Shiraz Disease

5.1. High Throughput Sequencing (HTS)

Although some leafroll viruses may produce SD-like symptoms [70], GVA has been proposed as the key pathogen associated with SD [71]. Therefore, an initial metagenomics HTS experiment using the Illumina Miseq platform [72] was conducted in several vineyards known to be infected with GVA with the goal of investigating the virus diversity in symptomatic and non-symptomatic grapevines. In our initial HTS results, we sequenced vines of four Shiraz isolates BV1, BV4, LC1, and LC16 selected from two regions (Table 4). The potential viral agents of SD are highlighted in bold. LC1 represented vines with severe Shiraz disease symptoms, and BV1 represented vines in which GVA and GLRaVs had been previously detected but only showed mild leafroll symptoms. BV4 and LC16 represented symptomless Shiraz vines from the same region. The virus profile for a given cultivar infected with SD was different; however, GVA and grapevine rupestris stem pitting-associated virus (GRSPaV) were always present. The latter, as well as grapevine yellow speckle viroid 1 (GYSVd-1) and hop stunt viroid, was present in both SD-affected and non-SD-affected vines (Table 4).

Table 4. Virus profiles in Shiraz Disease (SD)-affected and non-SD-affected Shiraz and Malbec grapevines from South Australia. The potential viral agents of SD are highlighted in bold.

Cultivar	Region	Sampling Year	Sample ID	Isolate Name	SD Symptoms	Viruses Identified	GVA Group
Shiraz	Barossa Valley	2018	BV1	Isolate 1	No	GRSPaV, GRVFV, **GLRaV-1**, **GVA**, GYSVd-1, HSVd	I
Shiraz	Barossa Valley	2018	BV4	Isolate 2	No	GRSPaV, GRVFV, GYSVd-1, HSVd	- [1]
Shiraz	Langhorne Creek	2018	LC1	Isolate 1	Yes	GRSPaV, **GVA, GLRaV-9,** GRVFV, GYSVd-1, HSV	II
Shiraz	Langhorne Creek	2018	LC16	Isolate 2	No	GRSPaV, GRVFV, GYSVd-1, HSVd	- [1]
Malbec	Padthaway	2016	Malbec	Malbec-Richter [2]	Yes	**GVA, GLRaV-3 (4 and its strains 5, 6 & 9),** GRSPaV	II

[1] No GVA present. [2] Malbec on Richter 110 rootstock.

5.2. Phylogenetic Analysis of Viruses Associated with Shiraz Disease

Several full-length and partial sequences of SD associated viruses obtained in this study using HTS are listed in Table 5. A summary of GVA and GLRaV-3 isolates from Australia and their phylogenetic groups is also provided in Table 5.

The sequence of the coat protein gene of the Australian GVA isolates was compared with 40 other isolates available on GenBank, and a phylogenetic tree was constructed (Figure 3). The tree showed that the coat protein (CP) sequences of SD-associated GVA isolates in South Africa (P163-M5, GTR1SD-1) and Australia (LC1-1, LC1-2, Malbec/Richter) are closely related and grouped together (Group II, Figure 3). These isolates are distinct from non-SD GVA isolates BV1-1 and BV1-2 (Group I) [8,73]. BV1-1 and BV1-2 were isolated from old vines (> 150 years old) that have undergone frequent virus testing. Recently, we found symptomless Shiraz grapevines in Clare Valley, SA that tested positive for GVA.

Table 5. Accession numbers of the Australian isolates of GVA and GLRaV-3 and their phylogenetic groups studied in this work.

Virus	Variety/ Rootstock	Sample ID (Isolate)	Accession#	Sequence Length (bp)	Location	Symptom on Shiraz	Group
GVA	Shiraz	BV1-1	MT070961	2751	Barossa Valley	None	I
GVA	Shiraz	BV1-2	MT070960	597	Barossa Valley	None	I
GVA	Shiraz	LC1-1	MT070963	7363	Langhorne Creek	SD	II
GVA	Shiraz	LC1-2	MT070962	7052	Langhorne Creek	SD	II
GVA	Malbec on Richter	Malbec-Richter	MT070959	598	Padthaway	SD	II
GLRaV-3	Shiraz on Ramsey	R3ShRam	MN984352	942	Riverland	SD	V
GLRaV-3	Shiraz on Ramsey	R4ShRam	MN984353	934	Riverland	SD	I
GLRaV-3	Shiraz on 101-14	R8Sh101	MN984354	941	Riverland	SD	I
GLRaV-3	Malbec on Richter	Malbec-Richter	N/A	N/A	Padthaway	SD	I [1]

[1] All the contigs of Malbec-Richter matched with the phylogenetic Group I. Malbec-Richter was not depicted in Figure 4 because of a truncated CP sequence.

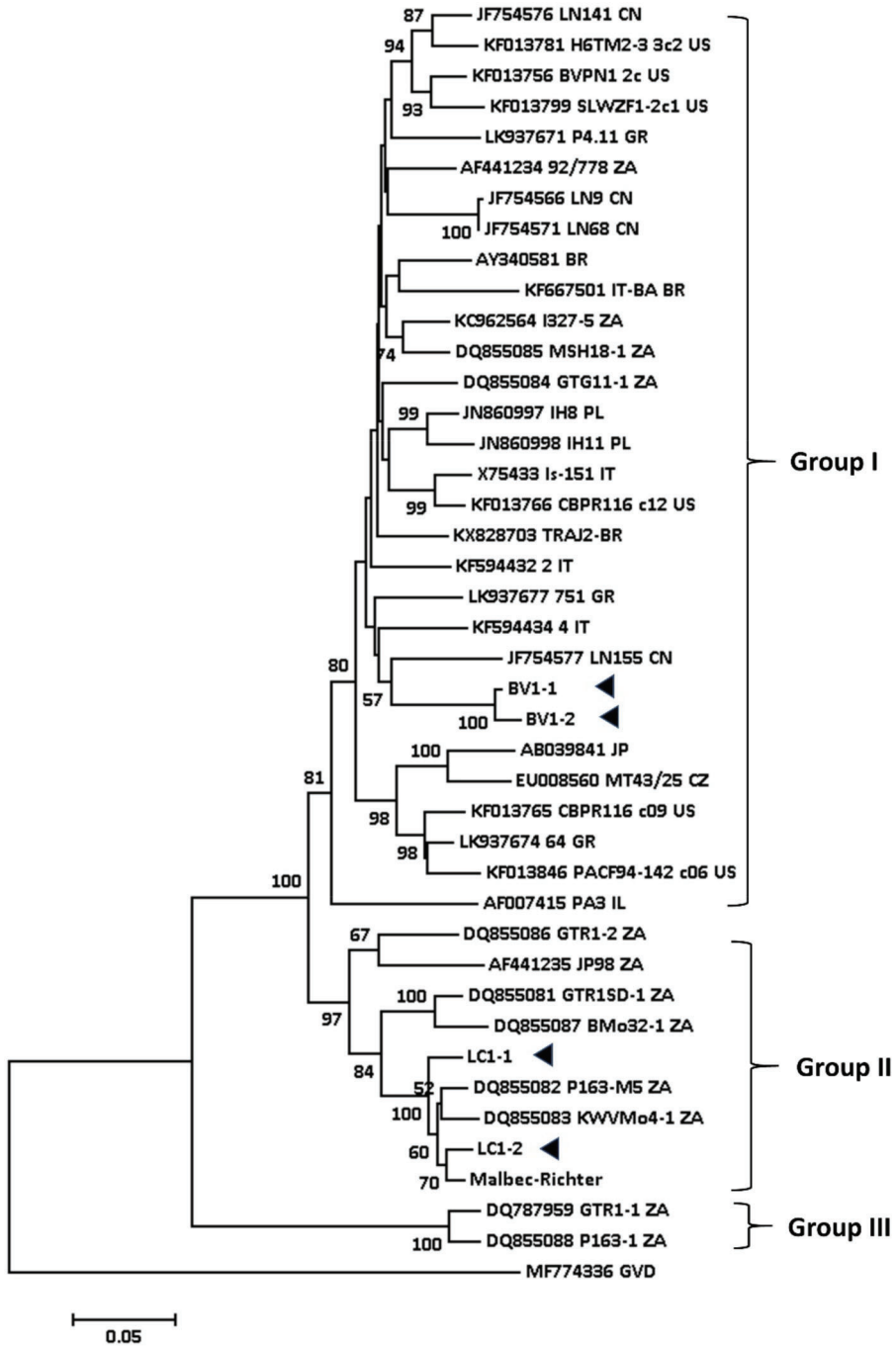

Figure 3. Phylogenetic tree constructed from the alignment of full-length nucleotide sequence of the coat protein of selected isolates of GVA detected in the grapevine using neighbour-joining method (Mega 7) with 1000 bootstrap replications. Bootstrap values less than 50% are not shown. Arrowheads denote the GVA isolates from Australia studied in this work. GVD (MF774336) presents outgroup of this tree.

For GLRaV-3, the phylogenetic study was based on nearly complete sequence of the viral CP gene (Figure 4). A total of seven groups were identified. This is slightly different from the grouping of GLRaV-3 isolates reported by Diaz-Lara and co-workers who found 10 phylogenetic groups, but Groups IV and VIII were not depicted in their tree [74]. The Australian isolates are assigned to Groups I, V, and VII (Figure 4 and Table 5).

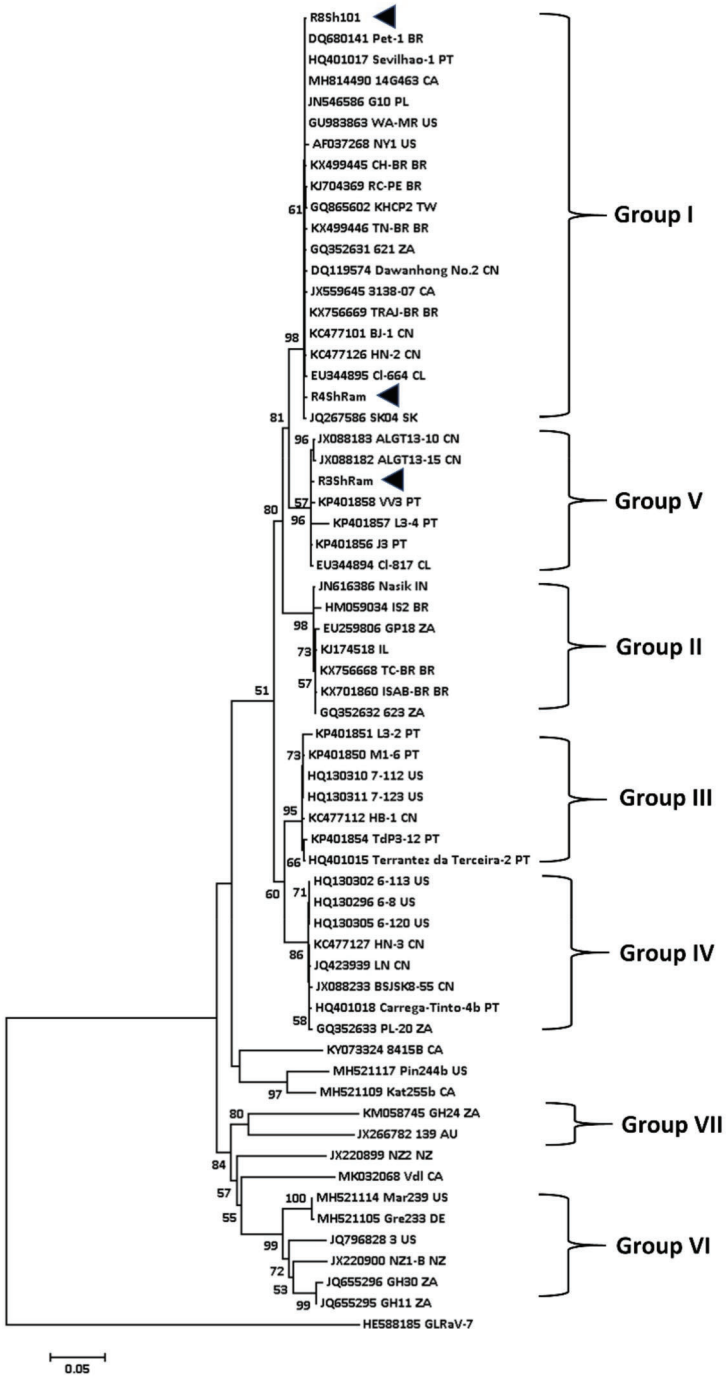

Figure 4. Phylogenetic tree constructed from the alignment of full-length nucleotide sequence of the coat protein of various isolates of GLRaV-3 (see also [73]) detected in the grapevine using Mega 7. A total of 1000 bootstrap replications were performed using neighbour-joining method. Bootstrap values less than 50% are not shown. Arrowheads denote the Australian isolates studied in this work. GLRaV-7 (HE588185) presents outgroup of this tree.

It is interesting to note that in R3ShRam andR4ShRam that were isolated from the same Shiraz vineyard in Riverland, SA, two different groups of GLRaV-3 (Groups I and IV) were detected (Table 5). Table 5 also shows the sequence of SD-affected Malbec (isolate Malbec-Richter). Based on the CP sequence of GVA and partial sequence of GLRaV-3, the isolate of Malbec-Richter was infected with Group II of GVA and Group I of GLRaV-3 (Table 5; [74]).

Two mild isolates of GLRaV-3 were detected in Australia, both belonging to Group VII. CSL isolated from Crimson Seedless (Accession MT081182) table grapes from Western Australia showed mild leafroll symptoms; this isolate clustered with a symptomless isolate 139 (Figure 4) of the virus detected in cultivar Sauvignon Blanc from the Adelaide Hills, SA (Accession JX266782). Both these isolates are clustered in Group VII, a group that appears to accommodate mild isolates of GLRaV-3. Isolate CSL (13,865 bp, ORF1 to 5) share 99% nucleotide sequence identity with the South African isolate GH24 (Accession KM058745), although only 300 nt of its ORF6 (CP) was sequenced. The truncated CP was not included in Figure 4.

6. Virus Effects on Vine Physiology and Fruit Composition

Virus-related diseases can affect grapevine physiological performance, vigour, yield, grape and wine composition, and quality [8,75]. Changes to vine physiology resulting from virus infection primarily relate to photosynthesis and chlorophyll *a* fluorescence, processes that directly or indirectly relate to the vine's ability to maintain vegetative and reproductive growth as well as ripen crop. Both photosynthesis and chlorophyll fluorescence were observed to be lower in GLRaV-3-infected Cabernet Franc grapevines in a Michigan (USA) vineyard compared to healthy vines after véraison [75]. Following véraison, sugar accumulates in grape berries, and reduced leaf photosynthesis would explain the lower sugar accumulation in the GLRaV-3-infected berries [8]. In the same Cabernet Franc vineyard, reductions in yield and grape soluble solids of 40% and 43%, respectively, were observed compared to uninfected vines. In the Finger Lakes region of New York (USA), Martinson and colleagues reported that grape soluble solids were lower by 2 °Brix in vines affected by GLD [76]. Yield losses have been reported in vines with leafroll disease as well as those associated with the rugose wood complex [7,77–81]. In a study involving several rootstocks, decreased vine vigour and pruning weights were observed in vines infected with GLRaV-1, GLRaV-3, GFLV, and rugose wood associated viruses [82]. In extreme cases, vine death has been observed with infections involving the rugose wood complex [81].

A study on Cabernet Sauvignon grapevines in Chile found that the main anthocyanin and sugar metabolism genes were down-regulated during fruit ripening in GLRaV-3-infected vines [83]. In Pinot Noir in Oregon, reduced total and individual anthocyanin concentrations were observed in GLD vines [80]. It is plausible that the reduced accumulation of grape primary metabolites, e.g., sugars, due to virus infection results in reduced accumulation of secondary metabolites, e.g., anthocyanins; this may be related to decreased phloem loading and hence accumulation of sugars in leaves [69]. Diminished grape composition resulting from changes in aroma compounds such as monoterpenes has been observed with leafroll infections [84].

A preliminary study in Southern Oregon, USA, on Grapevine red blotch virus (GRBV)-infected Cabernet Franc grapevines indicated that virus infections can be detected prior to véraison before the appearance of red leaf symptoms based on measurements of leaf chlorophyll fluorescence (Pagay and Martin, unpublished). Leaf reddening may be a response of grapevines to virus infection in which they accumulate anthocyanins that play a protective role as antioxidants in scavenging free radicals produced by the vine under biotic stress [69]. Nearly all the published studies to date, including those discussed above, have focused on the effects of GLD on red grape cultivars. Much less is known about the effects of GLD on white grape cultivars as well as about the effects of SD on vine physiology and fruit composition of both red and white cultivars. It was observed that GVA-infected Marzemino grapevines had reduced bud fertility, but surprisingly, when co-infected with GLRaV-1, the vines had neither significantly altered yields nor juice soluble solids, total acidity, pH, anthocyanins, or polyphenols [85].

Conversely, some virus species and isolates may not cause disease or impact yield or grape quality particularly when they infect grapevines in the absence of other viruses [86]. Interestingly, some studies suggest that there may be benefits from virus infection in grapevines. "Crimson Seedless" vines inoculated with a mixture of GLRaV-3 (Group VII; isolate CSL-WA), -5, and -9 and GVA were observed to have higher berry weight and lighter berry colour, which was more marketable compared

to uninfected grapevines [87]. Similarly, the mildly leafroll-affected cultivar "Emperor" produced larger and crisper berries compared to symptomless clones [88]. These studies highlight some of the positive effects of virus infections on grape composition.

Future studies could also consider investigating virus effects on grape berry development and potentially delayed ripening, which are becoming increasingly important in the context of climate change and regional warming [89,90].

7. Economic Impacts of GVA and GLRaV-3

Both GLD and SD are debilitating to vineyards due to economic losses associated with yield reductions, lower grape prices due to inferior fruit quality [25], and vine replacement costs. Unfortunately, there is a dearth of information on the economic impacts of both diseases. Below, we discuss the few published studies on the economic impacts of virus-related grapevine diseases that we are aware of.

In Australia, many grape growers may be complacent in their management of virus infections as they consider the magnitude of the issue insignificant relative to other pathogens in the vineyard including trunk diseases (e.g., Eutypa dieback) and powdery mildew. As a result, virus-infected vines are often ignored. A report on the economic impact of virus and related-infections on grapevines indicated that the reduced profit ranged from AU$34 to $103 ha^{-1} yr^{-1} for prevention and control [91]. In the same study, the economic loss due to viruses was estimated around AU$12 million yr^{-1}. Some conscious growers, or those whose economic impact is more significant, opt to rogue and replant the vines and even entire vineyards thereby decreasing the risk of virus spreading to neighbouring vines and vineyards. In Australia, the lifespan of a vineyard infected with SD may not exceed six years and is typically destroyed as it becomes economically unviable. In 2012 in the McLaren Vale and Barossa Valley viticulture regions of South Australia, entire blocks of Shiraz vines grafted on to GVA positive Chardonnay were removed six years after grafting due to lack of productivity (N. Habili, unpublished). It is estimated that the cost of removing virus infected vines and replanting in Australia is around AU$70,000 ha^{-1} [7].

8. Management of Shiraz Disease and Grapevine Leafroll Disease in Australian Vineyards

Virus-infected grapevines serve as inoculum for vector-based spreading of viruses in vineyards. Inaction will likely result in the spread of viruses within and between vineyard blocks resulting in larger pools of inoculum, much like fungal diseases that are better known to viticulturists. Atallah and co-workers modelled the spread of disease within and between blocks and found that costs of managing the disease are overestimated when only inter-block spatial dynamics, e.g., virus transmission from neighbouring vineyards via vectors, compared to when the effects of within-block disease spread are additionally considered [92]. Several mitigation strategies can be adopted, if grapevines develop visual symptoms of virus infection, e.g., show restricted spring growth, leaf discoloration post-véraison, or cupping of leaf margins. An integrated approach will undoubtedly be the most effective strategy in dealing with any epidemic. The following three-pronged approach has been shown to be highly effective in controlling viruses in South African and New Zealand vineyards [25]: (i) eliminating potential vectors of grapevine viruses such as mealybugs and scale insects to prevent additional spread of the viruses across vineyard blocks [93]; (ii) rogueing infected vines based on *both* visual symptoms and confirmation with molecular diagnosis; and (iii) replanting with certified plant material from an established grapevine nursery with clean source blocks and good sanitation practices.

Routine scouting of vineyard blocks for both virus symptoms and potential vectors such as mealybugs and scale insects should be done to minimize disruption to vine productivity and reduce economic losses associated with virus-related diseases. A combination of systemic and contact insecticides to control mealybugs and scales, in particular at the early stage in the lifecycle, i.e., first and second instar nymphs, or the use of biological control agents, e.g., parasitoids and mating disruption (pheromone traps), can be effective in minimizing the spread of GVA and GLRaV-3 in vineyards [94]. The use of fungicides such as sulphur applied at high rates in vineyards for the chemical control of

powdery mildew (*Erysiphe necator*) may indirectly contribute to increases in virus vector populations via their negative effects on parasitoids [95].

GVA and GLRaV-3 have been detected in and transmitted by, amongst others, grapevine scale insects (*Parthenolecanium persicae*), which are the predominant scale species in Australian vineyards [96]. This scale species has an annual lifecycle (one generation per season). Eggs are typically laid early in the growing season between bud burst and flowering in Australian vineyards. The young crawlers inhabit the underside of leaves moving onto the woody structures of the vine later in the season. Due to the high activity levels (feeding, movement) of juvenile scale insects, it is more critical to control them upon emergence compared to the more sedentary adults. Scale control includes using petroleum-based oil sprays, biological control agents, and broad-spectrum insecticides. Petroleum-based oil sprays are effective in reducing scale populations and have less negative effects on beneficial insects as compared to conventional broad-spectrum insecticides [97].

It is now well-documented that mealybugs are a primary vector of GLRaV-3 [28,98] and GVA [23] (Table 2); hence, mealybug control is of vital importance in any management strategy of viruses in vineyards. Mealybug control in vineyards has been effective using insecticides based on buprofezin or organophosphate chemistries early in the growing season, prior to flowering [99,100]. Removal of bark (bark stripping) prior to the application of sprays will increase the efficacy of contact insecticides due to better penetration into the bark where mealybugs often overwinter. Since crawlers are active and potentially effective in spreading viruses, spraying contact insecticides that coincide with their emergence is an appropriate approach. Insecticide application when more than 15 mealybugs per trap are collected has been recommended in South Africa [101].

As part of any vector management strategy, vineyard hygiene practices including cleaning vineyard equipment and removing dead leaves that can harbor mealybugs and destroying ant nests should be implemented. Observing the patterns of potential virus infection within a block can often provide clues on the source of the virus and mode of spread. Infections at or around points of entry into a vineyard suggest the possible role of humans and/or equipment in aiding the spread of vectors.

Roguing and Replanting

Rogueing and replanting is usually the last resort to deal with any virus infections in a vineyard and less than desirable since it makes vine management more challenging with vines of different ages that also affects the overall quality of the crop [102]. This technique has, however, shown to be highly effective in South Africa where the incidence of GLD in a 41 ha vineyard decreased from 100% (fully infected) to 0.027% over 10 years [98].

In an established vineyard, routine scouting for virus symptoms both early and late in the growing season is critical for effective management of any potential infection. Restricted shoot growth in the spring shortly after bud burst is typical in SD vines (Figure 1b); however, since this symptom can be mistaken for other conditions, appropriate diagnosis is required. GLD-infected vines do not typically display restricted shoot growth and only begin to show symptoms of curling leaf margins and reddening around or shortly after véraison. Vines that show any indications of virus-like infection should be flagged for testing using a molecular assay prior to rogueing. Using a spatial bioeconomic model to determine the optimum rogueing strategy in a leafroll-infected vineyard was recommended to rogue symptomatic vines. Their non-symptomatic neighbours should only be rogued when tested positive for virus. This strategy increased net present value (NPV) by 18-19% compared to no intervention [103].

When establishing a new vineyard, or replanting rogued vines, it is essential to use only clean, certified, and virus-tested planting material as no cure for virus-infected vines currently exists once they are established in a vineyard [93]. In many countries, including Australia, certified planting material is available through established and reputable grapevine nurseries that practice good hygiene, conduct regular virus testing of their source blocks, and routinely scout for viruses and their vectors. Nurseries that use shoot tip cultures to propagate and establish their clean mother blocks are generally reliable sources of virus-free material. Routine virus-testing of mother blocks should also be conducted by vine improvement groups and grapevine nurseries.

9. Observations of Shiraz Disease in South Australian Vineyards

Over several seasons, observations of mature (established) grapevines indicated consistent patterns of SD expression in regional vineyards across South Australia, the state with the largest winegrape area in Australia (76,292 ha, approx. 52% of Australian winegrape plantings; National Wine Scan, Wine Australia 2019 https://www.wineaustralia.com/market-insights/national-vineyard-scan-2018). These symptoms vary based on phenological stage, environmental conditions, as well as cultivar. In this section, we provide specific regional examples of SD and the symptoms elicited.

Early in the growing season, SD-infected grapevines typically have delayed budburst relative to healthy (non-SD infected grapevines, Figure 5a–c). This delay has been observed to range from several days to one week. Infrequently, in mature blocks where the virus is more established, buds do not burst resulting in a lack of shoot formation and crop and consequent vine decline, as observed in some Riverland vineyards (Figure 5a,c). In the same Riverland vineyard, an uninfected Shiraz grapevine planted next to a GVA-infected stump tested positive two years after planting (Figure 5d).

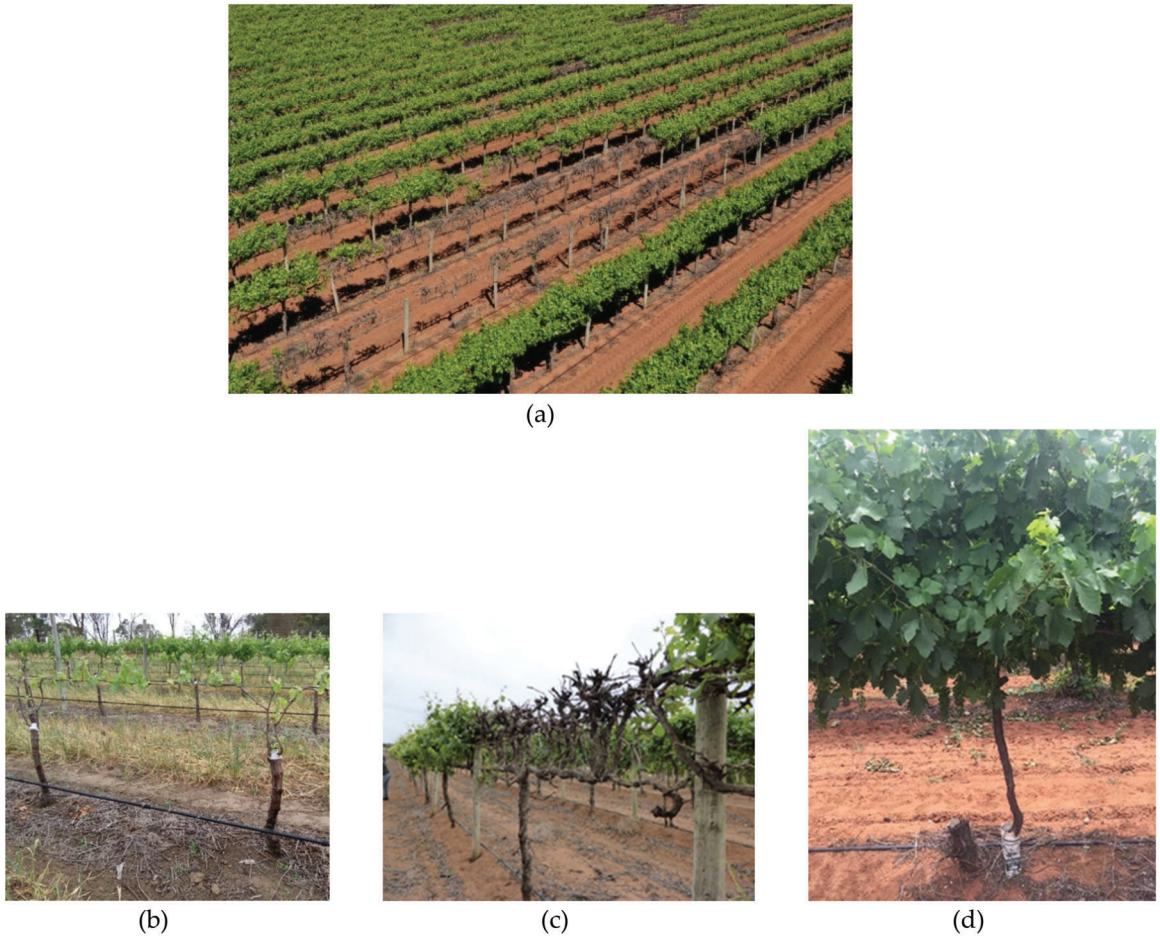

Figure 5. SD-infected grapevines in Australian vineyards. (**a**) Aerial view of a Riverland (South Australia) Shiraz vineyard showing prevalence of Shiraz disease: declining or dead vines with few or no leaves associated with GVA compared to symptomless GVA-infected Chardonnay (two rows on the right); (**b**) Malbec grapevines in a Langhorne Creek (South Australia) vineyard showing typical SD symptoms of restricted spring shoot growth; (**c**) same Shiraz block showing dieback associated with both SD and fungal trunk diseases; (**d**) Shiraz grapevine planted next to a stump, which tested positive for GVA two years later.

These vines were subsequently tested and found to be positive for GVA and occasionally GLRaV-3 (Table 4). Vine decline related to SD has only been observed in warmer viticultural regions of South

Australia, e.g., Riverland. A complicating factor to the SD story was the discovery of *Diplodia serratia*, a member of *Botryosphaeridae* in the SD affected vines that showed decline in the Riverland, South Australia (Figure 5a). Sequencing of the PCR products using Internal Transcribed Spacer (ITS1, ITS4) primers confirmed the association of this fungus with vine decline. The sequence showed 99% homology with the fungus isolate present in vineyards of southern Spain (accession number: MG745835). Based on this finding, we hypothesise that GVA increases the vulnerability of the vines to fungal pathogen infections. In the same Riverland vineyard (Figure 5a), all the non-SD vines tested positive for *Diplodia* and yet no vine decline was observed, which supports our virus-fungus co-infection hypothesis (N. Habili, unpublished). The cultivar specificity of SD was observed in the same vineyard: adjacent rows of Chardonnay grapevines tested positive for GVA and occasionally for GLRaV-3 but did not show vine decline (Figure 5a, two rows on right). A survey of potential vectors in this "hot spot" of Shiraz and Chardonnay grapevines revealed the presence of mealybugs and grapevine scale that would likely have vectored the viruses.

In vines that had successful budburst, SD infections typically resulted in restricted (or retarded) shoot growth during early stages of vine development. We observed retarded shoot growth symptoms in vineyards in Riverland, McLaren Vale, and Langhorne Creek regions (Figure 5b,c). Shoot growth tends to be retarded when budburst is delayed. This could be a consequence of SD stress-induced reduction in carbohydrate accumulation during bud development resulting from SD. Virus testing of Malbec vines in the Langhorne Creek vineyard confirmed the presence of GVA and GRSPaV. GRSPaV is present in most grapevines worldwide [104] and has been reported to have little or no negative effects on vine productivity [105]. Similar symptoms were observed in an adjacent block planted with Malbec that was previously top-worked onto GVA-infected Chardonnay grapevines confirming that the virus is graft transmissible.

In summary, our observations of SD in Australian vineyards indicate that the disease has the potential to cause vine decline manifested in delayed or no bud burst, retarded shoot development, and low or no crop. SD appears to be cultivar specific, with Shiraz and Malbec showing typical SD symptoms. Other red-berried cultivars such as Gamay, Merlot and Sumoll are also known to show SD symptoms, while Cabernet Sauvignon does not despite specific clones, e.g., SA125 and Reynella, that are infected with GVA.

10. Conclusions and Future Work

GVA and GLRaV-3 pose an ongoing threat to Australian vineyards due to their negative consequences on vine vigour, yield, and economic returns to the grower. In a few extreme cases, vineyards experienced yield losses of up to 98%, underscoring the importance of improving our understanding of these viruses; their source; methods of spread; potential vectors and their control; differences in cultivar susceptibility; and, most importantly, the specific interaction between the virus species on grapevine productivity. Systematic research needs to be undertaken to shed light on these open questions and to determine the long-term implications of virus-infected blocks including developing the best strategies to maintain their viability. Advances in proximal and remote sensing technologies provide opportunities for non-destructive detection of virus-infected grapevines [106,107] in a cost-effective manner and on a large spatial scale via airborne platforms [108]. Initial detection using these techniques should be followed by traditional or novel molecular-based testing such as HTS for confirmation of the virus infection. Search for novel viruses, for example, the negative sense RNA viruses of *Bunyavirales* [109], should continue using HTS. Effective virus management in vineyards begins with recognizing virus symptoms, early detection and confirmation, vector control, and rogueing and replanting infected vines with certified material. These management practices have proved effective in several major viticultural regions around the world, and Australian grape growers would be well served to adopt such an approach.

Author Contributions: Writing—original draft preparation, V.P., Q.W. and N.H.; writing—review and editing, V.P., Q.W., F.C., M.A.R., D.E.G. and N.H.; data and photos, V.P., Q.W., Y.W., F.C. and N.H. All authors have read and agreed to the published version of the manuscript.

Funding: This research received no external funding. The APC was funded by contributions from the authors and their affiliate organizations.

Conflicts of Interest: The authors declare no conflicts of interest.

References

1. Fuchs, M. Grapevine viruses: A multitude of diverse species with simple but overall poorly adopted management solutions in the vineyard. *J. Plant Pathol.* **2020**. [CrossRef]
2. Du Preez, J.; Stephan, D.; Mawassi, M.; Burger, J.T. The grapevine-infecting vitiviruses, with particular reference to grapevine virus A. *Arch. Virol.* **2011**, *156*, 1495–1503. [CrossRef] [PubMed]
3. Constable, F.E.; Nicholas, P.; Rodoni, B.C. *Development and Validation of Diagnostic Protocols for the Detection of Endemic and Exotic Pathogens of Grapevines*; Final Report to Grape and Wine Research & Development Corporation; Wine Australia: Adelaide, Australia, 2010; p. 283. Available online: http://www.gwrdc.com.au/wp-content/uploads/2012/09/DPI-05-04.pdf (accessed on 14 May 2020).
4. Constable, F.; Tassie, E.; McLoughlin, S. A Comprehensive Review of Grapevine Pinot Gris Virus (GPGV). Final Report to Wine Australia; Project No. VHA 1701; 2019. Available online: https://www.wineaustralia.com/getmedia/62a813e4-b27f-4a27-a32e-9b75c2c23103/VHA-1701-FINAL-REPORT.pdf (accessed on 23 June 2020).
5. IPPC. Official Pest Reports—Australia (2015-06-25) Absence of Grapevine Fanleaf Virus from Australia. Available online: https://www.ippc.int/en/countries/australia/pestreports/2015/06/absence-of-grapevine-fanleaf-virus-from-australia/ (accessed on 10 July 2020).
6. Meng, B.; Martelli, G.P.; Golino, D.; Fuchs, M. *Grapevine Viruses: Molecular Biology, Diagnostics and Management*; Springer: Cham, Switzerland, 2017; p. 698.
7. Habili, N.; Wu, Q.; Pagay, V. Virus-associated Shiraz Disease may lead Shiraz to become an endangered variety in Australia. *Wine Vitic. J.* **2016**, *31*, 47–50.
8. Alabi, O.J.; Casassa, F.; Gutha, L.R.; Larsen, R.C.; Henick-Kling, T.; Harbertson, J.F.; Naidu, R.A. Impacts of grapevine leafroll disease on fruit yield and grape and wine chemistry in a wine grape (*Vitis vinifera* L.) cultivar. *PLoS ONE* **2016**, *11*. [CrossRef] [PubMed]
9. Goszczynski, D.E.; Habili, N. Grapevine virus A variants of group II associated with Shiraz disease in South Africa are present in plants affected by Australian Shiraz disease, and have also been detected in the USA. *Plant Pathol.* **2012**, *61*, 205–214. [CrossRef]
10. Corbett, M.K.; Wiid, J. Closterovirus-like particles in extracts from diseased grapevines. In Proceedings of the 8th Meeting of the International Council for the study of Viruses and Virus Diseases of the Grapevine, Bari, Italy, 3–7 September 1984; pp. 91–100.
11. Goszczynski, D.E.; Jooste, A.E.C. Identification of divergent variants of Grapevine virus A. *Eur. J. Plant Pathol.* **2003**, *109*, 397–403. [CrossRef]
12. Habili, N. Australian Shiraz Disease: An emerging virus disease of *Vitis vinifera* cv. Shiraz. *Wine Vitic. J.* **2013**, *28*, 59–61.
13. Grenan, S.; Renault-Spilmont, A.S.; Boursiquot, J.-M. Syrah decline in France: Historical background and first approaches. In Proceedings of the Syrah Vine Health Symposium, University of California, Davis, CA, USA, 6 November 2007; p. 3.
14. Puckett, J.M.; Dangl, G.; Golino, D.; Al Rwahnih, M. Evidence to support Syrah Decline is a non-infectious genetic syndrome in several Syrah selections. In Proceedings of the 19th Congress of ICVG, Santiago, Chile, 9–12 April 2018; pp. 78–79.
15. Constable, F.; Drew, C. Review of vine health parameters, implementation priorities and capabilities for vine improvement groups and accredited nurseries. In *Final Report to the Grape and Wine Research & Development Corporation*; Project number NVH 03/01; Scholefield Robinson Horticultural Services Pty. Ltd.: Adelaide, Australia, 2004; p. 105. Available online: https://www.wineaustralia.com/getmedia/0807646b-1fb9-4cfd-80df-61b96d76809d/NVH-03-01 (accessed on 12 January 2020).

16. Martin, R.R.; Constable, F.; Tzanetakis, I.E. Quarantine regulations and the impact of modern detection methods. *Ann. Rev. Phytopathol.* **2016**, *54*, 189–205. [CrossRef]
17. Rakimov, A.; Ben-Dov, Y.; White, V.; Hoffmann, A.A. Soft scale insects (Hemiptera: Coccoidea: Coccidae) on grapevines in Australia. *Aust. J. Entomol.* **2013**, *52*, 371–378. [CrossRef]
18. PGIBSA. *A Growers' Guide to Top.-Working Grapevines*; Phylloxera and Grape Industry Board of South Australia: Adelaide, SA, Australia, 2004; p. 20.
19. Tsai, C.W.; Chau, J.; Fernandez, L.; Bosco, D.; Daane, K.M.; Almeida, R.P.P. Transmission of Grapevine leafroll-associated virus 3 by the vine mealybug (*Planococcus ficus*). *Phytopathology* **2008**, *98*, 1093–1098. [CrossRef]
20. Krueger, K.; Douglas-Smit, N. Grapevine leafroll-associated virus 3 (GLRaV-3) transmission by three soft scale insect species (Hemiptera: Coccidae) with notes on their biology. *Afr. Entomol.* **2013**, *21*, 1–8. [CrossRef]
21. Golino, D.; Sim, S.; Gill, R.; Rowhani, A. California mealybugs can spread grapevine leafroll disease. *Calif. Agric.* **2002**, *56*, 196–201. [CrossRef]
22. La Notte, P.; Buzkan, N.; Choueiri, E.; Minafra, A.; Martelli, G.P. Acquisition and transmission of grapevine virus A by the mealybug *Pseudococcus longispinus*. *J. Plant Pathol.* **1997**, *79*, 79–85.
23. Rosciglione, B.; Castellano, M.A.; Martelli, G.P.; Savino, V.; Cannizzaro, G. Mealybug transmission of Grapevine Virus-A. *Vitis* **1983**, *22*, 331–347.
24. Naidu, R.; Rowhani, A.; Fuchs, M.; Golino, D.; Martelli, G.P. Grapevine leafroll: A complex viral disease affecting a high-value fruit crop. *Plant Dis.* **2014**, *98*, 1172–1185. [CrossRef]
25. Almeida, R.P.P.; Daane, K.M.; Bell, V.A.; Blaisdell, G.K.; Cooper, M.L.; Herrbach, E.; Pietersen, G. Ecology and management of grapevine leafroll disease. *Front. Microbiol.* **2013**, *4*, 94. [CrossRef]
26. Le Maguet, J.; Fuchs, J.J.; Chadoeuf, J.; Beuve, M.; Herrbach, E.; Lemaire, O. The role of the mealybug *Phenacoccus aceris* in the spread of Grapevine leafroll-associated virus-1 (GLRaV-1) in two French vineyards. *Eur. J. Plant Pathol.* **2013**, *135*, 415–427. [CrossRef]
27. Habili, N.; Nutter, F.W., Jr. Temporal and spatial analysis of grapevine leafroll-associated virus 3 in Pinot Noir grapevines in Australia. *Plant Dis.* **1997**, *81*, 625–628. [CrossRef]
28. Herrbach, E.; Alliaume, A.; Prator, C.A.; Daane, K.M.; Cooper, M.L.; Almeida, R.P.P. Vector transmission of grapevine leafroll-associated viruses. In *Grapevine Viruses: Molecular Biology, Diagnostics and Management*; Meng, B., Martelli, G.P., Golino, D.A., Fuchs, M., Eds.; Springer: Cham, Switzerland, 2017; pp. 483–503.
29. Wistrom, C.M.; Blaisdell, G.K.; Wunderlich, L.R.; Almeida, R.P.P.; Daane, K.M. *Ferrisia gilli* Gullan (Hemiptera: Pseudococcidae) transmits grapevine leafroll associated viruses. *J. Econ. Entomol.* **2016**, *109*, 1519–1523. [CrossRef]
30. Bertin, S.; Cavalieri, V.; Gribaudo, I.; Sacco, D.; Marzachi, C.; Bosco, D. Transmission of Grapevine virus A and Grapevine leafroll-associated virus 1 and 3 by *Heliococcus bohemicus* (Hemiptera: Pseudococcidae) nymphs from plants with mixed infections. *J. Econ. Entomol.* **2016**, *109*, 1504–1511. [CrossRef]
31. Bertin, S.; Pacifico, D.; Cavalieri, V.; Marzachi, C.; Bosco, D. Transmission of Grapevine virus A and Grapevine leafroll-associated viruses 1 and 3 by *Planococcus ficus* and *Planococcus citri* fed on mixed-infected plants. *Ann. Appl. Biol.* **2016**, *169*, 53–63. [CrossRef]
32. Sforza, R.; Boudon-Padieu, E.; Greif, C. New mealybug species vectoring Grapevine leafroll-associated viruses-1 and-3 (GLRaV-1 and-3). *Eur. J. Plant Pathol.* **2003**, *109*, 975–981. [CrossRef]
33. Zorloni, A.; Prati, S.; Bianco, P.A.; Belli, G. Transmission of Grapevine virus A and Grapevine leafroll-associated virus 3 by *Heliococcus bohemicus*. *J. Plant Pathol.* **2006**, *88*, 325–328.
34. Le Maguet, J.; Beuve, M.; Herrbach, E.; Lemaire, O. Transmission of six ampeloviruses and two vitiviruses to grapevine by *Phenacoccus aceris*. *Phytopathology* **2012**, *102*, 717–723. [CrossRef]
35. Cabaleiro, C.; Segura, A. Some characteristics of the transmission of grapevine leafroll associated virus 3 by *Planococcus citri* Risso. *Eur. J. Plant Pathol.* **1997**, *103*, 373–378. [CrossRef]
36. Cabaleiro, C.; Segura, A. Field transmission of grapevine leafroll associated virus 3 (GLRaV-3) by the mealybug *Planococcus citri*. *Plant Dis.* **1997**, *81*, 283–287. [CrossRef]
37. Mahfoudhi, N.; Digiaro, M.; Dhouibi, M.H. Transmission of grapevine leafroll viruses by *Planococcus ficus* (Hemiptera: Pseudococcidae) and *Ceroplastes rusci* (Hemiptera: Coccidae). *Plant Dis.* **2009**, *93*, 999–1002. [CrossRef]
38. Engelbrecht, D.; Kasdorf, G. Transmission of grapevine leafroll disease and associated closteroviruses by the vine mealybug, *Planococcus ficus*. *Phytophylactica* **1990**, *22*, 341–346.

39. Garau, R.; Prota, V.A.; Boscia, D.; Fiori, M.; Prota, U. *Pseudococcus affinis* mask, a new vector of grapevine Trichovirus-A and Triochovirus-B. *Vitis* **1995**, *34*, 67–68.
40. Nakaune, R.; Toda, S.; Mochizuki, M.; Nakano, M. Identification and characterization of a new vitivirus from grapevine. *Arch. Virol.* **2008**, *153*, 1827–1832. [CrossRef]
41. Fuchs, M.; Marsella-Herrick, P.; Loeb, G.M.; Martinson, T.E.; Hoch, H.C. Diversity of ampeloviruses in mealybug and soft scale vectors and in grapevine hosts from leafroll-affected vineyards. *Phytopathology* **2009**, *99*, 1177–1184. [CrossRef] [PubMed]
42. Petersen, C.L.; Charles, J.G. Transmission of grapevine leafroll-associated closteroviruses by *Pseudococcus longispinus* and *P. calceolariae*. *Plant Pathol.* **1997**, *46*, 509–515. [CrossRef]
43. Douglas, N.; Kruger, K. Transmission efficiency of Grapevine leafroll-associated virus 3 (GLRaV-3) by the mealybugs *Planococcus ficus* and *Pseudococcus longispinus* (Hemiptera: Pseudococcidae). *Eur. J. Plant Pathol.* **2008**, *122*, 207–212. [CrossRef]
44. Ng, J.C.K.; Zhou, J.S. Insect vector-plant virus interactions associated with non-circulative, semi-persistent transmission: Current perspectives and future challenges. *Curr. Opin. Virol.* **2015**, *15*, 48–55. [CrossRef]
45. Zhou, J.S.; Drucker, M.; Ng, J.C.K. Direct and indirect influences of virus-insect vector-plant interactions on non-circulative, semi-persistent virus transmission. *Curr. Opin. Virol.* **2018**, *33*, 129–136. [CrossRef] [PubMed]
46. Tsai, C.W.; Rowhani, A.; Golino, D.A.; Daane, K.M.; Almeida, R.P.P. Mealybug transmission of grapevine leafroll viruses: An analysis of virus-vector specificity. *Phytopathology* **2010**, *100*, 830–834. [CrossRef]
47. Blaisdell, G.K.; Zhang, S.; Rowhani, A.; Klassen, V.; Cooper, M.L.; Daane, K.M.; Almeida, R.P.P. Trends in vector-borne transmission efficiency from coinfected hosts: Grapevine leafroll-associated virus-3 and Grapevine Virus. A. *Eur. J. Plant Pathol.* **2020**, *156*, 1163–1167. [CrossRef]
48. Hommay, G.; Komar, V.; Lemaire, O.; Herrbach, E. Grapevine virus A transmission by larvae of *Parthenolecanium corni*. *Eur. J. Plant Pathol.* **2008**, *121*, 185–188. [CrossRef]
49. Daane, K.M.; Almeida, R.P.P.; Bell, V.A.; Walker, J.T.S.; Botton, M.; Fallahzadeh, M.; Mani, M.; Miano, J.L.; Sforza, R.; Walton, V.M.; et al. Biology and management of mealybugs in vineyards. In *Arthropod Management in Vineyards: Pests, Approaches, and Future Directions*; Bostanian, N.J., Vincent, C., Isaacs, R., Eds.; Springer: Dordrecht, The Netherlands, 2012; pp. 271–307. [CrossRef]
50. Gutierrez, A.P.; Daane, K.M.; Ponti, L.; Walton, V.M.; Ellis, C.K. Prospective evaluation of the biological control of vine mealybug: Refuge effects and climate. *J. Appl. Ecol.* **2008**, *45*, 524–536. [CrossRef]
51. Burger, J.T.; Maree, H.J.; Gouveia, P.; Naidu, R.A. Grapevine leafroll-associated virus3. In *Grapevine Viruses: Molecular Biology, Diagnostics and Management*; Meng, B., Martelli, G.P., Golino, D.A., Fuchs, M., Eds.; Springer: Cham, Switzerland, 2017; pp. 167–195.
52. Tanne, E.; Ben-Dov, Y.; Raccah, B.; Dov, Y.B. Transmission of the corky-bark disease by the mealybug *Planococcus ficus*. *Phytoparasitica* **1989**, *17*, 55. [CrossRef]
53. Barras, I.C.; Jerie, P.; Ward, S.A. Aerial dispersal of first- and second-instar longtailed mealybug, *Pseudococcus longispinus* (Targioni-Tozzetti) (Pseudococcidae: Hemiptera). *Aust. J. Exp. Agric.* **1994**, *34*, 1205–1208. [CrossRef]
54. Hommay, G.; Wiss, L.; Chadoeuf, J.; Maguet, J.l.; Beuve, M.; Herrbach, E.; Le Maguet, J. Gone with the wind: Aerial dispersal of *Parthenolecanium corni* crawlers in a newly planted grapevine plot. *Ann. Appl. Biol.* **2019**, *174*, 372–387. [CrossRef]
55. Habili, N.; Kominek, P.; Little, A. Grapevine leafroll-associated virus 1 as a common grapevine pathogen. *Plant Viruses* **2007**, *1*, 63–68.
56. Hayes, A.; Neeman, T.; Cooper, P.D. Overwintering survival of grapevine scale *Parthenolecanium persicae* (Hemiptera: Coccidae) in the Canberra region of Australia. *Aust. Entomol.* **2019**, *58*, 346–353. [CrossRef]
57. Simbiken, N.A. Feeding and Ecology of Grapevine Scales, *Parthenolecanium Persicae* and *P. pruinosum*, on Different Varieties of Grapevine. Master's Thesis, Australian National University, Canberra, Australia, 2014.
58. Simbiken, N.A. Development and feeding effect of frosted scale *Parthenolecanium pruinosum* Cocquillet (Hemiptera: Coccidae) on selected *Vitis vinifera* L. cultivars. *Aust. J. Grape Wine Res.* **2015**, *21*, 451–457. [CrossRef]

59. Habili, N.; Wu, Q. Simultaneous Transmission of Grapevine Leafroll-Assocaited Virus 3 and Grapevine Virus A by the Scale Insect Parthenolecanium persicae in Australia 2015; Report number: 20151225.3890790. Available online: http://www.promedmail.org/post/3890790 (accessed on 23 May 2020).
60. Belli, G.; Fortusini, A.; Casati, P.; Belli, L.; Bianco, P.A.; Prati, S. Transmission of a grapevine leafroll associated closterovirus by the scale insect *Pulvinaria vitis* L. *Riv. Di Patol. Veg.* **1994**, *4*, 105–108.
61. Fuchs, M.; Martinson, T.E.; Loeb, G.M.; Hoch, H.C. Survey for the three major leafroll disease-associated viruses in Finger Lakes vineyards in New York. *Plant Dis.* **2009**, *93*, 395–401. [CrossRef]
62. Predajna, L.; Glasa, M. Partial Sequence Analysis of Geographically Close Grapevine virus A Isolates Reveals their High Regional Variability and an Intra-Isolate Heterogeneity. *J. Phytopathol.* **2016**, *164*, 427–431. [CrossRef]
63. Glasa, M.; Predajna, L.; Soltys, K.; Sihelska, N.; Nagyova, A.; Wetzel, T.; Sabanadzovic, S. Analysis of Grapevine rupestris stem pitting-associated virus in Slovakia reveals differences in intra-host population diversity and naturally occurring recombination events. *Plant Pathol. J.* **2017**, *33*, 34–42. [CrossRef]
64. Hily, J.M.; Beuve, M.; Vigne, E.; Demangeat, G.; Candresse, T.; Lemaire, O. A genome-wide diversity study of grapevine rupestris stem pitting-associated virus. *Arch. Virol.* **2018**, *163*, 3105–3111. [CrossRef]
65. Puckett, J.M.; Al Rwahnih, M.; Klassen, V.; Golino, D. The Davis grapevine virus collection—A current perspective. Proceedings of 19th Congress of ICVG, Santiago, Chile, 9–12 April 2018.
66. Krake, L.R.; Scott, N.S.; Rezaian, M.A.; Taylor, R.H. *Graft-Transmitted Diseases of Grapevines*; CSIRO Publishing: Melbourne, Australia, 1999.
67. Martelli, G.P. Directory of virus and virus-like diseases of the grapevine and their agents. *J. Plant Pathol.* **2014**, *96*, 1–136.
68. Constable, F.E.; Connellan, J.; Nicholas, P.; Rodoni, B.C. Comparison of enzyme-linked immunosorbent assays and reverse transcription-polymerase chain reaction for the reliable detection of Australian grapevine viruses in two climates during three growing seasons. *Aust. J. Grape Wine Res.* **2012**, *18*, 239–244. [CrossRef]
69. Naidu, R.A.; Maree, H.J.; Burger, J.T. Grapevine leafroll disease and associated viruses: A unique pathosystem. *Annu. Rev. Phytopathol.* **2015**, *53*, 613–634. [CrossRef]
70. Habili, N.; Randles, J.W. Descriptors for Grapevine virus A-associated syndrome in Shiraz, Merlot and Ruby Cabernet in Australia, and its similarity to Shiraz Disease in South Africa. *Aust. New Zealand Grapegrow. Winemak.* **2004**, *488*, 71–74.
71. Goszczynski, D.E.; du Preez, J.; Burger, J.T. Molecular divergence of Grapevine virus A (GVA) variants associated with Shiraz disease in South Africa. *Virus Res.* **2008**, *138*, 105–110. [CrossRef] [PubMed]
72. Saldarelli, P.; Giampetruzzi, A.; Maree, H.J.; Al Rwahnih, M. High-Throughput Sequencing: Advantages beyond virus identification. In *Grapevine Viruses: Molecular Biology, Diagnostics and Management*; Meng, B., Martelli, G.P., Golino, D.A., Fuchs, M., Eds.; Springer: Cham, Switzerland, 2017; pp. 625–642.
73. Maree, H.J.; Almeida, R.P.P.; Bester, R.; Chooi, K.; Cohen, D.; Dolja, V.V.; Fuchs, M.F.; Golino, D.A.; Jooste, A.E.C.; Martelli, G.P.; et al. Grapevine leafroll-associated virus 3. *Front. Microbiol.* **2013**, *4*, 82. [CrossRef] [PubMed]
74. Diaz-Lara, A.; Klaassen, V.; Stevens, K.; Sudarshana, M.R.; Rowhani, A.; Maree, H.J.; Chooi, K.M.; Blouin, A.G.; Habili, N.; Song, Y.; et al. Characterization of grapevine leafroll-associated virus 3 genetic variants and application towards RT-qPCR assay design. *PLoS ONE* **2018**, *13*, e208862. [CrossRef] [PubMed]
75. Endeshaw, S.T.; Sabbatini, P.; Romanazzi, G.; Schilder, A.C.; Neri, D. Effects of grapevine leafroll associated virus 3 infection on growth, leaf gas exchange, yield and basic fruit chemistry of *Vitis vinifera* L. cv. Cabernet Franc. *Sci. Hortic.* **2014**, *170*, 228–236. [CrossRef]
76. Martinson, T.E.; Fuchs, M.; Loeb, G.; Hoch, H.C. Grapevine leafroll: An increasing problem in the Finger Lakes, the US and the world. *Finger Lakes Vineyard Notes* **2008**, *6*, 6–11.
77. Guidoni, S.; Mannini, F.; Ferrandino, A.; Argamante, N.; Di Stefano, R. Effect of virus status on leaf and berry phenolic compounds in two wine grapevine vitis vinifera cultivars. *Acta Hortic.* **2000**, 445–452. [CrossRef]
78. Komar, V.; Vigne, E.; Demangeat, G.; Lemaire, O.; Fuchs, M. Comparative performance of virus-infected *Vitis vinifera* cv. Savagnin rose grafted onto three rootstocks. *Am. J. Enol. Vitic.* **2010**, *61*, 68–73.
79. Kovacs, L.G.; Hanami, H.; Fortenberry, M.; Kaps, M.L. Latent infection by leafroll agent GLRaV-3 is linked to lower fruit quality in French-American hybrid grapevines Vidal blanc and St Vincent. *Am. J. Enol. Vitic.* **2001**, *52*, 254–259.

80. Lee, J.M.; Martin, R.R. Influence of grapevine leafroll associated viruses (GLRaV-2 and -3) on the fruit composition of Oregon *Vitis vinifera* L. cv. Pinot noir: Phenolics. *Food Chem.* **2009**, *112*, 889–896. [CrossRef]
81. Tomazic, I.; Korosec-Koruza, Z.; Petrovic, N. Sanitary status of Slovenian indigenous grapevine cultivar refosk. *J. Int. Sci. Vigne Vin.* **2005**, *39*, 19–22. [CrossRef]
82. Credi, R.; Babini, A.R. Effect of virus and virus-like infections on the growth of grapevine rootstocks. *Adv. Hortic. Sci.* **1996**, *10*, 95–98.
83. Vega, A.; Gutierrez, R.A.; Pena-Neira, A.; Cramer, G.R.; Arce-Johnson, P. Compatible GLRaV-3 viral infections affect berry ripening decreasing sugar accumulation and anthocyanin biosynthesis in *Vitis vinifera*. *Plant Mol. Biol.* **2011**, *77*, 261–274. [CrossRef]
84. Flamini, R.; Vedova, A.D.; Panighel, A.; Biscaro, S.; Borgo, M.; Calo, A. Characterization of Torbato (*V. vinifera*) aroma and study of leaf-roll effects on the grape aroma compounds Caratterizzazione aromatica del Torbato (*V. vinifera*) e studio degli effetti dell'accartocciamento fogliare sui composti aromatici delle sue uve. *Riv. Vitic. Enol.* **2006**, *59*, 13–26.
85. Bertamini, M.; Malossini, U.; Krishnasamy, M.; Namachevayam, N.; Muthuchelian, K.; Nedunchezhian, N. Physiological response of field grown grapevine (*Vitis vinifera* L. cv. Marzemino) to grapevine leafroll-associated virus (GLRaV-1). *Phytopathol. Mediterr.* **2005**, *44*, 256–265.
86. Clingeleffer, P.R.; Krake, L.R. Light (minimal) pruning enhances expression of higher yield from clones of *Vitis vinifera* L cv Sultana following thermotherapy for virus attenuation. *Aust. J. Grape Wine Res.* **2002**, *8*, 95–100. [CrossRef]
87. Brar, H.S.; Zora, S.; Swinny, E.; Cameron, I.; Singh, Z. Girdling and grapevine leafroll associated viruses affect berry weight, colour development and accumulation of anthocyanins in 'Crimson Seedless' grapes during maturation and ripening. *Plant Sci.* **2008**, *175*, 885–897. [CrossRef]
88. Cameron, I.J. Emperor clonal selection and the effect of leafroll virus on table grape quality. In *Proceedings of the First Table Grape Industry Technical Conference*; Department of Agriculture: Mildura, VIC, Australia, 1984; pp. 43–47.
89. Van Leeuwen, C.; Darriet, P. The impact of climate change on viticulture and wine quality. *J. Wine Econ.* **2016**, *11*, 150–167. [CrossRef]
90. Webb, L.B.; Whetton, P.H.; Bhend, J.; Darbyshire, R.; Briggs, P.R.; Barlow, E.W.R. Earlier wine-grape ripening driven by climatic warming and drying and management practices. *Nat. Clim. Chang.* **2012**, *2*, 259–264. [CrossRef]
91. Scholefield, P.; Morison, J. Assessment of Economic Cost of Endemic Pests and Diseases on the Australian Grape and Wine Industry; Final Report to the GWRDC, Project GWR 08/04; 2010. Available online: https://www.wineaustralia.com/getmedia/3ca22df5-54be-4c82-a711-bcf8d00ed698/GWR-08-04 (accessed on 24 June 2020).
92. Atallah, S.S.; Gomez, M.I.; Conrad, J.M. Specification of Spatial-Dynamic Externalities and Implications for Strategic Behavior in Disease Control. *Land Econ.* **2017**, *93*, 209–229. [CrossRef]
93. Naidu, R.A. Grapevine leafroll-associated virus 1. In *Grapevine Viruses: Molecular Biology, Diagnostics and Management*; Meng, B., Martelli, G.P., Golino, D.A., Fuchs, M., Eds.; Springer International Publishing: Cham, Switzerland, 2017; pp. 127–139. [CrossRef]
94. Lucchi, A.; Ricciardi, R.; Benelli, G.; Bagnoli, B. What do we really know on the harmfulness of *Cryptoblabes gnidiella* (Milliere) to grapevine? From ecology to pest management. *Phytoparasitica* **2019**, *47*, 1–15. [CrossRef]
95. Martinson, T.; Williams III, L.; English-Loeb, G. Compatibility of chemical disease and insect management practices used in New York vineyards with biological control by *Anagrus* spp. (Hymenoptera: Mymaridae), parasitoids of Erythroneura leafhoppers. *Biol. Control.* **2001**, *22*, 227–234. [CrossRef]
96. Rakimov, A.; Hoffmann, A.A.; Malipatil, M.B. Natural enemies of soft scale insects (Hemiptera: Coccoidea: Coccidae) in Australian vineyards. *Aust. J. Grape Wine Res.* **2015**, *21*, 302–310. [CrossRef]
97. Cotsaris, D.; Burne, P.; Pietsch, A. Vineyard Scale. In *CCW Factsheet No. 3.*; CCW Cooperative, Ltd.: Berri, SA, Australia, 2009; Available online: http://www.ccwcoop.com.au/__files/f/4381 (accessed on 12 September 2019).
98. Pietersen, G.; Spreeth, N.; Oosthuizen, T.; Rensburg, A.v.; Rensburg, M.v.; Lottering, D.; Rossouw, N.; Tooth, D.; van Rensburg, A.; van Rensburg, M. Control of grapevine leafroll disease spread at a commercial wine estate in South Africa: A case study. *Am. J. Enol. Vitic.* **2013**, *64*, 296–305. [CrossRef]
99. Daane, K.M.; Bentley, W.J.; Walton, V.; Malakar-Kuenen, R.; Millar, J.G.; Ingels, C.; Weber, E.; Gispert, C. New controls investigated for vine mealybug. *Calif. Agric.* **2006**, *60*, 31–38. [CrossRef]

100. Mani, M.; Shivaraju, C. *Mealybugs and Their Management in Agricultural and Horticultural Crops*; Springer: New Delhi, India, 2016.
101. Bonfiglioli, R.; Hoskins, N. Managing virus in New Zealand vineyards. *Aust. New Zealand Grapegrow. Winemak.* **2006**, *45*, 43–46.
102. Bell, V.A.; Hedderley, D.I.; Pietersen, G.; Lester, P.J. Vineyard-wide control of grapevine leafroll-associated virus 3 requires an integrated response. *J. Plant Pathol.* **2018**, *100*, 399–408. [CrossRef]
103. Atallah, S.S.; Gomez, M.I.; Conrad, J.M.; Nyrop, J.P. A plant-level, spatial, bioeconomic model of plant disease diffusion and control: Grapevine leafroll disease. *Am. J. Agric. Econ.* **2015**, *97*, 199–218. [CrossRef]
104. Meng, B.; Rowhani, A. Grapevine ruperstris stem pitting-associated virus. In *Grapevine Viruses: Molecular Biology, Diagnostics and Management*; Springer: Cham, Switzerland, 2017; pp. 257–287.
105. Reynolds, A.G.; Lanterman, W.S.; Wardle, D.A. Yield and berry composition of five Vitis cultivars as affected by rupestris stem pitting virus. *Am. J. Enol. Vitic.* **1997**, *48*, 449–458.
106. Naidu, R.A.; Perry, E.M.; Pierce, F.J.; Mekuria, T. The potential of spectral reflectance technique for the detection of Grapevine leafroll-associated virus-3 in two red-berried wine grape cultivars. *Comput. Electron. Agric.* **2009**, *66*, 38–45. [CrossRef]
107. Pagay, V.; Habili, N.; Wu, Q.; Coleman, D. Rapid and non-destructive detection of Shiraz Disease and Grapevine Leafroll Disease on asymptomatic grapevines in Australian vineyards. In Proceedings of the 19th Congress of ICVG, Santiago, Chile, 9–12 April 2018.
108. MacDonald, S.L.; Staid, M.; Staid, M.; Cooper, M.L. Remote hyperspectral imaging of grapevine leafroll-associated virus 3 in cabernet sauvignon vineyards. *Comput. Electron. Agric.* **2016**, *130*, 109–117. [CrossRef]
109. Diaz-Lara, A.; Navarro, B.; Di Serio, F.; Stevens, K.; Hwang, M.S.; Kohl, J.; Vu, S.T.; Falk, B.W.; Golino, D.; Al Rwahnih, M. Two novel negative-sense RNA viruses infecting grapevine are members of a newly proposed genus within the family *Phenuiviridae*. *Viruses* **2019**, *11*, 685. [CrossRef]

2. Research aims and theoretical framework

2.1. Project title: Molecular epidemiology and physiology of Shiraz Disease with an emphasis on Grapevine virus A.

To date, 93 viruses have been recorded worldwide to affect grapevines [9-11]. Virus infections and associated diseases can reduce grapevine performance, yield, and berry quality. In Australian vineyards, SD is one of the most severe virus diseases that is threatening Shiraz production and reducing wine quality. The disease may result in significant economic losses to the viticulture industry in Australia. Symptoms include restricted spring growth (RSG), un-lignified canes and late autumn leaf reddening. A similar disease also occurs in South Africa, and it has been claimed that SD has always been associated with grapevine virus A (GVA). The epidemiology of SD, intra-host diversity of GVA, and its impact on grapevine performance and wine composition will be addressed in this study.

2.2. Project summary

The aim of this project was to study the molecular epidemiology of SD under Australian conditions. SD affected and unaffected grapevines (non-SD) from three South Australian vineyards in the Barossa Valley (BV), Willunga (WIL), and Langhorne Creek (LC) were analysed using metagenomics and amplicon high-throughput sequencing (Meta- and amplicon-HTS) and bioinformatics to better understand the specific association between variants of GVA and symptom expressions. This project also aimed to evaluate the impact of SD on Shiraz grapevines in two of the South Australian vineyards, WIL and LC, by measuring several basic grapevine physiological parameters as well as monitoring canopy development and berry ripening. Here, it is worthwhile noting that no SD has been detected in the Barossa Valley vineyard. Mini-scale wine was made to study the effect of SD on wine composition.

2.3. Research questions

GVA has been proposed as the key pathogen of SD in Australia. However, GLRaVs that have been detected in some SD-affected grapevines were suspected to be involved in symptom development. Therefore, this research aimed to better understand the viral aetiology of SD:

- Does GVA by itself produce SD symptoms or are other GLRaVs viruses required?
- Is the genetic diversity of GVA important for symptom expression of SD?
- What is the impact of SD on grapevine physiology and berry fruit quality and wine composition?

2.4. Aims/Objectives of the project

The aim of this PhD thesis is to improve understanding of SD aetiology and measure the impact under warm Australian conditions.

2.5. Theoretical framework and methods.

The basis of this thesis was to provide evidence that SD has a viral origin. This can be achieved by four major domains, each described in a

separate chapter in this thesis. Meta-HTS was used to examine viromes of SD affected and non-SD grapevines (Chapter 2). A virus new to Australia that was discovered by Meta-HTS was published as a plant disease note (Chapter 6). Amplicon-HTS was employed to study intra-host genetic diversity and the potential evolutionary history of GVA associated with SD (Chapter 3). Several basic parameters of grapevine physiology and berry composition were measured to determine the impact of SD on berry quality and grapevine performance in two commercial vineyards (Chapter 4). Small scale wines were made from SD grapevines and non–SD controls. Juice and wine chemical parameters and wine aroma compounds were compared to address the impact of SD on wine characteristics (Chapter 5). A general conclusion was written in Chapter 7.

2.5.1. Meta-HTS (Chapter 2)

GVA infected Shiraz grapevines were sampled from three vineyards at Langhorne Creek (LC), Willunga (WIL) and Barossa Valley (BV). Asymptomatic (non-SD) and symptomatic (SD) grapevines were selected and tagged based on symptoms and detection by RT-PCR. The virus status of the selected grapevines was also tested by endpoint RT-PCR, targeting 10 viruses as well as a specific GVA variant (see Chapter 2). Fifty more samples from the three vineyards were sequenced by Meta-HTS using the validated extraction and pre-treatment method to study the virus status of the SD and non-SD grapevines as well as studying the potential infection source of the WIL site by analysing the sequencing data obtained from Meta-HTS. Results were validated by RT-PCR of the two major viruses GVA and GLRaV-3.

2.5.2. Amplicon HTS (Chapter 3)

Amplicon-HTS experiments aimed to study the diversity of virus populations in grapevines infected with GVA and showing different types of symptoms. Samples from LC and WIL showed typical SD symptoms while those from BV showed mild LRD symptoms. GVA was amplified from each of the grapevines by RT-PCR using three pairs of primers from the MP (ORFs 3), CP (ORFs 4) and RB (ORFs 5) genes and sequenced by the MiSeq platform with 301 bp paired-end reads. The raw reads were quality trimmed and clustered at 100% nucleotide identity. The major variant of each sample were determined by copy numbers and the relationship between variants were shown by median joining networks (MJNs). For each gene, the 20 variants with the largest sequence copy numbers of all samples from WIL, LC and BV were combined to construct a MJN to display the overall evolutionary history of GVA.

2.5.3. Grapevine physiological performance and berry composition (Chapter 4)

This part of the study aimed to evaluate how SD affects vine performance and grapevine berry composition. Canopy size (plant area indexing), and berry development of SD and non-SD grapevines were monitored during three growing seasons from 2018 to 2021. Various important parameters such as gas exchange, water potential, leaf chlorophyll (Chl), berry mass and total soluble solids (TSS) were measured.

2.5.4. Small scale winemaking (Chapter 5)

Since no previous data can be found on how SD affects wine composition, this chapter aimed to address this knowledge gap. Small-scale wines were made from SD and non-SD grapevines and chemical composition of these and berry juice investigated. Although berries from SD grapevines were at an earlier ripening stage compared to non-SD grapevines, they were harvested at the same time to minimize the environmental variations between all technical replicates.

2.5.5. First report of grapevine rupestris vein feathering virus (GRVFV) (Chapter 6)

GRVFV was detected from SA and Western Australia by Meta-HTS and a short report has been published [226].

2.6. Concluding remarks

Meta and amplicon HTS results provide an insight into the virome of SD and the potential evolutionary history of GVA. The data on grapevine, berry, juice and wine compositions informs industry of the economic importance of this disease. The physiological data may indicate a connection between the dieback of SD grapevines and the level of biotic or abiotic stress, including grapevine trunk disease (GTD).

2.7. Significance/Contribution to the discipline.

- More than a hundred and fifty complete viral genome sequences of Australian GVA, GLRaVs, GRSPaV and GRVFV isolates were obtained, which will now be available for future grapevine virus studies.
- Six viruses (GRVFV published, and five unpublished viruses) new to Australia were reported to Vine Health Australia and relevant bio-security departments.
- There was evidence that symptom types and severity were related to phylogenetic groups of GVA.
- The impact of SD on Shiraz grapevine performance, berry ripening, and wine composition was studied for the first time and the results of which can be used to inform industry in the management of SD

3. References (Chapter 1)

1. Walsh, G. The Wine Industry of Australia 1788-1979. Available online: http://artserve.anu.edu.au/raid1/student_projects/wine/wia.html (accessed on 21 July 2022).
2. International Organisation of Vine and wine sector in 2020. Available online: https://www.oiv.int/public/medias/7909/oiv-state-of-the-world-vitivinicultural-sector-in-2020.pdf (accessed on 11 November 2022).
3. International Organisation of Vine and Wine world wine production outlook. Available online: https://www.oiv.int/public/medias/8553/en-oiv-2021-world-wine-production-first-estimates-to-update.pdf (accessed on 22/11/2022).
4. Wine Australia. National vintage report 2021. Available online: https://www.wineaustralia.com/getmedia/1195b141-323e-4a8d-8f99-9ae3005e40fd/MI_VintageReport2021.pdf (accessed on 7 February 2022).
5. Tolley, J.H. The first commercial wine vineyard planted in South Australia. *JHSSA* **2014**, *42*, 71-80.
6. Simpson, J. Vertical integration and the development of commercial wine production in Argentina, Australia and California, c1870-1914. In Proceedings of the Australian Agricultural and Resource Economics Society, Adelaide, South Australia, 7-9 February, 2010; pp. 1-29.
7. Adelaide Hills Wine. Our story. Available online: https://www.adelaidehillswine.com.au/region/our-story/#:~:text=The%20first%20South%20Australian%20vineyard,and%20hastily%20planted%20on%20arrival. (accessed on 11 November 2022).
8. Lee, V.D.P. *The South Australian Wine Story*; Lee, V.D.P., Ed.; Primedia eLaunch LlC: 2019.
9. Fuchs, M. Grapevine viruses: A multitude of diverse species with simple but overall poorly adopted management solutions in the vineyard. *J. Plant Pathol.* **2020**, *102*, 643-653, doi:10.1007/s42161-020-00579-2.
10. Al Rwahnih, M.; Alabi, O.J.; Hwang, M.S.; Tian, T.; Mollov, D.; Golino, D. Characterization of a new Nepovirus infecting grapevine. *Plant Dis.* **2021**, *105*, 1432-1439, doi:10.1094/PDIS-08-20-1831-RE.
11. Shvets, D.; Sandomirsky, K.; Porotikova, E.; Vinogradova, S. Metagenomic analysis of ampelographic collections of dagestan revealed the presence of two novel grapevine viruses. *Viruses* **2022**, *14*, 2623, doi:10.3390/v14122623.
12. Martelli, G.P. An overview on grapevine viruses, viroids, and the diseases they cause. In *Grapevine viruses: molecular biology, diagnostics and management*, Meng, B., Martelli, G.P., Golino, D.A., Fuchs, M., Eds.; Springer: Berlin/Heidelberg, Germany, 2017; pp. 31-46.
13. Wu, Q.; Habili, N.; Constable, F.; Al Rwahnih, M.; Goszczynski, D.E.; Wang, Y.; Pagay, V. Virus pathogens in Australian vineyards with an emphasis on Shiraz disease. *Viruses* **2020**, *12*, 818, doi:10.3390/v12080818.
14. Tsai, C.-W.; Rowhani, A.; Golino, D.A.; Daane, K.M.; Almeida, R.P.P. Mealybug transmission of grapevine leafroll viruses: An analysis of virus–vector specificity. *Phytopathology* **2010**, *100*, 830-834, doi:10.1094 / PHYTO-100-8-0830.
15. Bertin, S.; Pacifico, D.; Cavalieri, V.; Marzachì, C.; Bosco, D. Transmission of grapevine virus A and grapevine leafroll-associated viruses 1 and 3 by Planococcus ficus and Planococcus citri fed on mixed-infected plants. *Ann. Appl. Biol.* **2016**, *169*, 53-63, doi:10.1111/aab.12279.
16. Herrbach, E.; Alliaume, A.; Prator, C.A.; Daane, K.M.; Cooper, M.L.; Almeida, R.P.P. Vector transmission of grapevine leafroll-associated viruses. In *Grapevine viruses: molecular biology, diagnostics and management*, Meng, B., Martelli, G.P., Golino, D.A., Fuchs, M., Eds.; Springer: 2017; pp. 483-503.
17. Martelli, G.P.; Ghanem-Sabanadzovic, N.A.; Agranovsky, A.A.; Al Rwahnih, M.; Dolja, V.V.; Dovas, C.I.; Fuchs, M.; Gugerli, P.; Hu, J.S.; Jelkmann, W.; et al. Taxonomic revision of the family Closteroviridae with special reference to the grapevine leafroll-associated members of the genus Ampelovirus and the putative species unassigned to the family. *J. Plant Pathol.* **2012**, *94*, 7-19.
18. Al Rwahnih, M.; Dolja, V.V.; Daubert, S.; Koonin, E.V.; Rowhani, A. Genomic and biological analysis of Grapevine leafroll-associated virus 7 reveals a possible new genus within the family Closteroviridae. *Virus Res.* **2012**, *163*, 302-309, doi:10.1016/j.virusres.2011.10.018.
19. Jelkmann, W.; Mikona, C.; Turturo, C.; Navarro, B.; Rott, M.E.; Menzel, W.; Saldarelli, P.; Minafra, A.; Martelli, G.P. Molecular characterization and taxonomy of grapevine leafroll-associated virus 7. *Arch. Virol.* **2012**, *157*, 359-362, doi:10.1007/s00705-011-1176-8.
20. Schmitt-Keichinger, C.; Hemmer, C.; Berthold, F.; Ritzenthaler, C. Molecular, cellular, and structural biology of grapevine fanleaf virus. In *Grapevine viruses: molecular biology, diagnostics and management*, Meng, B., Martelli, G.P., Golino, D.A., Fuchs, M., Eds.; Springer: 2017; pp. 83-107.
21. Martelli, G.P. Virus diseases of grapevine. *John Wiley & Sons, Ltd: Chichester* **2014**, doi:10.1002/9780470015902.a0000766.pub3.

22. Oliver, J.E.; Fuchs, M.F. *Fanleaf degeneration/decline disease of grapevines*; New York state integrated pest management program; 2011.
23. Andret-Link, P.; Laporte, C.; Valat, L.; Ritzenthaler, C.; Demangeat, G.; Vigne, E.; Laval, V.; Pfeiffer, P.; Stussi-Garaud, C.; Fuchs, M. Grapevine fanleaf virus: still a major threat to the grapevine industry. *J. Plant Pathol.* **2004**, *86*, 183-195.
24. International Plant Protection Convention. Absence of grapevine fanleaf virus from Australia. Available online: https://www.ippc.int/en/countries/australia/pestreports/2015/06/absence-of-grapevine-fanleaf-virus-from-australia/ (accessed on 17 Feb 2023).
25. Martelli, G.P. Directory of virus and virus-like diseases of the grapevine and their agents. *J. Plant Pathol.* **2014**, *96*, 1-4.
26. El Beaino, T.; Sabanadzovic, S.; Digiaro, M.; Ghanem-Sabanadzovic, N.A.; Rowhani, A.; Kyriakopoulou, P.E.; Martelli, G.P. Molecular detection of grapevine fleck virus-like viruses. *Vitis* **2001**, *40*, 65-68.
27. Ghanem-Sabanadzovic, N.A.; Sabanadzovic, S.; Martelli, G.P. Sequence analysis of the 3′ end of three grapevine fleck virus-like viruses from grapevine. *Virus Genes* **2003**, *27*, 11-16.
28. Sabanadzovic, S.; Abou-Ghanem, N.; Castellano, M.A.; Digiaro, M.; Martelli, G.P. Grapevine fleck virus-like viruses in Vitis. *Arch. Virol.* **2000**, *145*, 553-565.
29. Sabanadzovic, S.; Aboughanem-Sabanadzovic, N.; Martelli, G.P. Grapevine fleck and similar viruses. In *Grapevine viruses: molecular biology, diagnostics and management*, Meng, B., Martelli, G.P., Golino, D.A., Fuchs, M., Eds.; Springer: 2017; pp. 331-349.
30. Basso, M.F.; Fajardo, T.V.M.; saldarelli, P. Grapevine virus diseases: economic impact and current advances in viral prospection and management. *Rev. Bras. Frutic.* **2017**, *39*, doi:10.1590/0100-29452017 411.
31. Meng, B.; Johnson, R.; Peressini, S.; Forsline, P.L.; Gonsalves, D. Rupestris stem pitting associated virus-1 is consistently detected in grapevines that are infected with rupestris stem pitting. *Eur. J. Plant Pathol.* **1999**, *105*, 191-199.
32. Garau, R.; Prota, V.A.; Piredda, R.; Boscia, D.; Prota, U. On the possible relationship between Kober stem grooving and grapevine virus A. *Vitis* **1994**, *33*, 161-163.
33. Zhang, Y.-P.; Uyemoto, J.K.; Golino, D.A.; Rowhani, A. Nucleotide sequence and RT-PCR detection of a virus associated with grapevine rupestris stem-pitting disease. *Phytopathology* **1998**, *88*, 1231-1237.
34. Meng, B.; Zhu, H.-Y.; Gonsalves, D. Rupestris stem pitting associated virus-1 consists of a family of sequence variants. *Arch. Virol.* **1999**, *144*, 2071-2085.
35. Bonavia, M.; Digiaro, M.; Boscia, D.; Boari, A.; Bottalico, G.; Savino, V.; Martelli, G.P. Studies on" corky rugose wood" of grapevine and on the diagnosis of grapevine virus B. *Vitis* **1996**, *35*, 53-58.
36. Boscia, D.; Savino, V.; Minafra, A.; Namba, S.; Elicio, V.; Castellano, M.A.; Gonsalves, D.; Martelli, G.P. Properties of a filamentous virus isolated from grapevines affected by corky bark. *Arch. Virol.* **1993**, *130*, 109-120.
37. Credi, R. Characterization of grapevine rugose wood disease sources from Italy. *Plant Dis.* **1997**, *81*, 1288-1292.
38. Golino, D.A. Potential interactions between rootstocks and grapevine latent viruses. *Am. J. Enol. Vitic.* **1993**, *44*, 148-152.
39. Martelli, G.P. *Graft-transmissible diseases of grapevines: handbook for detection and diagnosis*; Martelli, G.P., Ed.; Food and Agriculture Organization of the United Nations: 1993.
40. Goszczynski, D.E.; Du Preez, J.; Burger, J.T. Molecular divergence of grapevine virus A (GVA) variants associated with Shiraz disease in South Africa. *Virus Res.* **2008**, *138*, 105-110, doi:10.1016/j.virusres.2008.08.014.
41. Habili, N.; Randles, J.W. Descriptors for grapevine virus A-associated syndrome in Shiraz, Merlot and Ruby Cabernet in Australia, and its similarity to Shiraz disease in South Africa. *Aust. N.Z. Grapegrow. Winemak.* **2004**, *488*, 71-74.
42. Goszczynski, D.E.; Habili, N. Grapevine virus A variants of group II associated with Shiraz disease in South Africa are present in plants affected by Australian Shiraz disease, and have also been detected in the USA. *Plant Pathol.* **2012**, *61*, 205-214, doi:10.1111/j.1365-3059.2011.02499.x.
43. Sudarshana, M.R.; Perry, K.L.; Fuchs, M.F. Grapevine red blotch-associated virus, an emerging threat to the grapevine industry. *Phytopathology* **2015**, *105*, 1026-1032, doi:10.1094/PHYTO-12-14-0369-FI.
44. Calvi, B.L. Effects of red-leaf disease on Cabernet Sauvignon at the Oakville experimental vineyard and mitigation by harvest delay and crop adjustment. University of California, Davis, 2011.
45. Yepes, L.M.; Cieniewicz, E.; Krenz, B.; McLane, H.; Thompson, J.R.; Perry, K.L.; Fuchs, M. Causative role of grapevine red blotch virus in red blotch disease. *Phytopathology* **2018**, *108*, 902-909.

46. Bahder, B.W.; Zalom, F.G.; Jayanth, M.; Sudarshana, M.R. Phylogeny of geminivirus coat protein sequences and digital PCR aid in identifying Spissistilus festinus as a vector of grapevine red blotch-associated virus. *Phytopathology* **2016**, *106*, 1223-1230.
47. Flasco, M.; Hoyle, V.; Cieniewicz, E.J.; Roy, B.G.; McLane, H.L.; Perry, K.L.; Loeb, G.; Nault, B.; Heck, M.; Fuchs, M. Grapevine red blotch virus is transmitted by the three-cornered alfalfa hopper in a circulative, nonpropagative mode with unique attributes. *Phytopathology* **2021**, *111*, 1851-1861.
48. Kahl, D.; Úrbez-Torres, J.R.; Kits, J.; Hart, M.; Nyirfa, A.; Lowery, D.T. Identification of candidate insect vectors of Grapevine red blotch virus by means of an artificial feeding diet. *Can. J. Plant Pathol.* **2021**, *43*, 905-913.
49. Krenz, B.; Thompson, J.R.; McLane, H.L.; Fuchs, M.; Perry, K.L. Grapevine red blotch-associated virus is widespread in the United States. *Phytopathology* **2014**, *104*, 1232-1240, doi:10.1094/ PHYTO-02-14-0053-R
50. Poojari, S.; Lowery, D.T.; Rott, M.; Schmidt, A.M.; Úrbez-Torres, J.R. Incidence, distribution and genetic diversity of grapevine red blotch virus in British Columbia. *Can. J. Plant Pathol.* **2017**, *39*, 201-211.
51. Gasperin-Bulbarela, J.; Licea-Navarro, A.F.; Pino-Villar, C.; Hernández-Martínez, R.; Carrillo-Tripp, J. First report of grapevine red blotch virus in Mexico. *Plant Dis.* **2019**, *103*, 381-381.
52. Luna, F.; Debat, H.; Moyano, S.; Zavallo, D.; Asurmendi, S.; Gomez-Talquenca, S. First report of grapevine red blotch virus infecting grapevine in Argentina. *J. Plant Pathol.* **2019**, *101*, 1239-1239.
53. Poojari, S.; Lowery, D.; Rott, M.; Schmidt, A.; Úrbez-Torres, J. Incidence, distribution and genetic diversity of Grapevine red blotch virus in British Columbia. *Can. J. Plant Pathol.* **2017**, *39*, 201-211, doi:10.1080/07060661.2017.1312532.
54. Marwal, A.; Kumar, R.; Paul Khurana, S.M.; Gaur, R.K. Complete nucleotide sequence of a new geminivirus isolated from Vitis vinifera in India: A symptomless host of grapevine red blotch virus. *Virusdisease* **2019**, *30*, 106-111, doi:10.1007/s13337-018-0477-x.
55. Lim, S.; Igori, D.; Zhao, F.; Moon, J.S.; Cho, I.-S.; Choi, G.-S. First report of Grapevine red blotch-associated virus on grapevine in Korea. *Plant Dis.* **2016**, *100*, 1957-1957.
56. Bertazzon, N.; Migliaro, D.; Rossa, A.; Filippin, L.; Casarin, S.; Giust, M.; Brancadoro, L.; Crespan, M.; Angelini, E. Grapevine red blotch virus is sporadically present in a germplasm collection in Northern Italy. *J. Plant Dis. Prot.* **2021**, *128*, 1115-1119.
57. Vine Health Australia. Grapevine red blotch virus detections: your questions answered. Available online: https://vinehealth.com.au/2022/09/grapevine-red-blotch-virus-detections-in-australia-your-questions-answered/ (accessed on 12 November 2022).
58. Walter, B.; Bass, P.; Legin, R.; Martin, C.; Vernoy, R.; Collas, A.; Vesselle, G. The use of a green–grafting technique for the detection of virus–like diseases of the grapevine. *J. Phytopathol.* **1990**, *128*, 137-145.
59. Pathirana, R.; McKenzie, M.J. A modified green-grafting technique for large-scale virus indexing of grapevine (Vitis vinifera L.). *Sci. Hortic.* **2005**, *107*, 97-102.
60. Constable, F.E.; Connellan, J.; Nicholas, P.; Rodoni, B.C. The reliability of woody indexing for detection of grapevine virus-associated diseases in three different climatic conditions in Australia. *Aust. J. Grape Wine Res.* **2012**, *19*, 74-80, doi:10.1111/j.1755-0238.2012.00204.x.
61. Katz, D.; Kohn, A. Immunosorbent electron microscopy for detection of viruses. *Adv. Virus Res.* **1984**, *29*, 169-194.
62. Derrick, K.S.; Brlansky, R.H. Assay for viruses and mycoplasmas using serologically specific electron microscopy. *Phytopathology* **1976**, *66*, 815-820.
63. Milne, R.G.; Conti, M.; Lesemann, D.E.; Stellmach, G.; Tanne, E.; Cohen, J. Closterovirus-like particles of two types associated with diseased grapevines. *J. Phytopathol.* **1984**, *110*, 360-368.
64. Corbett, M.K.; Wiid, J. Closterovirus-like particles in extracts from diseased grapevines. *Phytopathol. Mediterr.* **1985**, *24*, 91-100.
65. Zimmermann, D.; Bass, P.; Legin, R.; Walter, B. Characterization and serological detection of four closterovirus-like particles associated with leafroll disease on grapevine. *J. Phytopathol.* **1990**, *130*, 205-218.
66. Conti, M.; Milne, R.G.; Luisoni, E.; Boccardo, G. A closterovirus from a stem-pitting-diseased grapevine. *Phytopathology* **1980**, *70*, 394-399.
67. Njukeng, A.P.; Atiri, G.I.; Hughes, J.d.A. Comparison of TAS-ELISA, dot and tissue blot, ISEM and immunocapture RT-PCR assays for the detection of yam mosaic virus in yam tissues. *Crop Prot.* **2005**, *24*, 513-519, doi:10.1016/j.cropro.2004.10.002.
68. Clark, M.F.; Adams, A.N. Characteristics of the microplate method of enzyme-linked immunosorbent assay for the detection of plant viruses. *J. Gen. Virol.* **1977**, *34*, 475-483.
69. Torrance, L.; Jones, R.A.C. Recent developments in serological methods suited for use in routine testing for plant viruses. *Plant Pathol.* **1981**, *30*, 1-24.

70. Fiore, N.; Prodan, S.; Montealegre, J.; Aballay, E.; Pino, A.M.; Zamorano, A. Survey of grapevine viruses in Chile. *J. Plant Pathol.* **2008**, *90*, 125-130.
71. Fiore, N.; Prodan, S.; Pino, A.M. Monitoring grapevine viruses by ELISA and RT-PCR throughout the year. *J. Plant Pathol.* **2009**, *91*, 489-493.
72. Boonham, N.; Kreuze, J.; Winter, S.; van der Vlugt, R.; Bergervoet, J.; Tomlinson, J.; Mumford, R. Methods in virus diagnostics: from ELISA to next generation sequencing. *Virus Res.* **2014**, *186*, 20-31.
73. Bruisson, S.; Lebel, S.; Walter, B.; Prevotat, L.; Seddas, S.; Schellenbaum, P. Comparative detection of a large population of grapevine viruses by TaqMan RT-qPCR and ELISA. *J. Virol. Methods* **2017**, *240*, 73-77.
74. Niimi, Y.; Han, D.-S.; Mori, S.; Kobayashi, H. Detection of cucumber mosaic virus, lily symptomless virus and lily mottle virus in Lilium species by RT-PCR technique. *Sci. Hortic.* **2003**, *97*, 57-63.
75. Hung, T.H.; Wu, M.L.; Su, H.J. A rapid method based on the one-step reverse transcriptase-polymerase chain reaction (RT-PCR) technique for detection of different strains of citrus tristeza virus. *J. Phytopathol.* **2000**, *148*, 469-475.
76. Rowhani, A.; Maningas, M.A.; Lile, L.S.; Daubert, S.D.; Golino, D.A. Development of a detection system for viruses of woody plants based on PCR analysis of immobilized virions. *Phytopathology* **1995**, *85*, 347-352.
77. Rowhani, A.; Chay, C.; Golino, D.A.; Falk, B.W. Development of a polymerase chain reaction technique for the detection of grapevine fanleaf virus in grapevine tissue. *Phytopathology* **1993**, *83*, 749-758.
78. La Notte, P.; Minafra, A.; Saldarelli, P. A spot-PCR technique for the detection of phloem-limited grapevine viruses. *J. Virol. Methods* **1997**, *66*, 103-108.
79. MacKenzie, D.J.; McLean, M.A.; Mukerji, S.; Green, M. Improved RNA extraction from woody plants for the detection of viral pathogens by reverse transcription-polymerase chain reaction. *Plant Dis.* **1997**, *81*, 222-226.
80. Nassuth, A.; Pollari, E.; Helmeczy, K.; Stewart, S.; Kofalvi, S.A. Improved RNA extraction and one-tube RT-PCR assay for simultaneous detection of control plant RNA plus several viruses in plant extracts. *J. Virol. Methods* **2000**, *90*, 37-49.
81. Constable, F.E.; Connellan, J.; Nicholas, P.; Rodoni, B.C. Comparison of enzyme-linked immunosorbent assays and reverse transcription-polymerase chain reaction for the reliable detection of Australian grapevine viruses in two climates during three growing seasons. *Aust. J. Grape Wine Res.* **2012**, *18*, 239-244, doi:10.1111/j.1755-0238.2012.00188.x.
82. Osman, F.; Leutenegger, C.; Golino, D.; Rowhani, A. Comparison of low-density arrays, RT-PCR and real-time TaqMan RT-PCR in detection of grapevine viruses. *J. Virol. Methods* **2008**, *149*, 292-299.
83. Osman, F.; Leutenegger, C.; Golino, D.; Rowhani, A. Real-time RT-PCR (TaqMan) assays for the detection of grapevine leafroll associated viruses 1–5 and 9. *J. Virol. Methods* **2007**, *141*, 22-29, doi:10.1016/j.jviromet.2006.11.035.
84. Beuve, M.; Sempé, L.; Lemaire, O. A sensitive one-step real-time RT-PCR method for detecting grapevine leafroll-associated virus 2 variants in grapevine. *J. Virol. Methods* **2007**, *141*, 117-124, doi:10.1016/j.jviromet.2006.11.042.
85. Bester, R.; Jooste, A.E.; Maree, H.J.; Burger, J.T. Real-time RT-PCR high-resolution melting curve analysis and multiplex RT-PCR to detect and differentiate grapevine leafroll-associated virus 3 variant groups I, II, III and VI. *Virol J.* **2012**, *9*, 219, doi:10.1186/1743-422X-9-219.
86. Schaad, N.W.; Frederick, R.D. Real-time PCR and its application for rapid plant disease diagnostics. *Can. J. Plant Pathol.* **2002**, *24*, 250-258.
87. López-Fabuel, I.; Wetzel, T.; Bertolini, E.; Bassler, A.; Vidal, E.; Torres, L.B.; Yuste, A.; Olmos, A. Real-time multiplex RT-PCR for the simultaneous detection of the five main grapevine viruses. *J. Virol. Methods* **2013**, *188*, 21-24.
88. Fan, X.D.; Dong, Y.F.; Zhang, Z.P.; Ren, F.; Hu, G.J.; Zhu, H.J. RT-LAMP assay for detection of grapevine rupestris stem pitting-associated virus. *Acta Phyto. Sin.* **2013**, *43*, 286-293.
89. Walsh, H.A.; Pietersen, G. Rapid detection of grapevine leafroll-associated virus type 3 using a reverse transcription loop-mediated amplification method. *J. Virol. Methods* **2013**, *194*, 308-316.
90. Romero Romero, J.L.; Carver, G.D.; Arce Johnson, P.; Perry, K.L.; Thompson, J.R. A rapid, sensitive and inexpensive method for detection of grapevine red blotch virus without tissue extraction using loop-mediated isothermal amplification. *Arch. Virol.* **2019**, *164*, 1453-1457.
91. Zhang, Y.; Xin, Y.; Li, G.; Qian, Y. Development of a RT-LAMP assay for detection of grapevine virus A. *Sci. Agric. sin.* **2016**, *49*, 103-109.

92. Almasi, M. Establishment and application of a reverse transcription loop-mediated isothermal amplification assay for detection of grapevine fanleaf virus. *Mol. Biol.* **2015**, *4*, 149-157, doi:10.4172/2168-9547.1000149.
93. Kogovšek, P.; Mehle, N.; Pugelj, A.; Jakomin, T.; Schroers, H.-J.; Ravnikar, M.; Dermastia, M. Rapid loop-mediated isothermal amplification assays for grapevine yellows phytoplasmas on crude leaf-vein homogenate has the same performance as qPCR. *Eur. J. Plant Pathol.* **2017**, *148*, 75-84, doi:10.1007/s10658-016-1070-z.
94. Wang, X.; Yin, F.; Bi, Y.; Cheng, G.; Li, J.; Hou, L.; Li, Y.; Yang, B.; Liu, W.; Yang, L. Rapid and sensitive detection of Zika virus by reverse transcription loop-mediated isothermal amplification. *J. Virol. Methods* **2016**, *238*, 86-93.
95. Parida, M.; Posadas, G.; Inoue, S.; Hasebe, F.; Morita, K. Real-time reverse transcription loop-mediated isothermal amplification for rapid detection of West Nile virus. *J. Clin. Microbiol.* **2004**, *42*, 257-263, doi:10.1128/JCM.42.1.257–263.2004.
96. Gadkar, V.J.; Goldfarb, D.M.; Gantt, S.; Tilley, P.A.G. Real-time detection and monitoring of loop mediated amplification (LAMP) reaction using self-quenching and de-quenching fluorogenic probes. *Sci. Rep.* **2018**, *8*, 5548-5557, doi:10.1038/s41598-018-23930-1.
97. Kashir, J.; Yaqinuddin, A. Loop mediated isothermal amplification (LAMP) assays as a rapid diagnostic for COVID-19. *Med. Hypotheses* **2020**, *141*, 109786.
98. Sanger, F.; Air, G.M.; Barrell, B.G.; Brown, N.L.; Coulson, A.R.; Fiddes, J.C.; Hutchison, C.A.; Slocombe, P.M.; Smith, M. Nucleotide sequence of bacteriophage φX174 DNA. *Nature* **1977**, *265*, 687-695.
99. Sanger, F.; Nicklen, S.; Coulson, A.R. DNA sequencing with chain-terminating inhibitors. *Proc. Natl. Acad. Sci.* **1977**, *74*, 5463-5467.
100. Bentley, D.R. The human genome project—an overview. *Med. Res. Rev.* **2000**, *20*, 189-196.
101. Collins, F.S.; Morgan, M.; Patrinos, A. The Human Genome Project: lessons from large-scale biology. *Science* **2003**, *300*, 286-290.
102. Massart, S.; Adams, I.; Al Rwahnih, M.; Baeyen, S.; Bilodeau, G.J.; Blouin, A.G.; Boonham, N.; Candresse, T.; Chandellier, A.; De Jonghe, K. Guidelines for the reliable use of high throughput sequencing technologies to detect plant pathogens and pests. *Peer community J.* **2022**, *2*, e62, doi:10.24072/pcjournal.181.
103. Oliveira, L.M.; Orílio, A.F.; Inoue-Nagata, A.K.; Nagata, T.; Blawid, R. A novel vitivirus-like sequence found in Arracacia xanthorrhiza plants by high throughput sequencing. *Arch. Virol.* **2017**, *162*, 2141-2144, doi:10.1007/s00705-017-3326-0.
104. Fox, A.; Fowkes, A.R.; Skelton, A.; Harju, V.; Buxton-Kirk, A.; Kelly, M.; Forde, S.M.D.; Pufal, H.; Conyers, C.; Ward, R. Using high-throughput sequencing in support of a plant health outbreak reveals novel viruses in Ullucus tuberosus (Basellaceae). *Plant Pathol.* **2019**, *68*, 576-587, doi:10.1111/ppa.12962.
105. Behjati, S.; Tarpey, P.S. What is next generation sequencing? *Arch. Dis. Child.: Educ. Pract. Ed.* **2013**, *98*, 236-238.
106. Margulies, M.; Egholm, M.; Altman, W.E.; Attiya, S.; Bader, J.S.; Bemben, L.A.; Berka, J.; Braverman, M.S.; Chen, Y.-J.; Chen, Z. Genome sequencing in microfabricated high-density picolitre reactors. *Nature* **2005**, *437*, 376-380, doi:10.1038/nature03959.
107. Aksyonov, S.A.; Bittner, M.; Bloom, L.B.; Reha-Krantz, L.J.; Gould, I.R.; Hayes, M.A.; Kiernan, U.A.; Niederkofler, E.E.; Pizziconi, V.; Rivera, R.S. Multiplexed DNA sequencing-by-synthesis. *Anal. Biochem.* **2006**, *348*, 127-138.
108. Liu, L.; Li, Y.; Li, S.; Hu, N.; He, Y.; Pong, R.; Lin, D.; Lu, L.; Law, M. Comparison of next-generation sequencing systems. *J. Biomed. Biotechnol.* **2012**, *2012*, doi:10.1155/2012/251364.
109. Sevim, V.; Lee, J.; Egan, R.; Clum, A.; Hundley, H.; Lee, J.; Everroad, R.C.; Detweiler, A.M.; Bebout, B.M.; Pett-Ridge, J. Shotgun metagenome data of a defined mock community using Oxford Nanopore, PacBio and Illumina technologies. *Sci. Data* **2019**, *6*, 285, doi:10.1038/s41597-019-0287-z.
110. Illumina. Applications of NGS. Available online: https://sapac.illumina.com/science/technology/next-generation-sequencing.html (accessed on 8 July 2022).
111. Illumina. Illumina sequencing platforms. Available online: https://sapac.illumina.com/systems/sequencing-platforms.html (accessed on 8 August 2022).
112. Eid, J.; Fehr, A.; Gray, J.; Luong, K.; Lyle, J.; Otto, G.; Peluso, P.; Rank, D.; Baybayan, P.; Bettman, B. Real-time DNA sequencing from single polymerase molecules. *Science* **2009**, *323*, 133-138, doi:10.1126/science.1162986.
113. Pacific Biosciences. Pacbio sequencing technology overview. Available online: https://www.pacb.com/technology/ (accessed on 8 August 2022).

114. Korlach, J.; Gedman, G.; Kingan, S.B.; Chin, C.-S.; Howard, J.T.; Audet, J.-N.; Cantin, L.; Jarvis, E.D. De novo PacBio long-read and phased avian genome assemblies correct and add to reference genes generated with intermediate and short reads. *Gigascience* **2017**, *6*, gix085, doi:10.1093/gigascience/gix085.
115. Roberts, R.J.; Carneiro, M.O.; Schatz, M.C. The advantages of SMRT sequencing. *Genome Biol.* **2013**, *14*, 405, doi:10.1186/gb-2013-14-6-405.
116. Deamer, D.; Akeson, M.; Branton, D. Three decades of nanopore sequencing. *Nat. Biotechnol.* **2016**, *34*, 518-524, doi:10.1038/nbt.3423.
117. Oxford nanopore. Company history. Available online: https://nanoporetech.com/about-us/history (accessed on 8 August 2022).
118. Deamer, D.W.; Akeson, M. Nanopores and nucleic acids: prospects for ultrarapid sequencing. *Trends Biotechnol.* **2000**, *18*, 147-151, doi:10.1016/S0167-7799(00)01426-8.
119. Kasianowicz, J.J.; Brandin, E.; Branton, D.; Deamer, D.W. Characterization of individual polynucleotide molecules using a membrane channel. *Proc. Natl. Acad. Sci.* **1996**, *93*, 13770-13773, doi:10.1073/pnas.93.24.13770.
120. Venkatesan, B.M.; Bashir, R. Nanopore sensors for nucleic acid analysis. *Nat. Nanotechnol.* **2011**, *6*, 615-624.
121. Amarasinghe, S.L.; Su, S.; Dong, X.; Zappia, L.; Ritchie, M.E.; Gouil, Q. Opportunities and challenges in long-read sequencing data analysis. *Genome Biol.* **2020**, *21*, 30, doi:10.1186/s13059-020-1935-5.
122. Ansorge, W.J. Next-generation DNA sequencing techniques. *N. Biotechnol.* **2009**, *25*, 195-203, doi:10.1016/j.nbt.2008.12.009.
123. Barzon, L.; Lavezzo, E.; Militello, V.; Toppo, S.; Palù, G. Applications of next-generation sequencing technologies to diagnostic virology. *Int. J. Mol. Sci.* **2011**, *12*, 7861-7884, doi:10.3390/ijms12117861.
124. Buermans, H.P.J.; Den Dunnen, J.T. Next generation sequencing technology: advances and applications. *BBA* **2014**, *1842*, 1932-1941, doi:10.1016/j.bbadis.2014.06.015.
125. Sharpton, T.J. An introduction to the analysis of shotgun metagenomic data. *Front. Plant Sci.* **2014**, *5*, 209, doi:10.3389/FPLS.2014.00209.
126. Quince, C.; Walker, A.W.; Simpson, J.T.; Loman, N.J.; Segata, N. Shotgun metagenomics, from sampling to analysis. *Nat. Biotechnol.* **2017**, *35*, 833-844.
127. Sedlar, K.; Kupkova, K.; Provaznik, I. Bioinformatics strategies for taxonomy independent binning and visualization of sequences in shotgun metagenomics. *Comput. Struct. Biotechnol. J.* **2017**, *15*, 48-55, doi:10.1016/j.csbj.2016.11.005.
128. Adams, I.P.; Glover, R.H.; Monger, W.A.; Mumford, R.; Jackeviciene, E.; Navalinskiene, M.; Samuitiene, M.; Boonham, N. Next-generation sequencing and metagenomic analysis: a universal diagnostic tool in plant virology. *Mol. Plant Pathol.* **2009**, *10*, 537-545, doi:10.1111/J.1364-3703.2009.00545.X.
129. Al Rwahnih, M.; Daubert, S.; Golino, D.; Rowhani, A. Deep sequencing analysis of RNAs from a grapevine showing Syrah decline symptoms reveals a multiple virus infection that includes a novel virus. *Virology* **2009**, *387*, 395-401, doi:10.1016/j.virol.2009.02.028.
130. Ito, T.; Nakaune, R. Molecular characterization of a novel putative ampelovirus tentatively named grapevine leafroll-associated virus 13. *Arch. Virol.* **2016**, *161*, 2555-2559, doi:10.1007/s00705-016-2914-8.
131. Jo, Y.; Song, M.-K.; Choi, H.; Park, J.-S.; Lee, J.-W.; Lian, S.; Lee, B.C.; Cho, W.K. Genome sequence of grapevine virus K, a novel vitivirus infecting grapevine. *Genome Announc.* **2017**, *5*, e00994-00917, doi:10.1128/genomeA.00994-17.
132. Jo, Y.; Song, M.-K.; Choi, H.; Park, J.-S.; Lee, J.-W.; Lian, S.; Lee, B.C.; Cho, W.K. Genome sequence of grapevine virus T, a novel Foveavirus infecting grapevine. *Genome Announc.* **2017**, doi:10.1128/genomeA.00995-17.
133. Maliogka, V.I.; Olmos, A.; Pappi, P.G.; Lotos, L.; Efthimiou, K.; Grammatikaki, G.; Candresse, T.; Katis, N.I.; Avgelis, A.D. A novel grapevine badnavirus is associated with the Roditis leaf discoloration disease. *Virus Res.* **2015**, *203*, 47-55, doi:10.1016/j.virusres.2015.03.003.
134. Zhang, Y.; Singh, K.; Kaur, R.; Qiu, W. Association of a novel DNA virus with the grapevine vein-clearing and vine decline syndrome. *Phytopathology* **2011**, *101*, 1081-1090, doi:10.1094 / PHYTO-02-11-0034.
135. Giampetruzzi, A.; Roumi, V.; Roberto, R.; Malossini, U.; Yoshikawa, N.; La Notte, P.; Terlizzi, F.; Credi, R.; Saldarelli, P. A new grapevine virus discovered by deep sequencing of virus-and viroid-derived small RNAs in Cv Pinot gris. *Virus Res.* **2012**, *163*, 262-268, doi:10.1016/j.virusres.2011.10.010.
136. Simmonds, P.; Adams, M.J.; Benkő, M.; Breitbart, M.; Brister, J.R.; Carstens, E.B.; Davison, A.J.; Delwart, E.; Gorbalenya, A.E.; Harrach, B. Virus taxonomy in the age of metagenomics. *Nat. Rev. Microbiol.* **2017**, *15*, 161-168, doi:10.1038/nrmicro.2016.177.
137. Choueiri, E.; Abou-Ghanem, N.; Boscia, D. Grapevine virus A and grapevine virus D are serologically distantly related. *Vitis* **1997**, *36*, 39-41.

138. Boscia, D.; Digiaro, M.; Safi, M.; Garau, R.; Zhou, Z.; Minafra, A.; Ghanem-Sabanadzovic, N.A.; Bottalico, G.; Potere, O. Production of monoclonal antibodies to grapevine virus D and contribution to the study of its aetiological role in grapevine diseases. *Vitis* **2001**, *40*, 69-74.
139. Nakaune, R.; Toda, S.; Mochizuki, M.; Nakano, M. Identification and characterization of a new vitivirus from grapevine. *Arch. Virol.* **2008**, *153*, 1827-1832, doi:10.1007/s00705-008-0188-5.
140. Coetzee, B.; Maree, H.J.; Stephan, D.; Freeborough, M.-J.; Burger, J.T. The first complete nucleotide sequence of a grapevine virus E variant. *Arch. Virol.* **2010**, *155*, 1357-1360, doi:10.1007/s00705-010-0685-1.
141. Coetzee, B.; Freeborough, M.-J.; Maree, H.J.; Celton, J.-M.; Rees, D.J.G.; Burger, J.T. Deep sequencing analysis of viruses infecting grapevines: virome of a vineyard. *Virology* **2010**, *400*, 157-163, doi:10.1016/j.virol.2010.01.023.
142. Al Rwahnih, M.; Sudarshana, M.R.; Uyemoto, J.K.; Rowhani, A. Complete genome sequence of a novel vitivirus isolated from grapevine. *Genome Announc.* **2012**, 9545, doi:10.1128/JVI.01444-12.
143. Molenaar, N.; Burger, J.T.; Maree, H.J. Detection of a divergent variant of grapevine virus F by next-generation sequencing. *Arch. Virol.* **2015**, *160*, 2125-2127, doi:10.1007/s00705-015-2466-3.
144. Blouin, A.G.; Keenan, S.; Napier, K.R.; Barrero, R.A.; MacDiarmid, R.M. Identification of a novel vitivirus from grapevines in New Zealand. *Arch. Virol.* **2018**, *163*, 281-284, doi:10.1007/s00705-017-3581-0.
145. Blouin, A.; Chooi, K.; Warren, B.; Napier, K.; Barrero, R.; MacDiarmid, R. Grapevine virus I, a putative new vitivirus detected in co-infection with grapevine virus G in New Zealand. *Arch. Virol.* **2018**, *163*, 1371-1374, doi:10.1007/s00705-018-3738-5.
146. Candresse, T.; Theil, S.; Faure, C.; Marais, A. Determination of the complete genomic sequence of grapevine virus H, a novel vitivirus infecting grapevine. *Arch. Virol.* **2018**, *163*, 277-280, doi:10.1007/s00705-017-3587-7.
147. Diaz-Lara, A.; Golino, D.; Al Rwahnih, M. Genomic characterization of grapevine virus J, a novel virus identified in grapevine. *Arch. Virol.* **2018**, *163*, 1965-1967, doi:10.1007/s00705-018-3793-y.
148. Debat, H.; Zavallo, D.; Brisbane, R.S.; Vončina, D.; Almeida, R.P.P.; Blouin, A.G.; Al Rwahnih, M.; Gomez-Talquenca, S.; Asurmendi, S. Grapevine virus L: a novel vitivirus in grapevine. *Eur. J. Plant Pathol.* **2019**, *155*, 319-328, doi:10.1007/s10658-019-01727-w.
149. Alabi, O.J.; McBride, S.; Appel, D.N.; Al Rwahnih, M.; Pontasch, F.M. Grapevine virus M, a novel vitivirus discovered in the American hybrid bunch grape cultivar Blanc du Bois in Texas. *Arch. Virol.* **2019**, *164*, 1739-1741, doi:10.1007/s00705-019-04252-7.
150. Gauthier, N.P.G.; Nelson, C.; Bonsall, M.B.; Locher, K.; Charles, M.; MacDonald, C.; Krajden, M.; Chorlton, S.D.; Manges, A.R. Nanopore metagenomic sequencing for detection and characterization of SARS-CoV-2 in clinical samples. *PLoS One* **2021**, *16*, e0259712, doi:10.1371/journal.pone.0259712.
151. Lewandowski, K.; Xu, Y.; Pullan, S.T.; Lumley, S.F.; Foster, D.; Sanderson, N.; Vaughan, A.; Morgan, M.; Bright, N.; Kavanagh, J. Metagenomic nanopore sequencing of influenza virus direct from clinical respiratory samples. *J. Clin. Microbiol.* **2019**, *58*, e00963-00919, doi:10.1128/JCM.00963-19.
152. Harismendy, O.; Ng, P.C.; Strausberg, R.L.; Wang, X.; Stockwell, T.B.; Beeson, K.Y.; Schork, N.J.; Murray, S.S.; Topol, E.J.; Levy, S. Evaluation of next generation sequencing platforms for population targeted sequencing studies. *Genome Biol.* **2009**, *10*, R32, doi:10.1186/gb-2009-10-3-r32.
153. Han, S.-W.; Kim, H.-P.; Shin, J.-Y.; Jeong, E.-G.; Lee, W.-C.; Lee, K.-H.; Won, J.-K.; Kim, T.-Y.; Oh, D.-Y.; Im, S.-A. Targeted sequencing of cancer-related genes in colorectal cancer using next-generation sequencing. *PLoS One* **2013**, *8*, e64271, doi:10.1371/journal.pone.0064271.
154. Guerrero-Preston, R.; Godoy-Vitorino, F.; Jedlicka, A.; Rodríguez-Hilario, A.; González, H.; Bondy, J.; Lawson, F.; Folawiyo, O.; Michailidi, C.; Dziedzic, A.; et al. 16S rRNA amplicon sequencing identifies microbiota associated with oral cancer, human papilloma virus infection and surgical treatment. *Oncotarget* **2016**, *7*, 51320.
155. Ding, D.; Lou, X.; Hua, D.; Yu, W.; Li, L.; Wang, J.; Gao, F.; Zhao, N.; Ren, G.; Li, L. Recurrent targeted genes of hepatitis B virus in the liver cancer genomes identified by a next-generation sequencing–based approach. *PLoS Genet.* **2012**, *8*, e1003065.
156. Hugerth, L.W.; Andersson, A.F. Analysing microbial community composition through amplicon sequencing: from sampling to hypothesis testing. *Front. Microbiol.* **2017**, *8*, 1561, doi:10.3389/fmicb.2017.01561.
157. Ranjan, R.; Rani, A.; Metwally, A.; McGee, H.S.; Perkins, D.L. Analysis of the microbiome: Advantages of whole genome shotgun versus 16S amplicon sequencing. *Biochem. Biophys. Res. Commun.* **2016**, *469*, 967-977, doi:10.1016/j.bbrc.2015.12.083.

158. Schöler, A.; Jacquiod, S.; Vestergaard, G.; Schulz, S.; Schloter, M. Analysis of soil microbial communities based on amplicon sequencing of marker genes. *Biol. Fertil. Soils* **2017**, *53*, 485-489, doi:10.1007/s00374-017-1205-1.
159. Piry, S.; Wipf-Scheibel, C.; Martin, J.-F.; Galan, M.; Berthier, K. High throughput amplicon sequencing to assess within-and between-host genetic diversity in plant viruses. *bioRxiv* **2017**, 168773, doi:10.1101/168773.
160. Kinoti, W.M.; Constable, F.E.; Nancarrow, N.; Plummer, K.M.; Rodoni, B. Generic amplicon deep sequencing to determine Ilarvirus species diversity in Australian Prunus. *Front. Microbiol.* **2017**, *8*, doi:10.3389/fmicb.2017.01219.
161. Kinoti, W.M.; Constable, F.E.; Nancarrow, N.; Plummer, K.M.; Rodoni, B. Analysis of intra-host genetic diversity of Prunus necrotic ringspot virus (PNRSV) using amplicon next generation sequencing. *PLoS One* **2017**, *12*, e0179284, doi:10.1371journal.pone.0179284.
162. Kinoti, W.M.; Constable, F.E.; Nancarrow, N.; Plummer, K.M.; Rodoni, B. The incidence and genetic diversity of apple mosaic virus (ApMV) and prune dwarf virus (PDV) in Prunus species in Australia. *Viruses* **2018**, *10*, 136, doi:10.3390/v10030136.
163. Maina, S.; Zheng, L.; Rodoni, B.C. Targeted genome sequencing (TG-Seq) approaches to detect plant viruses. *Viruses* **2021**, *13*, 583, doi:10.3390/v13040583.
164. Dana, H.; Chalbatani, G.M.; Mahmoodzadeh, H.; Karimloo, R.; Rezaiean, O.; Moradzadeh, A.; Mehmandoost, N.; Moazzen, F.; Mazraeh, A.; Marmari, V. Molecular mechanisms and biological functions of siRNA. *Int. J. Biomed. Sci.* **2017**, *13*, 48-57.
165. Ding, S.-W.; Voinnet, O. Antiviral immunity directed by small RNAs. *Cell* **2007**, *130*, 413-426, doi:10.1016/j.cell.2007.07.039.
166. Pantaleo, V.; Vitali, M.; Boccacci, P.; Miozzi, L.; Cuozzo, D.; Chitarra, W.; Mannini, F.; Lovisolo, C.; Gambino, G. Novel functional microRNAs from virus-free and infected Vitis vinifera plants under water stress. *Sci. Rep.* **2016**, *6*, 20167, doi:10.1038/srep20167.
167. Pantaleo, V.; Saldarelli, P.; Miozzi, L.; Giampetruzzi, A.; Gisel, A.; Moxon, S.; Dalmay, T.; Bisztray, G.; Burgyan, J. Deep sequencing analysis of viral short RNAs from an infected Pinot Noir grapevine. *Virology* **2010**, *408*, 49-56, doi:10.1016/j.virol.2010.09.001.
168. Alabi, O.J.; Zheng, Y.; Jagadeeswaran, G.; Sunkar, R.; Naidu, R.A. High-throughput sequence analysis of small RNAs in grapevine (Vitis vinifera L.) affected by grapevine leafroll disease. *Mol. Plant Pathol.* **2012**, *13*, 1060-1076, doi:10.1111/J.1364-3703.2012.00815.X.
169. Prasad, A.; Sharma, N.; Muthamilarasan, M.; Rana, S.; Prasad, M. Recent advances in small RNA mediated plant-virus interactions. *Crit. Rev. Biotechnol.* **2019**, *39*, 587-601, doi:10.1080/07388551.2019.1597830.
170. Massart, S.; Chiumenti, M.; De Jonghe, K.; Glover, R.; Haegeman, A.; Koloniuk, I.; Komínek, P.; Kreuze, J.; Kutnjak, D.; Lotos, L. Virus detection by high-throughput sequencing of small RNAs: Large-scale performance testing of sequence analysis strategies. *Phytopathology* **2019**, *109*, 488-497, doi:10.1094/PHYTO-02-18-0067-R.
171. Xu, C.; Sun, X.; Taylor, A.; Jiao, C.; Xu, Y.; Cai, X.; Wang, X.; Ge, C.; Pan, G.; Wang, Q. Diversity, distribution, and evolution of tomato viruses in China uncovered by small RNA sequencing. *J. Virol.* **2017**, *91*, e00173-00117, doi:10.1128/JVI.00173-17.
172. Gouveia, P.; Dandlen, S.; Costa, Â.; Marques, N.; Nolasco, G. Identification of an RNA silencing suppressor encoded by grapevine leafroll-associated virus 3. *Eur. J. Plant Pathol.* **2012**, *133*, 237-245, doi:10.1007/s10658-011-9876-1.
173. Agrawal, N.; Dasaradhi, P.V.N.; Mohmmed, A.; Malhotra, P.; Bhatnagar, R.K.; Mukherjee, S.K. RNA interference: biology, mechanism, and applications. *Microbiol. Mol. Biol. Rev.* **2003**, *67*, 657-685, doi:10.1128/MMBR.67.4.657-685.2003.
174. Kreuze, J. siRNA deep sequencing and assembly: piecing together viral infections. In *Detection and diagnostics of plant pathogens*, Gullino, M.L., Bonants, P.J.M., Eds.; Springer: 2014; Volume 5, pp. 21-38.
175. Santala, J.; Valkonen, J.P.T. Sensitivity of small RNA-based detection of plant viruses. *Front. Microbiol.* **2018**, *9*, 939, doi:10.3389/fmicb.2018.00939.
176. Kreuze, J.F.; Perez, A.; Untiveros, M.; Quispe, D.; Fuentes, S.; Barker, I.; Simon, R. Complete viral genome sequence and discovery of novel viruses by deep sequencing of small RNAs: a generic method for diagnosis, discovery and sequencing of viruses. *Virology* **2009**, *388*, 1-7, doi:10.1016/j.virol.2009.03.024.
177. Maliogka, V.I.; Minafra, A.; Saldarelli, P.; Ruiz-García, A.B.; Glasa, M.; Katis, N.; Olmos, A. Recent advances on detection and characterization of fruit tree viruses using high-throughput sequencing technologies. *Viruses* **2018**, *10*, 436, doi:10.3390/v10080436.

178. Villamor, D.E.V.; Ho, T.; Al Rwahnih, M.; Martin, R.R.; Tzanetakis, I.E. High throughput sequencing for plant virus detection and discovery. *Phytopathology* **2019**, *109*, 716-725, doi:10.1094/PHYTO-07-18-0257-RVW.
179. Gauthier, M.-E.A.; Lelwala, R.V.; Elliott, C.E.; Windell, C.; Fiorito, S.; Dinsdale, A.; Whattam, M.; Pattemore, J.; Barrero, R.A. Side-by-side comparison of post-entry quarantine and high throughput sequencing methods for virus and viroid diagnosis. *Biology* **2022**, *11*, 263, doi:10.3390/biology11020263.
180. Whattam, M.; Dinsdale, A.; Elliott, C.E. Evolution of plant virus diagnostics used in Australian post entry quarantine. *Plants* **2021**, *10*, 1430, doi:10.3390/plants10071430.
181. Goszczynski, D.E. Single-strand conformation polymorphism (SSCP), cloning and sequencing reveal a close association between related molecular variants of grapevine virus A (GVA) and Shiraz disease in South Africa. *Plant Pathol.* **2007**, *56*, 755-762, doi:10.1111/j.1365-3059.2007.01624.x.
182. Engelbrecht, D.J.; Kasdorf, G.G.F. Occurrence and transmission of grapevine virus A in South African grapevines. *South African J. Enol. Vitic.* **1987**, *8*, 23-29.
183. Minafra, A.; Hadidi, A.; Martelli, G.P. Detection of grapevine closterovirus-A in infected grapevine tissue by reverse transcription-polymerase chain-reaction. *Vitis* **1992**, *31*, 221-227.
184. Martelli, G.P.; Candresse, T.; Namba, S. Trichovirus, a new genus of plant viruses. *Arch. Virol.* **1994**, *137*, 451.
185. Minafra, A.; Saldarelli, P.; Martelli, G.P. Grapevine virus A: nucleotide sequence, genome organization, and relationship in the Trichovirus genus. *Arch. Virol.* **1997**, *142*, 417-423.
186. Goszczynski, D.E.; Kasdorf, G.G.F.; Pietersen, G. Western blots reveal that grapevine viruses A and B are serologically related. *J. Phytopathol.* **1996**, *144*, 581-583, doi:10.1111/j.1439-0434.1996.tb00302.x.
187. Martelli, G.P.; Minafra, A.; Saldarelli, P. Vitivirus, a new genus of plant viruses. *Archives of Virology* **1997**, *142*, 1929-1932.
188. Santana, V.S.; Mariutti, R.B.; Eberle, R.J.; Ullah, A.; Caruso, I.P.; Arni, R.K. *Betaflexiviridae-Family*; Elsevier Inc.: 2012; pp. 920-941.
189. Santana, V.; Mariutti, R.; Eberle, R.; Ullah, A.; Caruso, I.; Arni, R. *Betaflexiviridae-Family*; Elsevier Inc.: 2012; pp. 920-941.
190. Minafra, A.; Saldarelli, P.; Grieco, F.; Martelli, G. Nucleotide sequence of the 3′ terminal region of the RNA of two filamentous grapevine viruses. *Arch. Virol.* **1994**, *137*, 249-261.
191. Minafra, A.; Saldarelli, P.; Grieco, F.; Martelli, G.P. Nucleotide sequence of the 3' terminal region of the RNA of two filamentous grapevine viruses. *Arch. Virol.* **1994**, *137*, 249-261.
192. Goszczynski, D.E.; Jooste, A.E.C. Identification of divergent variants of grapevine virus A. *Eur. J. Plant Pathol.* **2003**, *109*, 397-403, doi:10.1023/a:1023555018700.
193. Habili, N.; Wu, Q.; Pagay, V. Virus-associated Shiraz disease may lead Shiraz to become an endangered variety in Australia. *Wine and Viticulture J.* **2016**, *31*, 47-50.
194. Habili, N. It's not worth the gamble: serious problems associated with top-working virus-infected vines. *Aust. N.Z. Grapegrow. Winemak.* **2003**, *476*, 84-89.
195. Habili, N.; Randles, J.W. Major yield loss in Shiraz vines infected with Australian Shiraz disease associated with grapevine virus A. In Proceedings of the 17th Meeting of the International Council for the Study of Viruses and Virus-like Diseases of the Grapevine, Davis, California, USA, 7–14 October 2012; pp. 164-165.
196. Goszczynski, D.E.; Jooste, A.E.C. Identification of grapevines infected with divergent variants of grapevine virus A using variant-specific RT-PCR. *J. Virol. Methods* **2003**, *112*, 157-164, doi:10.1016/s0166-0934(03)00198-8.
197. Saldarelli, P.; Dell'Orco, M.; Minafra, A. Infectious cDNA clones of two grapevine viruses. *Arch. Virol.* **2000**, *145*, 397-405, doi:10.1007/s007050050031.
198. Galiakparov, N.; Tanne, E.; Sela, I.; Gafny, R. Infectious RNA transcripts from grapevine virus a cDNA clone. *Virus Genes* **1999**, *19*, 235-242, doi:10.1023/a:1008192831883.
199. Galiakparov, N.; Tanne, E.; Mawassi, M.; Gafny, R.; Sela, I. ORF 5 of grapevine virus A encodes a nucleic acid-binding protein and affects pathogenesis. *Virus Genes* **2003**, *27*, 257-262, doi:10.1023/a:1026395815980.
200. Vaghchhipawala, Z.; Rojas, C.M.; Senthil-Kumar, M.; Mysore, K.S. Agroinoculation and agroinfiltration: simple tools for complex gene function analyses. In *Plant reverse genetics: methods and protocols*, Pereira, A., Ed.; Springer: 2011; Volume 678, pp. 65-76.
201. Muruganantham, M.; Moskovitz, Y.; Haviv, S.; Horesh, T.; Fenigstein, A.; du Preez, J.; Stephan, D.; Burger, J.T.; Mawassi, M. Grapevine virus A-mediated gene silencing in Nicotiana benthamiana and Vitis vinifera. *J. Virol. Methods* **2009**, *155*, 167-174, doi:10.1016/j.jviromet.2008.10.010.

202. Goszczynski, D.E. Brief report of the construction of infectious DNA clones of South African genetic variants of grapevine virus A and grapevine virus B. *Springerplus* **2015**, *4*, 739-746, doi:10.1186/s40064-015-1517-2.
203. Meng, B.; Venkataraman, S.; Li, C.; Wang, W.; Dayan-Glick, C.; Mawassi, M. Construction and biological activities of the first infectious cDNA clones of the genus Foveavirus. *Virology* **2013**, *435*, 453-462, doi:10.1016/j.virol.2012.09.045.
204. Tarquini, G.; Zaina, G.; Ermacora, P.; De Amicis, F.; Franco-Orozco, B.; Loi, N.; Martini, M.; Bianchi, G.L.; Pagliari, L.; Firrao, G. Agroinoculation of grapevine Pinot gris virus in tobacco and grapevine provides insights on viral pathogenesis. *PLoS One* **2019**, *14*, e0214010, doi:10.1371/journal.pone.0214010.
205. Jarugula, S.; Gowda, S.; Dawson, W.O.; Naidu, R.A. Development of infectious cDNA clones of grapevine leafroll-associated virus 3 and analyses of the 5′ non-translated region for replication and virion formation. *Virology* **2018**, *523*, 89-99, doi:10.1016/j.virol.2018.07.023.
206. Haviv, S.; Iddan, Y.; Goszczynski, D.E.; Mawassi, M. The ORF5 of grapevine virus A is involved in symptoms expression in Nicotiana benthamiana plants. *Ann. Appl. Biol.* **2012**, *160*, 181-190, doi:10.1111/j.1744-7348.2012.00531.x.
207. Galiakparov, N.; Tanne, E.; Sela, I.; Gafny, R. Functional analysis of the grapevine virus A genome. *Virology* **2003**, *306*, 42-50, doi:10.1016/S0042-6822(02)00019-3.
208. Rowhani, A.; Golino, D.A.; Klaassen, V.; Sim, S.T.; Gouran, M.; Al Rwahnih, M. Grapevine leafroll associated virus-3: effects on rootstocks, vine performance, yield and berries. In Proceedings of the 18th Meeting of the International Council for the Study of Viruses and Virus-like Diseases of the Grapevine, Ankara, Turkey, 7–11 September, 2015; pp. 161-162.
209. Girardello, R.C.; Cooper, M.L.; Smith, R.J.; Lerno, L.A.; Bruce, R.C.; Eridon, S.; Oberholster, A. Impact of grapevine red blotch disease on grape composition of Vitis vinifera Cabernet Sauvignon, Merlot, and Chardonnay. *J. Agric. Food Chem.* **2019**, *67*, 5496-5511, doi:10.1021/acs.jafc.9b01125.
210. Guidoni, S.; Mannini, F.; Ferrandino, A.; Argamante, N.; Di Stefano, R. The effect of grapevine leafroll and rugose wood sanitation on agronomic performance and berry and leaf phenolic content of a Nebbiolo clone (Vitis vinifera L.). *Am. J. Enol. Vitic.* **1997**, *48*, 438-442.
211. Cabaleiro, C.; Segura, A.; Garcia-Berrios, J.J. Effects of grapevine leafroll-associated virus 3 on the physiology and must of Vitis vinifera L. cv. Albarino following contamination in the field. *Am. J. Enol. Vitic.* **1999**, *50*, 40-44.
212. Komar, V.; Vigne, E.; Demangeat, G.; Fuchs, M. Beneficial effect of selective virus elimination on the performance of Vitis vinifera cv. Chardonnay. *Am. J. Enol. Vitic.* **2007**, *58*, 202-210.
213. Giribaldi, M.; Purrotti, M.; Pacifico, D.; Santini, D.; Mannini, F.; Caciagli, P.; Rolle, L.; Cavallarin, L.; Giuffrida, M.G.; Marzachì, C. A multidisciplinary study on the effects of phloem-limited viruses on the agronomical performance and berry quality of Vitis vinifera cv. Nebbiolo. *Journal of proteomics* **2011**, *75*, 306-315.
214. Mannini, F.; Mollo, A.; Credi, R. Field performance and wine quality modification in a clone of Vitis vinifera cv. Dolcetto after GLRaV-3 elimination. *Am. J. Enol. Vitic.* **2012**, *63*, 144-147, doi:10.5344/ajev.2011.11020.
215. Moutinho-Pereira, J.; Correia, C.M.; Gonçalves, B.; Bacelar, E.A.; Coutinho, J.F.; Ferreira, H.F.; Lousada, J.L.; Cortez, M.I. Impacts of leafroll-associated viruses (GLRaV-1 and-3) on the physiology of the Portuguese grapevine cultivar 'Touriga Nacional'growing under field conditions. *Ann. Appl. Biol.* **2012**, *160*, 237-249, doi:10.1111/j.1744-7348.2012.00536.x.
216. Endeshaw, S.T.; Sabbatini, P.; Romanazzi, G.; Schilder, A.C.; Neri, D. Effects of grapevine leafroll associated virus 3 infection on growth, leaf gas exchange, yield and basic fruit chemistry of Vitis vinifera L. cv. Cabernet Franc. *Sci. Hortic.* **2014**, *170*, 228-236, doi:10.1016/j.scienta.2014.03.021.
217. Bota, J.; Cretazzo, E.; Montero, R.; Rosselló, J.; Cifre, J. Grapevine fleck virus (GFkV) elimination in a selected clone of Vitis vinifera L. cv. Manto negro and its effects on photosynthesis. *J. Int. Sci. Vigne Vin* **2014**, *48*, 11-19.
218. El Aou-ouad, H.; Montero, R.; Medrano, H.; Bota, J. Interactive effects of grapevine leafroll-associated virus 3 (GLRaV-3) and water stress on the physiology of Vitis vinifera L. cv. Malvasia de Banyalbufar and Giro-Ros. *J. Plant Physiol.* **2016**, *196*, 106-115, doi:10.1016/j.jplph.2016.04.003.
219. El Aou-ouad, H.; Pou, A.; Tomás, M.; Montero, R.; Ribas-Carbo, M.; Medrano, H.; Bota, J. Combined effect of virus infection and water stress on water flow and water economy in grapevines. *Physiol. Plant.* **2017**, *160*, 171-184, doi:10.1111/ppl.12541.

220. Reynard, J.-S.; Brodard, J.; Dubuis, N.; Zufferey, V.; Schumpp, O.; Schaerer, S.; Gugerli, P. Grapevine red blotch virus: Absence in Swiss vineyards and analysis of potential detrimental effect on viticultural performance. *Plant Dis.* **2018**, *102*, 651-655, doi:10.1094/PDIS-07-17-1069-RE.
221. Halldorson, M.M.; Keller, M. Grapevine leafroll disease alters leaf physiology but has little effect on plant cold hardiness. *Planta* **2018**, *248*, 1201-1211, doi:10.1007/s00425-018-2967-x.
222. Bowen, P.; Bogdanoff, C.; Poojari, S.; Usher, K.; Lowery, T.; Úrbez-Torres, J.R. Effects of grapevine red blotch disease on Cabernet franc vine physiology, bud hardiness, and fruit and wine quality. *Am. J. Enol. Vitic.* **2020**, *71*, 308-318, doi:10.5344/ajev.2020.20011.
223. Swamy, P.; Pattathil, S.; Unda, F.; Mansfield, S.D. Grapevine red blotch disease affects carbohydrate homeostasis and cell call characteristics in Vitis vinifera L. *Res. Sq. Prepr.* **2021**, doi:10.21203/rs.3.rs-428067/v1.
224. Copp, C.R.; Levin, A.D. Irrigation improves vine physiology and fruit composition in grapevine red blotch virus-infected Vitis vinifera L. *Am. J. Enol. Vitic.* **2021**, *72*, 307-317, doi:10.5344/ajev.2021.21007.
225. Jež-Krebelj, A.; Rupnik-Cigoj, M.; Stele, M.; Chersicola, M.; Pompe-Novak, M.; Sivilotti, P. The physiological impact of GFLV virus infection on grapevine water status: First observations. *Plants* **2022**, *11*, 161, doi:10.3390/plants11020161.
226. Wu, Q.; Kehoe, M.; Kinoti, W.M.; Wang, C.; Rinaldo, A.; Tyerman, S.; Habili, N.; Constable, F.E. First report of grapevine rupestris vein feathering virus in grapevine in Australia. *Plant Dis.* **2021**, *105*, 515.

Chapter 2: A Metagenomic Investigation of the Viruses Associated with Shiraz Disease in Australia

Wu, Q.; Habili, N.; Kinoti, W.M.; Tyerman, S.D.; Rinaldo, A.; Zheng, L.; Constable, F.E. A Metagenomic Investigation of the Viruses Associated with Shiraz Disease in Australia. Viruses 2023, 15, 774, doi:10.3390/v15030774.

Statement of Authorship

Title of Paper	Metagenomic Investigation of the Viruses Associated with Shiraz Disease in Australia
Publication Status	☒ Published ☐ Accepted for Publication ☐ Submitted for Publication ☐ Unpublished and Unsubmitted work written in manuscript style
Publication Details	Journal: MDPI-Viruses Year 2023, volume: 15, issue 774, page 1-21 https://doi.org/10.3390/v15030774

Principal Author

Name of Principal Author (Candidate)	Qi Wu		
Contribution to the Paper	Conception, acquiring data, knowledge, analysis, drafting		
Overall percentage (%)	30%		
Certification:	This paper reports on original research I conducted during the period of my Higher Degree by Research candidature and is not subject to any obligations or contractual agreements with a third party that would constrain its inclusion in this thesis. I am the primary author of this paper.		
Signature		Date	27/04/2023

Co-Author Contributions

By signing the Statement of Authorship, each author certifies that:

i. the candidate's stated contribution to the publication is accurate (as detailed above);

ii. permission is granted for the candidate in include the publication in the thesis; and

iii. the sum of all co-author contributions is equal to 100% less the candidate's stated contribution.

Name of Co-Author	Nuredin Habili		
Contribution to the Paper	Conception, knowledge, drafting		
Signature		Date	28/4/2023

Name of Co-Author	Wycliff M. Kinoti

Contribution to the Paper	Acquiring data, knowledge, analysis, drafting		
Signature		Date	27/04/2023

Name of Co-Author	Stephen D. Tyerman		
Contribution to the Paper	Conception, knowledge, drafting		
Signature		Date	27/04/2023

Name of Co-Author	Amy Rinaldo		
Contribution to the Paper	Conception, knowledge, drafting		
Signature		Date	27/04/2023

Name of Co-Author	Linda Zheng		
Contribution to the Paper	Acquiring data, knowledge, drafting		
Signature		Date	28/4/2023

Name of Co-Author	Fiona Constable		
Contribution to the Paper	Conception, knowledge, analysis, drafting		
Signature		Date	27/04/2023

viruses

MDPI

Article

A Metagenomic Investigation of the Viruses Associated with Shiraz Disease in Australia

Qi Wu [1,2,*], Nuredin Habili [1,2], Wycliff M. Kinoti [3], Stephen D. Tyerman [1], Amy Rinaldo [2], Linda Zheng [3] and Fiona E. Constable [3,4]

1 School of Agriculture, Food and Wine, University of Adelaide, Waite Precinct, PMB 1, Glen Osmond, SA 5064, Australia
2 Australian Wine Research Institute, Wine Innovation Central Building, Hartley Grove crn Paratoo Road, Urrbrae, SA 5064, Australia
3 Agriculture Victoria Research, Department of Energy, Environment and Climate Action, AgriBio, Centre for AgriBioscience, 5 Ring Road, Bundoora, VIC 3083, Australia
4 School of Applied Systems Biology, La Trobe University, Bundoora, VIC 3086, Australia
* Correspondence: qi.wu@adelaide.edu.au

Abstract: Shiraz disease (SD) is an economically important virus-associated disease that can significantly reduce yield in sensitive grapevine varieties and has so far only been reported in South Africa and Australia. In this study, RT-PCR and metagenomic high-throughput sequencing was used to study the virome of symptomatic and asymptomatic grapevines within vineyards affected by SD and located in South Australia. Results showed that grapevine virus A (GVA) phylogroup II variants were strongly associated with SD symptoms in Shiraz grapevines that also had mixed infections of viruses including combinations of grapevine leafroll-associated virus 3 (GLRaV-3) and grapevine leafroll-associated virus 4 strains 5, 6 and 9 (GLRaV-4/5, GLRaV-4/6, GLRaV-4/9). GVA phylogroup III variants, on the other hand, were present in both symptomatic and asymptomatic grapevines, suggesting no or decreased virulence of these strains. Similarly, only GVA phylogroup I variants were found in heritage Shiraz grapevines affected by mild leafroll disease, along with GLRaV-1, suggesting this phylogroup may not be associated with SD.

Keywords: Shiraz disease; Australia; grapevine virus A; grapevine leafroll-associated virus 3; metagenomic sequencing; grapevine leafroll-associated virus 4; phylogenetic groups; dsRNA

Citation: Wu, Q.; Habili, N.; Kinoti, W.M.; Tyerman, S.D.; Rinaldo, A.; Zheng, L.; Constable, F.E. A Metagenomic Investigation of the Viruses Associated with Shiraz Disease in Australia. *Viruses* **2023**, *15*, 774. https://doi.org/10.3390/v15030774

Academic Editor: Hernan Garcia-Ruiz

Received: 21 February 2023
Revised: 14 March 2023
Accepted: 15 March 2023
Published: 17 March 2023

1. Introduction

Shiraz disease (SD) and grapevine leafroll disease (LRD) are the two major viral diseases that pose a serious threat to Australia's AUD 45.5 billion dollar grape and wine industry [1–3]. LRD is associated with grapevine leafroll-associated viruses (GLRaVs) of the genera *Ampelovirus*, *Closterovirus* and *Velarivirus* within the family *Closteroviridae* [4]. Grapevine leafroll-associated virus 3 (GLRaV-3) is considered to be the most important GLRaV species due to its global prevalence, the severity of associated disease and impact on production [5]. In red berry varieties, LRD symptoms include downwards rolling of red leaves with green veins, which commences at veraison [5]. Studies have shown that sensitive grapevine varieties infected with GLRaV-3 can have a significant reduction in vigour, yield, juice sugar and berry anthocyanins [6–8]. Conversely, white berry varieties are often asymptomatic where vigour, fruit quality and yield may not be affected [5,9].

SD is only known to occur in South Africa and Australia and the disease is associated with significant yield losses and grapevine decline [1,2,10,11]. SD was first reported from South Africa, affecting Shiraz and Merlot grapevines grafted onto 101-14 rootstock [12]. The symptoms of SD include uneven lignification of canes (ULC) and purple leaves that remain longer on affected grapevines at the end of the growing season as compared to the asymptomatic grapevines [12]. SD was also described in Australia as early as 2001 [13], with

affected grapevines showing late bud burst, restricted spring growth (RSG), leaf reddening and ULC in autumn [14,15]. In both countries, SD is associated with grapevine virus A (GVA), and in South Africa, a strong association was observed between GVA variants in phylogenetic group II (GVA^{II}) [11]. The association between specific GVA variants and SD in Australia has not been explored in depth, although GVA^{II} variants were found in seven SD-affected plants of cv. Shiraz and Merlot [10]. Symptoms of SD vary between grapevine varieties. Red berry varieties including Shiraz, Merlot, Malbec, Gamay, Ruby Cabernet and Sumoll express typical SD symptoms when infected with GVA, whereas Cabernet Sauvignon, Grenache, Nero d'Avola, and most white berry varieties and rootstocks are consistently asymptomatic when infected with GVA [1,2,16].

GVA has five open reading frames (ORFs): ORF1 encodes a 194 kDa polypeptide functioning as an RNA-dependent RNA polymerase (RdRp), ORF2 encodes a 19 kDa polypeptide with unknown function, ORF3 encodes a 31 kDa movement protein (MP), ORF4 encodes a 21.5 kDa coat protein (CP) and ORF 5 encodes a 10 kDa polypeptide putatively involved in RNA-binding (RB) functions by suppressing RNA-silencing responses [17,18]. Symptom severity in *Nicotiana benthamiana* inoculated with GVA depended upon the eighth amino acid (aa) from the N-terminus of the RNA-binding gene [19,20]. However, the association between specific genes or changes in specific nucleotides or amino acids and symptoms of SD within the grapevine is not known.

In this study, we use endpoint reverse transcription polymerase chain reaction (RT-PCR) and metagenomic high-throughput sequencing (Meta-HTS) to investigate the association between SD and GVA, its variants and other viruses in affected Australian grapevines.

2. Materials and Methods

2.1. Vineyard Locations and Grapevine Selection

Two commercial vineyards with SD-affected grapevines cv Shiraz, at Langhorne Creek (LC) and Willunga (WIL; blocks 1 and 2 Figure S1) in South Australia (SA), and one commercial vineyard with mild LRD-affected heritage Shiraz at Barossa Valley (BV), SA, were chosen for this study. A total of 116 grapevines, including SD- or LRD-affected and asymptomatic grapevines, were selected to investigate the virome and association of viruses and their strains to disease. Samples were collected over three years, in May to July of 2018–2019, March 2019 and August 2020 for RT-PCR testing (Table 1 and Table S1). Forty-one samples, which represent distinct symptom types at each location, were selected from the 116 samples for Meta-HTS. The SD grapevines were selected based on the presence of both the RSG symptoms in the early growing stages around EL stage 15 (8 leaves separated [21]), and leaf reddening observed [1] (Figure 1a,b) from EL stage 35 (veraison) to leaf-fall. The LRD grapevines were selected based on field observations of red leaves with green veins around EL stage 38 (harvest). Mild LRD symptoms refer to pinkish reddening leaves (BV) or slight red leaves without rolling (Figure 1c). Asymptomatic grapevines did not show RSG, SD or LRD at the time of selection and appeared healthy (Figure 1d). Symptom types were identified twice by field observation at EL stage 15 for RSG and at EL stage 38 for leaf reddening at each study site, from 2018 to 2020.

To investigate the potential for spread between WIL and adjoining blocks of grapevines, four grapevines (Cabw1, 2, 11 and 12) from an adjoining block of Cabernet Sauvignon (clone SA125) and a grapevine (Merlot1) from an abandoned neighbouring Merlot block were selected for virome analysis (Figure S1, Table 1). Merlot1 showed typical SD symptoms and Cabernet Sauvignon showed LRD symptoms at EL-38 (Table 1).

Two asymptomatic own-rooted Shiraz (clone BVRC12) grapevines (Shiraz_OR_P5 and Shiraz_OR_P6) and two Cabernet Sauvignon (clone SA125) grapevines (CabSA125_R3V30 and CabSA125_R3V44) with mild LRD symptoms located in the Coombe's research vineyard (CV), Waite Campus, University of Adelaide, SA, were selected as controls for diseased grapevines' virome comparison (Table 1).

Table 1. The number of grapevines, their location, variety/clone, year planted and symptoms selected for the reverse transcription polymerase chain reaction (RT-PCR) and metagenomics high-throughput sequencing (Meta-HTS) experiments.

Location	Year Selected	Variety and Clone	Year Established	Grafted on Rootstock?	Total Grapevines		No. of SD Grapevines		No. of LRD Grapevines		No. of Asymptomatic Grapevines	
					RT-PCR	HTS	RT-PCR	HTS	RT-PCR	HTS	RT-PCR	HTS
Langhorne Creek [1] (LC)	2018	Shiraz BVRC12	2004	Chardonnay	30	14	15	9	N/A	0	15	5
Willunga (WIL)	2018&2020	Shiraz BVRC12	2004	No	80 [4]	24	8	13	7	7	15	4
	2020	Cabernet Sauvignon SA125 [2]	2004	No	4	4	N/A	N/A	4	4	N/A	N/A
	2020	Merlot unknown clone [2]	Unknown	Unknown	1	1	1	1	N/A	N/A	N/A	N/A
Barossa Valley [3] (BV)	2018	heritage Shiraz, unknown clone	≈1900σ	No	6	3	N/A	N/A	3	2	3	1
Coombe vineyard (CV)	2020	Shiraz [2] BVRC12	1993	No	2	2	N/A	N/A	N/A	N/A	2	2
	2020	Cabernet Sauvignon SA125 [2]	1993	No	2	2	N/A	N/A	2	2	N/A	N/A

[1] No grapevine with leafroll disease symptoms was found at the LC site. [2] For studying the infection source at the WIL site only. [3] BV grapevines showed mild leafroll disease symptoms. [4] Thirty LC grapevines were chosen in 2018 but were subsequently removed, therefore 50 additional WIL grapevines were sampled in 2020 for the analysis.

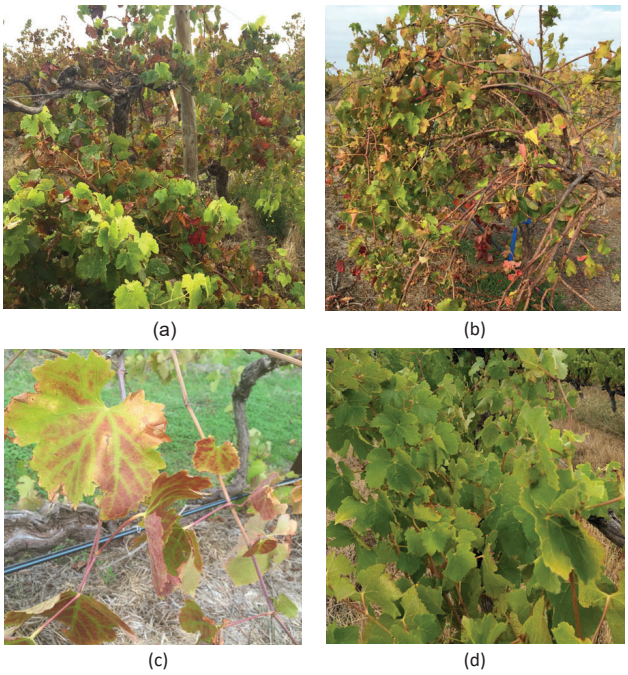

Figure 1. Symptoms of grapevine virus A (GVA)-infected Shiraz from the Willunga, Langhorne Creek and Barossa Valley sites. Symptoms of Shiraz-disease-affected Shiraz grapevines at (**a**) Willunga and (**b**) Langhorne Creek, and infected with GVA^{II} variants (**c**) mild grapevine leafroll disease symptoms on an unknown clone of Shiraz that tested positive to GVA^{I} variant and grapevine leafroll-associated virus 1 at Barossa Valley. (**d**) An asymptomatic Shiraz, clone BVRC12 at Willunga.

2.2. Sample Collection

The sampling time and tissue type for the RT-PCR and HTS experiments are listed in Table S1. Petioles (5 per grapevine) or dormant canes (3 per grapevine) were collected in autumn (March or May) or in winter (June–August), respectively. When collecting samples, canes or petioles were randomly selected from across the whole canopy of each grapevine. Samples were stored at 4 °C until they were processed.

2.3. Nucleic Acid Extraction

2.3.1. Nucleic Acid Extraction for RT-PCR

Total nucleic acid (TNA) extraction for virus detection by RT-PCR was performed as follows. A stock silica slurry was prepared by washing one gram of silica (Sigma-Aldrich, cat.S5631, Darmstadt, Germany) with PCR-grade water (Thermo Fisher Scientific, Waltham, MA, USA), centrifuging at 6900× *g*, discarding the supernatant and resuspending the pellet in 1.5 mL of guanidine hydrochloride (GHC) extraction buffer (4 M guanidine hydrochloride, 0.2 M sodium acetate, pH 5.0, 0.2 M EDTA, 0.5% (*w*/*w*) PVP-40 (Sigma-Aldrich, Darmstadt, Germany) and 0.5% (*w*/*w*) sodium metabisulfite (Sigma-Aldrich, Darmstadt, Germany). Plant tissue from an equivalent proportion of each sampled leaf or cane were pooled and homogenized in GHC extraction buffer at a ratio of 100 mg tissue to 1 mL buffer. One twentieth volume of 20% (*wt*/*vol*) sarkosyl (Sigma-Aldrich, Darmstadt, Germany) was added to the homogenate and incubated at 65 °C for 10 min. The homogenate was mixed with one-third volume of chloroform: isoamyl alcohol mixture (24:1, Sigma-Aldrich, Darmstadt, Germany) and centrifuged at 6900× *g* for 10 min. Then, 350 µL of 100% ethanol was added to 500 µL of clear supernatant and mixed with 30 µL of the GHC silica slurry. The sample was mixed for 5 min on a rotating wheel to allow the TNA to bind to the silica particles. Silica was then pelleted and washed once in 700 µL of GHC buffer without PVP40 and twice with 1 mL of wash buffer (75% ethanol, 10 mM Tris-HCl pH 7.5, 100 mM LiCl). Pellet was dried at 65 °C for 1 min then left at ambient temperature until completely dried. This was then resuspended in 50 µL of elution buffer (10 mM Tris-HCl, pH 8.5) and incubated at 65 °C for 1 min. Silica was then pelleted by centrifugation and supernatant transferred to a fresh tube and stored at −20 °C.

2.3.2. Nucleic Acid Extraction for HTS

For HTS, ribosomal RNA depleted double-stranded RNA (dsRNA) was used. The dsRNA was extracted from each sample using a previously published CF-11-based method [22] that was modified. Briefly, 3 g of tissue was homogenized in 8 mL of GHC buffer. About 7.5 mL of homogenate was mixed with one-third volume of chloroform: isoamyl alcohol mixture (24:1, Sigma-Aldrich, Darmstadt, Germany) and centrifuged for 10 min at 4200× *g*. Seven mL of the clear homogenate was transferred into a 15 mL centrifuge tube, and the volume adjusted to 20% ethanol (ethanol: homogenate ratio 1:4 *vol*/*vol*). Then 0.1 g of Whatman® CF-11 cellulose powder (Sigma-Aldrich, Darmstadt, Germany) was added to the homogenate and the mixture was rotated for 10 min. The mixture was centrifuged at 4200× *g* for 2 min and supernatant discarded. The CF-11 was washed and centrifuged twice with 5 mL of STE/20% ethanol buffer (20% ethanol (*vol*/*vol*), in 10 mM Tris-HCl pH 8.0, 100 mM NaCl and 1 mM EDTA). A final 3 mL of 80% STE buffer (in 20% ethanol) was added to CF-11 and vortexed to resuspend. The CF-slurry was dispensed into a syringe containing 0.2 gm of autoclaved glass wool fibre (SiO_2) and the CF-11 was dried by gently pressing the plunger to remove any remaining buffer. The dsRNA was eluted in 1 mL of preheated (65 °C) 1× STE buffer.

2.3.3. Nucleic Acid Quality Control

Prior to RT-PCR and Meta-HTS, the quality, integrity and quantity of RNA for RT-PCR and dsRNA for HTS were evaluated using a Nanodrop TM 1000 spectrophotometer (Thermo Fisher Scientific, Waltham, MA, USA) and a Qubit fluorometer (Thermo Fisher Scientific, Waltham, MA, USA), according to the manufacturer's instructions. Samples with

the OD 260/280 and OD 260/230 values outside of the acceptable range were re-extracted (260/280 >1.8, 260/230 ≈ 2.0). In addition, all RNA used for virus detection by RT-PCR was tested using the RubiscoL internal control RT-PCR assay (Table S2) [23] to ensure RNA was present and detection was not affected by inhibitors. Each Meta-HTS sample was tested for expected viruses including GVA, GLRaV-1, GLRaV-3, GLRaV-4 strain 6 and 9, grapevine rupestris stem pitting-associated virus (GRSPaV) using virus specific RT-PCR assays listed in Table S2.

2.4. RT-PCR Reaction Conditions

A total of 10 µL RT-PCR reactions contained 4 units of ProtoScript® II reverse transcriptase (New England Biolabs, Ipswich, MA, USA), 0.15 units of EpiMark® Hot Start Taq DNA polymerase (New England Biolabs, Ipswich, MA, USA), 2 µL 5XGoTaq® Flexi Reaction Buffer (Promega, Madison, WI, USA), 0.2 mM of each dNTP, 1.5 mM of $MgCl_2$, 0.2 µM of each forward and reverse primer, PCR-grade water (Thermo Fisher Scientific, Waltham, MA, USA) and 1 µL of TNA. Reaction conditions were as follows: reverse transcription at 43 °C for 45 min and initial denaturation at 95 °C for 30 s, followed by 35 cycles of denaturation at 95 °C for 20 s, annealing (assay dependent, see Table S2) for 20 s, and extension at 68 °C for 30 s, and then a final extension at 68 °C for 5 min.

2.5. Metagenomic High-Throughput Sequencing (Meta-HTS)

2.5.1. Nucleic Acid Pretreatments, Library Preparation and Sequencing

Prior to library preparation, dsRNA was concentrated using isopropanol and sodium acetate as previously described [24]. The concentrated dsRNA was DNase-treated to remove DNA using the Ambion™ DNase I kit (Invitrogen, Waltham, MA, USA) according to manufacturers' instructions.

Libraries of the Meta-HTS samples were prepared using the TruSeq Stranded Total RNA with Ribo-Zero Plant (Illumina, San Diego, CA, USA) kits, following the manufacturer's instructions. The concentration of libraries was determined using a Nanodrop, Qubit fluorometer, and TapeStation (Agilent, Santa Clara, CA, USA) and pooled to equivalent concentration. The pooled library was sequenced using a NovaSeq instrument with 2 × 150 bp read length.

2.5.2. *De Novo* Assembly

Illumina adapters were trimmed and the raw reads with a quality score below 20 and length below 50 bp were removed using TrimGalore (v. 0.4.2) [25]. Trimmed reads were *de novo* assembled using SPAdes (v. 3.12.0) with default settings [26]. Assembled contigs were compared against the local database built with the exemplar isolate of each virus species identified by the International Committee on Taxonomy of Viruses (ICTV) and latest release of the viral sequences from the GenBank database using the "makeblastdb" function of BLAST+ (v. 2.11.0). The contigs were blasted against the local database to obtain a list of virus species in each sample using the "blastn" function [27]. The number of raw and quality trimmed reads, number of contigs and contig length were obtained using the "stats" and "readlength" functions of the BBMap (v. 35.85). To obtain the average coverage of each *de novo* assembled contig (complete genome sequence used in the phylogenetic analysis) of each virus, quality trimmed reads were mapped back to each *de novo* assembled virus contig using the "bbmap" function of the BBMap [28].

2.5.3. Phylogenetic and Sequence Similarity Analysis

GVA, GLRaV-3 and GLRaV-4 contigs longer than 7000 nucleotides (nts), 17,000 nts and 13,000 nts, respectively, were used for phylogenetic analysis of each virus. Each virus contig was aligned to all publicly available GenBank complete genome sequences (Tables S7–S9) using Muscle (v.3.8.31) [29]. Nucleotide (nt) identity and amino acid (aa) similarity were determined using the sequence demarcation tool (SDT, v. Linux64) [30]. Phylogenetic trees were constructed using the neighbour-joining method with 1000 bootstrap replicates by

MEGA (v. 7.0.26) [31]. The neighbour-joining method was used to enable comparison of GVA phylogenetic groupings reported in previous studies [11]. Phylogenetic trees of GVA were constructed using complete genomes as well as nt and aa sequences from all gene regions excluding ORF2. The phylogenetic groups of GVA contigs were assigned based on the clades of the phylogenetic tree of the full genomes and the coat protein (CP) gene. Phylogenetic trees of GLRaV-3 were constructed using complete genome sequences and complete nt sequences of the CP gene. Phylogenetic trees of GLRaV-4 were constructed using complete genome sequences and complete aa sequences of the RdRp, heat shock protein 70 homologue (HSP70h) and CP genes.

2.5.4. Phylogenetic Group Identification of the Grapevine Virus A Contigs

When phylogenetic groups of the complete genome sequences from both GenBank and Meta-HTS experiments were determined using the phylogenetic analysis described above, they were used as a reference database by BLAST+ to build a local blast. All short contigs were blasted against the reference database using the "blastn" function [27]. The phylogroup of each short contig was obtained by the best match that gave the highest percentage nucleotide identity to this contig.

2.5.5. Multiple Sequence Alignment of the GVA RNA-Binding Protein

The GVA RB gene nucleotide sequence was translated to amino acid sequence using the "translate to protein" function and aligned to coding protein sequences from GenBank using the "create alignment" function within the CLC Genomics Workbench (v. 21.0.3; Qiagen, Aarhus, Denmark). The SD status of each GenBank isolate was obtained from publications [11,19,32,33] and listed in Table S7.

2.5.6. Recombination Analysis

Complete or near-complete viral contigs of GVA, GLRaV-3 and GLRaV-4 were combined with all publicly available full genome sequences from GenBank (Tables S7–S9) and aligned using Muscle (v. 3.8.31). The sequence alignment was trimmed according to the shortest sequences and analysed by RDP5 (v. Beta 5.23) [34]. Seven methods RDP [35], GENECONV [36], Chimaera [37], MaxChi [38], BootScan [39], SiScan [40], 3Seq [41] were selected to detect recombination events. If more than four out of seven methods detected the same recombination event for a contig, it was considered as a recombined sequence and excluded from the phylogenetic analysis.

3. Results

3.1. Virome Analysis by Endpoint RT-PCR and Meta-HTS

A summary of the overall number of grapevines with identical virus status by RT-PCR is given in Table S3. The virus status of each individual grapevine by RT-PCR but not by Meta-HTS can be found in Table S4. The virus status by both methods can be found in Table S5. The viruses detected by RT-PCR and/or Meta-HTS in grapevines across WIL, LC, BV and CV were GVA, GLRaV-1, GLRaV-3, GLRaV-4 (including strains 4/5, 4/6 and 4/9), grapevine rupestris vein feathering virus (GRVFV), GRSPaV, grapevine virus F (GVF) and grapevines red globe virus (GRGV).

3.1.1. RT-PCR

Across all Shiraz grapevines from WIL, LC and BV (n = 116), the viruses that were detected by endpoint RT-PCR included, GVA (51/116), GLRaV-1 (3/116), GLRaV-3 (50/116), GLRaV-4/6 (34/116), GLRaV-4/9 (52/116), GRVFV (76/116) and GRSPaV (116/116). GRVFV was found in 72/80 (90%) grapevines in the WIL vineyard but only 4/30 (13.3%) at LC. The frequency of GLRaV-4 strains 6 and 9 at WIL was 33/80 (41.25%) and 43/80 (53.75%), respectively (Tables S4 and S5). At the LC site, GLRaV-4 strain 6 only occurred in 1/30 (3.3%) grapevines and GLRaV-4 strain 9 was detected in 9/30 (30%) of the total tested grapevines. GLRaV-1 was detected at BV in 3/6 grapevines with mild LRD symptoms,

which also had GVA and GRSPaV, but it was not detected at any other site. GLRaV-3, GLRaV-4 strain 6 or 9, GRSPaV and GRVFV may also be present in SD-affected grapevines, but they were not consistently associated with SD, or they were also found in grapevines without SD (Table S3).

In the 16 SD-affected Shiraz grapevines at the WIL site, 16/16 were positive by the general purpose GVA endpoint RT-PCR assay using primer pairs Ah587/Ac995 and H7038/C7273 that detect phylogroups I and II, and 5/16 were also positive using the phylogenetic group III (GVA^{III}) specific endpoint RT-PCR assay. Among 35 LRD and 29 asymptomatic Shiraz grapevines, none were positive by the general purpose GVA assays (Tables 2 and S5). A total of 12/35 LRD and 5/29 asymptomatic Shiraz grapevines were positive by the GVA^{III} assay (Tables 2 and S5).

Table 2. The presence of grapevine virus A (GVA), and grapevine leafroll-associated viruses 3 (GLRaV-3) and -4 (GLRaV-4) determined by endpoint RT-PCR and metagenomic high-throughput sequencing (Meta-HTS), and associated symptoms, in 50 grapevines.

Sample ID [1]	Total Number of Grapevines with Symptom and Virus Status Combination	Symptoms [2]	GVA (I,II,II), GLRaV-1 (1), GLRaV-3 (3) and GLRaV-4 (4) Status by RT-PCR [3]	GVA (I,II,III), GLRaV-1 (1), GLRaV-3 (3) and GLRaV-4 (4) Status by Meta-HTS [4]
WIL19, WIL22	2	Asymptomatic	4	4
WIL17, LC16, LC18, LC20, LC24, LC27, BV6, CVP5, CVP6	9		None	None
WIL24	1		None	4
WIL14, 15	2	LRD	3, 4	3, 4
WIL9, WIL10, WIL11, WIL12	4		III, 3, 4	III, 3, 4
Cabw1, Cabw2, Cabw12	3		I/II, III, 3, 4	II and III, 3, 4
Cabw11	1		I/II, 3, 4	II, 3, 4
WIL13 *	1		3, 4	III, 3, 4
BV1, 3	2	Mild LRD	I/II, 1	I, 1
CabSA125_R3V30, CabSA125_R3V44	2		I/II, III, 4	II and III, 4
WIL8	1	SD	I/II, III, 3, 4	II and III, 3, 4
LC10, LC11, LC12, LC13, LC14	5		I/II, 4	II, 4
WIL48, WIL49, WIL50, WIL53	4		1/II, 3	II, 3
WIL4, WIL5, WIL6, WIL7	4		I/II, 3, 4	II, 3, 4
LC5, LC6, LC7, LC9 *	4		I/II	II, 4
WIL47 *	1		I/II, 3	III, 3
Melort1 *	1		I/II, III, 3	II and III, 3, 4
WIL1, WIL2, WIL3 *	3		I/II, III, 3, 4	II andIII, 4

[1] WIL = Willunga, LC = Langhorne Creek, BV = Barossa Valley, CV = Coombe's Vineyard. All grapevines listed are var. Shiraz except Cabw = Cabernet Sauvignon from Willunga and CabSA125 = Cabernet Sauvignon clone SA125 from Coombe's Vineyard. [2] I = GVA^{I}, II = GVA^{II}, I/II = GVA^{I}/GVA^{II} (the two groups cannot be discriminated by RT-PCR), III = GVA^{III}, 1 = GLRaV-1, 3 = GLRaV-3, 4 = GLRaV-4. [3] SD = Shiraz disease, LRD = leafroll disease. [4] GVA^{I}, GVA^{II} and GVA^{III} phylogenetic groups were identified using contigs generated by Meta-HTS (Table S7). * RT-PCR and Meta-HTS results mismatched.

For the Cabernet Sauvignon and Merlot grapevines from WIL and CV, 6/6 were positive by the GVA general purpose endpoint RT-PCR assay and 5/6 were positive by the GVA^{III} specific RT-PCR (Tables 2 and S5). The two Shiraz grapevines from CV were positive for GRSPaV and GRVFV only.

Grapevine yellow speckle viroid 1 and hop stunt viroid were frequently detected in most of the samples by Meta-HTS (Table S6), but no further analysis was performed on the viroids.

3.1.2. Comparison of Virome Detection between Meta-HTS and Endpoint RT-PCR

The viromes from a total of 50 grapevines, including 43 Shiraz grapevines across all vineyards, including WIL (n = 24), LC (n = 14), BV (n = 3) and CV (n = 2), plus one Merlot grapevine from WIL and six Cabernet Sauvignon grapevines from WIL (n = 4) and CV (n = 2), were analysed by Meta-HTS and compared with the endpoint RT-PCR results (Table 2). For the presence of GVA strains, GLRaV-3 and the GLRaV-4 strains, comparable results were obtained in 40/50 grapevines. Meta-HTS detected GVA and GLRaV-4 in 6/50 grapevines that were missed by RT-PCR, and the presence of GLRaV-3 was missed by Meta-HTS in 3/50 grapevines (Table 2).

Near-complete or partial genomes of GVA^{II} were obtained from 21/50 and 7/50 grapevines, respectively, including all SD-affected shiraz grapevines (n = 29) at WIL and LC, one SD-affected Merlot grapevine at WIL and all six LRD-affected Cabernet Sauvignon SA125 grapevines from WIL (4/6) and CV (2/6) (Table 2). In 10/50 grapevines, two distinct partial or near full-length genomes of GVA were assembled (Tables S6 and S7).

The detection of GVA by Meta-HTS generally corresponded with the results of the endpoint RT-PCR assays with some exceptions. This included the designation of phylogroup type based on sequence comparison of whole genomes and comparisons of the RdRp, MP and CP genes (Table 2, Figure 2). Meta-HTS showed that GVA^{II} isolates were always associated with SD in Shiraz and Merlot, except in WIL 47 (Shiraz) where GVA^{III} was detected by Meta-HTS, but the RT-PCR results suggested phylogenetic group I (GVA^{I}) or GVA^{II} were present (Table 2). GVA was also detected in nine LRD-affected Shiraz grapevines from WIL (7/9) and BV (2/9) by Meta-HTS and RT-PCR (Table 2). Seven out of nine were positive by Meta-HTS and 6/7 of the same grapevines by RT-PCR (Table 2). Meta-HTS indicated GVA^{I} was present in the two mild LRD-affected grapevines at BV and GVA^{III} was present in the five LRD-affected grapevines at WIL (Table 2). GVA was not detected in any of the asymptomatic Shiraz grapevines from WIL, LC, BV and CV (Table 2). GVA^{II} and GVA^{III} were detected in 6/6 and 5/6 LRD-affected Cabernet Sauvignon grapevines (Table 2).

GLRaV-3 was detected in all SD- affected grapevines (n = 13) at WIL by RT-PCR, but genomes were only assembled from 10/13 of the affected grapevines. GLRaV-3 was also detected from the single SD-affected Merlot and all LRD-affected Cabernet Sauvignon (n = 4) grapevines at WIL by both methods. GLRaV-3 was not detected in SD-affected or asymptomatic grapevines from LC and Cabernet Sauvignon grapevines from CV. Genomes and RT-PCR confirmed the detection of GLRaV-3 in the same LRD-affected grapevines at WIL and the detection of GLRaV-1 in mild LRD-affected grapevines at BV.

At WIL, GLRaV-4 strains were detected by RT-PCR and genomes assembled in the same 8/13 SD-affected Shiraz grapevines and in all seven LRD-affected Shiraz grapevines. Additionally, GLRaV-4 strains were detected by RT-PCR and genomes were assembled in 2/4 and 3/4 asymptomatic Shiraz grapevines. GLRaV-4 was detected by RT-PCR and genomes assembled in 5/9 and 9/9 SD-affected grapevines at LC, but it was not detected in asymptomatic grapevines. GLRaV-4 was also found in all LRD-affected Cabernet Sauvignon grapevines at WIL and CV by RT-PCR and Meta-HTS.

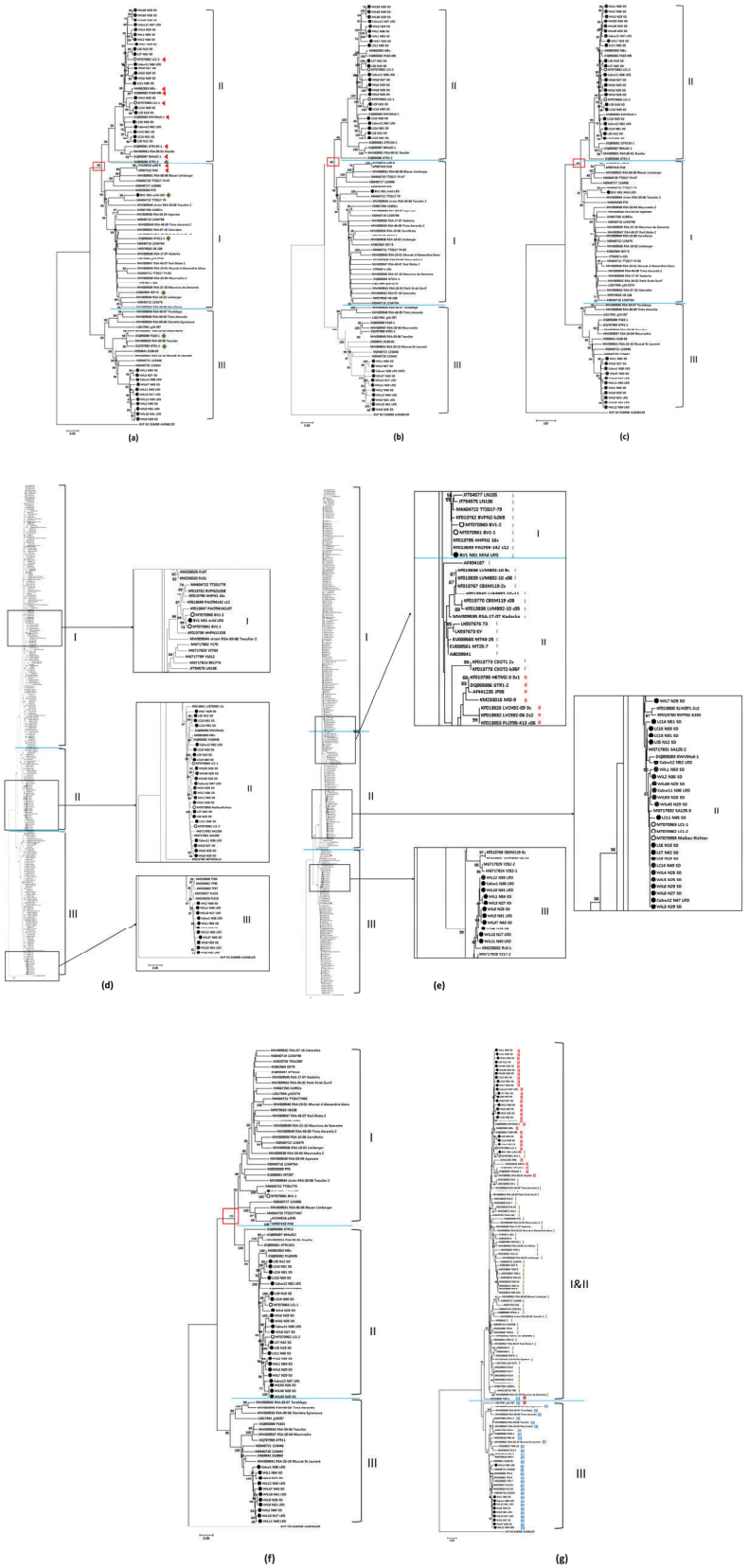

Figure 2. Neighbour-joining phylogenetic analysis of grapevine virus A (GVA) using 35 metagenomic sequences and all available sequences from GenBank. A neighbour-joining tree using (**a**) complete genome sequences alignment above 6991 nts, (GVA isolates associated with SD-affected grapevines are labelled with red triangles and isolates associated with asymptomatic grapevines are labelled with

green rhombus), (**b**) full-length nucleotide (nt) sequences of RNA-dependent RNA polymerase (RdRp), (**c**) full-length amino acid (aa) sequences of RdRp, (**d**) nt sequences of complete coat protein (CP) gene, (**e**) aa sequence of CP gene, (**f**) nt sequence of complete movement protein (MP) gene, (**g**) nt sequences of RNA-binding (RB) gene. All phylogenetic trees were constructed using MEGA (7.0.26) software and the neighbour-joining method with 1000 bootstrap replicates. Bootstrap values below 50% were not shown. Australian sequences generated by a previous study by Meta-HTS [1] are labelled using open circles and sequences generated by NovaSeq are labelled by black dots. Isolates for which the phylogroup assigned differed depending on the gene used is marked by * in figure (**g**). The red squares indicate the primary branches which show $\geq$ 99% bootstrap values. The colour-coded I, II and III labelled in figure (**g**) is based on the phylogroup assigned using the CP gene, for comparison. Grapevine virus F (GVF) isolate AUD46129 (accession no. NC018458) was used as an outgroup.

GRSPaV was detected in all 50 grapevines by RT-PCR and Meta-HTS (Tables S4 and S5). GRVFV was detected by RT-PCR and by Meta-HTS in 24/50 and 32/50 grapevines, respectively, including SD, LRD and asymptomatic grapevines from WIL, LC, BV and CV (Tables S4 and S5). GRGV was not tested using RT-PCR but was found by Meta-HTS in five LRD-affected Cabernet Sauvignon grapevines from WIL and CV (Table S5). GVF was only found from the WIL site in 2/4 of the Cabernet Sauvignon grapevines, but not in the Cabernet Sauvignon from CV by Meta-HTS only (Table S5).

Two own-rooted asymptomatic Shiraz BVRC12 grapevines at CV did not have the same virus profile as grapevines from WIL and LC and only GRSPaV and GRVFV were detected by Meta-HTS (Table S5).

3.2. Phylogenetic Analysis of Grapevine Virus A (GVA)

3.2.1. Phylogenetic Groups (Phylogroups) of Grapevine Virus A (GVA)

The GVA isolates used for analysis are listed in Table S7. Three major GVA phylogroups, GVA^{I}, GVA^{II} and GVA^{III}, were formed when phylogenetic analysis was used to compare the nucleotide sequence of the 35 whole genomes and the RdRp, CP and MP genes from the same 35 Australian GVA isolates and isolates available in GenBank (Figure 2a,b,d,f; Table S7). Three clusters were also formed when amino acid sequences of the RdRp, CP and MP gene products were analysed (Figures 2c,e and S2a). In most cases, the phylogenetic clade designation of each Australian isolate was the same when comparing across all gene nt or aa sequences (Figure 2 and S2; Table S7). However, some isolates designated as group I based on the nt sequence of the CP gene (Figure 2d) shifted into the group II clade when the corresponding aa sequences were compared (Figure 2e).

Only two distinct clusters were formed when phylogenetic analyses were used to compare the nt (Figure 2g) and aa sequences (Figure S2b) of the RB gene. The first cluster comprised of the isolates that were previously identified as GVA^{I} and GVA^{II} using the CP gene, and the second RB cluster included those previously identified as GVA^{III} using the CP gene.

3.2.2. Similarity within Phylogroups and between Australian GVA Isolates

The range of percentage nt identities and aa similarities within each GVA phylogroup for whole genomes, RdRp, CP, MP and RB genes within Australian isolates from this study, and all previously identified Australian and international isolates, is given in Table 3. The data show that all isolates within GVA^{I}, GVA^{II} and GVA^{III}, at the full genome level, share 76.33–99.8%, 79.92–99.90% and 76.52–99.94% nt identities, respectively. Isolates within Australia share nt identities between 91.45–99.94% at full genome level. Among all Australian isolates, the lowest nt identities and aa similarities are 90.65% and 91.45%, respectively, when RdRp, CP, MP and RB genes were analysed. The sequence similarity between all available isolates across all three phylogroups of RdRp, CP, MP and RB genes were 74.76–99.96% nt and 84.72–100% aa (RdRp), 77.30–100% nt and 78.85–100% aa (MP),

77.39–100% nt and 79.90–100% aa (CP), and 86.08 to 100% nt and 84.62–100% aa, identities and similarities, respectively. Only two Australian isolates belonging to the GVA^{I} phylogroup were found, BV1_N31_mild_LRD and BV1-1 (accession no. MT070961), both from the BV vineyard (Tables 3 and S7) [1]. The highest nucleotide identity shared between local and international GVA^{I} isolates was 90.76% and this was between Australian isolate BV1_N31_mild_LRD and French isolate TT2017-79 (accession no. MK404722) from Pinot Noir (Table S7).

Table 3. Sequence similarity within and between phylogroups of grapevine virus A (GVA) of the Australian isolates obtained by metagenomic high-throughput sequencing and international isolates from the GenBank database.

Genes Compared [1]		I [2]		II [2]		III [2]	
		Australian Isolates Only	All Isolates	Australian Isolates Only	All Isolates	Australian Isolates Only	All Isolates
Whole genome		N/A [3]	76.33–99.80	91.45–99.90	79.92–99.90	94.85–99.94	76.52–99.94
RdRp	RdRp nt	N/A	74.96–99.88	90.65–99.90	79.53–99.90	94.12–99.96	74.76–99.96
	RdRp aa	N/A	84.72–99.53	96.60–100	90.28–100	97.25–100	86.59–100
MP	MP nt	99.88 [4]	77.30–100	91.07–100	83.03–100	96.31–100	81.67–100
	MP aa	100 [4]	78.85–100	92.47–100	89.25–100	95.70–100	87.46–100
CP	CP nt	98.49–99.83	80.23–99.66	94.30–100	84.09–100	97.82–100	77.39–100
	CP aa	98.99–100	79.90–100	96.98–100	88.94–100	98.99–100	82.41–100
RB	RB nt	95.24–100 [5]	86.08–100 [5]	See GVA^{I}		97.43–100	91.58–100
	RB aa	94.51–100 [5]	84.62–100 [5]			97.80–100	92.31–100

[1] RdRp = RNA-dependent RNA polymerase, MP = movement protein, CP = coat protein, RB = RNA-binding protein, nt = percentage nucleotide identity, aa = percentage amino acid similarity. [2] I = GVA^{I}, II = GVA^{II}, III = GVA^{III}, grapevine virus A isolates from the phylogroups I, II and III. [3] Only one whole genome sequence from group I was available from Australia. [4] Only two sequences were compared. [5] Identities or similarities obtained from both GVA^{I} and GVA^{II} isolates.

3.3. Association between Amino acid Sequence of RNA-Binding Gene and Symptom Expression of Grapevine Virus A

Amino acid sequences of the RB gene of GVA isolates obtained from Meta-HTS in this study, and GVA isolates associated with SD from previous studies [11,19,32,33] were aligned and the results are shown in Figure 3. All Australian GVA^{III} isolates from this study have an extra four aa residues at the c-terminus, whereas the two GVA^{III} isolates from South Africa, P163-1 and GTR1-1, and other GVA^{I} and GVA^{II} isolates, lack these residues. No association between symptom expression and amino acid residue changes were observed consistently between GVA^{I} and GVA^{II} isolates from SD-affected and -unaffected grapevines. GVA^{III} isolates consistently had a leucine residue at position 31, which was not found in GVA ^{I} and GVA^{II} isolates (Figure 3), and a glutamic acid residue at position 61 that was only found in one GVA^{II} isolate (WIL2_N36_SD).

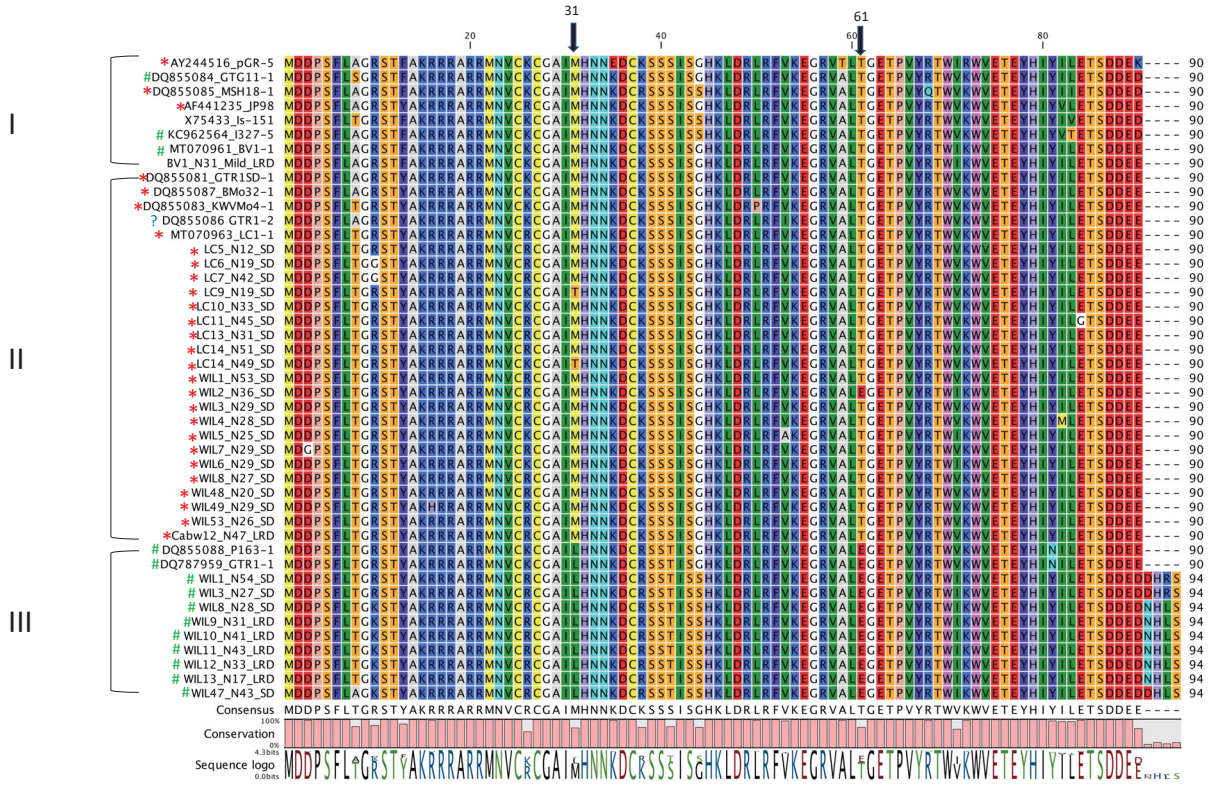

Figure 3. Amino acid alignment of the N-terminal (90–94 aa) of the RNA-binding gene of grapevine virus A (GVA) of Australian and international isolates. The phylogenetic group (I, II or III) of each isolate is on the left. Red * indicates isolates associated with Shiraz disease (SD) and green # indicates isolates not associated with SD. The blue question mark indicates a SD-negative isolate in phylogenetic group II [11]. The two black arrows point to positions 31 and 61 of the alignment.

3.4. Phylogenetic Analysis of Grapevine Leafroll-Associated Virus 3

The nucleotide sequences of 77 near-complete genome sequences from GenBank and 21 genome sequences from this study were analysed (Figure 4 and Table S8). The phylogenetic trees obtained from the complete genome sequence (above 17,027 nts) and CP gene alignments both show five major phylogenetic groups. Group names were redefined based on the genetic distance to the exemplar isolate NY1 (nt identities high to low) of the full genome sequences (Figure 4a) and CP genes (Figure 4b). The 21 Meta-HTS sequences of this study share 99.86 to 99.99% nt identities with each other using alignment of the complete genome sequences of 18,1713 nts. They all clustered into group I with the exemplar isolate NY1 from USA. Phylogenetic analysis of the RdRp and HSP70h genes confirmed the five-group system. The CP sequences within phylogroup I, II, III, IV and V share 94.59–99.47%, 92.46–92.78%, 91.4–91.72%, 81.1–82.70% and 74.31–79.83% nt identities, respectively, when compared to the isolate NY1 (Table S8). The standard length of the GLRaV-3 CP gene is 942 nts, with only one unique isolate, 3m-139 (accession no. JX266782) from *Vitis vinifera* cv. Sauvignon Blanc from Australia has an extra 15 nts insertion compared to other isolates. This isolate is believed to be an asymptomatic variant of GLRaV-3 [42,43].

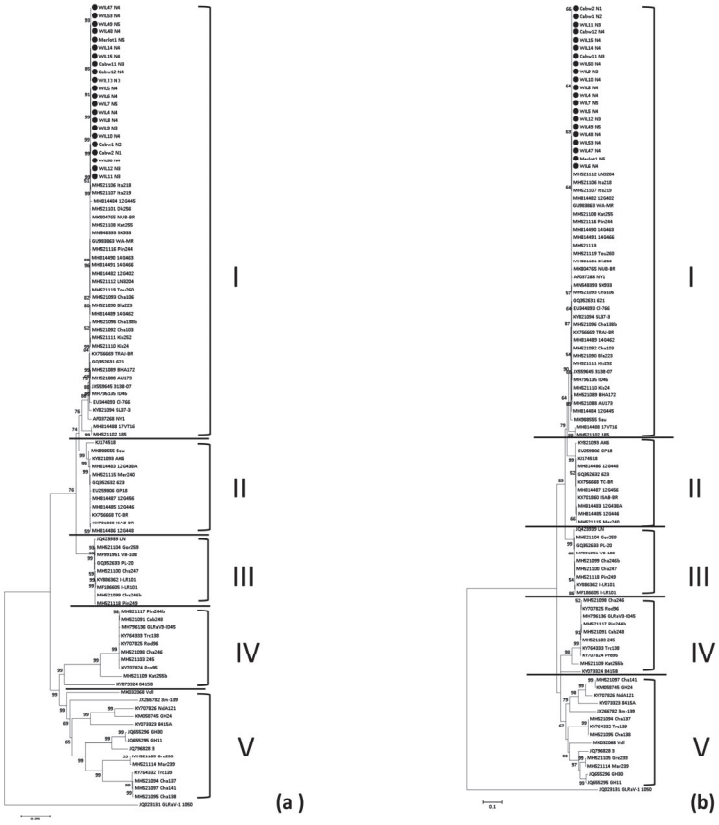

Figure 4. Phylogenetic analysis of 21 near-complete genome sequences (above 17,027 nts) of Australian grapevine leafroll-associated virus 3 (GLRaV-3) isolates and 77 publicly available full genome GLRaV-3 sequences from GenBank. A neighbour-joining tree of (**a**) complete genome sequences, (**b**) nucleotide sequence of the coat protein gene, was constructed with 1000 bootstrap replicates by MEGA software. Black dots denote sequences generated by Meta-HTS of this study. The bootstrap values below 50% are not shown. Sequences generated by this study are labelled by black dots. Roman numerals I–V represent the five distinct GLRaV-3 phylogroups observed in this study.

3.5. Phylogenetic Analysis of Grapevine Leafroll-Associated Virus 4, Strains 5, 6 and 9

The Meta-HTS assembled a total of 35 near-complete genome sequences of GLRaV-4 isolates from 31 grapevines including 5/31 that had two distinct strains, and they were compared with all complete genome sequences available in the GenBank database. The phylogenetic analysis of the complete genome sequence and aa sequences of the RdRp, HPS70h and CP gene showed five major clades, which represent strains 4, 5, 6, 9 and 10 (Figure 5). Table S9 shows the amino acid pairwise similarities of the RdRp, HPS70h and CP genes for each isolate with the exemplar isolate LR106 (accession no. FJ467503). GLRaV-4 strain 9 is more frequently found among all Meta-HTS sequences of GLRaV-4 (26 out of 36), followed by strain 6 (8 out of 36) (Figure 5; Table S9). GLRaV-4 strain 5 is the most uncommon strain that was only found in three grapevines at WIL (WIL13 to WIL15) (Tables S6 and S9). The two unique strains Ob and Car are phylogenetically distantly related to other strains used for analysis, as indicated by the star symbols in Figure 5a. Strain Ob shares the lowest aa similarity of 72.54% with the exemplar isolate LR106 in the RdRp gene (Table S9). It is nine amino acids longer than other GLRaV-4 strains (527 aa compares to 518 aa). The isolate Car has one amino acid extra in the HSP70h protein compared to other isolates (535 aa compares to 534 aa). By pairwise similarity matrix, Ob and Car had the lowest pairwise aa similarity to other isolates in the HSP70h gene, ranging from 66.17 to 71.35% (Table S9).

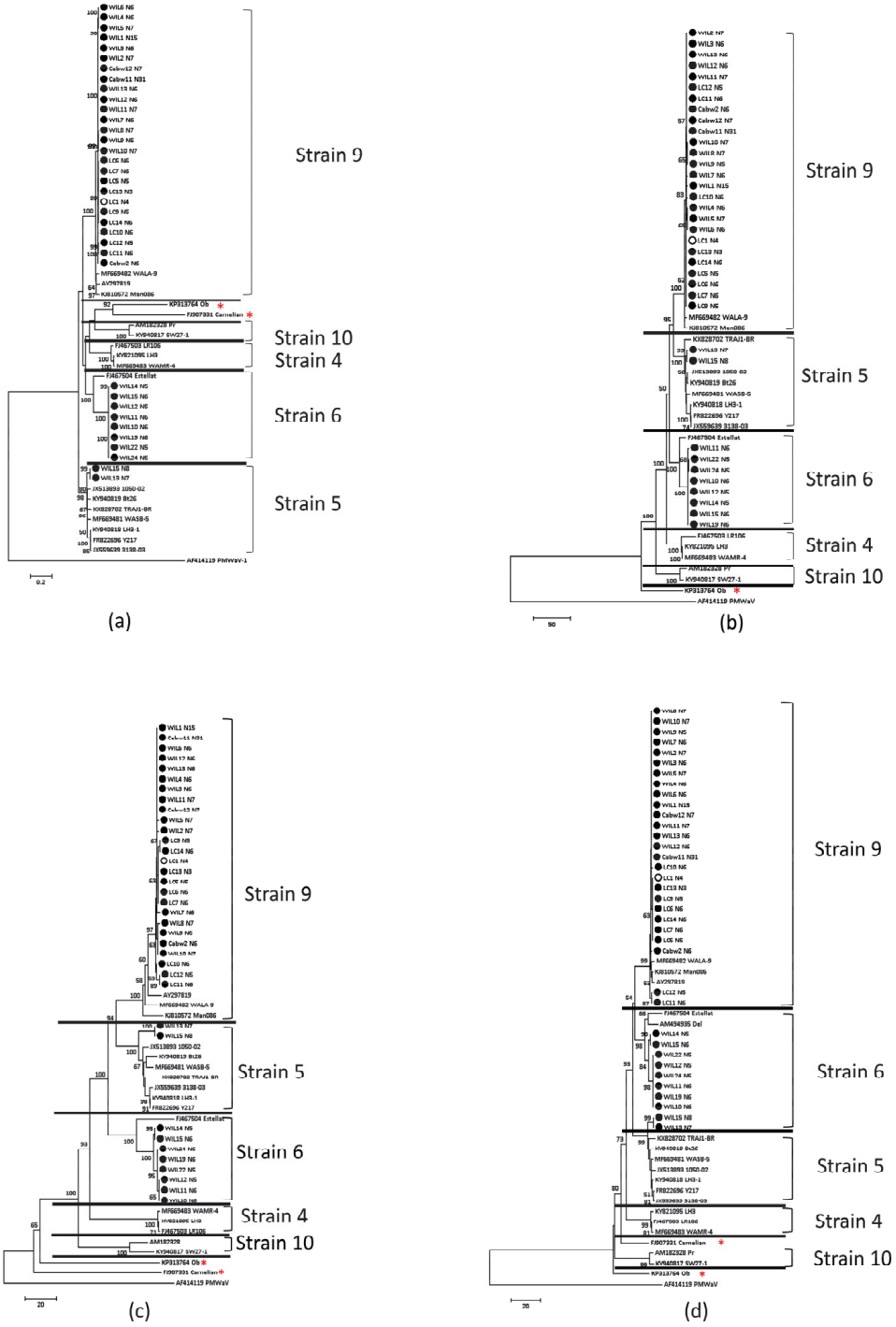

Figure 5. Neighbour-joining phylogenetic trees of grapevine leafroll-associated virus 4 (GLRaV-4) detected by metagenomic high-throughput sequencing and isolates from the GenBank database. Phylogenetic trees constructed by alignments of (**a**) complete genome sequences (above 12600 nts), (**b**) amino acid (aa) sequences of the RNA-dependent RNA polymerase (RdRp), (**c**) aa sequences of the heat shock protein 70 homologue (HSP70h) and (**d**) aa sequences of the coat protein (CP) gene. Bootstrap values less than 50% are not shown. * Indicates GLRaV-4 isolates with similarities to the exemplar isolate LR106 (accession no. FJ467503) below the demarcation of this species. Open circles indicate sequences generated by a previous study [1] and black dots display the sequences by this study.

Based on the length of the CP aa sequence, all isolates of strain 4 and strain 10 had 273 aa, all isolates of strains 5 and 9 had 268 aa and all isolates of 6 had 269 aa. The CP gene protein homology shows that strains 5, 6 and 9 are phylogenetically more similar than strains 4, 10, Car and Ob. Within strain 4, 5, 6, 9 and 10, pairwise aa similarity of the CP gene to the exemplar isolate LR106 (accession no. FJ467503) shares 99.26–99.63%, 81.02–83.21%, 79.93–80.66%, 81.39–82.48% and 77.01% (only one isolate), respectively, using similarity matrix of all GenBank available isolates and Australian isolates listed in Table S9.

3.6. Recombination Analysis

Recombination analysis was performed for all Meta-HTS sequences along with complete genome sequences from GenBank (Tables S7–S9) used in phylogenetic analysis. No recombination events were detected in GVA, GLRaV-3 and GLRaV-4 sequences obtained from this study.

4. Discussion

4.1. Association between SD and Phylogenetic Groups of GVA

In this comprehensive virome study, further evidence of the association between GVA^{II} variants and SD in Australia was shown, supporting previous studies both in Australia and South Africa [10]. This study indicated that GVA^{II} variants might also be associated with SD in Merlot, although only one grapevine was analysed. Although GVA^{III} variants were often found in mixed infections with GVA^{II} variants, the results presented in this study suggest they are unlikely to be associated with SD symptoms on Shiraz because they were also present in LRD and asymptomatic grapevines in the absence of GVA^{II} variants (Tables 2 and S5). GVA^{III} was only found in one SD-affected grapevine (WIL47) with Meta-HTS, but this sample was positive by endpoint RT-PCR, which detects GVA^{I} and GVA^{II} variants. Therefore, it is possible that a GVA^{II} variant was present in WIL47 but the titre was too low for detection by Meta-HTS. GVA^{I} was only found in a few LRD-affected grapevines from BV, and in this study, was not associated with SD.

Although a strong association between GVA^{II} and SD was observed, it is possible that some GVA^{I} and GVA^{III} variants could cause SD, and that some GVA^{II} variants may not. For example, isolate GTR1-2 from South Africa was identified as SD-negative and induced mild vein clearing symptoms on *N. benthamiana* [11] and yet it belongs to group II (Figure 2a). This is likely due to the ORF1, ORF3, 5′NTR and 3′NTR, which were clearly divergent from other GVA^{II} isolates [11]. Although the current data suggest that GVA^{II} variants are most likely to be the key pathogen of SD in Australia, phylogenetic grouping of a variant should not be used alone to predict virulence. Broader surveillance of SD-sensitive varieties, with and without SD, across multiple grape-growing regions should be performed to further confirm the association between specific GVA phylogroups and SD.

4.2. Amino Acid Sequence of RNA-Binding Gene of GVA and Symptom Expression

ORF5 of GVA, which encodes a 10 kDa RNA-binding protein, was reported to play an important role in symptom expression on *N. benthamiana*. When ORF5 of the infectious clone of isolate PA3 was modified, this virulent clone no longer induced symptoms on *N. benthamiana* [20]. Later, it was demonstrated that an association between symptom severity in *N. benthamiana* plants inoculated with seven South African GVA isolates was dependent on the eighth amino acid sequence from the N-terminus [22]. Therefore, we investigated if this change could be involved in SD symptom expression in Australian isolates, but it was not demonstrated in this study. Goszczynski and Habili [10] reported the South African GVA^{II} isolate, P163-M5 (accession no. DQ855082), has a 119 nt insertion on ORF 2 and this isolate induced stronger leaf mottling symptoms on *N. benthamiana* compared to other South African GVA isolates. ORF 2 encodes a putative 19-kDa protein with no significant sequence identity to other proteins in the database. Only one other GVA^{II} isolate, M5v (accession no. MK982553), has this insertion at the same position. This study therefore illustrates that this insertion is not associated with SD symptom expression

in Australian isolates. This study did highlight residues at positions 31 and 61, which differentiated the GVA^{III} phylogroup from GVA^{II} isolates consistently, and GVA^{I} isolates in most cases (Figure 3). This may highlight important residues that could impact the virulence of GVA; however, further studies are required to test this hypothesis. Further comparative genomic analyses and functional genomic studies are required to investigate the specific sequences that interact with the host to cause SD in sensitive varieties.

4.3. GVA Diversity

Phylogenetic relationships between GVA^{I} and GVA^{II} isolates, based on genomes and individually analysed RdRp, MP and CP genes, indicate that they are more closely related to each other than either group are to GVA^{III}. They share the same primary branch with ≥99% bootstrap support (Figures 2 and S2, in red square), and cannot be differentiated using the neighbour-joining trees of the RNA-binding gene by both nt and aa sequence (Figures 2g and S2b). In addition, some GVA isolates were placed within the GVA^{I} clade when analysing nt sequences of the CP gene but placed within the GVA^{II} clade when using the aa sequence of the same gene (Figure 2e). This all supports the hypothesis that GVA^{I} and GVA^{II} phylogroups may have diverged from the same ancestor.

Diversity between GVA^{II} and GVA^{III} strains was observed in Shiraz, Cabernet Sauvignon and Merlot grapevines at WIL, although some Shiraz grapevines had GVA strains that were almost identical (Figure 2a). When the longest GVA^{III} contigs from each of the Cabernet Sauvignon, Merlot and Shiraz samples were analysed by pairwise nt identity, the identities of GVA^{II} and GVA^{III} contigs were between 91.05–99.96% and 95.04–99.95%, respectively (Figure S3). This suggests GVA infection may have originated from multiple sources. One Cabernet Sauvignon grapevine (Cabw12) had two distinct GVA^{II} strains, and both strains clustered with GVA^{II} strains from SD-affected grapevines at WIL and LC but were not identical (Figure 2a and Table S6). Therefore, although some spread may have occurred between Shiraz grapevines and adjacent vineyards, infections are also likely to have been introduced from other sources.

4.4. GLRaV-3

As a part of this study, the diversity of GLRaV-3 and GLRaV-4 were also investigated in SD and asymptomatic grapevines due to previous observations that these viruses may play a role in this disease [1]. Using all available GLRaV-3 sequences from GenBank, and Australian isolates from this study, a tree with five phylogroups was produced and new naming of these proposed based on the aa sequence similarity of the CP gene from high (phylogroup I) to low (phylogroup V) to the exemplar isolate NY1. This finding contrasts to several previous studies, including our preliminary study, which identified seven phylogroups [1], and that described by Diaz-Lara et al. (2018) that identified 10 phylogroups [44]. It appears the addition of a larger number of full-length GLRaV-3 genomes and CP gene sequences in our most recent phylogenetic analysis has more clearly defined the evolutionary relationship between isolates, resulting in the collapse of previously described phylogroups to a smaller number. This proposed grouping was also reflected in one previous study, which used all available GenBank sequences of the full-length CP gene when assessing GLRaV-3 isolates obtained from Portuguese grapevine varieties [45]. This study demonstrated that the phylogroup of any novel GLRaV-3 isolates could be identified using any of CP, RdRp, HSP70h or full-length sequences since they provided consistent results (Figure 4 and Table S9).

In this study, low diversity between all Australian GLRaV-3 strains was observed that were all isolated from grapevines located in the WIL vineyard. These all clustered in phylogroup I, including those infecting Shiraz, Cabernet Sauvignon SA125 (Cabw1, 2, 11, 12) and Merlot (Merlot 1), and shared 99.86 to 99.99% nt identity. This suggests a single origin of the virus at the WIL site, potentially from the same source, and then transmitted by natural spread through insect vectors. According to the phylogenetic analysis of GLRaV-3,

all Australian GLRaV-3 isolates clustered with the NY1, which could indicate they might have originated from the USA.

4.5. GLRaV-4

GLRaV-4 species are the most genetically diverse groups within the *Ampelovirus* genus, and GLRaV-4 strains 4/5, 4/6, 4/9, 4/10, 4/Car, 4/De and 4/Pr were previously thought to be independent virus species. In 2012 they were classified by Martelli et al. [4] into a single species based on their serological relationships, genome structure, size, and biological and epidemiological characteristics. Strains Ob and Car have been classified as strains of GLRaV-4, but they have lower homology to other strains of this virus [46,47].

In this study, genomes of Australian isolates of GLRaV-4/5, -4/6 and -4/9 are reported for the first time. GLRaV-4 strains 6 and 9 in Shiraz from WIL and LC showed low diversity and close phylogenetic relationships to the GLRaV-4 isolates in Cabernet Sauvignon from WIL (Figure 5). This suggests the GLRaV-4 in Shiraz from WIL and LC may have originated from the same source, possibly the Cabernet Sauvignon clone SA125.

4.6. Other Viruses

Other viruses that were detected in grapevines in this study included GLRaV-1, GRVFV, GRSPaV, GVF and GRGV. GRVFV and GRSPaV were two abundant viruses in all the South Australian vineyards studied and were found in SD- and LRD-affected and -unaffected grapevines. They are therefore, not considered to be associated with SD or LRD and were not studied further. GLRaV-1, GVF and GRGV were infrequently found and also not considered to be associated with SD. This is the first report of GVF and GRGV in Australia. The detection of these two viruses will be described in a different paper in the near future.

4.7. Variability in Virus Detection

Variability in the detection of some viruses by Meta-HTS and RT-PCR was observed. The detection of viruses by Meta-HTS and not by RT-PCR is most likely due to sequence variability at the RT-PCR primer binding sites. For example, in this study, the primer pair H7038/C7273 from Goszczynski and Jooste [33], that were claimed to detect all GVA strains, only detected strains GVA^{I} and GVA^{II}, and a third assay was required to detect GVA^{III} variants. The failure to detect GLRaV-4/9 and GRVFV in some samples by Meta-HTS could be due to low virus titre in the extracts, which could be below the detection threshold due to seasonal fluctuation or uneven distribution of the virus in the sampled tissue [48,49].

4.8. Association between SD and LRD Species

In all SD-affected grapevines, at least one grapevine leafroll virus species, either GLRaV-3 or GLRaV-4, was also present with GVA (Table 2, Tables S4 and S5). This may be associated with the enhanced transmission efficiency of GVA by insect vectors in the presence of GLRaVs [50]. It is possible that the presence of a GLRaV species is important in SD symptom expression; however, there was no association to a specific GLRaV species. Additionally, strains of GLRaV-3 and GLRaV-4 were found in LRD-only-affected grapevines and asymptomatic grapevines, suggesting they are not the sole cause of SD.

In conclusion, this study showed a strong association between GVA^{II} variants and SD. SD has only been reported from two countries, Australia and South Africa. This distribution could be due to the low prevalence of SD-related GVA^{II} variants in the USA and other countries (Table S7). Another reason for the prevalence of SD in Australia could also be due to more conducive environmental conditions or more efficient insect vectors. In this study, clone SA125 of Cabernet Sauvignon was tolerant to infection by GVA^{II} as SD symptoms were not observed. This clone is one of the most widely planted Cabernet Sauvignon clones in South Australia and could present a risk for the spread of GVA and SD disease but could also pose a risk if infected grapevines are top worked with sensitive varieties, as has previously been observed [51]. Further work to investigate the prevalence and relationships between strains within and between vineyards to estimate the risk of the

disease in other regions is still required. A better understanding of vector efficiency for the transmission of GVA and GLRaVs is also required. This highlights the importance of pathogen testing and the provision of high-quality planting material to ensure disease-free sustainable vineyards.

Supplementary Materials: The following supporting information can be downloaded at: https://www.mdpi.com/article/10.3390/v15030774/s1, Figure S1: Vineyard map of the Willunga site. Figure S2: Neighbor-joining phylogenetic analysis of amino acid (aa) sequences of full-length movement protein (MP) and RNA-binding (RB) genes of grapevine virus A (GVA) using metagenomic sequences and sequences from GenBank; Figure S3: Color coded percentage of nucleotide (nt) pairwise identities of grapevine virus A (GVA) contigs in this study; Table S1: Sampling time, numbers of canes or petioles sampled per grapevine, tissue type and sample codes for samples used in the reverse transcription polymerase chain reaction (RT-PCR) and metagenomics high throughput sequencing (Meta-HTS) experiments; Table S2: Primers sequences for virus detection using endpoint RT-PCR [52–60]; Table S3: Symptom observation and the viruses detected in Shiraz grapevines at the Willunga, Langhorne Creek, Barossa, and Adelaide University (Coombe's) vineyards using endpoint RT-PCR; Table S4: Virus detection of samples tested by RT-PCR but not tested by high throughput sequencing, and the symptoms that were observed; Table S5: Virus status detected by RT-PCR and metagenomic high-throughput sequencing (Meta-HTS) and the GVA phylogroup that was identified; Table S6: Basic statistics and list of contigs of the 50 grapevine samples sequenced by the NovaSeq (Illumina) instrument; Table S7: Details of grapevine virus A (GVA) isolate sequences used for the phylogenetic analysis; Table S8: Details of the Australian grapevine leafroll-associate virus 3 (GLRaV-3) isolates generated by metagenomic high-throughput sequencing and the publicly available isolates used for the phylogenetic analysis; Table S9: Pairwise amino acid similarity of grapevine leafroll-associated virus 4 (GLRaV-4) to the exemplar isolate LR106 (GLRaV-4 strain 4, accession no. FJ467503).

Author Contributions: Conceptualization, Q.W., F.E.C. and N.H.; methodology, Q.W., F.E.C. and N.H.; data and photos, Q.W., W.M.K., L.Z. and F.E.C.; writing—original draft preparation, Q.W., F.E.C. and N.H.; writing—review and editing, Q.W., F.E.C., N.H., W.M.K., A.R. and S.D.T.; project administration, F.E.C. and S.D.T.; funding acquisition, F.E.C., S.D.T. and A.R. All authors have read and agreed to the published version of the manuscript.

Funding: This work was supported by Wine Australia under the project WAPh1706, with levies from Australia's grapegrowers and winemakers and matching funds from the Australian Government. It was also supported by funding from Agriculture Victoria Research, the University of Adelaide and the Australian Wine Research Institute.

Institutional Review Board Statement: Not applicable.

Informed Consent Statement: Not applicable.

Data Availability Statement: The sequencing data were submitted to the GenBank database and can be accessed using the accession numbers provided at the National Center of Biotechnology Information website [61].

Acknowledgments: I would like to thank the managers and owners of the Barossa valley, Willunga, Langhorne Creek and Coombe's vineyards for supporting this study.

Conflicts of Interest: The authors declare no conflict of interest.

References

1. Wu, Q.; Habili, N.; Constable, F.; Al Rwahnih, M.; Goszczynski, D.E.; Wang, Y.; Pagay, V. Virus pathogens in Australian vineyards with an emphasis on Shiraz disease. *Viruses* **2020**, *12*, 818. [CrossRef]
2. Habili, N.; Randles, J.W. Major yield loss in Shiraz vines infected with Australian Shiraz disease associated with grapevine virus A. In Proceedings of the 17th Meeting of the International Council for the Study of Viruses and Virus-like Diseases of the Grapevine, Davis, CA, USA, 7–14 October 2012; pp. 164–165.
3. Australian Grape and Wine. Available online: https://www.agw.org.au/ (accessed on 6 February 2023).

4. Martelli, G.P.; Ghanem-Sabanadzovic, N.A.; Agranovsky, A.A.; Al Rwahnih, M.; Dolja, V.V.; Dovas, C.I.; Fuchs, M.; Gugerli, P.; Hu, J.S.; Jelkmann, W.; et al. Taxonomic revision of the family Closteroviridae with special reference to the grapevine leafroll-associated members of the genus Ampelovirus and the putative species unassigned to the family. *J. Plant Pathol.* **2012**, *94*, 7–19.
5. Maree, H.J.; Almeida, R.P.P.; Bester, R.; Chooi, K.M.; Cohen, D.; Dolja, V.V.; Fuchs, M.F.; Golino, D.A.; Jooste, A.E.C.; Martelli, G.P.; et al. Grapevine leafroll-associated virus 3. *Front. Microbiol.* **2013**, *4*, 82. [CrossRef] [PubMed]
6. Cabaleiro, C.; Segura, A.; Garcia-Berrios, J.J. Effects of grapevine leafroll-associated virus 3 on the physiology and must of *Vitis vinifera* L. cv. Albarino following contamination in the field. *Am. J. Enol. Vitic.* **1999**, *50*, 40–44. [CrossRef]
7. Mannini, F.; Mollo, A.; Credi, R. Field performance and wine quality modification in a clone of *Vitis vinifera* cv. Dolcetto after GLRaV-3 elimination. *Am. J. Enol. Vitic.* **2012**, *63*, 144–147. [CrossRef]
8. Endeshaw, S.T.; Sabbatini, P.; Romanazzi, G.; Schilder, A.C.; Neri, D. Effects of grapevine leafroll associated virus 3 infection on growth, leaf gas exchange, yield and basic fruit chemistry of *Vitis vinifera* L. cv. Cabernet Franc. *Sci. Hortic.* **2014**, *170*, 228–236. [CrossRef]
9. Almeida, R.; Daane, K.; Bell, V.; Blaisdell, G.K.; Cooper, M.; Herrbach, E.; Pietersen, G. Ecology and management of grapevine leafroll disease. *Front. Microbiol.* **2013**, *4*, 94. [CrossRef] [PubMed]
10. Goszczynski, D.E.; Habili, N. Grapevine virus A variants of group II associated with Shiraz disease in South Africa are present in plants affected by Australian Shiraz disease, and have also been detected in the USA. *Plant Pathol.* **2012**, *61*, 205–214. [CrossRef]
11. Goszczynski, D.E.; Du Preez, J.; Burger, J.T. Molecular divergence of grapevine virus A (GVA) variants associated with Shiraz disease in South Africa. *Virus Res.* **2008**, *138*, 105–110. [CrossRef]
12. Corbett, M.K.; Wiid, J. Closterovirus-like particles in extracts from diseased grapevines. *Phytopathol. Mediterr.* **1985**, *24*, 91–100.
13. Habili, N.; Scliefert, L. The increasing threat of grapevine virus A and its association with restricted spring growth in Australia. *Aust. N. Z. Grapegrow. Winemak.* **2001**, *452*, 22–26.
14. Symons, B.; Habili, N. Grapevine virus A is associated with restricted growth in the spring. *Aust. N. Z. Grapegrow. Winemak.* **2000**, *443*, 17–19.
15. Habili, N.; Randles, J.W. Descriptors for grapevine virus A-associated syndrome in Shiraz, Merlot and Ruby Cabernet in Australia, and its similarity to Shiraz disease in South Africa. *Aust. N. Z. Grapegrow. Winemak.* **2004**, *488*, 71–74.
16. Habili, N. It's not worth the gamble: Serious problems associated with top-working virus-infected vines. *Aust. N. Z. Grapegrow. Winemak.* **2003**, *476*, 84–89.
17. Minafra, A.; Saldarelli, P.; Grieco, F.; Martelli, G.P. Nucleotide sequence of the 3′ terminal region of the RNA of two filamentous grapevine viruses. *Arch. Virol.* **1994**, *137*, 249–261. [CrossRef] [PubMed]
18. Minafra, A.; Saldarelli, P.; Martelli, G.P. Grapevine virus A: Nucleotide sequence, genome organization, and relationship in the Trichovirus genus. *Arch. Virol.* **1997**, *142*, 417–423. [CrossRef] [PubMed]
19. Haviv, S.; Iddan, Y.; Goszczynski, D.E.; Mawassi, M. The ORF5 of grapevine virus A is involved in symptoms expression in *Nicotiana benthamiana* plants. *Ann. Appl. Biol.* **2012**, *160*, 181–190. [CrossRef]
20. Galiakparov, N.; Tanne, E.; Mawassi, M.; Gafny, R.; Sela, I. ORF 5 of grapevine virus A encodes a nucleic acid-binding protein and affects pathogenesis. *Virus Genes* **2003**, *27*, 257–262. [CrossRef]
21. Dry, P.R.; Coombe, B.G.; Anderson, C.J. *Viticulture: Volume 2. Practices*, 2nd ed.; Winetitles: Adelaide, Australia, 2004.
22. Balijja, A.; Kvarnheden, A.; Turchetti, T. A non-phenol–chloroform extraction of double-stranded RNA from plant and fungal tissues. *J. Virol. Methods* **2008**, *152*, 32–37. [CrossRef] [PubMed]
23. Nassuth, A.; Pollari, E.; Helmeczy, K.; Stewart, S.; Kofalvi, S.A. Improved RNA extraction and one-tube RT-PCR assay for simultaneous detection of control plant RNA plus several viruses in plant extracts. *J. Virol. Methods* **2000**, *90*, 37–49. [CrossRef]
24. Green, M.R.; Sambrook, J. Precipitation of RNA with Ethanol. *Cold Spring Harb. Protoc.* **2020**, *101717*, 89–91. [CrossRef] [PubMed]
25. Krueger, F. Trim Galore, v. 0.4.2. 2012. Available online: https://github.com/FelixKrueger/TrimGalore (accessed on 20 February 2021).
26. Bankevich, A.; Nurk, S.; Antipov, D.; Gurevich, A.A.; Dvorkin, M.; Kulikov, A.S.; Lesin, V.M.; Nikolenko, S.I.; Pham, S.; Prjibelski, A.D. SPAdes: A new genome assembly algorithm and its applications to single-cell sequencing. *J. Comput. Biol.* **2012**, *19*, 455–477. [CrossRef]
27. Altschul, S.F.; Madden, T.L.; Schäffer, A.A.; Zhang, J.; Zhang, Z.; Miller, W.; Lipman, D.J. Gapped BLAST and PSI-BLAST: A new generation of protein database search programs. *Nucleic Acids Res.* **1997**, *25*, 3389–3402. [CrossRef] [PubMed]
28. Bushnell, B. *BBMap: A Fast, Accurate, Splice-Aware Aligner*; Lawrence Berkeley National Lab (LBNL): Berkeley, CA, USA, 2014.
29. Edgar, R.C. MUSCLE: Multiple sequence alignment with high accuracy and high throughput. *Nucleic Acids Res.* **2004**, *32*, 1792–1797. [CrossRef] [PubMed]
30. Muhire, B.M.; Varsani, A.; Martin, D.P. SDT: A virus classification tool based on pairwise sequence alignment and identity calculation. *PLoS ONE* **2014**, *9*, e108277. [CrossRef]
31. Kumar, S.; Stecher, G.; Tamura, K. MEGA7: Molecular evolutionary genetics analysis version 7.0 for bigger datasets. *Mol. Biol. Evol.* **2016**, *33*, 1870–1874. [CrossRef]
32. Goszczynski, D.E. Single-strand conformation polymorphism (SSCP), cloning and sequencing reveal a close association between related molecular variants of Grapevine virus A (GVA) and Shiraz disease in South Africa. *Plant Pathol.* **2007**, *56*, 755–762. [CrossRef]

33. Goszczynski, D.E.; Jooste, A.E.C. Identification of grapevines infected with divergent variants of grapevine virus A using variant-specific RT-PCR. *J. Virol. Methods* **2003**, *112*, 157–164. [CrossRef]
34. Martin, D.P.; Varsani, A.; Roumagnac, P.; Botha, G.; Maslamoney, S.; Schwab, T.; Kelz, Z.; Kumar, V.; Murrell, B. RDP5: A computer program for analyzing recombination in, and removing signals of recombination from, nucleotide sequence datasets. *Virus Evol.* **2021**, *7*, veaa087. [CrossRef]
35. Martin, D.; Rybicki, E. RDP: Detection of recombination amongst aligned sequences. *Bioinformatics* **2000**, *16*, 562–563. [CrossRef]
36. Sawyer, S.A. *GENECONV: A Computer Package for the Statistical Detection of Gene Conversion*; Department of Mathematics, Washington University in Louis: Washington, WA, USA, 1999.
37. Posada, D.; Crandall, K.A. Evaluation of methods for detecting recombination from DNA sequences: Computer simulations. *Proc. Natl. Acad. Sci. USA* **2001**, *98*, 13757–13762. [CrossRef] [PubMed]
38. Smith, J.M. Analyzing the mosaic structure of genes. *J. Mol. Evol.* **1992**, *34*, 126–129. [CrossRef] [PubMed]
39. Salminen, M.O.; Carr, J.K.; Burke, D.S.; McCutchan, F.E. Identification of breakpoints in intergenotypic recombinants of HIV type 1 by bootscanning. *AIDS Res. Hum. Retrovir.* **1995**, *11*, 1423–1425. [CrossRef] [PubMed]
40. Gibbs, M.J.; Armstrong, J.S.; Gibbs, A.J. Sister-scanning: A Monte Carlo procedure for assessing signals in recombinant sequences. *Bioinformatics* **2000**, *16*, 573–582. [CrossRef]
41. Boni, M.F.; Posada, D.; Feldman, M.W. An exact nonparametric method for inferring mosaic structure in sequence triplets. *Genetics* **2007**, *176*, 1035–1047. [CrossRef]
42. Rast, H.E.; James, D.; Habili, N.; Masri, S.A. Genome organisation and characterization of a novel variant of grapevine leafroll-associated virus 3. In Proceedings of the 17th Meeting of the International Council for the Study of Virus and Virus-like Diseases of the Grapevine, Davis, CA, USA, 7–14 October 2012; pp. 61–63.
43. Habili, N.; Cameron, I.; Randles, J. A mild strain of grapevine leafroll-associated virus 3 is present in desirable clones of Crimson seedless table grapes in Western Australia. In Proceedings of the 16th Meeting of the International Council for the Study of Virus and Virus-like Diseases of the Grapevine, Dijon, France, 31 August–4 September 2009; pp. 237–238.
44. Diaz-Lara, A.; Klaassen, V.; Stevens, K.; Sudarshana, M.R.; Rowhani, A.; Maree, H.J.; Chooi, K.M.; Blouin, A.G.; Habili, N.; Song, Y.; et al. Characterization of grapevine leafroll-associated virus 3 genetic variants and application towards RT-qPCR assay design. *PLoS ONE* **2018**, *13*, e0208862. [CrossRef]
45. Gouveia, P.; Santos, M.T.; Eiras-Dias, J.E.; Nolasco, G. Five phylogenetic groups identified in the coat protein gene of grapevine leafroll-associated virus 3 obtained from Portuguese grapevine varieties. *Arch. Virol.* **2011**, *156*, 413–420. [CrossRef]
46. Ghanem-Sabanadzovic, A.; Sabanadzovic, S.; Uyemoto, J.K.; Golino, D.; Rowhani, A. A putative new ampelovirus associated with grapevine leafroll disease. *Arch. Virol.* **2010**, *155*, 1871–1876. [CrossRef]
47. Reynard, J.-S.; Schneeberger, P.H.H.; Frey, J.E.; Schaerer, S. Biological, serological, and molecular characterization of a highly divergent strain of grapevine leafroll-associated virus 4 causing grapevine leafroll disease. *Phytopathology* **2015**, *105*, 1262–1269. [CrossRef]
48. Osman, F.; Leutenegger, C.; Golino, D.; Rowhani, A. Comparison of low-density arrays, RT-PCR and real-time TaqMan® RT-PCR in detection of grapevine viruses. *J. Virol. Methods* **2008**, *149*, 292–299. [CrossRef]
49. Čepin, U.; Gutiérrez-Aguirre, I.; Balažic, L.; Pompe-Novak, M.; Gruden, K.; Ravnikar, M. A one-step reverse transcription real-time PCR assay for the detection and quantitation of grapevine fanleaf virus. *J. Virol. Methods* **2010**, *170*, 47–56. [CrossRef]
50. Le Maguet, J.; Beuve, M.; Herrbach, E.; Lemaire, O. Transmission of six ampeloviruses and two vitiviruses to grapevine by Phenacoccus aceris. *Phytopathology* **2012**, *102*, 717–723. [CrossRef]
51. Habili, N.; Wu, Q.; Pagay, V. Virus-associated Shiraz disease may lead Shiraz to become an endangered variety in Australia. *Wine Vitic. J.* **2016**, *31*, 47–50.
52. Minafra, A.; Hadidi, A. Sensitive detection of grapevine virus A, B, or leafroll-associated III from viruliferous mealybugs and infected tissue by cDNA amplification. *J. Virol. Methods* **1994**, *47*, 175–187. [CrossRef]
53. Fazeli, C.F.; Rezaian, M.A. Nucleotide sequence and organization of ten open reading frames in the genome of grapevine leafroll-associated virus 1 and identification of three subgenomic RNAs. *J. Gen. Virol.* **2000**, *81*, 605–615. [CrossRef] [PubMed]
54. Bertazzon, N.; Angelini, E. Advances in the detection of grapevine leafroll-associated virus 2 variants. *J. Plant Pathol.* **2004**, *86*, 283–290.
55. Habili, N.; Fazeli, C.F.; Ewart, A.; Hamilton, R.; Cirami, R.; Saldarelli, P.; Minafra, A.; Rezaian, M.A. Natural spread and molecular analysis of grapevine leafroll-associated virus 3 in Australia. *Phytopathology* **1995**, *85*, 1418–1422. [CrossRef]
56. Good, X.; Monis, J. Partial genome organization, identification of the coat protein gene, and detection of Grapevine leafroll-associated virus-5. *Phytopathology* **2001**, *91*, 274–281. [CrossRef]
57. Mahfoudhi, N.; Habili, N.; Masri, S.A.; Dhouibi, M.H. First report on the occurrence of grapevine leafroll-associated viruses 5 and 9 in Tunisian grapevines. *Plant Dis.* **2007**, *91*, 1359. [CrossRef]
58. Wu, Q.; Kehoe, M.; Kinoti, W.M.; Wang, C.; Rinaldo, A.; Tyerman, S.; Habili, N.; Constable, F.E. First report of grapevine rupestris vein feathering virus in grapevine in Australia. *Plant Dis.* **2020**, *105*, 515. [CrossRef] [PubMed]
59. Zhang, Y.-P.; Uyemoto, J.K.; Golino, D.A.; Rowhani, A. Nucleotide sequence and RT-PCR detection of a virus associated with grapevine rupestris stem-pitting disease. *Phytopathology* **1998**, *88*, 1231–1237. [CrossRef] [PubMed]

60. MacKenzie, D.J.; McLean, M.A.; Mukerji, S.; Green, M. Improved RNA extraction from woody plants for the detection of viral pathogens by reverse transcription-polymerase chain reaction. *Plant Dis.* **1997**, *81*, 222–226. [CrossRef] [PubMed]
61. National Center of Biotechnology Information. Available online: https://www.ncbi.nlm.nih.gov/ (accessed on 13 February 2023).

Supplementary Material

Table S1. Sampling time, numbers of canes or petioles sampled per grapevine, tissue type and sample codes for samples used in the reverse transcription polymerase chain reaction (RT-PCR) and metagenomics high throughput sequencing (Meta-HTS) experiments. Samples were collected from four vineyards between May 2018 and December 2020.

Sampling time	Vineyard locations[3]	tissue type	No. of canes/petioles per grapevine	Total no. of samples	Sample code
May to July 2018[1]	WIL, LC and BV	autumn or dormant canes	3	66	WIL1-30, LC1-30 and BV1-6
March 2019[1,2]	WIL, LC and BV	petioles	5	66	WIL1-30, LC1-30 and BV1-6
August 2020[1,2]	WIL	dormant canes	5	50	WIL31-81 (exclude WIL46)
December 2020[1,2]	WIL and CV	petioles	5	9	Cabw1, 2, 11 and 12, Merlot1 (WIL), Shiraz_OR_P5 and P6, CabSA125_R3V30 and R3V44 (CV)

[1] Samples for RT-PCR virus detection.
[2] Samples for metagenomics high throughput sequencing.
[3] WIL = Willunga, LC = Langhorne Creek, BV = Barossa Valley, CV= Coombe's Vineyard. All grapevines listed are var. Shiraz except Cabw = Cabernet Sauvignon clone SA125 from Willunga and CabSA125 = Cabernet Sauvignon clone SA125 from Coombe's Vineyard.

Table S2. Primers sequences for virus detection using endpoint RT-PCR.

Virus	Primers	Primer sequence (5′- 3′)	Annealing Temperature (°C)	Gene	Amplicon size	Reference
GVA	Ah587 Ac995	GACAAATGGCACACTACG AAGCCTGACCTAGTCATCTTGG	56	CP	430bp	[52]
GVA	H7038 C7273	AGGTCCACGTTTGCTAAG CATCGTCTGAGGTTTCTACTAT	56	RNA binding	273bp	[33]

GVA	GVAgroupIIIF[2] GVAgroupIIIR[2]	GGAGAGGTAGATATAGTAGGACC CTTCTTGCAGAGTCAAGGTC	56	CP	315	Modified from primer pair 6591F/6906R [33]
GLRaV-1	p35LR17589f p35LR17763r	AATCCTATGCGTCAGTATGC TGGCATCGTTGCTAAATTGAG	56	CP	174 bp	[53]
GLRaV-2	LR2-U2 LR2-L2	ATAATTCGGCGTACATCCCCACTT GCCCTCCGCGCAACTAATGACAG	56	HSP 70-like protein	332 bp	[54]
GLRaV-3	HSP70 HSP7070	GGGTCAAGTGCTCTAGTTAAGGTCA AAAGTGTCCACCAGTCTCAGTCC	58	HSP 70-like protein	167bp	[44]
GLRaV-3	LR3P-H420 LR3P-C629	GATTTAAGCGCGTTTTTCAGGAC CGGCACGATCGTACTTTCTAA	58	Hsp90-like protein	210 bp	[55]
GLRaV-4 strain 4	LR4CP298F LR4CP298R	CCTGTTACGCCGCCTACTAC GGTGCTTGTCACTCTCCGAA	56	CP	298bp	This study
GLRaV-4 strain 5[1]	LR5-1F LR5-1R	CCCGTGATACAAGGTAGGACA CAGACTTCACCTCCTGTTAC	55	3′-URT	690bp	[56]
GLRaV-4 strain 6	LR6_CPF LR6_CPR	AAATTCCGCGCCTMTTCAATG ATGTCTGGGGCCACCTTAGT	58	CP	563bp	This study
GLRaV-4 strain 9	LR9F LR9R	ACA GTG GTC GGC ATA AGA AAA G ACACAA ACA TGC AGG CCA AAG	56	Hsp90-like protein	250bp	[57]
GRVFV	GRVFV237F GRVFV237R	ACTGAGCTACAAGGTGAATTGC AGCAACCCACTGGAAGGGGATGG	60	Polyprotein	237bp	[58]
GRSPaV	RSP48 RSP49	AGCTGGGATTATAAGGGAGGT CCAGCCGTTCCACCACTAAT	56	CP	330bp	[59]
GVB	H6980 C7439	GTGCTAAGAACGTCTTCACAGC ATCAGCAAACACGCTTGAACCG	56	RNA binding	460bp	[60]
RubiscoL internal control	RBCL-H535 RBCL-C705	CTTTCCAAGGCCCGCCTCA CATCATCTTTGGTAAAATCAAGTCCA	56	N/A	171bp	[23]

[1] For Sanger sequencing only.
[2] Grapevine virus A phylogroup III specific RT-PCR assay.

Table S3. Symptom observation and the viruses detected in Shiraz grapevines at the Willunga, Langhorne Creek, Barossa, and Adelaide University (Coombe's) vineyards using endpoint RT-PCR.

Location	Symptoms	Variety and Clone	Virus detected by RT-PCR#	Number of grapevines with given virus
Willunga	Asymptomatic	Shiraz BVRC12	GRSPaV	1
			GRVFV, GRSPaV	3
			GLRaV-4/6, GRSPaV	1
			GLRaV-4/9, GRSPaV	2
			GLRaV-4/6, GRVFV, GRSPaV	10
			GLRaV-4/9, GRVFV, GRSPaV	7
			GLRaV-4/6, GLRaV-4/9, GRVFV, GRSPaV	5
	LRD	Shiraz BVRC12	GLRaV-3, GRSPaV	1
			GLRaV-3, GLRaV-4/6, GRSPaV	1
			GLRaV-3, GRVFV, GRSPaV	7
			GLRaV-3, GLRaV-4/9, GRVFV, GRSPaV	10
			GLRaV-3, GLRaV-4/6, GRVFV, GRSPaV	4
			GLRaV-3, GLRaV-4/6, GLRaV-4/9, GRVFV, GRSPaV	12
		Cabernet Sauvignon SA125	GVA, GLRaV-3, GLRaV-4/9, GRSPaV	4
	SD	Shiraz BVRC12	GVA, GLRaV-3, GRSPaV	2
			GVA, GLRaV-3, GRVFV, GRSPaV	5
			GVA, GLRaV-4/9, GRVFV, GRSPaV	1

			GVA, GLRaV-3, GLRaV-4/9, GRVFV, GRSPaV	8
		Merlot	GVA, GLRaV-3, GRSPaV	1
Langhorne Creek	Asymptomatic	Shiraz	GRSPaV	14
			GRVFV, GRSPaV	1
	SD		GVA, GRSPaV	5
			GVA, GLRaV-4/9	7
			GVA, GLRaV-4/9, GRVFV, GRSPaV	2
			GVA, GLRaV-4/6, GRVFV, GRSPaV	1
Barossa	Mild LRD	heritage Shiraz	GVA*, GLRaV-1, GRSPaV	3
	Asymptomatic		GRSPaV	3
Coombe's	Mild LRD	Cabernet Sauvignon SA125	GVA, GLRaV-4/9, GRSPaV	2
	Asymptomatic	Shiraz BVRC12	GRVFV, GRSPaV	2

*Grapevine virus A detected in the grapevine with mild leafroll disease symptoms in Barossa valley.
#GRSPaV = grapevine rupestris stem pitting-associated virus, GRVFV = grapevine rupestris vein feathering virus, GLRaV-1, -3 = grapevine leafroll-associated virus 1, and 3, GLRaV-4/6, -4/9 = grapevine leafroll-associated virus 4 strains 6 and 9, GVA = grapevine virus A.

Table S4. Virus detection of samples tested by RT-PCR but not tested by high throughput sequencing, and the symptoms that were observed.

Sample ID[1]	**Virus status by RT-PCR[2]**	**Symptoms[3]**
WIL16	GRVFV, GRSPaV	Asymptomatic
WIL18	GLRaV-4/6, GRVFV, GRSPaV	Asymptomatic
WIL20	GLRaV-4/6, GRVFV, GRSPaV	Asymptomatic
WIL21	GLRaV-4/6, GRVFV, GRSPaV	Asymptomatic
WIL23	GLRaV-4/6, GRVFV, GRSPaV	Asymptomatic
WIL25	GLRaV-4/6, GRVFV, GRSPaV	Asymptomatic
WIL26	GRVFV, GRSPaV	Asymptomatic

WIL27	GLRaV-4/6, GRVFV, GRSPaV	Asymptomatic
WIL28	GLRaV-4/6, GRSPaV	Asymptomatic
WIL29	GLRaV-4/6, GLRaV-4/9, GRVFV, GRSPaV	Asymptomatic
WIL30	GLRaV-4/6, GLRaV-4/9, GRVFV, GRSPaV	Asymptomatic
WIL31	GVA#, GLRaV-4/9, GRVFV, GRSPaV	Asymptomatic
WIL32	GVA*#, GLRaV-4/9, GRVFV, GRSPaV	SD
WIL33	GVA#, GLRaV-3, GLRaV-4/9, GRVFV, GRSPaV	LRD
WIL34	GVA#, GLRaV-4/9, GRVFV, GRSPaV	Asymptomatic
WIL35	GVA#, GLRaV-3, GRVFV, GRSPaV	LRD
WIL36	GLRaV-3, GRVFV, GRSPaV	LRD
WIL37	GLRaV-3, GRVFV, GRSPaV	LRD
WIL38	GVA#, GLRaV-3, GLRaV-4/6, GLRaV-4/9, GRVFV, GRSPaV	LRD
WIL39	GVA#, GLRaV-4/6, GLRaV-4/9, GRVFV, GRSPaV	Asymptomatic
WIL40	GVA#, GLRaV-3, GLRaV-4/6, GLRaV-4/9, GRVFV, GRSPaV	LRD
WIL41	GLRaV-3, GLRaV-4/6, GLRaV-4/9, GRVFV, GRSPaV	LRD
WIL42	GLRaV-3, GLRaV-4/6, GRVFV, GRSPaV	LRD
WIL43	GVA#, GLRaV-3, GLRaV-4/6, GRVFV, GRSPaV	LRD
WIL44	GLRaV-4/9, GRVFV, GRSPaV	Asymptomatic
WIL45	GVA#, GLRaV-4/9, GRVFV, GRSPaV	Asymptomatic
WIL51	GVA*, GLRaV-3, GRVFV, GRSPaV	SD
WIL52	GVA*, GLRaV-3, GRVFV, GRSPaV	SD
WIL54	GLRaV-3, GLRaV-4/9, GRVFV, GRSPaV	LRD
WIL55	GLRaV-3, GLRaV-4/9, GRVFV, GRSPaV	LRD
WIL56	GVA#, GLRaV-4/9, GRVFV, GRSPaV	Asymptomatic
WIL57	GLRaV-4/9, GRSPaV	Asymptomatic
WIL58	GLRaV-4/9, GRSPaV	Asymptomatic
WIL59	GLRaV-4/9, GRVFV, GRSPaV	Asymptomatic

WIL60	GLRaV-3, GLRaV-4/9, GRVFV, GRSPaV	LRD
WIL61	GLRaV-3, GLRaV-4/9, GRVFV, GRSPaV	LRD
WIL62	GVA#, GLRaV-3, GLRaV-4/9, GRVFV, GRSPaV	LRD
WIL63	GLRaV-3, GLRaV-4/9, GRVFV, GRSPaV	LRD
WIL64	GLRaV-3, GLRaV-4/9, GRVFV, GRSPaV	LRD
WIL65	GLRaV-3, GRVFV, GRSPaV	LRD
WIL66	GLRaV-3, GLRaV-4/6, GLRaV-4/9, GRVFV, GRSPaV	LRD
WIL67	GVA#, GLRaV-3, GLRaV-4/6, GLRaV-4/9, GRVFV, GRSPaV	LRD
WIL68	GVA#, GLRaV-3, GLRaV-4/6, GLRaV-4/9, GRVFV, GRSPaV	LRD
WIL69	GLRaV-3, GLRaV-4/6, GLRaV-4/9, GRVFV, GRSPaV	LRD
WIL70	GLRaV-3, GLRaV-4/6, GLRaV-4/9, GRVFV, GRSPaV	LRD
WIL71	GLRaV-4/6, GLRaV-4/9, GRVFV, GRSPaV	Asymptomatic
WIL72	GLRaV-4/6, GLRaV-4/9, GRVFV, GRSPaV	Asymptomatic
WIL73	GLRaV-3, GLRaV-4/6, GRVFV, GRSPaV	LRD
WIL74	GLRaV-4/6, GRVFV, GRSPaV	Asymptomatic
WIL75	GLRaV-4/6, GRVFV, GRSPaV	Asymptomatic
WIL76	GLRaV-4/9, GRVFV, GRSPaV	Asymptomatic
WIL77	GLRaV-3, GRVFV, GRSPaV	LRD
WIL78	GLRaV-3, GLRaV-4/6, GRSPaV	LRD
WIL79	GLRaV-3, GRVFV, GRSPaV	LRD
WIL80	GLRaV-3, GRSPaV	LRD
WIL81	GLRaV-3, GRVFV, GRSPaV	LRD
LC1	GVA*, GLRaV-4/9, GRVFV, GRSPaV	SD
LC2	GVA*, GLRaV-4/9, GRSPaV	SD
LC3	GVA*, GLRaV-4/6, GRVFV, GRSPaV	SD
LC4	GVA*, GRSPaV	SD
LC8	GVA*, GLRaV-4/9, GRSPaV	SD

LC15	GVA*, GLRaV-4/9, GRVFV, GRSPaV	SD
LC17	GRSPaV	Asymptomatic
LC19 to LC30	GRSPaV	Asymptomatic
BV2	GVA*, GLRaV-1, GRSPaV	Mild LRD
BV4	GRSPaV	Asymptomatic
BV5	GRSPaV	Asymptomatic

[1] WIL = Willunga, LC = Langhorne Creek, BV = Barossa Valley. All grapevines listed are var. Shiraz
[2] GRSPaV = grapevine rupestris stem pitting-associated virus, GRVFV = grapevine rupestris vein feathering virus, GLRaV-1, -3 = grapevine leafroll-associated virus 1, and 3, GLRaV-4/6, -4/9 = grapevine leafroll-associated virus 4 strain 6 and 9, GVA = grapevine virus A.
[3] SD = Shiraz disease, LRD = leafroll disease (LRD)
*GVA positives by primer pairs Ah587/Ac995 and H7038/C7273.
GVA positives by primer pairs GVAgroupIIIF/R.

Table S5. Virus status detected by RT-PCR and metagenomic high-throughput sequencing (Meta-HTS) and the GVA phylogroup that was identified.

Sample ID[1]	**Symptoms[2]**	**Virus status by RT-PCR[4]**	**Virus status by Meta-HTS[4]**	**Phylo groups[3]**
WIL1	SD	GVA*#, GLRaV-3, GLRaV-4/9,GRVFV,GRSPaV	GVA, GLRaV-4/9, GRSPaV, GRVFV	II[3a] &III[3a]
WIL2	SD	GVA*#, GLRaV-3,GLRaV-4/9, GRVFV,GRSPaV	GVA, GLRaV-4/9, GRVFV, GRSPaV	II[3a] &III[3a]
WIL3	SD	GVA*#, GLRaV-3, GLRaV-4/9,GRVFV,GRSPaV	GVA, GLRaV-4/9, GRVFV, GRSPaV	II[3a] &III[3a]
WIL4	SD	GVA*, GLRaV-3, GLRaV-4/9,GRSPaV,GRVFV	GVA, GLRaV-3, GLRaV-4/9, GRVFV, GRSPaV	II[3a]
WIL5	SD	GVA*, GLRaV-3,GLRaV-4/9,GRVFV,GRSPaV	GVA, GLRaV-3, GLRaV-4/9, GRVFV, GRSPaV	II[3a]
WIL6	SD	GVA*, GLRaV-3,GLRaV-4/9,GRVFV,GRSPaV	GVA, GLRaV-3, GLRaV-4/9, GRVFV, GRSPaV	II[3a]
WIL7	SD	GVA*, GLRaV-3,GLRaV-4/9,GRVFV,GRSPaV	GVA, GLRaV-3, GLRaV-4/9, GRVFV, GRSPaV	II[3a]
WIL8	SD	GVA*#, GLRaV-3,GLRaV-4/9,GRSPaV,GRVFV	GVA, GLRaV-3, GLRaV-4/9, GRVFV, GRSPaV	II[3a] &III[3a]
WIL9	LRD	GVA#,GLRaV-3,GLRaV-4/9,GRVFV,GRSPaV	GVA, GLRaV-3, GLRaV-4/6, GLRaV-4/9, GRVFV, GRSPaV	III[3a]

WIL10	LRD	GVA#,GLRaV-3,GLRaV-4/6,GLRaV-4/9,GRVFV,GRSPaV	GVA, GLRaV-3, GLRaV-4/6, GLRaV-4/9,GRVFV,GRSPaV	III[3a]
WIL11	LRD	GVA#,GLRaV-3,GLRaV-4/6,GLRaV-4/9,GRVFV,GRSPaV	GVA, GLRaV-3, GLRaV-4/6, GLRaV-4/9, GRVFV,GRSPaV	III[3a]
WIL12	LRD	GVA#,GLRaV-3,GLRaV-4/6,GLRaV-4/9,GRVFV,GRSPaV	GVA, GLRaV-3, GLRaV-4/6, GLRaV-4/9,GRVFV,GRSPaV	III[3a]
WIL13	LRD	GLRaV-3, GLRaV-4/9,GRVFV,GRSPaV	GVA, GLRaV-3, GLRaV-4/5, GLRaV-4/9, GRVFV,GRSPaV	III[3a]
WIL14	LRD	GLRaV-3,GLRaV-4/6,GLRaV-4/9,GRVFV,GRSPaV	GLRaV-3, GLRaV-4/5, GLRaV-4/6, GLRaV-4/9, GRVFV,GRSPaV	Neg
WIL15	LRD	GLRaV-3, GLRaV-4/6,GRVFV,GRSPaV	GLRaV-3, GLRaV-4/5, GLRaV-4/6, GRVFV, GRSPaV	Neg
WIL17	Asymptomatic	GRVFV, GRSPaV	GRVFV, GRSPaV	Neg
WIL19	Asymptomatic	GLRaV-4/6,GRVFV,GRSPaV	GLRaV-4/6, GRVFV,GRSPaV	Neg
WIL22	Asymptomatic	GLRaV-4/6,GRVFV,GRSPaV	GLRaV-4/6, GRVFV,GRSPaV	Neg
WIL24	Asymptomatic	GRSPaV	GLRaV-4/6, GRVFV,GRSPaV	Neg
WIL47	SD	GVA*,GLRaV-3,GRVFV,GRSPaV	GVA, GLRaV-3, GRVFV, GRSPaV	III[3a]
WIL48	SD	GVA*,GLRaV-3,GRVFV,GRSPaV	GVA, GLRaV-3, GRSPaV	II[3a]
WIL49	SD	GVA*,GLRaV-3,GRVFV,GRSPaV	GVA, GLRaV-3, GRVFV, GRSPaV	II[3a]
WIL50	SD	GVA*,GLRaV-3, GRSPaV	GVA, GLRaV-3, GRSPaV	II[3b]
WIL53	SD	GVA*, GLRaV-3,GRSPaV	GVA, GLRaV-3, GRVFV, GRSPaV	II[3a]
LC5	SD	GVA*, GRSPaV	GVA, GLRaV-4/9, GRSPaV	II[3a]
LC6	SD	GVA*, GRSPaV	GVA, GLRaV-4/9, GRSPaV	II[3a]
LC7	SD	GVA*,GRSPaV	GVA, GLRaV-4/9, GRSPaV	II[3a]
LC9	SD	GVA*,GRSPaV	GVA, GLRaV-4/9, GRSPaV	II[3a]
LC10	SD	GVA*,GLRaV-4/9, GRSPaV,	GVA, GLRaV-4/9, GRSPaV	II[3a]

LC11	SD	GVA*,GLRaV-4/9, GRSPaV,	GVA, GLRaV-4/9, GRVFV, GRSPaV	II[3a]
LC12	SD	GVA*,GLRaV-4/9, GRSPaV,	GVA, GLRaV-4/9, GRSPaV	II[3b]
LC13	SD	GVA*,GLRaV-4/9, GRSPaV	GVA, GLRaV-4/9, GRSPaV	II[3a]
LC14	SD	GVA*,GLRaV-4/9, GRSPaV	GVA, GLRaV-4/9, GRSPaV	II[3a]
LC16	Asymptomatic	GRVFV, GRSPaV	GRVFV,GRSPaV	Neg
LC18	Asymptomatic	GRSPaV	GRVFV, GRSPaV	Neg
LC20	Asymptomatic	GRSPaV	GRSPaV	Neg
LC24	Asymptomatic	GRSPaV	GRSPaV	Neg
LC27	Asymptomatic	GRSPaV	GRVFV, GRSPaV	Neg
BV1	Mild LRD	GVA*, GLRaV-1, GRSPaV	GVA, GLRaV-1, GRVFV, GRSPaV	I[3a]
BV3	Mild LRD	GVA*, GLRaV-1, GRSPaV	GVA, GLRaV-1, GRSPaV	I[3b]
BV6	Asymptomatic	GRSPaV	GRVFV, GRSPaV	Neg
Cabw1	LRD	GVA*#, GLRaV-3, GLRaV-4/9, GRSPaV	GVA, GVF, GLRaV-3, GLRaV-4/9, GRSPaV, GRGV	II[3b]&III[3a]
Cabw2	LRD	GVA*#, GLRaV-3, GLRaV-4/9, GRSPaV	GVA, GVF, GLRaV-3, GLRaV-4/9, GRSPaV, GRGV	II[3b]&III[3b]
Cabw11	LRD	GVA*, GLRaV-3, GLRaV-4/9, GRSPaV	GVA, GLRaV-3, GLRaV-4/9, GRSPaV, GRVFV, GRGV	II[3a]
Cabw12	LRD	GVA*#, GLRaV-3, GLRaV-4/9, GRSPaV	GVA, GLRaV-3, GLRaV-4/9, GRSPaV, GRVFV, GRGV	II[3a]&III[3b]
Melort1	SD	GVA#*, GLRaV-3, GRSPaV	GVA, GLRaV-3, GLRaV-4/9, GRSPaV	II[3b]&III[3b]
Shiraz_OR_P5	Asymptomatic	GRVFV, GRSPaV	GRVFV, GRSPaV	Neg

Shiraz_OR_P6	Asymptomatic	GRVFV, GRSPaV	GRVFV, GRSPaV	Neg
CabSA125_R3V30	LRD	GVA*#, GLRaV-4/9, GRSPaV,	GVA, GLRaV-4/9, GRSPaV, GRGV	II^{3b}&III^{3b}
CabSA125_R3V44	LRD	GVA*#, GLRaV-4/9, GRSPaV	GVA, GLRaV-4/9, GRSPaV	II^{3b}&III^{3b}

[1] WIL = Willunga, LC = Langhorne Creek, BV = Barossa Valley, CV= Coombe's Vineyard. All grapevines listed are var. Shiraz except Cabw = Cabernet Sauvignon from Willunga and CabSA125 = Cabernet Sauvignon clone SA125 from Coombe's Vineyard, Merlot = Merlot from Willunga.
[2] SD = Shiraz disease, LRD = leafroll disease (LRD)
[3] Phylogenetic groups were identified using contigs generated by Meta-HTS and phylogroups of each sample was identified based on the phylogroup of each GVA contig obtained from Meta-HTS (Tables S6 and S7). [3a] Phylogenetic group of GVA was identified using near complete sequences.
[3b] Phylogroup by partial sequences.
[4] GRSPaV = grapevine rupestris stem pitting-associated virus, GRVFV = grapevine rupestris vein feathering virus, GLRaV-1, -3 = grapevine leafroll-associated virus 1, and 3, GLRaV-4/5, -4/6, -4/9 = grapevine leafroll-associated virus 4 strains 5, 6 and 9, GVA = grapevine virus A, GVF = grapevine virus F, GRGV= grapevine red globe virus
*GVA positives by the generic assays using both primer pairs Ah587/Ac995 and H7038/C7273.
GVA positives by the group III specific assay using primer pairs GVAgroupIIIF/R.

Table S6. Basic statistics and list of contigs of the 50 grapevine samples sequenced by the NovaSeq (Illumina) instrument.

Sample ID[1]	Raw reads	Trimmed reads	Avg length after trim (bp)	Total no.contigs	Viroid contigs*	Virus contigs	Virus detected in this sample[4]	Exemplar isolate	Genus	Contig ID	Contig length (nts)	Average coverage (x)	Percentage of genome covered	Similarity to exemplar isolate
WIL1	8,844,230	8,819,752	130.4	87202	4	7	GVA^{II}	Is151 (X75433)	*Vitivirus*	WIL1_N53_SD	7398	714.76	93.91%	5478/6903 (79.36%)
							GVA^{III}	Is151 (X75433)	*Vitivirus*	WIL1_N54_SD	7348	460.279	23.11%	1366/1699 (80.4%)
							GLRaV-4/9	LR106 (FJ467503)	*Ampelovirus*	WIL1_N15	13954	1657.313	53.79%	5692/7439 (78.29%)
							GRSPaV	3138-07 (JX559646)	*Foveavirus*	WIL1_N23	8723	111.188	99.84%	8141/8712 (93.45%)

							GRSPaV	3138-07 (JX559646)	*Foveavirus*	WIL1_N35	8706	322.036	95.50%	6643/8333 (79.72%)
							GRVFV	Mauzac (KY513701)	*Marafivirus* (tentative)	WIL1_N74	6738	74.103	100.00%	5835/6744 (86.52%)
WIL2	7,711,315	7,692,915	130.7	82796	4	8	GVA^{II}	Is151 (X75433)	*Vitivirus*	WIL2_N36_SD	7335	329.159	93.84%	5475/6898 (79.37%)
							GVA^{III}	Is151 (X75433)	*Vitivirus*	WIL2_N40_SD	7183	545.375	20.91%	1207/1537 (78.53%)
							GLRaV-4/9	LR106 (FJ467503)	*Ampelovirus*	WIL2_N7	13837	1083.389	55.12%	5966/7623 (78.26%)
							GRSPaV	3138-07 (JX559646)	*Foveavirus*	WIL2_N21	8728	98.879	99.97%	8168/8723 (93.64%)
							GRSPaV	3138-07 (JX559646)	*Foveavirus*	WIL2_N22	8707	211.968	95.50%	6646/8333 (79.76%)
							GRVFV	Mauzac (KY513701)	*Marafivirus* (tentative)	WIL2_N88	5940	49.075	88.40%	5158/5949 (86.7%)
WIL3	7,515,198	7,487,210	131	80649	3	7	GVA^{II}	Is151 (X75433)	*Vitivirus*	WIL3_N29_SD	7338	281.229	93.92%	5489/6904 (79.5%)
							GVA^{III}	Is151 (X75433)	*Vitivirus*	WIL3_N27_SD	7366	1010.957	68.22%	3839/5015 (76.55%)
							GLRaV-4/9	LR106 (FJ467503)	*Ampelovirus*	WIL3_N6	13987	1825.827	55.14%	5973/7626 (78.32%)
							GRSPaV	3138-07 (JX559646)	*Foveavirus*	WIL3_N17	8712	125.018	99.85%	8142/8713 (93.45%)
							GRSPaV	3138-07 (JX559646)	*Foveavirus*	WIL3_N20	8286	168.353	90.60%	6263/7906 (79.22%)
							GRVFV	Mauzac (KY513701)	*Marafivirus* (tentative)	WIL3_N49	6718	86.218	100.00%	5745/6731 (85.35%)
							GRVFV	Mauzac (KY513701)	*Marafivirus* (tentative)	WIL3_N57	6383	87.836	95.02%	5559/6395 (86.93%)
WIL4	6,510,068	6,491,857	128.5	60366	2	18	GVA^{II}	Is151 (X75433)	*Vitivirus*	WIL4_N28_SD	7322	513.125	93.95%	5481/6906 (79.37%)

							GLRaV-3	NY1 (AF037268)	*Ampelovirus*	WIL4_N4	18785	2069.145	100.00%	17548/17919 (97.93%)
							GLRaV-4/9	LR106 (FJ467503)	*Ampelovirus*	WIL4_N6	13984	1046.354	53.88%	5837/7451 (78.34%)
							GRSPaV	3138-07 (JX559646)	*Foveavirus*	WIL4_N17	8807	72.847	99.95%	8161/8722 (93.57%)
							GRSPaV	3138-07 (JX559646)	*Foveavirus*	WIL4_N18	8710	52.755	95.98%	6676/8375 (79.71%)
							GRVFV	Mauzac (KY513701)	*Marafivirus* (tentative)	WIL4_N417	3466	18.067	51.50%	2919/3466 (84.22%)
WIL5	5,471,483	5,450,378	124.9	59171	6	14	GVA^{II}	Is151 (X75433)	*Vitivirus*	WIL5_N25_SD	7330	214.968	93.46%	5451/6870 (79.34%)
							GLRaV-3	NY1 (AF037268)	*Ampelovirus*	WIL5_N4	18634	647.413	100.00%	17549/17919 (97.94%)
							GLRaV-4/9	LR106 (FJ467503)	*Ampelovirus*	WIL5_N7	13900	471.646	53.88%	5838/7452 (78.34%)
							GRSPaV	3138-07 (JX559646)	*Foveavirus*	WIL5_N15	8753	138.559	95.98%	6678/8375 (79.74%)
							GRSPaV	3138-07 (JX559646)	*Foveavirus*	WIL5_N16	8710	102.693	99.77%	8149/8706 (93.6%)
							GRVFV	Mauzac (KY513701)	*Marafivirus* (tentative)	WIL5_N148	3874	24.803	57.64%	3316/3879 (85.49%)
WIL6	6,061,385	6,028,858	129	66387	2	11	GVA^{II}	Is151 (X75433)	*Vitivirus*	WIL6_N29_SD	7356	428.922	93.61%	5464/6881 (79.41%)
							GLRaV-3	NY1 (AF037268)	*Ampelovirus*	WIL6_N4	18681	935.641	100.00%	17550/17919 (97.94%)
							GLRaV-4/9	LR106 (FJ467503)	*Ampelovirus*	WIL6_N6	13827	617.582	53.80%	5827/7440 (78.32%)
							GRSPaV	3138-07 (JX559646)	*Foveavirus*	WIL6_N14	8701	28.127	74.41%	5203/6493 (80.13%)
							GRSPaV	3138-07 (JX559646)	*Foveavirus*	WIL6_N21	8713	67.368	99.85%	8152/8713 (93.56%)

							GRVFV	Mauzac (KY513701)	*Marafivirus* (tentative)	WIL6_N5518	1262	9.194	18.72%	1054/1260 (83.65%)
WIL7	6,307,477	6,275,973	129.2	63855	4	14	GVA^{II}	Is151 (X75433)	*Vitivirus*	WIL7_N29_SD	7336	148.576	93.97%	5505/6908 (79.69%)
							GLRaV-3	NY1 (AF037268)	*Ampelovirus*	WIL7_N5	18485	1159.452	99.92%	17531/17905 (97.91%)
							GLRaV-4/9	LR106 (FJ467503)	*Ampelovirus*	WIL7_N6	13857	780.61	53.80%	5823/7440 (78.27%)
							GRSPaV	3138-07 (JX559646)	*Foveavirus*	WIL7_N16	8761	104.034	92.36%	6463/8059 (80.2%)
							GRVFV	Mauzac (KY513701)	*Marafivirus* (tentative)	WIL7_N640	3082	22.426	45.66%	2625/3073 (85.42%)
WIL8	8,229,748	8,198,038	132.4	64064	2	17	GVA^{II}	Is151 (X75433)	*Vitivirus*	WIL8_N27_SD	7361	302.566	92.57%	5395/6805 (79.28%)
							GVA^{III}	Is151 (X75433)	*Vitivirus*	WIL8_N28_SD	7346	427.954	46.17%	2714/3394 (79.96%)
							GLRaV-3	NY1 (AF037268)	*Ampelovirus*	WIL8_N4	18569	1646.454	100.00%	17547/17919 (97.92%)
							GLRaV-4/9	LR106 (FJ467503)	*Ampelovirus*	WIL8_N7	13838	673.864	66.99%	7175/9265 (77.44%)
							GRSPaV	3138-07 (JX559646)	*Foveavirus*	WIL8_N16	8718	102.419	99.86%	8153/8714 (93.56%)
							GRSPaV	3138-07 (JX559646)	*Foveavirus*	WIL8_N17	8712	85.609	95.98%	6677/8375 (79.73%)
							GRVFV	Mauzac (KY513701)	*Marafivirus* (tentative)	WIL8_N376	3334	23.328	49.58%	2888/3337 (86.54%)
WIL9	7,436,140	7,409,318	131.8	75379	3	18	GVA^{III}	Is151 (X75433)	*Vitivirus*	WIL9_N31_LRD	7364	386.726	23.10%	1357/1698 (79.92%)
							GLRaV-3	NY1 (AF037268)	*Ampelovirus*	WIL9_N3	18523	830.866	100.00%	17548/17919 (97.93%)
							GLRaV-4/6	LR106 (FJ467503)	*Ampelovirus*	WIL9_N25253	558	181.254	4.03%	431/558 (77.24%)

							GLRaV-4/9	LR106 (FJ467503)	*Ampelovirus*	WIL9_N5	13850	956.128	66.99%	7176/9265 (77.45%)
							GRSPaV	3138-07 (JX559646)	*Foveavirus*	WIL9_N19	8788	263.662	95.52%	6639/8335 (79.65%)
							GRSPaV	3138-07 (JX559646)	*Foveavirus*	WIL9_N21	8724	293.566	92.20%	6430/8045 (79.93%)
							GRSPaV	3138-07 (JX559646)	*Foveavirus*	WIL9_N22	8705	131.032	99.76%	8132/8705 (93.42%)
							GRVFV	Mauzac (KY513701)	*Marafivirus* (tentative)	WIL9_N4759	1464	33.023	21.72%	1257/1462 (85.98%)
WIL10	8,132,470	8,107,226	130.8	74459	3	11	GVA^{III}	Is151 (X75433)	*Vitivirus*	WIL10_N41_LRD	7384	493.56	23.09%	1357/1697 (79.96%)
							GLRaV-3	NY1 (AF037268)	*Ampelovirus*	WIL10_N4	18319	830.274	99.91%	17531/17902 (97.93%)
							GLRaV-4/6	LR106 (FJ467503)	*Ampelovirus*	WIL10_N6	13957	803.428	55.67%	5938/7699 (77.13%)
							GLRaV-4/9	LR106 (FJ467503)	*Ampelovirus*	WIL10_N7	13854	577.642	66.99%	7177/9265 (77.46%)
							GRSPaV	3138-07 (JX559646)	*Foveavirus*	WIL10_N19	8788	186.984	99.97%	8169/8723 (93.65%)
							GRSPaV	3138-07 (JX559646)	*Foveavirus*	WIL10_N21	8706	162.929	95.91%	6668/8369 (79.67%)
							GRVFV	Mauzac (KY513701)	*Marafivirus* (tentative)	WIL10_N82	6175	43.267	90.85%	5119/6114 (83.73%)
WIL11	7,348,392	7,327,397	131.3	70213	3	18	GVA^{III}	Is151 (X75433)	*Vitivirus*	WIL11_N43_LRD	7365	550.786	23.11%	1361/1699 (80.11%)
							GLRaV-3	NY1 (AF037268)	*Ampelovirus*	WIL11_N3	18692	843.165	100.00%	17546/17919 (97.92%)
							GLRaV-4/6	LR106 (FJ467503)	*Ampelovirus*	WIL11_N6	13925	898.052	55.65%	5934/7696 (77.1%)
							GLRaV-4/9	LR106 (FJ467503)	*Ampelovirus*	WIL11_N7	13815	521.005	53.65%	5804/7420 (78.22%)

							GRSPaV	3138-07 (JX559646)	*Foveavirus*	WIL11_N24	8710	154.401	95.48%	6640/8332 (79.69%)
							GRSPaV	3138-07 (JX559646)	*Foveavirus*	WIL11_N26	8459	208.263	89.26%	6209/7789 (79.71%)
							GRVFV	Mauzac (KY513701)	*Marafivirus* (tentative)	WIL11_N2122	2324	43.434	34.59%	2017/2328 (86.64%)
WIL12	7,188,416	7,170,862	130.9	70252	4	14	GVA^{III}	Is151 (X75433)	*Vitivirus*	WIL12_N33_LRD	7343	302.104	23.29%	1363/1712 (79.61%)
							GLRaV-3	NY1 (AF037268)	*Ampelovirus*	WIL12_N3	18552	778.591	100.00%	17548/17919 (97.93%)
							GLRaV-4/6	LR106 (FJ467503)	*Ampelovirus*	WIL12_N5	13846	662.026	55.68%	5940/7700 (77.14%)
							GLRaV-4/9	LR106 (FJ467503)	*Ampelovirus*	WIL12_N6	13827	197.208	53.86%	5831/7449 (78.28%)
							GRSPaV	3138-07 (JX559646)	*Foveavirus*	WIL12_N21	8741	97.715	99.84%	8161/8712 (93.68%)
							GRSPaV	3138-07 (JX559646)	*Foveavirus*	WIL12_N22	8713	123.795	95.55%	6635/8338 (79.58%)
							GRVFV	Mauzac (KY513701)	*Marafivirus* (tentative)	WIL12_N352	3874	42.252	57.62%	3313/3878 (85.43%)
WIL13	6,529,218	6,499,025	114.9	50341	4	14	GVA^{III}	Is151 (X75433)	*Vitivirus*	WIL13_N17_LRD	7380	386.722	23.11%	1365/1699 (80.34%)
							GLRaV-3	NY1 (AF037268)	*Ampelovirus*	WIL13_N3	18496	960.277	99.98%	17544/17916 (97.92%)
							GLRaV-4/5	LR106 (FJ467503)	*Ampelovirus*	WIL13_N7	13817	675.435	67.76%	7435/9371 (79.34%)
							GLRaV-4/9	LR106 (FJ467503)	*Ampelovirus*	WIL13_N6	13835	469.602	53.88%	5831/7451 (78.26%)
							GRSPaV	3138-07 (JX559646)	*Foveavirus*	WIL13_N13	8708	86.657	95.91%	6676/8369 (79.77%)
							GRSPaV	3138-07 (JX559646)	*Foveavirus*	WIL13_N14	8531	108.4	96.53%	7877/8423 (93.52%)

							GRVFV	Mauzac (KY513701)	*Marafivirus* (tentative)	WIL13_N74	4675	29.422	69.58%	3960/4683 (84.56%)
WIL14	7,491,817	7,475,282	131.3	74114	3	19	GLRaV-3	NY1 (AF037268)	*Ampelovirus*	WIL14_N4	18628	1148.426	100.00%	17551/17919 (97.95%)
							GLRaV-4/5	LR106 (FJ467503)	*Ampelovirus*	WIL14_N48	7283	172.25	16.98%	1994/2349 (84.89%)
							GLRaV-4/6	LR106 (FJ467503)	*Ampelovirus*	WIL14_N5	13892	599.815	57.92%	6166/8010 (76.98%)
							GLRaV-4/9	LR106 (FJ467503)	*Ampelovirus*	WIL14_N1317	2729	90.403	18.16%	1983/2512 (78.94%)
							GRSPaV	3138-07 (JX559646)	*Foveavirus*	WIL14_N19	8709	104.825	95.51%	6632/8334 (79.58%)
							GRSPaV	3138-07 (JX559646)	*Foveavirus*	WIL14_N20	8709	82.695	99.81%	8155/8709 (93.64%)
							GRSPaV	3138-07 (JX559646)	*Foveavirus*	WIL14_N21	8701	113.332	92.05%	6414/8032 (79.86%)
							GRVFV	Mauzac (KY513701)	*Marafivirus* (tentative)	WIL14_N338	4155	28.068	61.58%	3429/4144 (82.75%)
WIL15	7,789,197	7,711,086	126.7	63971	3	15	GLRaV-3	NY1 (AF037268)	*Ampelovirus*	WIL15_N4	18563	1298.621	100.00%	17549/17919 (97.94%)
							GLRaV-4/5	LR106 (FJ467503)	*Ampelovirus*	WIL15_N8	13095	179.913	67.61%	7415/9351 (79.3%)
							GLRaV-4/6	LR106 (FJ467503)	*Ampelovirus*	WIL15_N6	14017	678.683	57.92%	6166/8010 (76.98%)
							GRSPaV	3138-07 (JX559646)	*Foveavirus*	WIL15_N15	8740	102.612	99.84%	8158/8712 (93.64%)
							GRSPaV	3138-07 (JX559646)	*Foveavirus*	WIL15_N16	8796	249.931	93.15%	6508/8128 (80.07%)
							GRVFV	Mauzac (KY513701)	*Marafivirus* (tentative)	WIL15_N478	3358	41.478	49.91%	2853/3359 (84.94%)
WIL17	6,146,002	6,124,074	128.5	57552	3	13	GRSPaV	3138-07 (JX559646)	*Foveavirus*	WIL17_N13	8709	144.958	95.54%	6646/8337 (79.72%)

							GRSPaV	3138-07 (JX559646)	*Foveavirus*	WIL17_N14	8705	138.686	99.76%	8130/8705 (93.39%)
							GRVFV	Mauzac (KY513701)	*Marafivirus* (tentative)	WIL17_N147	4331	25.129	64.44%	3677/4337 (84.78%)
WIL19	7,469,836	7,439,964	129.8	60025	4	10	GLRaV-4/6	LR106 (FJ467503)	*Ampelovirus*	WIL19_N6	13930	546.193	56.25%	6011/7780 (77.26%)
							GRSPaV	3138-07 (JX559646)	*Foveavirus*	WIL19_N13	8763	92.843	99.84%	8163/8712 (93.7%)
							GRSPaV	3138-07 (JX559646)	*Foveavirus*	WIL19_N14	8709	163.499	95.54%	6645/8337 (79.7%)
							GRVFV	Mauzac (KY513701)	*Marafivirus* (tentative)	WIL19_N522	2942	23.692	43.76%	2505/2945 (85.06%)
WIL22	6,389,640	6,375,696	130.9	58491	4	15	GLRaV-4/6	LR106 (FJ467503)	*Ampelovirus*	WIL22_N5	13805	454.366	55.65%	5935/7696 (77.12%)
							GRSPaV	3138-07 (JX559646)	*Foveavirus*	WIL22_N12	8712	107.732	95.56%	6645/8339 (79.69%)
							GRSPaV	3138-07 (JX559646)	*Foveavirus*	WIL22_N13	8711	81.514	99.83%	8136/8711 (93.4%)
							GRVFV	Mauzac (KY513701)	*Marafivirus* (tentative)	WIL22_N148	4498	32.339	66.92%	3845/4504 (85.37%)
WIL24	7,389,330	7,361,985	133.5	68055	2	13	GLRaV-4/6	LR106 (FJ467503)	*Ampelovirus*	WIL24_N5	13867	642.107	55.68%	5939/7700 (77.13%)
							GRSPaV	3138-07 (JX559646)	*Foveavirus*	WIL24_N17	8740	78.037	95.56%	6664/8339 (79.91%)
							GRSPaV	3138-07 (JX559646)	*Foveavirus*	WIL24_N18	8702	51.304	99.74%	8122/8703 (93.32%)
							GRVFV	Mauzac (KY513701)	*Marafivirus* (tentative)	WIL24_N775	3070	17.366	45.29%	2585/3048 (84.81%)
LC5	3,641,648	3,577,621	125.2	39666	5	7	GVA^{II}	Is151 (X75433)	*Vitivirus*	LC5_N12_SD	7339	136.552	92.49%	5401/6799 (79.44%)
							GLRaV-4/9	LR106 (FJ467503)	*Ampelovirus*	LC5_N5	13847	269.42	53.88%	5828/7452 (78.21%)

							GRSPaV	3138-07 (JX559646)	*Foveavirus*	LC5_N7	8704	70.512	99.75%	8161/8704 (93.76%)
LC6	5,893,931	5,869,862	127.4	57289	5	7	GVA^{II}	Is151 (X75433)	*Vitivirus*	LC6_N19_SD	7348	137.147	93.61%	5456/6881 (79.29%)
							GLRaV-4/9	LR106 (FJ467503)	*Ampelovirus*	LC6_N6	13838	395.085	53.86%	5824/7449 (78.18%)
							GRSPaV	3138-07 (JX559646)	*Foveavirus*	LC6_N11	8712	84.278	99.84%	8167/8712 (93.74%)
							GRSPaV	3138-07 (JX559646)	*Foveavirus*	LC6_N12	8695	121.041	95.38%	6641/8323 (79.79%)
LC7	6,496,609	6,479,256	132.5	74472	5	7	GVA^{II}	Is151 (X75433)	*Vitivirus*	LC7_N42_SD	7339	205.542	93.58%	5454/6879 (79.28%)
							GLRaV-4/9	LR106 (FJ467503)	*Ampelovirus*	LC7_N6	13886	429.195	53.85%	5823/7448 (78.18%)
							GRSPaV	3138-07 (JX559646)	*Foveavirus*	LC7_N24	8707	154.287	95.46%	6641/8330 (79.72%)
							GRSPaV	3138-07 (JX559646)	*Foveavirus*	LC7_N25	8700	79.634	92.05%	6426/8032 (80%)
LC9	7,067,771	7,040,778	116	54559	5	7	GVA^{II}	Is151 (X75433)	*Vitivirus*	LC9_N19_SD	7336	107.851	93.93%	5464/6905 (79.13%)
							GLRaV-4/9	LR106 (FJ467503)	*Ampelovirus*	LC9_N5	13886	460.939	53.79%	5815/7439 (78.17%)
							GRSPaV	3138-07 (JX559646)	*Foveavirus*	LC9_N10	8746	49.552	99.85%	8166/8713 (93.72%)
							GRSPaV	3138-07 (JX559646)	*Foveavirus*	LC9_N13	8347	137.518	91.27%	6321/7964 (79.37%)
LC10	7,527,983	7,503,883	128.9	80310	4	6	GVA^{II}	Is151 (X75433)	*Vitivirus*	LC10_N33_SD	7326	201.187	93.85%	5486/6899 (79.52%)
							GLRaV-4/9	LR106 (FJ467503)	*Ampelovirus*	LC10_N6	13855	721.857	53.88%	5846/7452 (78.45%)
							GRSPaV	3138-07 (JX559646)	*Foveavirus*	LC10_N15	8778	97.815	99.87%	8173/8715 (93.78%)

							GRSPaV	3138-07 (JX559646)	*Foveavirus*	LC10_N16	8755	207.959	95.73%	6673/8353 (79.89%)
							GRSPaV	3138-07 (JX559646)	*Foveavirus*	LC10_N17	8708	210.924	92.87%	6498/8104 (80.18%)
LC11	8,104,889	8,047,276	133.2	76962	3	8	GVA^{II}	Is151 (X75433)	*Vitivirus*	LC11_N45_SD	7345	329.374	93.97%	5470/6908 (79.18%)
							GLRaV-4/9	LR106 (FJ467503)	*Ampelovirus*	LC11_N6	13853	1504.603	53.88%	5847/7451 (78.47%)
							GRSPaV	3138-07 (JX559646)	*Foveavirus*	LC11_N23	8824	208.7	95.32%	6643/8318 (79.86%)
							GRSPaV	3138-07 (JX559646)	*Foveavirus*	LC11_N24	8708	204.944	95.73%	6669/8353 (79.84%)
							GRSPaV	3138-07 (JX559646)	*Foveavirus*	LC11_N25	8699	122.517	99.69%	8144/8699 (93.62%)
							GRVFV	Mauzac (KY513701)	*Marafivirus* (tentative)	LC11_N65	6692	65.603	99.70%	5708/6710 (85.07%)
							GRVFV	Mauzac (KY513701)	*Marafivirus* (tentative)	LC11_N98	6116	70.257	90.82%	5118/6112 (83.74%)
LC12	5,786,465	5,765,655	130	60117	6	9	GVA^{II}	Is151 (X75433)	*Vitivirus*	LC12_N124_SD	4608	128.498	62.78%	3681/4615 (79.76%)
							GLRaV-4/9	LR106 (FJ467503)	*Ampelovirus*	LC12_N5	13847	706.131	53.88%	5848/7452 (78.48%)
							GRSPaV	3138-07 (JX559646)	*Foveavirus*	LC12_N11	8763	60.616	99.85%	8172/8713 (93.79%)
							GRSPaV	3138-07 (JX559646)	*Foveavirus*	LC12_N12	8710	115.289	95.55%	6658/8338 (79.85%)
LC13	6,381,939	6,366,843	128.4	69862	5	7	GVA^{II}	Is151 (X75433)	*Vitivirus*	LC13_N31_SD	7325	218.789	74.26%	4324/5459 (79.21%)
							GLRaV-4/9	LR106 (FJ467503)	*Ampelovirus*	LC13_N3	13836	599.363	53.62%	5792/7416 (78.1%)
							GRSPaV	3138-07 (JX559646)	*Foveavirus*	LC13_N16	8712	216.011	95.50%	6649/8333 (79.79%)

							GRSPaV	3138-07 (JX559646)	*Foveavirus*	LC13_N21	8176	210.55	21.12%	1443/1843 (78.3%)
LC14	7,454,524	7,438,758	133.3	80194	5	7	GVA^{II}	Is151 (X75433)	*Vitivirus*	LC14_N49_SD	7361	461.658	94.08%	5474/6916 (79.15%)
							GVA^{II}	Is151 (X75433)	*Vitivirus*	LC14_N51_SD	7305	465.173	93.55%	5444/6877 (79.16%)
							GLRaV-4/9	LR106 (FJ467503)	*Ampelovirus*	LC14_N6	13842	1053.333	53.88%	5826/7451 (78.19%)
							GRSPaV	3138-07 (JX559646)	*Foveavirus*	LC14_N30	8702	192.266	91.76%	6412/8007 (80.08%)
							GRSPaV	3138-07 (JX559646)	*Foveavirus*	LC14_N31	8702	119.366	99.72%	8154/8702 (93.7%)
							GRSPaV	3138-07 (JX559646)	*Foveavirus*	LC14_N33	8580	189.477	90.30%	6311/7880 (80.09%)
LC16	6,465,268	6,434,000	131.9	64080	12	7	GRSPaV	3138-07 (JX559646)	*Foveavirus*	LC16_N15	8739	195.301	99.97%	8169/8723 (93.65%)
							GRSPaV	3138-07 (JX559646)	*Foveavirus*	LC16_N16	8700	186.972	92.07%	6443/8034 (80.2%)
							GRVFV	Mauzac (KY513701)	*Marafivirus* (tentative)	LC16_N40	6476	79.407	96.51%	5431/6495 (83.62%)
LC18	7,790,861	7,770,023	132.5	69922	5	8	GRSPaV	3138-07 (JX559646)	*Foveavirus*	LC18_N16	8711	163.878	99.83%	8163/8711 (93.71%)
							GRSPaV	3138-07 (JX559646)	*Foveavirus*	LC18_N17	8709	330.907	95.48%	6636/8332 (79.64%)
							GRVFV	Mauzac (KY513701)	*Marafivirus* (tentative)	LC18_N18191	686	5.516	10.21%	571/687 (83.11%)
LC20	8,309,672	8,290,763	135.1	69527	3	6	GRSPaV	3138-07 (JX559646)	*Foveavirus*	LC20_N17	8779	252.426	99.97%	8179/8723 (93.76%)
							GRSPaV	3138-07 (JX559646)	*Foveavirus*	LC20_N22	8707	125.468	92.13%	6430/8039 (79.99%)
LC24	8,548,571	8,527,508	131.2	65729	3	5	GRSPaV	3138-07 (JX559646)	*Foveavirus*	LC24_N15	8727	244.805	99.84%	8159/8712 (93.65%)

							GRSPaV	3138-07 (JX559646)	*Foveavirus*	LC24_N19	8709	296.035	93.10%	6500/8124 (80.01%)
LC27	7,009,354	6,937,713	129.9	60293	3	8	GRSPaV	3138-07 (JX559646)	*Foveavirus*	LC27_N15	8704	142.126	99.75%	8163/8704 (93.78%)
							GRSPaV	3138-07 (JX559646)	*Foveavirus*	LC27_N16	8690	130.19	91.83%	6425/8013 (80.18%)
							GRVFV	Mauzac (KY513701)	*Marafivirus* (tentative)	LC27_N2994	1852	8.204	27.55%	1583/1854 (85.38%)
BV1	7,793,165	7,684,434	138.4	65632	5	14	GVA[I]	Is151 (X75433)	*Vitivirus*	BV1_N31_mild_LRD	7356	757.595	94.86%	5628/6973 (80.71%)
							GLRaV-1	1050 (JQ023131)	*Ampelovirus*	BV1_N3	18326	606.399	60.16%	9152/11226 (81.53%)
							GRSPaV	3138-07 (JX559646)	*Foveavirus*	BV1_N20	8709	426.948	95.55%	6663/8338 (79.91%)
							GRVFV	Mauzac (KY513701)	*Marafivirus* (tentative)	BV1_N2869	2158	10.479	32.08%	1850/2159 (85.69%)
BV3	6,823,261	6,801,634	130.8	45040	10	8	GVA[I]	Is151 (X75433)	*Vitivirus*	BV3_N260_mild_LRD	3217	333.538	43.98%	2678/3233 (82.83%)
							GLRaV-1	1050 (JQ023131)	*Ampelovirus*	BV3_N5	14324	181.667	49.67%	7681/9267 (82.89%)
							GRSPaV	3138-07 (JX559646)	*Foveavirus*	BV3_N9	8710	273.563	99.82%	8144/8710 (93.5%)
							GRSPaV	3138-07 (JX559646)	*Foveavirus*	BV3_N10	8657	450.294	94.90%	6600/8281 (79.7%)
BV6	6,021,139	5,998,506	131.4	47521	5	5	GRSPaV	3138-07 (JX559646)	*Foveavirus*	BV6_N11	8772	445.154	95.58%	6656/8340 (79.81%)
							GRVFV	Mauzac (KY513701)	*Marafivirus* (tentative)	BV6_N15461	597	4.702	8.87%	521/597 (87.27%)
Cabw1	7,450,095	7,434,263	129	74364	3	18	GVA[II]	Is151 (X75433)	*Vitivirus*	Cabw1_N153_LRD	5086	103.457	19.75%	1159/1452 (79.82%)
							GVA[III]	Is151 (X75433)	*Vitivirus*	Cabw1_N38_LRD	7343	379.453	23.28%	1374/1711 (80.3%)

							GVF	AUD46129 (JX105428)	*Vitivirus* (tentative)	Cabw1_N36	7520	79.977	99.55%	6734/7517 (89.49%)
							GLRaV-3	NY1 (AF037268)	*Ampelovirus*	Cabw1_N2	18502	1089.258	100.00%	17548/17919 (97.93%)
							GLRaV-4/9	LR106 (FJ467503)	*Ampelovirus*	Cabw1_N57	6596	197.098	46.91%	5106/6488 (78.7%)
							GRSPaV	3138-07 (JX559646)	*Foveavirus*	Cabw1_N45	6965	280.323	41.12%	2933/3588 (81.74%)
							GRGV	Graciano-T101 (KX171166)	*Maculavirus* (tentative)	Cabw1_N12057	919	6.351	13.64%	817/936 (87.29%)
Cabw2	5,679,378	5,670,120	118.4	60894	2	11	GVA^{II}	Is151 (X75433)	*Vitivirus*	Cabw2_N2273_LRD	1384	169.63	18.77%	1111/1380 (80.51%)
							GVA^{III}	Is151 (X75433)	*Vitivirus*	Cabw2_N6157_LRD	893	292.233	11.45%	716/842 (85.04%)
							GVF	AUD46129 (JX105428)	*Vitivirus* (tentative)	Cabw2_N17	7522	24.739	99.62%	6739/7522 (89.49%)
							GLRaV-3	NY1 (AF037268)	*Ampelovirus*	Cabw2_N1	18627	694.995	100.00%	17548/17919 (97.93%)
							GLRaV-4/9	LR106 (FJ467503)	*Ampelovirus*	Cabw2_N6	13818	174.28	53.86%	5832/7449 (78.29%)
							GRSPaV	3138-07 (JX559646)	*Foveavirus*	Cabw2_N11	8712	224.33	95.58%	6649/8340 (79.72%)
							GRSPaV	3138-07 (JX559646)	*Foveavirus*	Cabw2_N12	8712	139.557	99.84%	8151/8712 (93.56%)
							GRGV	Graciano-T101 (KX171166)	*Maculavirus* (tentative)	Cabw2_N17647	514	5.957	7.47%	439/513 (85.58%)
Cabw11	7,388,963	7,364,304	127.8	64873	3	15	GVA^{II}	Is151 (X75433)	*Vitivirus*	Cabw11_N36_LRD	7331	331.053	93.78%	5477/6894 (79.45%)
							GLRaV-3	NY1 (AF037268)	*Ampelovirus*	Cabw11_N3	18623	1219.735	100.00%	17543/17919 (97.9%)

							GLRaV-4/9	LR106 (FJ467503)	*Ampelovirus*	Cabw11_N31	13832	251.088	53.85%	5831/7448 (78.29%)
							GRSPaV	3138-07 (JX559646)	*Foveavirus*	Cabw11_N22	8738	227.72	99.95%	8169/8722 (93.66%)
							GRVFV	Mauzac (KY513701)	*Marafivirus* (tentative)	Cabw11_N1117	2784	16.009	41.38%	2384/2785 (85.6%)
							GRGV	Graciano-T101 (KX171166)	*Maculavirus* (tentative)	Cabw11_N40326	365	4.148	4.76%	277/327 (84.71%)
Cabw12	8,325,871	8,311,536	126.5	71483	3	16	GVA^{II}	Is151 (X75433)	*Vitivirus*	Cabw12_N47_LRD	7359	300.854	94.08%	5518/6916 (79.79%)
							GVA^{II}	Is151 (X75433)	*Vitivirus*	Cabw12_N52_LRD	7056	297.598	90.55%	5266/6656 (79.12%)
							GVA^{III}	Is151 (X75433)	*Vitivirus*	Cabw12_N650_LRD	3537	396.084	23.32%	1372/1714 (80.05%)
							GLRaV-3	NY1 (AF037268)	*Ampelovirus*	Cabw12_N4	18563	1096.171	100.00%	17548/17919 (97.93%)
							GLRaV-4/9	LR106 (FJ467503)	*Ampelovirus*	Cabw12_N7	13848	320.447	53.63%	5802/7417 (78.23%)
							GRSPaV	3138-07 (JX559646)	*Foveavirus*	Cabw12_N27	8752	273.132	99.89%	8155/8716 (93.56%)
							GRVFV	Mauzac (KY513701)	*Marafivirus (tentative)*	Cabw12_N1350	2775	17.089	41.32%	2377/2781 (85.47%)
							GRGV	Graciano-T101 (KX171166)	*Maculavirus (tentative)*	Cabw12_N10896	981	0	14.28%	877/980 (89.49%)
Merlot1	8,290,479	8,254,982	130.1	72852	2	15	GVA^{II}	Is151 (X75433)	*Vitivirus*	Merlot1_N121_SD	7356	175.8	93.50%	5434/6873 (79.06%)
							GVA^{III}	Is151 (X75433)	*Vitivirus*	Melort1_N1053_SD	2937	175.8	23.26%	1372/1710 (80.23%)
							GLRaV-3	NY1 (AF037268)	*Ampelovirus*	Merlot1_N5	18715	655.547	100.00%	17550/17919 (97.94%)

							GLRaV-4/9	LR106 (FJ467503)	*Ampelovirus*	Merlot1_N18	9339	271.871	51.33%	5526/7099 (77.84%)
							GRSPaV	3138-07 (JX559646)	*Foveavirus*	Merlot1_N23	8787	146.887	99.97%	8157/8723 (93.51%)
							GRSPaV	3138-07 (JX559646)	*Foveavirus*	Merlot1_N25	8708	244.398	95.53%	6655/8336 (79.83%)
WIL47	6,969,071	6,951,444	132.4	65411	4	7	GVA^{III}	Is151 (X75433)	*Vitivirus*	WIL47_N43_SD	7352	138.221	23.29%	1371/1712 (80.08%)
							GLRaV-3	NY1 (AF037268)	*Ampelovirus*	WIL47_N4	18722	1722.427	100.00%	17548/17919 (97.93%)
							GRSPaV	3138-07 (JX559646)	*Foveavirus*	WIL47_N22	8726	369.074	95.65%	6662/8346 (79.82%)
							GRSPaV	3138-07 (JX559646)	*Foveavirus*	WIL47_N23	8710	215.087	99.82%	8142/8710 (93.48%)
							GRVFV	Mauzac (KY513701)	*Marafivirus* (tentative)	WIL47_N404	4019	10.897	59.69%	3427/4017 (85.31%)
WIL48	6,642,608	6,621,321	128.2	53212	5	4	GVA^{II}	Is151 (X75433)	*Vitivirus*	WIL48_N20_SD	7322	116.535	93.78%	5487/6894 (79.59%)
							GLRaV-3	NY1 (AF037268)	*Ampelovirus*	WIL48_N4	18402	631.677	99.09%	17386/17756 (97.92%)
							GRSPaV	3138-07 (JX559646)	*Foveavirus*	WIL48_N11	8711	152.874	93.18%	6509/8131 (80.05%)
							GRSPaV	3138-07 (JX559646)	*Foveavirus*	WIL48_N12	8700	68.505	99.70%	8131/8700 (93.46%)
WIL49	8,918,793	8,887,686	132.7	76184	5	6	GVA^{II}	Is151 (X75433)	*Vitivirus*	WIL49_N29_SD	7333	158.202	93.77%	5479/6893 (79.49%)
							GLRaV-3	NY1 (AF037268)	*Ampelovirus*	WIL49_N5	18622	730.866	99.94%	17539/17909 (97.93%)
							GRSPaV	3138-07 (JX559646)	*Foveavirus*	WIL49_N12	8712	299.75	95.45%	6656/8329 (79.91%)
							GRSPaV	3138-07 (JX559646)	*Foveavirus*	WIL49_N13	8712	172.718	99.84%	8139/8712 (93.42%)

							GRVFV	Mauzac (KY513701)	*Marafivirus* (tentative)	WIL49_N5272	1514	5.488	22.51%	1301/1515 (85.87%)
WIL50	4,070,795	4,045,084	127	28893	3	7	GVA^{II}	Is151 (X75433)	*Vitivirus*	WIL50_N27_SD	4284	34.486	19.59%	1156/1440 (80.28%)
							GRSPaV	3138-07 (JX559646)	*Foveavirus*	WIL50_N7	8706	127.646	95.50%	6657/8333 (79.89%)
WIL53	8,291,340	8,242,006	126.1	54153	3	8	GVA^{II}	Is151 (X75433)	*Vitivirus*	WIL53_N26_SD	7330	256.071	93.86%	5487/6900 (79.52%)
							GLRaV-3	NY1 (AF037268)	*Ampelovirus*	WIL53_N4	18561	1261.987	100.00%	17547/17919 (97.92%)
							GRSPaV	3138-07 (JX559646)	*Foveavirus*	WIL53_N15	8711	95.738	99.83%	8144/8711 (93.49%)
							GRSPaV	3138-07 (JX559646)	*Foveavirus*	WIL53_N16	8704	264.03	95.45%	6638/8329 (79.7%)
							GRVFV	Mauzac (KY513701)	*Marafivirus* (tentative)	WIL53_N433	3087	19.299	45.57%	2622/3067 (85.49%)
Shiraz_OR_P5	7,412,911	7378996	126.5	45848	2	8	GRSPaV	3138-07 (JX559646)	*Foveavirus*	Shiraz_OR_P5_N18	8722	1443.013	93.14%	6507/8127 (80.07%)
							GRSPaV	3138-07 (JX559646)	*Foveavirus*	Shiraz_OR_P5_N24	8715	890.954	99.87%	8156/8715 (93.59%)
							GRVFV	Mauzac (KY513701)	*Marafivirus* (tentative)	Shiraz_OR_P5_N304	4168	137.484	60.74%	3567/4088 (87.26%)
Shiraz_OR_P6	11,034,624	10968905	127.2	52144	3	4	GRSPaV	3138-07 (JX559646)	*Foveavirus*	Shiraz_OR_P6_N26	8802	682.444	99.97%	8162/8723 (93.57%)
							GRVFV	Mauzac (KY513701)	*Marafivirus* (tentative)	Shiraz_OR_P6_N564	3718	66.938	55.35%	3183/3725 (85.45%)
CabSA125_R3V30	7,734,941	7673531	126.9	41987	1	20	GVA^{II}	Is151 (X75433)	*Vitivirus*	CabSA125_3R30_N89_LRD	5731	222.553	71.64%	4126/5266 (78.35%)
							GVA^{III}	Is151 (X75433)	*Vitivirus*	CabSA125_3R30_N1944_LRD	2218	270.229	23.15%	1368/1702 (80.38%)
							GLRaV-4/9	LR106 (FJ467503)	*Ampelovirus*	CabSA125_3R30_N13	11333	452.9	53.14%	5745/7349 (78.17%)

							GRSPaV	3138-07 (JX559646)	*Foveavirus*	CabSA125_3R30_N21	8644	706.123	99.06%	8083/8644 (93.51%)
							GRGV	Graciano-T101 (KX171166)	*Maculavirus* (tentative)	CabSA125_3R30_N8761	1008	7.688	14.28%	877/980 (89.49%)
CabSA125_R3V44	6,838,643	6817153	128.4	49351	1	11	GVA[II]	Is151 (X75433)	*Vitivirus*	CabSA125_3R44_N55_LRD	6784	153.798	86.23%	5001/6339 (78.89%)
							GVA[III]	Is151 (X75433)	*Vitivirus*	CabSA125_3R44_N1182_LRD	2795	169.145	23.09%	1357/1697 (79.96%)
							GLRaV-4/9	LR106 (FJ467503)	*Ampelovirus*	CabSA125_3R44_N46	7274	218.01	51.89%	5602/7176 (78.07%)
							GRSPaV	3138-07 (JX559646)	*Foveavirus*	CabSA125_3R44_N24	8772	347.321	95.56%	6648/8339 (79.72%)
							GRSPaV	3138-07 (JX559646)	*Foveavirus*	CabSA125_3R44_N25	8710	142.797	99.82%	8125/8710 (93.28%)

[1] WIL = Willunga, LC = Langhorne Creek, BV = Barossa Valley, CV= Coombe's Vineyard. All grapevines listed are var. Shiraz except Cabw = Cabernet Sauvignon from Willunga and CabSA125 = Cabernet Sauvignon clone SA125 from Coombe's Vineyard, Merlot = Merlot from Willunga.
[2] Including number of contigs from grapevine yellow speckle viroid 1 and hop stunt viroid.
[3] Percentage of genome covered is calculated based on the pairwise alignment of this contig to the exemplar isolate of this virus using the "Blastn" command previously described.
[4] GRSPaV = grapevine rupestris stem pitting-associated virus, GRVFV = grapevine rupestris vein feathering virus, GLRaV-1, -3 = grapevine leafroll-associated virus 1, and 3, GLRaV-4/5, -4/6, -4/9 = grapevine leafroll-associated virus 4 strains 5, 6 and 9, GVA = grapevine virus A, GVF = grapevine virus F, GRGV= grapevine red globe virus

Table S7. Details of grapevine virus A (GVA) isolate sequences used for the phylogenetic analysis.

GenBank accession No (if available)	Isolate	Country	Variety or other host	Symptom[1]	RdRp[2] (ORF1)	MP[2] (ORF3)	CP[2] (ORF4)	RNA-binding[2] (ORF5)	Complete genome[2]
OP752632	BV1_N31_Mild_LRD	Australia	Shiraz	mild LRD	I	I	I	I&II	I
OP752610	Cabw12_N47_LRD	Australia	Cabernet Sauvignon	LRD	II	II	II	I&II	II

OP752625	Cabw12_N52_LRD	Australia	Cabernet Sauvignon	LRD	II	II	II	N/A	II
OP752640	LC5_N12_SD	Australia	Shiraz	SD	II	II	II	I&II	II
OP752637	LC6_N19_SD	Australia	Shiraz	SD	II	II	II	I&II	II
OP752631	LC7_N42_SD	Australia	Shiraz	SD	II	II	II	I&II	II
OP752611	LC9_N19_SD	Australia	Shiraz	SD	II	II	II	I&II	II
OP752620	LC10_N33_SD	Australia	Shiraz	SD	II	II	II	I&II	II
OP752618	LC11_N45_SD	Australia	Shiraz	SD	II	II	II	I&II	II
OP752639	LC13_N31_SD	Australia	Shiraz	SD	II	II	II	I&II	II
OP752616	LC14_N49_SD	Australia	Shiraz	SD	II	II	II	I&II	II
OP752628	LC14_N51_SD	Australia	Shiraz	SD	II	II	II	I&II	II
OP752613	WIL1_N53_SD	Australia	Shiraz	SD	II	II	II	I&II	II
OP752635	WIL1_N54_SD	Australia	Shiraz	SD	III	III	III	III	III
OP752633	WIL2_N36_SD	Australia	Shiraz	SD	II	II	II	I&II	II
OP752608	WIL2_N40_SD	Australia	Shiraz	SD	III	III	III	N/A	III
OP752609	WIL3_N27_SD	Australia	Shiraz	SD	III	III	III	III	III
OP752623	WIL3_N29_SD	Australia	Shiraz	SD	II	II	II	I&II	II

OP752626	WIL4_N28_SD	Australia	Shiraz	SD	II	II	II	I&II	II
OP752621	WIL5_N25_SD	Australia	Shiraz	SD	II	II	II	I&II	II
OP752642	WIL6_N29_SD	Australia	Shiraz	SD	II	II	II	I&II	II
OP752629	WIL7_N29_SD	Australia	Shiraz	SD	II	II	II	I&II	II
OP752615	WIL8_N27_SD	Australia	Shiraz	SD	II	II	II	I&II	II
OP752619	WIL8_N28_SD	Australia	Shiraz	SD	III	III	III	III	III
OP752622	WIL9_N31_LRD	Australia	Shiraz	LRD	III	III	III	III	III
OP752612	WIL10_N41_LRD	Australia	Shiraz	LRD	III	III	III	III	III
OP752641	WIL12_N33_LRD	Australia	Shiraz	LRD	III	III	III	III	III
OP752638	WIL13_N17_LRD	Australia	Shiraz	LRD	III	III	III	III	III
OP752624	WIL47_N43_SD	Australia	Shiraz	LRD	III	III	III	III	III
OP752617	WIL48_N20_SD	Australia	Shiraz	LRD	II	II	II	I&II	II
OP752636	WIL49_N29_SD	Australia	Shiraz	LRD	II	II	II	I&II	II
OP752627	WIL53_N26_SD	Australia	Shiraz	LRD	II	II	II	I&II	II
OP752614	Cabw11_N36_LRD	Australia	Cabernet Sauvignon	LRD	II	II	II	I&II	II
OP752634	Cabw1_N38_LRD	Australia	Cabernet Sauvignon	LRD	III	III	III	III	III

DQ855085	MSH18-1	SouthAfrica	Shiraz	SD-affected	N/A	N/A	I	I&II	N/A
KF013755	BVPN1-21c	USA	Pinot Noir	unknown	N/A	N/A	I	N/A	N/A
DQ855088	P163-1	SouthAfrica	Cinsaut Blanc	SD-negative	N/A	III	III	III	III
DQ787959	GTR1-1	SouthAfrica	Shiraz	SD-negative	III	III	III	III	III
DQ855086	GTR1-2	SouthAfrica	Shiraz	SD-negative	II	II	II	N/A	II
AF441235	JP98	SouthAfrica	Shiraz	SD-affected	N/A	N/A	II	I&II	N/A
MT070962	LC1-2	Australia	Shiraz	SD	II	II	II	N/A	II
MT070963	LC1-1	Australia	Shiraz	SD	II	II	II	II	II
MT070959	Malbec-Richter	Australia	Malbec	SD	N/A	N/A	II	N/A	N/A
DQ855087	BMo32-1	SouthAfrica	Merlot	SD-affected	II	II	II	I&II	II
DQ855083	KWVMo4-1	SouthAfrica	Merlot	SD-affected	II	II	II	I&II	II
DQ855082	P163-M5	SouthAfrica	Cinsaut Blanc	SD-affected	II	II	II	I&II	II
AY244516	pGR-5	SouthAfrica	*Nicotiana benthamiana*	SD-affected	I	I	I	N/A	I
AF007415	PA3	SouthAfrica	*N. benthamiana*	SD-affected	I	I	I	I&II	I

MT070960	BV1-2	Australia	Shiraz	SD-negative	N/A	N/A	I	N/A	N/A
MT070961	BV1-1	Australia	Shiraz	SD-negative	N/A	I	I	I&II	N/A
MG717802	Y170	Armenia	Ambarry	unknown	N/A	N/A	I	N/A	N/A
KF013847	PACF94-142-c07	USA	Cabernet Franc	unknown	N/A	N/A	I	N/A	N/A
JF754577	LN155	China	Golden finger	unknown	N/A	N/A	I	N/A	N/A
KF013785	H6TM2-3-c11	USA	Tamar S1	unknown	N/A	N/A	II	N/A	N/A
KF013833	LVCS92-06	USA	Cabernet Sauvignon	unknown	N/A	N/A	I	N/A	N/A
KF013764	CBPR116-c03	USA	Primitivo CL4	unknown	N/A	N/A	I	N/A	N/A
KF013840	LVMB92-10c11	USA	Malbec	unknown	N/A	N/A	I	N/A	N/A
EU008561	MT25-7	Czech	Muller Thurgau	unknown	N/A	I	I	N/A	N/A
EU008560	MT43-25	Czech	Muller Thurgau	unknown	N/A	N/A	I	N/A	N/A
MG717800	Y170	Armenia	Ambarry	unknown	N/A	N/A	I	N/A	N/A
KF594432	2	Macedonia	Vranec variety	unknown	N/A	N/A	I	I&II	N/A
KM233029	Rc3-6	Portugal	Ricoca	unknown	N/A	N/A	I	I&II	N/A
MK404721	TT2017-74-53	France	Pinot Noir	unknown	I	I	I	N/A	I

KM233033	S3-1	Portugal	Sousao	unknown	N/A	N/A	I	I&II	N/A
JN860997	IH8	Poland	Vitis vinifera	unknown	N/A	N/A	I	N/A	N/A
JN860998	IH11	Poland	Vitis sp.	unknown	N/A	N/A	I	N/A	N/A
MK404720	TT2017-74-47	France	Pinot Noir	unknown	I	I	I	N/A	I
KC962564	I327-5	SouthAfrica	Shiraz	SD-negative	I	I	I	I&II	I
KM233003	TM3-1	Portugal	Tinta Martins	unknown	N/A	N/A	I	I&II	N/A
KM232996	BT3-11	Portugal	Bastardo Tinto	unknown	N/A	N/A	I	N/A	N/A
KF013766	CBPR116-c12	USA	Primitivo CL4	unknown	N/A	N/A	I	N/A	N/A
MF979533	VB-108	Croatia	Babica	unknown	I	I	I	I&II	I
KX828703	TRAJ2-BR	Brazil	Trajadura	unknown	N/A	I	I	I&II	I
DQ855081	GTR1SD-1	SouthAfrica	Shiraz	SD-affected	II	II	II	I&II	II
DQ855084	GTG11-1	SouthAfrica	Shiraz	SD-negative	I	I	I	I&II	I
X75433	Is-151	Italy	benthamiana	unknown	I	I	I	I&II	I
MK404722	TT2017-79	France	Pinot Noir	unknown	I	I	I	N/A	I
MG925333	P70	France	Pinot noir	unknown	N/A	I	I	I&II	I

JX559641	3138-03	Canada	Vitis vinifera	unknown	III	III	III	III	III
LC617941	g13-C57*	Japan	Vitis sp.	unknown	III	III	III	I&II	III
LC617944	g13-C274	Japan	Vitis sp.	unknown	I	I	I	I&II	I
KF013813	LV94-02	USA	Vitis vinifera	unknown	N/A	N/A	I	N/A	N/A
MG977014	p26	Iran	Vitis vinifera	unknown	N/A	N/A	I	N/A	N/A
KF013799	SLWZF1-2c1	USA	Zinfandel	unknown	N/A	N/A	I	N/A	N/A
JF754576	LN141	China	Mars Seedless	unknown	N/A	N/A	I	N/A	N/A
AF441234	92-788	SouthAfrica	Cabernet Sauvignon	SD-affected	N/A	N/A	I	I&II	N/A
KM233013	MI3-15	Portugal	Malandra	unknown	N/A	N/A	I	I&II	N/A
KM233012	Ml3-12	Portugal	Malandra	unknown	N/A	N/A	I	I&II	N/A
KF594433	3	Macedonia	Frankovka	unknown	N/A	N/A	I	I&II	N/A
KF594434	4	Macedonia	Vranec	unknown	N/A	N/A	I	I&II	N/A
KF594435	5	Macedonia	Vranec	unknown	N/A	N/A	I	I&II	N/A
AB039841		Japan	Vitis sp.	unknown	N/A	N/A	I	N/A	N/A
AF441236	P163-1	SouthAfrica	Cinsaut Blanc	unknown	III	N/A	III	III	N/A
DQ911145	LQ58	China	Vitis sp	unknown	N/A	N/A	III	N/A	N/A

JF754566	LN9	China	Vitis vinifera	unknown	N/A	N/A	I	N/A	N/A
JF754567	LN37	China	Vitis vinifera	unknown	N/A	N/A	I	N/A	N/A
JF754568	LN43	China	Autumn black	unknown	N/A	N/A	I	N/A	N/A
JF754569	LN50	China	Vitis vinifera	unknown	N/A	N/A	I	N/A	N/A
JF754570	LN60	China	Rosario Bianco	unknown	N/A	N/A	I	N/A	N/A
JF754571	LN68	China	Yatomi Rosa	unknown	N/A	N/A	I	N/A	N/A
JF754572	LN107	China	Renitaka	unknown	N/A	N/A	I	N/A	N/A
JF754573	LN121	China	Vitis vinifera	unknown	N/A	N/A	I	N/A	N/A
JF754574	LN126	China	Vitis vinifera	unknown	N/A	N/A	I	N/A	N/A
JF754575	LN136	China	Vitis vinifera	unknown	N/A	N/A	I	N/A	N/A
JF754578	LN68-2	China	Yatomi Rosa	unknown	N/A	N/A	I	N/A	N/A
JN565033	IH10	Poland	Vitis vinifera	unknown	N/A	N/A	I	N/A	N/A
JN860999	IH23	Poland	Vitis vinifera	unknown	N/A	N/A	I	N/A	N/A
JN861000	IH27	Poland	Vitis vinifera	unknown	N/A	N/A	I	N/A	N/A
KF013756	BVPN1-2c	USA	Pinot Noir	unknown	N/A	N/A	I	N/A	N/A
KF013757	BVPN1-11G	USA	Pinot Noir	unknown	N/A	N/A	III	N/A	N/A

KF013758	BVPN2-8c	USA	Pinot Noir	unknown	N/A	N/A	III	N/A	N/A
KF013759	BVPN2-13c	USA	Pinot Noir	unknown	N/A	N/A	I	N/A	N/A
KF013760	BVPN2-b15E	USA	Pinot Noir	unknown	N/A	N/A	II	N/A	N/A
KF013761	BVPN2-b23E	USA	Pinot Noir	unknown	N/A	N/A	II	N/A	N/A
KF013762	BVPN2-b26B	USA	Pinot Noir	unknown	N/A	N/A	I	N/A	N/A
KF013763	CBPR116-2c	USA	Primitivo CL 4	unknown	N/A	N/A	III	N/A	N/A
KF013765	CBPR116-c09	USA	Primitivo CL 4	unknown	N/A	N/A	I	N/A	N/A
KF013767	CBSM119-2c	USA	Sami S1	unknown	N/A	N/A	I	N/A	N/A
KF013768	CBSM119-3c	USA	Sami S1	unknown	N/A	N/A	III	N/A	N/A
KF013770	CBSM119_c08	USA	Sami S2	unknown	N/A	N/A	I	N/A	N/A
KF013771	CSOT1_14c	USA	Cabernet Sauvignon	unknown	N/A	N/A	I	N/A	N/A
KF013772	CSOT1_4c	USA	Cabernet Sauvignon	unknown	N/A	N/A	II	N/A	N/A
KF013774	CSOT1-b50H	USA	Cabernet Sauvignon	unknown	N/A	N/A	III	N/A	N/A
KF013775	CSOT2-19c	USA	Cabernet Sauvignon	unknown	N/A	N/A	I	N/A	N/A
KF013776	CSOT2-2c	USA	Cabernet Sauvignon	unknown	N/A	N/A	III	N/A	N/A
KF013777	CSOT2-2G	USA	Cabernet Sauvignon	unknown	N/A	N/A	III	N/A	N/A

KF013779	H6TM2-3_2c2	USA	Tamar S1	unknown	N/A	N/A	III	N/A	N/A
KF013780	H6TM2-3_3c1	USA	Tamar S1	unknown	N/A	N/A	II	N/A	N/A
KF013781	H6TM2-3_3c2	USA	Tamar S1	unknown	N/A	N/A	I	N/A	N/A
KF013782	H6TM2-3_c01	USA	Tamar S1	unknown	N/A	N/A	II	N/A	N/A
KF013783	H6TM2-3_c07	USA	Tamar S1	unknown	N/A	N/A	III	N/A	N/A
KF013784	H6TM2-3_c09	USA	Tamar S1	unknown	N/A	N/A	III	N/A	N/A
KF013786	HHCS1_17c	USA	Cabernet Sauvignon	unknown	N/A	N/A	III	N/A	N/A
KF013787	HHCS1_4c	USA	Cabernet Sauvignon	unknown	N/A	N/A	II	N/A	N/A
KF013788	HHCS2_13c	USA	Cabernet Sauvignon	unknown	N/A	N/A	III	N/A	N/A
KF013789	HHCS2_6c	USA	Cabernet Sauvignon	unknown	N/A	N/A	II	N/A	N/A
KF013790	HHCS3_2c	USA	Cabernet Sauvignon	unknown	N/A	N/A	I	N/A	N/A
KF013791	HHCS3_8c	USA	Cabernet Sauvignon	unknown	N/A	N/A	III	N/A	N/A
KF013792	HHCS3_7c	USA	Cabernet Sauvignon	unknown	N/A	N/A	II	N/A	N/A
KF013793	HHPN1_2c2	USA	Pinot Noir	unknown	N/A	N/A	I	N/A	N/A
KF013794	HHPN1_9c	USA	Pinot Noir	unknown	N/A	N/A	III	N/A	N/A
KF013795	HHPN1_16c	USA	Pinot Noir	unknown	N/A	N/A	I	N/A	N/A

KF013796	HHPN1-115B	USA	Pinot Noir	unknown	N/A	N/A	I	N/A	N/A
KF013797	HRPCH1_10c	USA	Chardonnay	unknown	N/A	N/A	I	N/A	N/A
KF013798	SLWZF1-11c	USA	Zinfandel	unknown	N/A	N/A	III	N/A	N/A
KF013800	SLWZF1-2c2	USA	Zinfandel	unknown	N/A	N/A	II	N/A	N/A
KF013801	SLWZF1-5c2	USA	Zinfandel	unknown	N/A	N/A	III	N/A	N/A
KF013802	SLWZF1-105E	USA	Zinfandel	unknown	N/A	N/A	II	N/A	N/A
KF013803	SLWZF1-5D	USA	Zinfandel	unknown	N/A	N/A	I	N/A	N/A
KF013804	SLWZF1-6	USA	Zinfandel	unknown	N/A	N/A	II	N/A	N/A
KF013806	VHLM1_5c	USA	Lemberger	unknown	N/A	N/A	I	N/A	N/A
KF013807	VHLM1_2c	USA	Lemberger	unknown	N/A	N/A	I	N/A	N/A
KF013808	VHLM1-8D	USA	Lemberger	unknown	N/A	N/A	I	N/A	N/A
KF013809	VHLM1-9D	USA	Lemberger	unknown	N/A	N/A	I	N/A	N/A
KF013810	LREP100_9c	USA	Emperor	unknown	N/A	N/A	III	N/A	N/A
KF013811	LREP100_c03	USA	Emperor	unknown	N/A	N/A	III	N/A	N/A
KF013812	LV94-02_2c	USA	Vitis vinifera	unknown	N/A	N/A	III	N/A	N/A
KF013814	LV94-02_c04	USA	Vitis vinifera	unknown	N/A	N/A	I	N/A	N/A

KF013815	LV94-02_c09	USA	Vitis vinifera	unknown	N/A	N/A	I	N/A	N/A
KF013816	LVCH92-04_4c2	USA	Chardonnay	unknown	N/A	N/A	III	N/A	N/A
KF013817	LVCH92-04_7c	USA	Chardonnay	unknown	N/A	N/A	III	N/A	N/A
KF013818	LVCH92-04_c06	USA	Chardonnay	unknown	N/A	N/A	III	N/A	N/A
KF013819	LVCH92-07_3c	USA	Chardonnay	unknown	N/A	N/A	III	N/A	N/A
KF013820	LVCH92-07_2c1	USA	Chardonnay	unknown	N/A	N/A	III	N/A	N/A
KF013821	LVCH92-07_2c2	USA	Chardonnay	unknown	N/A	N/A	III	N/A	N/A
KF013822	LVCH92-07_c05	USA	Chardonnay	unknown	N/A	N/A	III	N/A	N/A
KF013823	LVCH92-07_c09	USA	Chardonnay	unknown	N/A	N/A	III	N/A	N/A
KF013824	LVCH92-09_2c1	USA	Chardonnay	unknown	N/A	N/A	III	N/A	N/A
KF013825	LVCH92-09_2c2	USA	Chardonnay	unknown	N/A	N/A	III	N/A	N/A
KF013826	LVCH92-09_3c	USA	Chardonnay	unknown	N/A	N/A	II	N/A	N/A
KF013827	LVCH92-09_c07	USA	Chardonnay	unknown	N/A	N/A	III	N/A	N/A
KF013828	LVCH94-04_10c	USA	Chardonnay	unknown	N/A	N/A	I	N/A	N/A
KF013829	LVCH94-04_c11	USA	Chardonnay	unknown	N/A	N/A	III	N/A	N/A
KF013830	LVCS92-06_2c1	USA	Chardonnay	unknown	N/A	N/A	I	N/A	N/A

KF013831	LVCS92-06_3c2	USA	Chardonnay	unknown	N/A	N/A	III	N/A	N/A
KF013832	LVCS92-06_2c2	USA	Chardonnay	unknown	N/A	N/A	II	N/A	N/A
KF013834	LVCS92-06_c04	USA	Chardonnay	unknown	N/A	N/A	III	N/A	N/A
KF013835	LVCS92-06_c08	USA	Chardonnay	unknown	N/A	N/A	III	N/A	N/A
KF013836	LVMB92-10_5c	USA	Malbec	unknown	N/A	N/A	I	N/A	N/A
KF013837	LVMB92-10_2c	USA	Malbec	unknown	N/A	N/A	III	N/A	N/A
KF013838	LVMB92-10_c05	USA	Malbec	unknown	N/A	N/A	I	N/A	N/A
KF013839	LVMB92-10_c08	USA	Malbec	unknown	N/A	N/A	I	N/A	N/A
KF013841	LVSB91-02_11c	USA	Malbec	unknown	N/A	N/A	I	N/A	N/A
KF013842	LVZT93-09_12c	USA	Zante	unknown	N/A	N/A	II	N/A	N/A
KF013843	PACF94-142_3c	USA	Cabernet Franc	unknown	N/A	N/A	I	N/A	N/A
KF013844	PACF94-142_4c	USA	Cabernet Franc	unknown	N/A	N/A	III	N/A	N/A
KF013845	PACF94-142_c02	USA	Cabernet Franc	unknown	N/A	N/A	III	N/A	N/A
KF013846	PACF94-142_c06	USA	Cabernet Franc	unknown	N/A	N/A	I	N/A	N/A
KF013848	PACF94-142_c08	USA	Cabernet Franc	unknown	N/A	N/A	I	N/A	N/A
KF013849	PACF94-142_c12	USA	Cabernet Franc	unknown	N/A	N/A	I	N/A	N/A

KF013850	PLCF95-413_4c	USA	Cabernet Franc	unknown	N/A	N/A	III	N/A	N/A
KF013851	PLCF95-413_c02	USA	Cabernet Franc	unknown	N/A	N/A	I	N/A	N/A
KF013852	PLCF95-413_c05	USA	Cabernet Franc	unknown	N/A	N/A	III	N/A	N/A
KF013853	PLCF95-413_c06	USA	Cabernet Franc	unknown	N/A	N/A	II	N/A	N/A
KF013854	PLCF95-413_c10	USA	Cabernet Franc	unknown	N/A	N/A	II	N/A	N/A
LC387465	KGA	South Korea	Vitis sp.	unknown	N/A	N/A	I	N/A	N/A
LK937667	K4	Greece	Aidani white	unknown	N/A	N/A	III	N/A	N/A
LK937668	K12	Greece	Aidani red	unknown	N/A	N/A	III	N/A	N/A
LK937669	T2-11	Greece	Koumariano	unknown	N/A	N/A	III	N/A	N/A
LK937670	D9	Greece	Potamisi	unknown	N/A	N/A	III	N/A	N/A
LK937671	P4-11	Greece	Aidani white	unknown	N/A	N/A	I	N/A	N/A
LK937672	F15	Greece	Kakomauro	unknown	N/A	N/A	III	N/A	N/A
LK937673	5Y	Greece	140 Ru	unknown	N/A	N/A	I	N/A	N/A
LK937674	64	Greece	Vertzami	unknown	N/A	N/A	I	N/A	N/A
LK937675	72-1	Greece	Cabernet franc	unknown	N/A	N/A	III	N/A	N/A
LK937676	73	Greece	Roditis	unknown	N/A	N/A	I	N/A	N/A

LK937677	75-1	Greece	Cabernet	unknown	N/A	N/A	I	N/A	N/A
LK937678	89-3	Greece	Attiki	unknown	N/A	N/A	I	N/A	N/A
LK937679	95-4	Greece	Roditis	unknown	N/A	N/A	I	N/A	N/A
LK937680	P14	Greece	Korithiaki stafida	unknown	N/A	N/A	I	N/A	N/A
LR794210	73a	Greece	Roditis	unknown	N/A	N/A	III	N/A	N/A
LR794211	K11	Greece	Mandilaria	unknown	N/A	N/A	III	N/A	N/A
LR794212	D24	Greece	Karabraimi	unknown	N/A	N/A	III	N/A	N/A
MG977013	p25	Iran	Vitis vinifera	unknown	N/A	N/A	I	N/A	N/A
KM232988	TL3-5	Portugal	Tinta Lameira	unknown	N/A	N/A	I	N/A	N/A
KM232989	TL3-7	Portugal	Tinta Lameira	unknown	N/A	N/A	I	N/A	N/A
KM232990	TL3-13	Portugal	Tinta Lameira	unknown	N/A	N/A	I	N/A	N/A
KM232991	TL3-31	Portugal	Tinta Lameira	unknown	N/A	N/A	I	N/A	N/A
KM233034	S3-4	Portugal	Sousao	unknown	N/A	N/A	I	I&II	N/A
KM233033	S3-1	Portugal	Sousao	unknown	N/A	N/A	I	I&II	N/A
KM233032	Rc3-1	Portugal	Ricoca	unknown	N/A	N/A	III	III	N/A
KM233031	Rc3-12	Portugal	Ricoca	unknown	N/A	N/A	I	I&II	N/A

KM233030	Rc3-7	Portugal	Ricoca	unknown	N/A	N/A	I	I&II	N/A
KM233029	Rc3-6	Portugal	Ricoca	unknown	N/A	N/A	I	I&II	N/A
KM233028	Rs3-16	Portugal	Roseira	unknown	N/A	N/A	I	I&II	N/A
KM233027	Rs3-15	Portugal	Roseira	unknown	N/A	N/A	III	III	N/A
KM233026	Rs3-10	Portugal	Roseira	unknown	N/A	N/A	III	III	N/A
KM233025	Rs3-7	Portugal	Roseira	unknown	N/A	N/A	I	I&II	N/A
KM233024	Rs3-6	Portugal	Roseira	unknown	N/A	N/A	I	I&II	N/A
KM233023	Rs3-5	Portugal	Roseira	unknown	N/A	N/A	I	I&II	N/A
KM233022	Rs3-3	Portugal	Roseira	unknown	N/A	N/A	I	I&II	N/A
KM233021	Rs3-2	Portugal	Roseira	unknown	N/A	N/A	I	I&II	N/A
KM233020	Rs3-1	Portugal	Roseira	unknown	N/A	N/A	I	I&II	N/A
KM233019	Ml3-3	Portugal	Roseira	unknown	N/A	N/A	III	III	N/A
KM232992	BT3-1	Portugal	Bastardo Tinto	unknown	N/A	N/A	I	N/A	N/A
KM232993	BT3-3	Portugal	Bastardo Tinto	unknown	N/A	N/A	I	N/A	N/A
KM232994	BT3-6	Portugal	Bastardo Tinto	unknown	N/A	N/A	I	N/A	N/A
KM232995	BT3-9	Portugal	Bastardo Tinto	unknown	N/A	N/A	I	N/A	N/A

KM232997	BT3-14	Portugal	Bastardo Tinto	unknown	N/A	N/A	I	N/A	N/A
KM232998	BT3-33	Portugal	Bastardo Tinto	unknown	N/A	N/A	I	N/A	N/A
KM232999	TF3-6	Portugal	Tinta Ferreira	unknown	N/A	N/A	I	I&II	N/A
KM233000	TF3-3	Portugal	Tinta Ferreira	unknown	N/A	N/A	III	III	N/A
KM233001	TF3-5	Portugal	Tinta Ferreira	unknown	N/A	N/A	III	III	N/A
KM233002	TF3-7	Portugal	Tinta Ferreira	unknown	N/A	N/A	III	III	N/A
KM233004	TM3-5	Portugal	Tinta Martins	unknown	N/A	N/A	I	I&II	N/A
KM233005	TM3-6	Portugal	Tinta Martins	unknown	N/A	N/A	I	I&II	N/A
KM233006	TM3-4	Portugal	Tinta Martins	unknown	N/A	N/A	III	I&II	N/A
KM233007	Ml3-1	Portugal	Malandra	unknown	N/A	N/A	I	I&II	N/A
KM233008	Ml3-4	Portugal	Malandra	unknown	N/A	N/A	I	I&II	N/A
KM233009	Ml3-5	Portugal	Malandra	unknown	N/A	N/A	I	I&II	N/A
KM233010	Ml3-10	Portugal	Malandra	unknown	N/A	N/A	I	I&II	N/A
KM233011	Ml3-11	Portugal	Malandra	unknown	N/A	N/A	I	I&II	N/A
KM233014	Ml3-16A	Portugal	Malandra	unknown	N/A	N/A	I	I&II	N/A
KM233015	Ml3-9	Portugal	Malandra	unknown	N/A	N/A	II	I&II	N/A

KM233016	Ml3-7	Portugal	Malandra	unknown	N/A	N/A	III	III	N/A
KM233017	Ml3-13	Portugal	Malandra	unknown	N/A	N/A	III	III	N/A
KM233018	Ml3-14	Portugal	Malandra	unknown	N/A	N/A	III	III	N/A
MK982553	M5v	South Africa	Cinsaut Blanc	SD-affected	II	II	II	I&II	II
MG717789	Y245-1	Turkey	Karasakis	unknown	N/A	N/A	I	N/A	N/A
MG717790	Y245-2	Turkey	Karasakis	unknown	N/A	N/A	I	N/A	N/A
MG717791	Y273-1	Turkey	Narince	unknown	N/A	N/A	I	N/A	N/A
MG717792	Y273-2	Turkey	Narince	unknown	N/A	N/A	I	N/A	N/A
MG717793	Y273-3	Turkey	Narince	unknown	N/A	N/A	I	N/A	N/A
MG717794	Y273-4	Turkey	Narince	unknown	N/A	N/A	I	N/A	N/A
MG717795	Y307-1	Ukraine	Tanagos Kosky	unknown	N/A	N/A	I	N/A	N/A
MG717796	Y307-2	Ukraine	Tanagos Kosky	unknown	N/A	N/A	I	N/A	N/A
MG717797	Y307-4	Ukraine	Tanagos Kosky	unknown	N/A	N/A	I	N/A	N/A
MG717798	Y161-1	Lebanon	Agmi Assouad	unknown	N/A	N/A	III	N/A	N/A
MG717799	Y161-2	Lebanon	Agmi Assouad	unknown	N/A	N/A	I	N/A	N/A
MG717801	Y170- 2	Armenia	Ambarry	unknown	N/A	N/A	I	N/A	N/A

MG717803	Y170- 4	Armenia	Ambarry	unknown	N/A	N/A	I	N/A	N/A
MG717804	Y170- 5	Armenia	Ambarry	unknown	N/A	N/A	I	N/A	N/A
MG717805	Y170- 6	Armenia	Ambarry	unknown	N/A	N/A	I	N/A	N/A
MG717806	Y172-1	Azerbaijan	Ara Hirna	unknown	N/A	N/A	I	N/A	N/A
MG717807	Y172-2	Azerbaijan	Ara Hirna	unknown	N/A	N/A	I	N/A	N/A
MG717808	Y172-3	Azerbaijan	Ara Hirna	unknown	N/A	N/A	I	N/A	N/A
MG717809	Y172-4	Azerbaijan	Ara Hirna	unknown	N/A	N/A	I	N/A	N/A
MG717810	95-177-1	Italy	Italia	unknown	N/A	N/A	I	N/A	N/A
MG717811	95-177-2	Italy	Italia	unknown	N/A	N/A	I	N/A	N/A
MG717812	95-177-3	Italy	Italia	unknown	N/A	N/A	I	N/A	N/A
MG717813	95-177-4	Italy	Italia	unknown	N/A	N/A	I	N/A	N/A
MG717814	Y199-1	USA	Black Monucca	unknown	N/A	N/A	III	N/A	N/A
MG717815	Y199-3	USA	Black Monucca	unknown	N/A	N/A	III	N/A	N/A
MG717816	Y199-4	USA	Black Monucca	unknown	N/A	N/A	III	N/A	N/A
MG717817	Y217-1	USA	Emperor	unknown	N/A	N/A	III	N/A	N/A
MG717818	Y217-2	USA	Emperor	unknown	N/A	N/A	III	N/A	N/A

MG717819	Y217-3	USA	Emperor	unknown	N/A	N/A	III	N/A	N/A
MG717820	Y217-4	USA	Emperor	unknown	N/A	N/A	III	N/A	N/A
MG717821	Y276-1	USA	Otscha Bala	unknown	N/A	N/A	I	N/A	N/A
MG717822	Y276-2	USA	Otscha Bala	unknown	N/A	N/A	I	N/A	N/A
MG717823	Y276-3	USA	Otscha Bala	unknown	N/A	N/A	I	N/A	N/A
MG717824	Y252-1	USA	Koudsi	unknown	N/A	N/A	III	N/A	N/A
MG717825	Y252-2	USA	Koudsi	unknown	N/A	N/A	III	N/A	N/A
MG717826	Y252-4	USA	Koudsi	unknown	N/A	N/A	III	N/A	N/A
MG717827	A94-1	USA	Servant	unknown	N/A	N/A	III	N/A	N/A
MG717828	A94-2	USA	Servant	unknown	N/A	N/A	II	N/A	N/A
MG717829	A94-4	USA	Servant	unknown	N/A	N/A	II	N/A	N/A
MG717831	SA125-2	Australia	Cabernet Sauvignon	unknown	N/A	N/A	II	N/A	N/A
MG717832	SA125-3	Australia	Cabernet Sauvignon	unknown	N/A	N/A	II	N/A	N/A
MG717833	Y258-1	Azerbaijan	Lilia Bidona	unknown	N/A	N/A	I	N/A	N/A
KF667501	IT-BA	Brazil	Italia	unknown	N/A	N/A	I	N/A	N/A
AY340581	SP	Brazil	Niagra rosada.	unknown	N/A	N/A	I	N/A	N/A

ON567250	A1892o	Russia	Vitis vinifera	unknown	I	I	I	I&II	I
MW309530	RSA-03-04_Agawam	South Africa	Agawam	unknown	I	I	I	I&II	I
MW309531	RSA-06-08_Blauer_Limberger	South Africa	Blauer Limberger	unknown	I	I	I	I&II	I
MW309532	RSA-07-15_Cataratto	South Africa	Cataratto	unknown	I	I	I	I&II	I
MW309533	RSA-09-06_Clairette_Egreneuse	South Africa	Clairette Egreneuse	unknown	N/A	III	III	III	III
MW309534	RSA-10-06_Cornifesto	South Africa	Cornifesto	unknown	I	I	I	I&II	I
MW309535	RSA-17-07_Kadarka	South Africa	Kadarka	unknown	I	I	I	I&II	I
MW309536	RSA-18-02_Limberger	South Africa	Limberger	unknown	I	I	I	I&II	I
MW309537	RSA-20-04_Mourvedre	South Africa	Mourvedre	unknown	III	III	III	III	III
MW309538	RSA-20-04_Mourvedre_2	South Africa	Mourvedre	unknown	I	I	I	I&II	I
MW309539	RSA-22-15_Mourisco_de_Semente	South Africa	Mourisco de Semente	unknown	I	I	I	I&II	I
MW309540	RSA-23-01_Muscat_d_Alexandrie_blanc	South Africa	Alexandrie blanc	unknown	I	I	I	I&II	I
MW309541	RSA-23-15_Muscat_St_Laurent	South Africa	Muscat Saint Laurent	unknown	III	III	III	III	III
MW309542	RSA-26-02_Petit_Sirah_Durif	South Africa	Petit Sirah	unknown	I	I	I	I&II	I
MW309543	RSA-33-06_Teoulier	South Africa	Teoulier	unknown	III	III	III	III	III

MW309544	strain RSA-33-06_Teoulier_2	South Africa	Teoulier	unknown	I	I	I	I&II	I
MW309545	RSA-33-07_Teroldego	South Africa	Teroldego	unknown	III	III	III	III	III
MW309547	RSA-45-07_Red_Globe_2	South Africa	Red Globe	unknown	I	I	I	I&II	I
MW309548	RSA-48-09_Tinta_Amarela	South Africa	Tinta Amarela	unknown	III	III	III	III	III
MW309549	RSA-48-09_Tinta_Amarela_2	South Africa	Tinta Amarela	unknown	I	I	I	I&II	I
MW309551	RSA-55-01_Staufer	South Africa	Staufer	unknown	II	II	II	I&II	II
MZ440717	12G456	Canada	Vitis vinifera	unknown	I	I	I	I&II	I
MZ440718	12G479A	Canada	Vitis vinifera	unknown	I	I	I	I&II	I
MZ440719	2G479B	Canada	Vitis vinifera	unknown	I	I	I	I&II	I
MZ440720	12G442	Canada	Vitis vinifera	unknown	III	III	III	III	III
MZ440721	12G446	Canada	Vitis vinifera	unknown	III	III	III	III	III
MZ440722	12G475	Canada	Vitis vinifera	unknown	I	I	I	I&II	I
NC_018458	AUD46129	USA	Vitis vinifera	N/A	N/A	N/A	N/A	N/A	N/A

[1] SD = Shiraz disease, LRD = leafroll disease (LRD), SD-affect and SD-negative isolates refer to when grapevines infected with these isolates, they show typical SD symptoms, or they remain asymptomatic [11,32].
[2] I = GVA^{I}, II = GVA^{II}, III = GVA^{III} , phylogroup of GVA by RdRp, MP, CP, RNA-binding genes and complete genome by phylogenetic analysis.
*Two isolates assigned to different phylogroup when using different gene regions of GVA.

Table S8. Details of the Australian grapevine leafroll associate virus 3 (GLRaV-3) isolates generated by metagenomic high-throughput sequencing and the publicly available isolates used for the phylogenetic analysis.

Phylogroup	% nt identities of CP gene of each phylogroup	Accession no.	Isolate	Country	Variety	%nt identity to NY1[1]
V	74.31-79.83	KY073323	8415A	Canada	Riesling	74.31%
		MH521097	Cha141	USA	Chardonnay	76.82%
		KM058745	GH24	South Africa	Cabernet Sauvignon	76.82%
		JX266782	3m-139	Australia	Sauvignon Blanc	76.86%
		KY707826	NdA121	Italy	Nero d'Avola	77.88%
		MK032068	Vdl	Canada	Vidal	77.92%
		MH521095	Cha138	USA	Chardonnay	78.66%
		MH521094	Cha137	USA	Chardonnay	78.66%
		KY764332	Trc139	USA	Chardonnay	78.66%
		JQ796828	3	USA	Merlot	78.87%
		JQ655296	GH30	South Africa	Cabernet Sauvignon	79.09%
		JQ655295	GH11	South Africa	Cabernet Sauvignon	79.41%
		MH521105	Gre233	Germany	Green Veltliner	79.72%
		MH521114	Mar239	USA	Marzemino	79.83%
IV	81.1-82.70	MH521098	Cha246	USA	Chardonnay	81.10%
		MH521091	Cab248	USA	Cabernet Sauvignon	81.21%
		MH521117	Pin244b	USA	Pinot Noir	81.21%
		KY073324	8415B	Canada	Riesling	81.42%

		MH796136	GLRaV3-ID45	USA	Cabernet Sauvignon	81.42%
		KY707824	Pro95	USA	11184	81.53%
		KY707825	Rod96	Greece	Roditis	81.53%
		KY764333	Trc138	USA	Chardonnay	81.63%
		MH521103	245	USA	Vitis vinifera	81.63%
		MH521109	Kat255b	Canada	Katelin	82.70%
III	91.4-91.72	KY886362	I-LR101	USA	Vitis vinifera	91.40%
		MF186605	I-LR101	USA	Vitis vinifera	91.40%
		GQ352633	PL-20	South Africa	Vitis sp.	91.51%
		MH521099	Cha246b	USA	Chardonnay	91.61%
		MH521100	Cha247	USA	Chardonnay	91.61%
		MH521118	Pin249	USA	Pinot noir	91.61%
		JQ423939	LN	China	Venus Seedless	91.72%
		MF991951	VB-108	Croatia	Babica	91.72%
		MH521104	Gor259	France	Goron de Bovernier	91.72%
II	92.46-92.78	MH814485	12G446	Canada	Vitis vinifera	92.46%
		EU259806	GP18	South Africa	Vitis sp.	92.46%
		MH814483	12G438A	Canada	Vitis vinifera	92.57%
		MH521115	Mer240	USA	Merlot	92.57%
		KY821093	AK6	Pakistan	Sugra one	92.57%
		MH814487	12G456	Canada	Vitis vinifera	92.68%
		KX701860	ISAB-BR	Brazil	Isabel	92.68%
		KJ174518		Israel	Vitis sp.	92.68%

		MH814486	12G448	Canada	Vitis vinifera	92.78%
		GQ352632	623	South Africa	Ruby Cabernet	92.78%
		KX756668	TC-BR	Brazil	Tardia de Caxias	92.78%
I	94.59-99.47	MH521102	185	USA	Vitis vinifera	94.59%
		MH814488	17VT16	Canada	Vitis vinifera	94.59%
		MK988555	Sau	China	Cabernet Sauvignon	97.77%
		EU344893	Cl-766	Chile	Merlot	99.04%
		MH521089	BHA172	Spain	BHAU 19-010	99.04%
		MH521088	AU173	Spain	AU 33-057	99.15%
		JX559645	3138-07	Canada	Vitis vinifera	99.15%
		MH796135	ID46	USA	Cabernet sauvignon	99.15%
		MH521110	Kis24	Hungary	Kishmish Vatkana	99.15%
		MN548393	SK933	Slovakia	Vitis vinifera	99.15%
		MK804765	NUB-BR	Brazil	Vitis sp. cv. BRS Nubia	99.15%
		KY821094	SL37-3	Pakistan	Italia	99.26%
		MH521090	Bla223	USA	Black Muscat Alexandria	99.26%
		GQ352631	621	South Africa	Cabernet Sauvignon	99.26%
		MH521101	Dk256	USA	DK03	99.26%
		OP752692	Cabw2_N1	Australia	Cabernet Sauvignon	99.26%
		OP752684	Cabw1_N2	Australia	Cabernet Sauvignon	99.26%
		MH814484	12G445	Canada	Vitis vinifera	99.26%
		MH814489	14G462	Canada	Vitis vinifera	99.26%
		MH521096	Cha138b	USA	Chardonnay	99.36%

KX756669	TRAJ-BR	Brazil	Trajadura	99.36%
MH521092	Cha103	USA	Chardonnay	99.36%
MH521111	Kis252	Hungary	Kishmish Vatkana	99.36%
MH521093	Cha106	USA	Chardonnay	99.36%
MH521119	Tou260	Portugal	Touriga Franca	99.36%
MH814491	14G466	Canada	Vitis vinifera	99.36%
MH521112	LN3204	USA	LN33	99.36%
MH521106	Ita218	USA	Italia	99.36%
MH521107	Ita219	USA	Italia	99.36%
OP752688	Merlot1_N5	Australia	Merlot	99.36%
OP752695	WIL47_N4	Australia	Shiraz	99.36%
OP752680	WIL53_N4	Australia	Shiraz	99.36%
OP752698	WIL48_N4	Australia	Shiraz	99.36%
OP752693	WIL49_N5	Australia	Shiraz	99.36%
OP752690	WIL12_N3	Australia	Shiraz	99.36%
OP752683	WIL5_N4	Australia	Shiraz	99.36%
OP752678	WIL6_N4	Australia	Shiraz	99.36%
OP752682	WIL7_N5	Australia	Shiraz	99.36%
OP752687	WIL4_N4	Australia	Shiraz	99.36%
OP752681	WIL8_N4	Australia	Shiraz	99.36%
OP752685	WIL10_N4	Australia	Shiraz	99.36%
OP752689	WIL9_N3	Australia	Shiraz	99.36%
OP752691	WIL50_N4	Australia	Shiraz	99.36%
OP752686	Cabw11_N3	Australia	Cabernet Sauvignon	99.36%
OP752696	WIL14_N4	Australia	Shiraz	99.36%

OP752677	WIL15_N4	Australia	Shiraz	99.36%
OP752679	Cabw12_N4	Australia	Cabernet Sauvignon	99.36%
MH814482	12G402	Canada	Vitis vinifera	99.47%
GU983863	WAMR	USA	Merlot	99.47%
MH521108	Kat255	Canada	Katelin	99.47%
MH521116	Pin244	USA	Pinot Noir	99.47%
MH814490	14G463	Canada	Vitis vinifera	99.47%
MH521113	Mal162	USA	Malbec	99.47%
OP752630	WIL11_N43	Australia	Shiraz	99.68%
JQ023131	GLRaV-1_1050	Canada	Vitis sp.	N/A

[1] Pairwise nucleotide identity of coat protein gene to the exemplar isolate NY1 (AF037268).

Table S9. Pairwise amino acid similarity of grapevine leafroll-associated virus 4 (GLRaV-4) to the exemplar isolate LR106 (GLRaV-4 strain 4, accession no. FJ467503).

GenBank accession No.	Isolate names	Strain of GLRaV-4	Country	Variety	% aa similarity of RdRp[1] to LR106	% aa similarity of HSP70h[1] to LR106	% aa similarity of CP[1] to LR106
KP313764	Ob	unclassified	Switzerland	Otcha bala	72.54	70.6	74.63
FJ907331	Carnelian		USA	Carnelian	N/A	66.73	77.94
AM182328	Pr	10	Greece	Mantilaria	81.47	N/A	N/A
KY940817	SW27-1		Pakistan	Tarakya	82.05	78.09	77.01
FJ467503	LR106	4	USA	Vitis sp.	100	100	100
KY821095	LH3		Pakistan	Autumn Royal	95.75	99.81	99.26

MF669483	WAMR-4		USA	Merlot	95.75	99.63	99.63
AY297819	-		USA	Vitis sp.	N/A	82.02	81.39
KJ810572	Man086		Spain	Mantua	86.87	82.02	81.75
MF669482	WALA-9		USA	Lagrein	87.26	82.21	82.48
OP752673	Cabw2_N6		Australia	Cabernet Sauvignon	87.04	81.65	82.12
OP752652	LC10_N6		Australia	Shiraz	87.04	81.65	82.12
OP752665	LC12_N5		Australia	Shiraz	87.04	81.65	81.75
OP752651	LC11_N6		Australia	Shiraz	87.04	81.65	81.75
OP752643	LC13_N3		Australia	Shiraz	87.23	81.27	82.48
OP752676	LC5_N5	9	Australia	Shiraz	87.23	81.27	82.48
OP752645	LC6_N6		Australia	Shiraz	87.23	81.27	82.48
OP752646	LC7_N6		Australia	Shiraz	87.23	81.27	82.48
OQ092720	LC1_N4		Australia	Shiraz	87.23	81.27	82.48
OP752675	LC9_N5		Australia	Shiraz	87.23	81.27	82.48
OP752670	LC14_N6		Australia	Shiraz	87.23	81.27	82.48
OP752660	WIL9_N5		Australia	Shiraz	86.85	81.65	81.39
OP752650	WIL10_N7		Australia	Shiraz	86.85	81.65	81.39

OP752666	WIL8_N7		Australia	Shiraz	86.85	81.65	81.39
OP752647	Cabw12_N7		Australia	Cabernet Sauvignon	87.04	81.46	82.12
OP752657	WIL12_N6		Australia	Shiraz	87.04	81.46	82.12
OQ092719	WIL11_N7		Australia	Shiraz	87.04	81.46	82.12
OP752659	Cabw11_N31		Australia	Cabernet Sauvignon	87.04	81.46	82.12
OP752653	WIL13_N6		Australia	Shiraz	87.04	81.46	82.12
OP752644	WIL7_N6		Australia	Shiraz	86.85	81.27	81.75
OP752668	WIL5_N7		Australia	Shiraz	87.23	81.46	82.12
OP752674	WIL6_N6		Australia	Shiraz	87.23	81.46	82.12
OP752648	WIL4_N6		Australia	Shiraz	87.23	81.46	82.12
OP752658	WIL1_N15		Australia	Shiraz	86.85	81.46	82.12
OP752669	WIL3_N6		Australia	Shiraz	87.04	81.46	82.48
OP752655	WIL2_N7		Australia	Shiraz	87.04	81.46	82.48
OP752654	WIL10_N6		Australia	Shiraz	85.49	81.09	80.29
OP752661	WIL12_N5	6	Australia	Shiraz	85.49	81.09	80.29
OP752672	WIL11_N6		Australia	Shiraz	85.3	81.09	80.29

OP752663	WIL19_N6		Australia	Shiraz	85.49	81.27	80.29
OP752649	WIL22_N5		Australia	Shiraz	85.3	81.27	80.29
OP752662	WIL24_N5		Australia	Shiraz	85.3	81.27	80.29
OP752664	WIL14_N5		Australia	Shiraz	85.49	81.27	80.66
OP752656	WIL15_N6		Australia	Shiraz	85.49	81.27	80.66
FJ467504	Estellat		USA	Vitis sp.	86.68	78.28	79.93
OP752671	WIL15_N8	5	Australia	Shiraz	86.85	81.27	82.12
OP752667	WIL13_N7		Australia	Shiraz	86.85	81.27	82.12
KY940818	LH3-1		Pakistan	Autumn Royal	85.91	82.02	81.75
FR822696	Y217		France	White Emperor	85.71	82.02	82.12
JX559639	3138-03		Canada	Vitis vinifera	85.71	82.21	82.12
KX828702	TRAJ1-BR		Brazil	Trajadura	86.68	82.02	83.21
MF669481	WASB-5		USA	Sauvignon Blanc	85.91	82.21	82.12
JX513893	1050-02		Canada	Vitis vinifera	85.91	82.4	81.75
KY940819	Bt26		Pakistan	Flame Seedless	86.49	82.02	81.02
AF414119	PMWaV-1	Out group	USA	unknown	N/A	N/A	N/A

[1] RdRp = RNA-dependent RNA polymerase (RdRp), HSP70h = heat shock protein 70 homologue, CP = coat protein
[2] Strains classified based on phylogenetic analysis of GLRaV-4 (Figure 5).

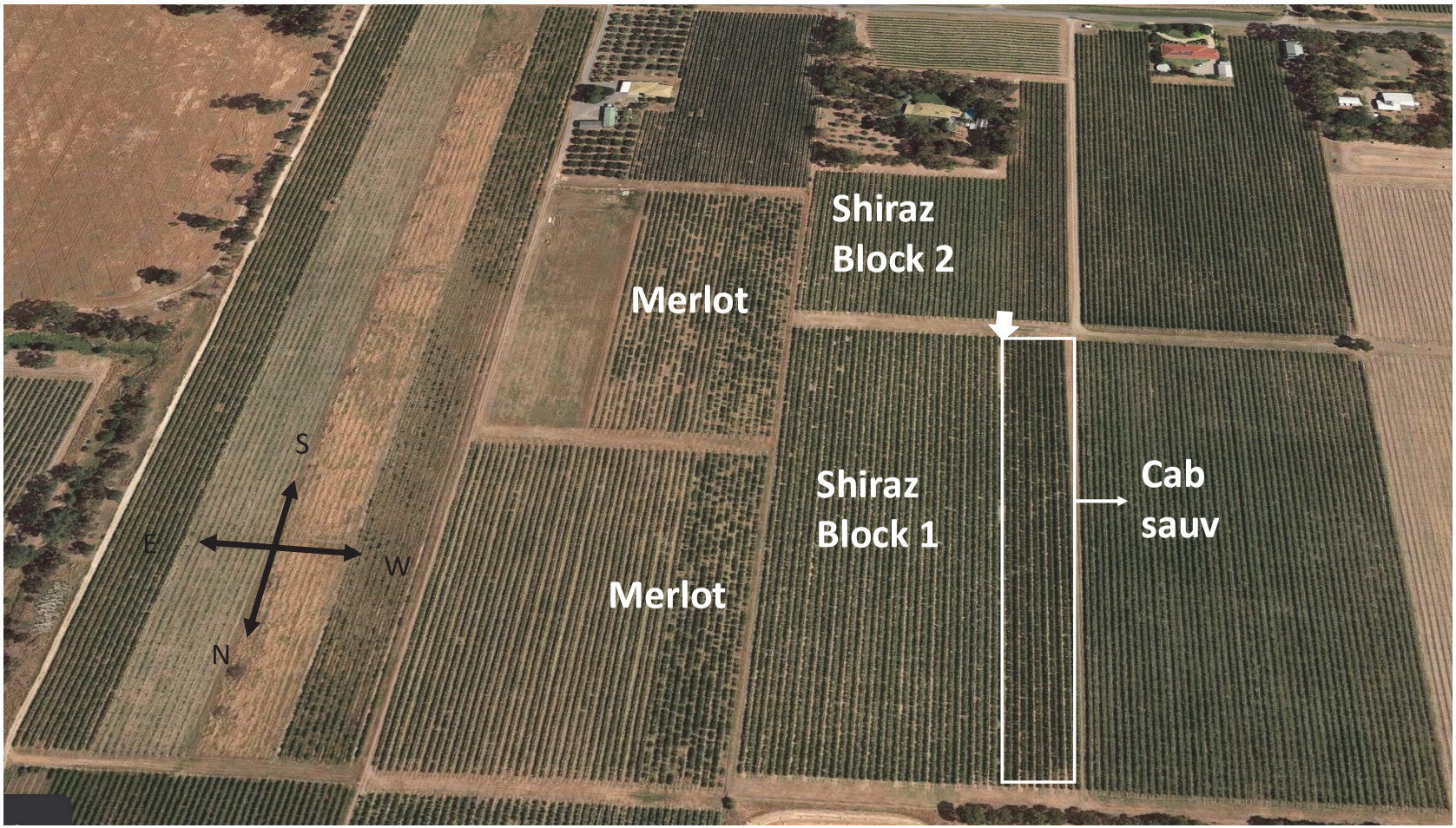

Figure S1. Vineyard map of the Willunga site. Shiraz grapevines from blocks 1 and 2 were used in the Metagenomic High Throughput Sequencing (Meta-HTS) andRT-PCR virus detection. The red arrow indicates Row 35 where symptoms of Shiraz disease (SD) were first discovered.

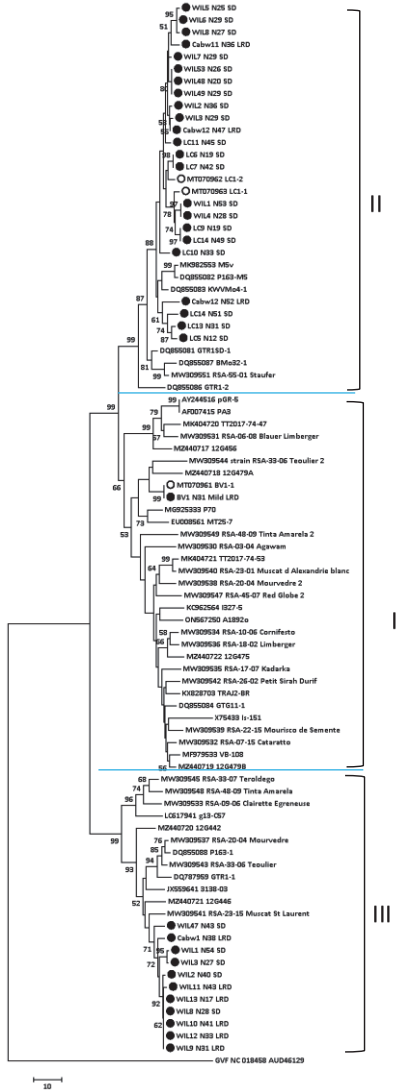
II
I
III
GVF NC 018458 AUD46129
10

(a)

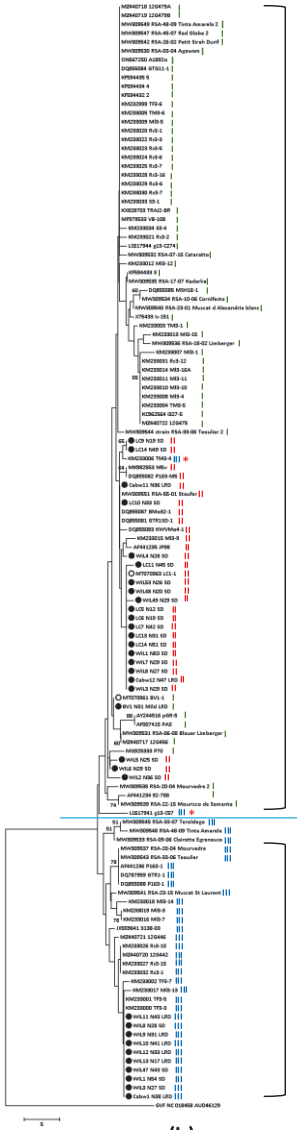
I&II
III
GVF NC 018458 AUD46129
5

(b)

Figure S2. Neighbor-joining phylogenetic analysis of amino acid (aa) sequences of full-length movement protein (MP) and RNA-binding (RB) genes of grapevine virus A (GVA) using metagenomic sequences and sequences from GenBank. (a) A neighbour-joining tree using full-length aa sequences of MP gene, (b) using complete aa sequences of CP gene. The phylogenetic trees were constructed using MEGA (7.0.26) software and the neighbour-joining method with 1000 bootstrap replicates. Only bootstrap values higher than 50% were shown. Sequences generated by the MiSeq and NovaSeq Meta-HTS experiments were labelled using circles and black dots, respectively. The variety, accession numbers and phylogroups assigned by each gene are listed in Table S6. Grapevine virus F (GVF) isolate AUD46129 (accession no. NC018458) was used as an outgroup. The phylogroup assigned by each gene was different for the two isolates (marked by *) in figure (b) and detailed in Table S6.

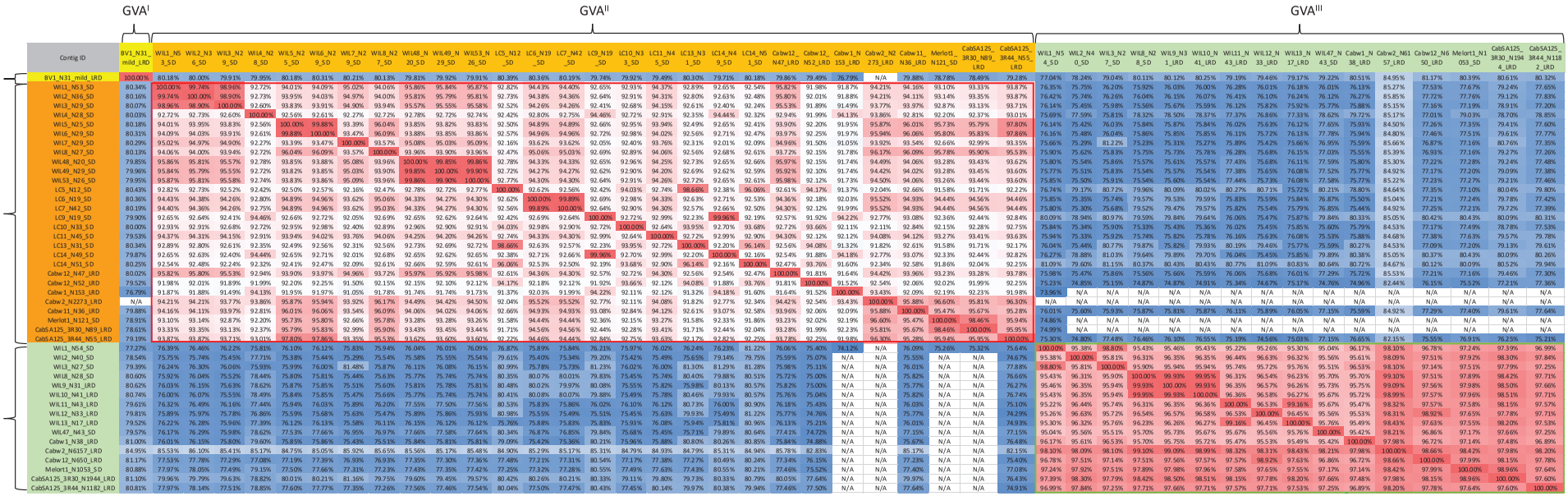

Figure S3. Color coded percentage of nucleotide (nt) pairwise identities of grapevine virus A (GVA) contigs in this study. GVA isolates from phylogenetic groups I, II and III are labeled as GVA^{I}, GVA^{II} and GVA^{III}. The contig IDs refer to Table S6. The pairwise identities were obtained by the the "blastn" function of Blast+. For contigs which do not share any comment genome region, identities are shown as N/A. The percentage of nt identities are color coded by the "3- color scale function" of Microsoft excel using blue (lowest value), white (midpoint) and red (highest value). The red and green squares show the sequence differences of GVA^{II} and GVA^{III} isolates between cv. Shiraz, Merlot and Cabernet Sauvignon, respectively.

Chapter 3: Genetic Diversity of Grapevine Virus A in Three Australian Vineyards Using Amplicon High Throughput Sequencing (Amplicon-HTS)

Abstract

Shiraz disease (SD) is one of the most destructive viral diseases of grapevines in Australia and is known to cause significant economic loss to local growers. Grapevine virus A (GVA) was reported to be the key pathogen associated with this disease. This study aimed to better understand the diversity of GVA variants both within and between individual SD and grapevine leafroll disease (LRD) affected grapevines located at vineyards in South Australia. Amplicon high throughput sequencing (Amplicon-HTS) combined with median-joining networks (MJNs) was used to analyse the variability in specific gene regions of GVA variants. MJNs analysis in individual samples, combined with phylogenetic analysis, demonstrated that GVA variants from phylogenetic group II (GVA^{II}) could be the ancestral phylogroup of all GVA variants. Several GVA^{II} variant groups contain samples from both vineyards studied suggesting that these GVA^{II} variants were from a common origin. Variant groups analysed by MJNs using the overall data set denote that there may be a possible relationship between variant groups of GVA and geographical location of the grapevines.

Keywords: amplicon sequencing; MiSeq; grapevine virus A, Shiraz Disease; intra-host diversity; median-joining haplotype networks; phylogenetic

1. Introduction

Shiraz disease (SD) affecting *Vitis vinifera* var. Shiraz and Merlot grafted onto 101-14 rootstock was first reported from South Africa in 1985 [1]. This disease was first detected in Australia in 2001 [2] and has since been frequently reported by Australian grape growers as one of the most destructive virus diseases that has resulted in significant canopy decline and yield lost [3-5]. The cost of removing infected grapevines, replanting, and considering the elapsed time ahead of the first profitable crop, is estimated to be around AU$12 million yr−1 [4]. In Australia, SD affected grapevines display restricted spring growth (RSG, late bud burst and delayed canopy growth) early in the growing season, leaf reddening, delayed leaf fall, and rubbery un-lignified shoots in autumn as compared to the asymptomatic grapevines [3,4,6].

Grapevine virus A (GVA), the core pathogen with a strong association with SD [4], is a positive-sense single-stranded RNA virus and is assigned into the family *Betaflexiviridae* under the genus *Vitivirus* [7]. This virus consists of 5 open reading frames (ORFs). ORF1 to 5 encode a 194 kilodaltons (kDa) RNA-dependent RNA polymerase (RdRp) (ORF1), a 19 kDa hypothetical protein (ORF2), a 31 kDa movement protein (MP) (ORF3), a 21.5 kDa coat protein (CP) and a 10 kDa RNA-binding protein (RB gene; p10 protein), respectively [8,9]. The p10 gene that was identified as the suppressor of gene silencing [10], consists of two major units, a basic arginine-rich domain and zinc-finger domain[11]. One of the early studies demonstrated that replacing cysteine residues by serine in the zinc-finger domain of GVA did not affect binding, however, compared to the wildtype, the mutated GVA infectious clone did not cause symptoms when inoculated onto *Nicotiana benthamiana* [11]. Another study also suggested the eighth amino acid counted from the N-terminus of the GVA RB gene is also involved in symptom severity [12]. Although these two studies indicate involvement of the RB protein in symptom expression in

an experimental host, others concluded that the specific GVA phylogenetic groups (phylogroup) II (GVA^{II}) and III (GVA^{III}), which are assigned based on the 3' terminal part of the genome including partial MP, entire CP and RB genes, were linked to the SD status in grapevines and symptom severity in *N. benthamiana* [13,14]. They suggest the GVA isolates from GVA^{II} are always associated with SD in grapevines and severe symptoms on *N. benthamiana*, whereas isolates belonging to GVA^{III} were consistently associated with asymptomatic grapevines or induce milder symptoms compared to GVA^{II} isolates [13]. Phylogroup I (GVA^{I}) was not associated with SD [Chapter 2].

During virus replication, mutants (variants) arise from error-prone replication mechanisms, recombination and reassortment giving rise to a population of viral quasispecies that can lead to molecular divergence and genetic variations within the same virus population [15-17]. Virus variation within its population can lead to breaking the resistance of the host [18,19] and to natural selection to adapt to the current environment [20]. However, most mutations are inconsequential or harmless, and are abandoned during virus evolution [20-22]. Studying virus evolutionary history and genetic diversity of a virus population can provide information on genomic epidemiology as well as a deep understanding of the epidemiologic model of how viral diseases emerge and spread.

Before the era of high-throughput sequencing (HTS) technology the traditional way of studying virus population, including variants, in an individual, involved reverse transcription polymerase chain reaction (RT-PCR), amplification of the gene of interest, then cloning amplicons into vectors followed by Sanger sequencing. Analysing sufficient clones to detect variants within an indivdual is time consuming and costly and may miss important low frequency variants [23,24]. Amplicon high-throughput sequencing (Amplicon-HTS), which is a targeted sequencing approach, clearly shows its advantages over Sanger sequencing when investigating the depth of diversity in viral populations. It does not require any cloning steps, and can identify thousands of variants in a single sample with the ability to detect low frequency variants [23], which may be an indicator of emerging pathogens. Amplicon-HTS has been successfully utilized in medical drug selection to detect drug resistance mutations [25-27], virus epidemiology studies for tracking the transmission of a viral outbreak [23,28,29], cancer research [30-33], investigating microbial diversity in environmental samples [34-38], and in human diseases [39-41]. Recently, this approach has been used to study virus evolutionary history, intra-host and inter-host diversities in plant virology, e.g., endive necrotic mosaic virus (ENMV) [42] in various hosts, several *Ilarvirus* species in *Prunus* species [43-45] and four viruses in legumes [46].

Median-joining networks (MJNs), a method that was first published in 1999 [47], is now widely used–to study biogeography, and most importantly to study the evolutionary relationships within a virus population [44,48-51]. The potential parent of a virus can be identified, and the evolutionary history can be visualized based on the principle of the median-join algorithm by which variants that are closely related in the network are also genetically closely related and the parent variants should have the highest number of connections to the descendant variants [49]. This algorithm is based on genetic distance of nucleotide sequence, which

is similar to one of the most popular methods, neighbor-joining algorithm, for constructing phylogenetic trees of viruses [52,53].

This study used deep amplicon sequencing combined with phylogenetic analysis and MJNs analysis to explore the intra- and inter-host diversity of GVA variants and the possible relationships between variant groups of GVA and relative geographical location of SD and LRD affected grapevines.

2. Materials and Methods

2.1. Sample selection

The Amplicon-HTS experiment was carried out on a total of 26 Shiraz grapevines from three South Australian vineyards: Langhorne Creek (LC1 to 15, clone BVRC12 grafted on Chardonnay rootstock), Willunga (WIL1 to 8, clone BVRC12 on one roots), and Barossa Valley (BV1 to 3, unknown heritage clone on own roots, planted around 1900), that tested positive to GVA by RT-PCR using the general-purpose primer pairs, Ah587/Ac995 and H7038/C7273 (Chapter 2, Table S2). The samples were collected between May to July of 2018 from LC and WIL vines that displayed typical Shiraz Disease (SD) symptoms, and BV1 to 3 vines that showed mild LRD symptoms (Chapter 2, Figure S1). Table 1 in Chapter 2 provides basic information on variety, clone, year of planting, number of grapevines per symptom type. Tables S4 and S5 in Chapter 2 detail the presence of all viruses of each sample as determined by RT-PCR and metagenomic high throughput sequencing (Meta-HTS).

2.2. Nucleic acid extraction method and RT-PCR amplification

Dormant canes (3 per grapevine) were randomly sampled from across the whole canopy of each grapevine from May to July in 2018 from the three vineyards. Total Nucleic Acid (TNA) extraction was performed using the modified Mackenzie method [54] outlined in Chapter 2 (2.3.1. Nucleic acid extraction for RT-PCR) for general purpose RT-PCR virus detection. A region from each of the MP, CP and RB genes were amplified from the 26 samples in a 25 µl reaction contains 0.1 µl of ProtoScript® II Reverse Transcriptase (New England Biolabs ®), 1.25 µl of each primer of 10 µM primers, 12.5 µl of Q5 master mix (contains Q5® High-Fidelity DNA Polymerase, New England Biolabs ®), 8.9 µl of PCR-grade water (Thermo Fisher Scientific) and 1 µl of TNA samples. The RT-PCR reaction conditions were as follows: reverse transcription at 42°C for 50 minutes and initial denaturation at 98°C for 30 seconds, followed by 35 cycles of denaturation at 98°C for 20 seconds, annealing at 56°C for 30 seconds, and extension at 72°C for 30 seconds, and a final extension at 72°C for 5 minutes. The desired amplicon sizes of MP, CP and RB were 404 base pair (bp), 565 bp and 236 bp, respectively. The primer sequences and annealing temperature for the RT-PCR of each set of primers can be found in Table S1.

2.3. Amplicon purification and library preparation

To ensure that the amplicons were successfully amplified, 10 µl of each RT-PCR product were run on 1.8% agarose gel electrophoresis and stained with SYBR Safe™ gel stain (Invitrogen™). The remaining 15 µl were transferred to a fresh tube for amplicon purification using Ampure

XP beads (Beckman Coulter) following the manufacturer's protocol. The purified amplicons were first adapter-ligated using the Illumina mpxPE1 and mpxPE2 adapters and then PCR-enriched using the in-house multiplex PE barcode primer as described previously [44]. The reaction conditions for the PCR-enrichment were the same as the RT-PCR amplification described previously, but only 15 cycles were used. The PCR-enriched amplicons were purified again using Ampure beads. The final concentrations of the 78 purified libraries were determined using the TapeStation system (Agilent) and Qubit fluorometer (Thermo Fisher Scientific). Libraries were pooled using an equal amount of each sample at a final concentration of 4 nM. The pooled libraries were then sequenced on an Illumina MiSeq instrument with 300 bp paired-end reads.

2.4. Amplicon raw reads trimming and filtering

Raw reads with a quality score of under 20, and a length below 50 bp as well as the Illumina adapter sequences were removed using AdapterRemoval (v. 2.2.2) [55] (quality trimming). The remaining reads from both directions were paired and merged using the "collapse" command of AdapterRemoval. Sequencing files were converted from "fastq" to the "fasta" format using the "reformat" function of BBmaps (v. 35.85) [56]. Amplicon sequences from the MP, CP, and RB genes were filtered to the designed size of MP, CP and RB genes ranged from 399 nucleotide (nt) to 404 nt, 560 nt to 564 nt, and 230 nt to 244 nt, respectively, using the "reformat" function of BBmaps (size trimming). A local database was built using all complete genome sequences of GVA from GenBank and the current study (Table S7 in Chapter 2) with the "makeblastdb" command using BLAST+ (v. 2.11.0) [57]. Amplicon sequences were compared against the local database to determine the sequence orientation and unspecific reads derived from the host plant were filtered out using the "blastn" command of BLAST+. The minus reads were first separated from the plus reads and reverse complemented using the "reformat" command of BBmaps, then combined with the plus reads. Reads from each sample were renamed by sample ID and numbers using the BBmap's "bbrename" command. Primer sequences were removed by the "cutadapt" function of Cutadapt (v. 3.4) [58], and they became self-aligned after primer trimming. In case of any sequence variation on the primer binding sites, the mismatching tolerant function was implemented when removing both reverse and forward primer sequences from amplicon reads. Any amplicon reads without any primer sequences were also discarded at the same time to ensure they were all at the same position. Reads were filtered again to the expected sizes of 364 bp, 524 bp, 198 bp for MP, CP, and RB genes, respectively, to ensure all amplicons for each gene have the same size. The extra 38 nt sequence from the intergenic region right before the CP gene was deleted from the original CP amplicon sequences using the Cutadapt's "cutadapt" command, resulting in a final amplicon size of 486 bp for the CP gene.

2.5. Amplicon reads error filtering and clustering

Reads with a frequency greater than 10 (cut-off value) in each sample were grouped at 100 percent nt identity using the Usearch's (v. 11.0. 667) "fastx uniques" command [59]. Nucleotide sequence clustering results in several hundreds of unique nt variants, each of which was labelled by the

copy number (N) obtained for that variant. The unique variants were named as Cluster 1 to N by the copy numbers from high to low, eg. Cluster 1 was the unique variant with the highest copy number (largest variant cluster) in a given sample from a particular gene. The unique nt variants were translated into aa sequences using the CLC Genomics Workbench (v. 21.0.3; Qiagen, Aarhus, Denmark). Protein sequences of each sample were clustered at 100% aa similarity again using the same "fastx uniques" command of Usearch.

After clustering of unique variants of each gene from each sample, data from all 26 samples of each gene were combined and again clustered as described above to obtain the combined pool of unique variants for each gene by clustering the combined data again with the Usearch at 100% nt or aa sequence similarity using the same Usearch command described above.

2.6. Phylogenetic group identification of amplicon variants

Phylogroups of all near-complete genome sequences obtained by metagenomic high throughput sequencing (Meta-HTS), and all publicly available GenBank sequences, of GVA were previously identified using a neighbour-joining tree (Chapter 2, Figure 1). The phylogroup of GVA^{I}, GVA^{II} or GVA^{III} were assigned to each isolate and implemented as the customized database of the BLAST+ by the "makeblastdb" command to identify phylogroups for all amplicon variants in this study. The phylogroup of unique variants from each sample were assigned according to the best match with the highest nt identity when blasted against the database described above using the "blastn" function of the BLAST+. To ensure the reliability of this method, the BLAST+ method was validated as follows. Variants containing phylogroup information were sorted by nt identities and sampled every 24 rows. The sampled variants were clustered with GenBank sequences of known phylogroups. A neighbour-joining phylogenetic tree was constructed using MEGA (v. 7.0.26) with 1000 bootstrap replicates [60]. The phylogroups, identified by the neighbour-joining tree and by the BLAST+ method, were compared to ensure they provided identical results before being applied to the isolates being analysed in this study.

2.7. Intra-host diversity based on lowest pairwise identities

In this study, the lowest percentage pairwise nt identities between any of the two amplicon variants in each sample were utilised as a parameter of genetic diversity within a virus population in an individual vine sample based on our hypothesis that a higher pairwise identity (closer to 100%) within a population has fewer sequence variations, whereas samples with lower nt identities contain deeper intra-host genetic diversity. The pairwise nt and amino acid (aa) identity between each two amplicon variants was determined using the command version of sequence demarcation tool (SDT, v. Linux64) [61]. The nt or aa identities were sorted from lowest to highest to find the lowest identities within the virus population using the default Shell command "sort" using the output generated from the SDT.

2.8. Intra-host genetic diversity by median-joining haplotype networks (MJNs)

As the unclustered files were too large for construction of a MJNs tree for each gene, only the 20 unique nt variants with the largest number of amplicon sequences (Cluster 1 to 20) from each gene of each sample were used for generating the scaled sequencing files as input files. In this study, a variant cluster consists of variants clustered at 100% nt identity extracted from the sequence data using the Usearch nt sequence clustering method as described above. The 20 largest clusters were used because together they represented more than 50% of the trimmed reads before clustering in the majority of samples. Three samples, each from a different site were selected as representative GVA infected grapevines for the MJNs analysis and included WIL3 and LC1, which displayed SD, and BV1, which displayed mild LRD. Individual MJNs were constructed for each gene of each sample using the median-joining algorithm [47] by the PopART software (http://popart.otago.ac.nz/index.shtml), thus a total of nine MJNs were constructed. GVA^{I}, GVA^{II} and GVA^{III} variants from each gene were identified using the Blast method described above and colored by different colors in the MJNs. The scale of the figure, to represent relative population size, for each gene of each sample was determined by dividing the number of sequence copies of larger clusters 1-20 by number of sequences in the smallest cluster 20.

2.9. Intra and inter-host diversity by MJNs

To study the evolutionary relationship among the GVA variants, the top 20 variant clusters from all 26 samples, in total 520 variants of each CP, MP and RB gene, were combined and analyzed by the MJNs method described above. In this analysis, each variant cluster may consist of identical sequences obtained from different locations.

3. Results

3.1. Sequencing reads of Amplicon-HTS

Basic statistical data of number of raw reads, number of reads after trimming, and the copy numbers of top 20 variant clusters of each sample after clustering as well as number of nonsense variants are reported in Table S2. After the quality, size and primer trimming, and before clustering, the total number of reads for the MP, CP, and RB genes, when all 26 samples were combined, was 2.13, 2.02, and 2.81 million, respectively (Table 1). Blast analysis of the discarded reads, after quality and size trimming, against the GenBank database indicated that shorter reads were either GVA associated or *V. vinifera* (host) associated (data not shown). The average proportion of reads for MP, CP, and RB per sample after quality, size and primer trimming were 64.44%, 46.08% and 73.36% (primer trimmed reads /total raw reads) (Table 1). It was observed that after the size trimming, the average proportion of the remaining reads for the MP gene of BV1, BV2 and BV3 were only 25.99%, 9.23% and 2.44% and proportion of the CP gene reads for WIL7 were 17.84%, which was much lower than the average proportion of reads for these genes (Table S2).

Table 1. Overall number of reads and unique variants before and after clustering of grapevine virus A amplicon sequences across 26 grapevines.

Gene[1]	MP	CP	RB
Total raw reads	6,466,112	8,784,286	7,568,478
Quality trimmed reads	2,805,669	3,877,170	3,399,212
Size trimmed reads	2,188,151	2,080,245	3,153,286
Primer trimmed reads	2,128,784	2,015,120	2,814,646
Proportion of trimmed reads in total raw reads (%)	64.44	46.08	73.36
Total nucleotide (nt) variants	12,983	13,103	10,052
Unique nt variants	10,454	10,899	6,366
Proportion of unique nt variants in total variants (%)	80.52	83.18	63.33
Total amino acid (aa) variants	6,593	5,389	6,192
Unique aa variants	4,402	2,250	1,900
Proportion of unique aa variants in total variants (%)	66.77	41.75	30.68

[1] MP = movement protein, CP = coat protein, RB = RNA binding protein

3.2. Nucleotide and amino acid sequence clustering

The nucleotide sequence of the amplicon reads which passed through all three trimming filters were clustered at 100% identity at nt and aa levels. The number of clustered unique nt and aa variants detected in each sample of each gene is listed in Table 1. After nucleotide sequence clustering, 10,454, 10,899, and 6,366 unique variants were discovered from MP, CP, and RB genes, respectively. The proportion of unique variants to total variants of the MP, CP, and RB sequences was 80.52%, 83.18%, and 63.33%, respectively (Table 1).

Each sample's unique nucleotide variants were translated to aa sequence and grouped again at 100% aa identity, resulting in a total of 6593, 5389, and 6192 protein variants for the MP, CP, and RB genes, respectively (Table 1). Among these, 4402, 2250, and 1900 are distinct protein variants, accounting for 66.77%, 41.75%, and 30.68% of total protein sequences of the MP, CP and RB genes, respectively.

Unique nonsense aa variants with premature stop codons were found in each of the three genes in 76/78 samples. Nonsense variants were found in the CP and RB genes but not in the MP gene of samples BV2 and BV3 (Table S2). Generally, they represented <10% of the total unique aa variants, except for the CP gene of isolate BV2 where unique nonsense variants represented 33.02% of the total (35 unique nonsense aa variants / 106 unique aa variants Table S2).

3.3. Intra- and inter-host diversity of amplicon variants

Table S3 provides the phylogroups of GVA variants in each sample. Variants from all three phylogroups were identified in the CP dataset, whereas only GVA^{I} and GVA^{II} variants were obtained from MP and RB genes. Within the MP data set, all variants from BV belonged to GVA^{I}, and all variants from LC and WIL belonged to GVA^{II}. For the CP data set, GVA^{III} variants were detected along with GVA^{II} in the same grapevine in three samples WIL2, 3 and 8 (Table 4). Only variants of GVA^{I} and GVA^{II} were identified from the MP gene dataset.

3.3.1. Intra-host diversity: Lowest pairwise identities within each sample

The largest genetic distance (the lowest nt identity) was found in the CP gene of WIL2, WIL3 and WIL8 when the GVA^{II} and GVA^{III} variants found within each of these samples were compared, ranging from 75.7-76.1% (Table S3). Comparisons within GVA^{II} and GVA^{III} variants populations in these three samples showed the lowest genetic distance ranging from 90.7-91% and 88.1-91% nt identity, respectively. This was higher than the genetic distance observed for the CP gene within other samples, which ranged from 93.6-99.1% nt identity and 93-97.5% for GVA^{II} and GVA^{I} variants, respectively. The highest genetic distance (90.11% nt identity) for the MP gene was observed within GVA^{II} variants in sample LC8, while the overall range of intra-host diversity amongst the other 25 samples ranged from 90.4-98.9% and 96.2-96.4% nt identity for GVA^{II} and GVA^{I} variants, respectively. For the RB gene, the highest genetic distance (91.4% nt identity) was observed within GVAI&II variants in samples LC3 and BV2; the overall range of intra-host diversity amongst the other 24 samples ranged from 93.9-97% nt identity.

3.3.2. Inter host diversity: Lowest percentage pairwise identities within each phylogroup

The MP, CP, and RB variants of GVA^{I}, GVA^{II} and GVA^{III} were compared across all 26 samples and the overall lowest pairwise nt and aa identities for each gene within each phylogroup across all 26 samples are listed in Table 2. Note that the lowest % nt identity of each phylogroup of GVA was obtained based on unequal number of samples of each phylogroup (Table S3). The lowest % nt and aa identities of GVA^{I}, GVA^{II}, and GVA^{III} were obtained from 3 (BV1 to BV3), 23 (whole data set excluding BV) and 3 (WIL2, WIL3 and WIL8) samples, respectively. The number of variants used to gain the % nt or aa nt identities of each phylogroup of GVA and each gene are given in Table S3. Based on the current data set, only the CP gene could be compared across all phylogroups. For this gene the nt % identity was higher in GVA^{I} variants, indicating lowest variability, but when the sequences were translated to aa the % identity was lower than that of GVA^{II} and GVA^{III} indicating high variability (Table2). The nt and aa % identity of the MP gene was higher for GVA^{I} compared to GVA^{II} indicating that the lower variability of the GVA^{II} variants (Table 2). Since GVA^{I} and GVA^{II} variants cannot be segregated based on the RB gene (Chapter 2, Figure 1g), the lowest % nt and aa identities of RB gene were calculated using combined variants from both groups. Therefore, identities for GVA^{II} RB gene were not shown in Table 2.

Table 2. Lowest percentage pairwise identities of grapevine virus A (GVA) phylogenetic groups (GVA^{I}, GVA^{II} and GVA^{III}) amongst 26 grapevine samples.

Lowest identity[a]	**MP[b]**		**CP[b]**		**RB[b]**	
	% nt identity[a]	**% aa identity[a]**	**% nt identity**	**% aa identity**	**% nt identity**	**% aa identity**
GVA^{I} variants	95.60%[1]	95.04%[1]	92.59%[1]	86.42%[1]	90.40%[3]	86.36%[3]
GVA^{II} variants	88.74%	90.08%	86.42%	87.04%	See GVA^{I}	
GVA^{III} variants	N/A		88.07%[2]	88.89%[2]	N/A	

[a] nt = percentage nucleotide identity, aa = percentage amino acid identity, GVA^{I}, GVA^{II}, GVA^{III} , grapevine virus A isolates from the phylogroups I, II and III, respectively. [b] MP = movement protein, CP = coat protein, RB = RNA binding protein. [1] Identities calculated from samples BV1, BV2 and BV3. [2] Identities calculated from GVA^{III} variants from samples WIL2, WIL3 and WIL8. [3]According to the phylogenetic analysis of grapevine virus A in Chapter 2, Figure 1g, variants of GVA ^{I} and GVA^{II} of the RB gene cannot be differentiated and therefore the sequences of all samples with these variants were combined.

3.4. Intra- and inter-host diversity analysis by median-joining haplotype networks (MJN)

3.4.1. MJNs of sample WIL3, BV1 and LC1

Intra-host diversity of GVA in three samples of grapevines each from a different region and displayed SD (WIL3, LC1) or mild LRD (BV1) were visualized by MJNs of the nt sequences of the MP, CP and RB genes (Figure 1). Each subfigure represents a given gene of a single sample. BV1 was chosen because it contains only GVA^{I} variants. Samples WIL3 (Figures 1a and 1b) and LC1 (Figures 1g and 1h) were chosen for analysis because they have the highest copy numbers of GVA^{II} variants for the CP and MP genes. WIL3 was also chosen because it also contains GVA^{III} CP variants that occur with much lower frequency compared to GVA^{II} variants (Figure 1a).

GVA^{II} variants were widely segregated from GVA^{III} variants of the CP gene in sample WIL3 as indicated by the large number of hatch marks (Figure 1a), which represent the number of mutation events separating the variants, and therefore evolutionarily distantly related. For the CP, MP and RB genes of the GVA^{II} variants in WIL3 there was one large cluster (Cluster 1) surrounded by and connected to smaller clusters and the smaller clusters were not connected, suggesting that Cluster 1 of each gene is likely the ancestor of other variants in this sample (Figures 1a, b, and c). The number of copies in both the Cluster 1 of the CP and the MP represented approximately 75% of the total number of copies amongst all clusters whereas the RB Cluster 1 represented 92% of all copies because it contains both GVA^{I} and GVA^{II} variants.

GVA^{I} variants of the CP gene from sample BV1 showed dispersed distribution and no major variant was found (Figure 1d). However, Cluster 8 which has 983 copies, has the highest number of connections to other clusters suggesting it may be a primary ancestor. Only one major cluster was found among GVA^{I} MP variants. As seen from Figure 1e, four mutation events gave rise to GVA^{I} MP Clusters 2, 15, 14 and then 4 and then two mutation events gave rise to Clusters 17 and 20, which are most distantly related to Cluster 1. The GVA^{I} variants of the RB gene, Cluster 2 has the highest number of links to other clusters and although Cluster1 and Cluster 3 appear to give rise to some other clusters they are closely related to Cluster 2 as they are only separated by one hatch mark. Therefore Cluster 2 is the most likely ancestor of this population (Figure 1f).

Two major variants were found for the LC1 GVA^{II} MP (Figure 1h) and RB genes (Figure 1i), whereas three were found for the CP gene (Figure 1g). In a previous experiment using Meta-HTS of sample LC1, two distinct molecular GVA^{II} variants were found, namely LC1-1 (accession no. MT070963) and LC1-2 (accession no MT070962), which share 92.90% nt identity by pairwise alignment of their genome sequences using Blast [57]. In the context of this study, the percentage of pairwise nt identities

of the largest five clusters of CP and MP genes show that the top 5 clusters have over 99.4% nt identity to the isolate LC1-1, or to LC1-2 (Table 3). The CP gene Cluster 3 and MP gene Cluster 1 were identical to isolate LC1-1 and CP gene Cluster 1 respectively, and MP gene Cluster 3 were identical to LC1-2, supporting the detection of distinct GVA^{II} variants in a single sample (Table 3). The nt identity of the same region of the CP (486 nt) and MP (364 nt) between LC1-1 and LC1-2 are 96.09% and 93.96%, respectively. CP Cluster 2 is the primary ancestor of sample LC since it is surrounded by Clusters 1, 4, 6, 19, 12, 15 and 18 (Figure 1g). Cluster 2 and 5 are distantly related (97.33% nt identity) compared to CP Clusters 3 and 5 (98.97% nt identity) (Figure 1g). CP Cluster 3 and MP Cluster 1 are smaller and give rise to fewer variants than CP Clusters 1 and MP Cluster 3, respectively (Figures 1g and 1h). Cluster 1 of the RB gene is identical to LC1-1, but the similarity between clusters and LC1-2 could not be calculated as the RB gene sequence of MT070962 is incomplete (Table 3). However, two distinct RB genes clusters were formed which could be representative of the LC1-1 and LC1-2 (Figures 1h and i).

Table 3. Sequence similarity of the largest 5 clusters to the two metagenomic high throughput sequencing isolates LC1-1 and LC1-2 that were obtained from the same grapevine LC1.

Gene[1]	Sample ID	No. of reads	% nucleotide (nt) identity to LC1-1[3]	% nt identity to LC1-2[3]
CP	LC1_CP_Cluster1#	9,679	96.09%	100.00%#
	LC1_CP_Cluster2#	8,968	96.30%	99.79%#
	LC1_CP_Cluster3*	7,105	100.00%*	96.09%
	LC1_CP_Cluster4#	4,359	96.09%	99.59%#
	LC1_CP_Cluster5	1,345	98.97%	97.12%
MP	LC1_MP_Cluster1*	22,327	100.00%*	93.96%
	LC1_MP_Cluster2*	16,980	99.73%*	94.23%
	LC1_MP_Cluster3#	3,972	93.96%	100.00%#
	LC1_MP_Cluster4#	547	94.51%	99.45%#
	LC1_MP_Cluster5*	377	99.18%*	94.78%
RB	LC1_RB_Cluster1*	61,140	100.00%*	N/A[2]
	LC1_RB_Cluster2	41,319	96.97%	N/A
	LC1_RB_Cluster3	8,577	96.46%	N/A
	LC1_RB_Cluster4	2,652	97.47%	N/A
	LC1_RB_Cluster5*	2,626	99.49%*	N/A

*Variants share more than 99.4% nt identities to LC1-1. #Variants share more than 99.4% nt identities to LC1-2. [1] MP = movement protein, CP = coat protein, RB = RNA binding protein. [2] Since isolate LC1-2 includes only partial sequences of the RB gene, sequence comparison was not performed for the RB gene and shown as N/A. [3] The isolate LC1-1 (accession no. MT070963) and LC1-2 (accession no. MT070962) were detected in the same grapevine LC1.

3.4.2. Intra and Inter-host diversity of MJNs by the overall data set

After sequence clustering, the top 20 variant clusters (one sequence per cluster) of each gene from each of the 26 grapevines were combined to draw an overall MJNs map for each gene (Figure 2). In this MJNs, the

size of variant cluster displays number of samples within a given cluster (100% nt identity) and the colors display sample locations. When the MJNs were constructed, variants were clustered together and formed into variant groups. There were 17, 14 and 10 variant groups formed in the MJNs for the CP, MP and RB genes for GVA^{II}, respectively (Table 4). For each gene, some variant groups were only represented by variants from a single grapevine (single-sample variant group), but some were represented by variants from multiple grapevines (multiple-sample variant group). Variant groups were each labelled with a variant group ID (VG1 to VG21) and the lowest % nt identities of variants within each variant group are given in Table 4. The multi-sample variant group 14 (VG14) of the RB gene contained GVA^{II} variants of ten grapevines with a total of 546,940 reads which count as 19.43% of the total amplicon reads for this gene after primer trimming (Table 4 and S2). GVA^{II} variants associated with grapevines located at LC (LC1, LC2) and WIL (WIL1) occurred in muti-sample variant group VG4 across all three genes (Table 4; Figures 2a, e, and h), and the MP, CP, and RB genes of the GVA^{II} variants across the three samples shared 38, 141, and 208 identical variants, respectively (data not shown).

GVA^{II} variant groups radiate from multi-sample variant group VG4 (grapevines LC1, LC2, WIL1) based on the CP and MP genes, suggesting that variants within these CP and MP variant groups are likely to be the ancestor of all other GVA^{II} variants (Figures 2a, 2b; supplementary Figures S1b and S1e; marked with green dots). However, the ancestral relationship was not supported by the RB gene, since variant groups appear to arise from multi-sample variant group VG14 that contains variants of WIL1 along with variants of nine other grapevines, but not those from LC1 and LC2 (Figure 2c). For the CP gene, GVA^{I} and GVA^{III} variants were not connected to each other, instead they were only connected to GVA^{II}. However, they were separated from GVA^{II} by a large number of hatch marks suggesting a distant genetic relationship (Figure 2a).

Based on current data of three samples BV1, BV2 and BV3, GVA^{I} variants formed a diverse and interconnected variant group of unique variants across all three genes. Based on the size and number of linkages to other clusters of the CP and RB genes, the potential ancestor variant of the three BV samples was labeled by red circles in supplementary Figures S1a and S1c. The evolutionary relations within the MP gene could not be determined (Figure S1b) likely due to the low number of reads that were obtained and analysed.

Table 4. Single-sample and multiple-sample variant subgroups identified for phylogroup II grapevine virus A (GVA) variants.

		CP[2]		**MP[2]**		**RB[2]**	
	Variant group ID[1]	**Sample ID**	**Lowest % nucleotide (nt) identity within the variant group**	**Sample ID**	**Lowest % nt identity within the variant group**	**Sample ID**	**Lowest % nt identity within the variant group**
Multiple-sample	VG1	LC8, 9, 14	95.68	LC8, 9, 14	97.53	LC8, 9, 14	95.96
	VG2	LC8, 14	98.77	LC8, 14	97.8	N/A	N/A

variant groups	VG3	LC5, 13	98.97	LC5, 13	97.53	N/A	N/A
	VG4	LC1,2; WIL1	98.56	LC1,2; WIL1	96.98	LC1,2; WIL1	95.96
	VG5	WIL2, 3	97.33	N/A	N/A	N/A	N/A
	VG6	LC3, 4, 11, 12	94.65	LC3, 4, 11, 12	96.98	N/A	N/A
	VG7	LC6, 7	98.97	LC6, 7	99.45	LC6, 7	97.98
	VG8	WIL5, 6	99.59	WIL5, 6	98.9	WIL5, 6	98.48
	VG9	LC1; WIL1a	99.38	LC1; WIL1a	98.63	N/A	N/A
	VG10	LC3, 12	98.56	N/A	N/A	N/A	N/A
	VG11	N/A	N/A	WIL2, 3; LC2	98.08	N/A	N/A
	VG12	N/A	N/A	LC10, 12	94.78	N/A	N/A
	VG13	LC1; WIL1b	99.38	N/A	N/A	N/A	N/A
	VG14*	N/A	N/A	N/A	N/A	LC3,4,5,11,12 ,13; WIL1,2,7,8*	97.47
Single-sample variant group	VG15	LC3	99.38	N/A	N/A	LC3	97.47
	VG16	LC15	99.38	LC15	99.45	LC15	98.99
	VG17	LC10	99.59	N/A	N/A	LC10	98.99
	VG18	WIL4	99.59	WIL4	98.9	WIL4	98.99
	VG19	WIL7	98.97	WIL7	99.18	N/A	N/A
	VG20	WIL8	98.97	WIL8	99.18	N/A	N/A
	VG21	N/A	N/A	N/A	N/A	WIL3	98.99

[1] Phylogroups contain phylogroup II GVA variants that were used to analyse the intra-and inter- host diversity in each of the 26 grapevines with either shiraz disease or mild leafroll disease in this study (Figure 2). [2] MP = movement protein, CP = coat protein, RB = RNA binding protein *Super variant groups of the RB gene.

3.4.3. Variant groups vs. geographical location

The relative geographical locations of the SD grapevines and their GVA CP gene variant groups were linked together in Figure 3. Generally, samples within the same GVA variant groups are geographically close to each other and are most frequently next to each other in a vineyard. There are exceptions, e.g., grapevines LC5 and LC13 are both within GVA CP variant group VG3 but they were physically distant within the vineyard (Figure 2a and 3a). In contrast, WIL1 is next to WIL2 and WIL3, but its GVA^{II} variants belongs to variant group VG4, which also contains GVA^{II} variants from grapevines LC1 and LC2 (Figures 2b and 3b). Grapevines WIL4, 5 and 6, are neighbors occurring in a row but GVA^{II} CP, MP and RB variants WIL5 and 6 occur in variant group VG8 and GVA^{II} variants in WIL4 occur in variant group VG18 (Figures 2 and 3b).

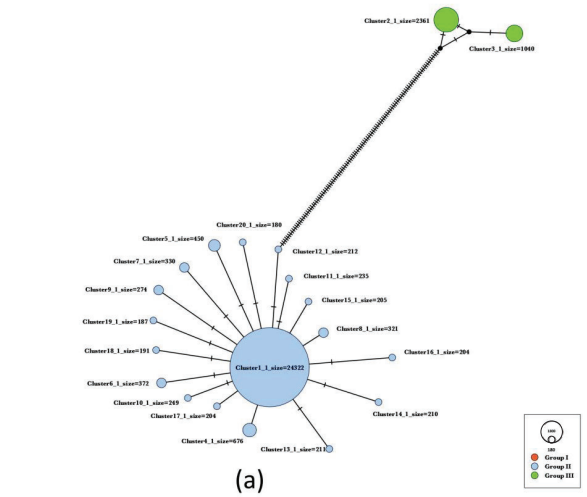
Cluster2_1_size=2361
Cluster3_1_size=1040
Cluster20_1_size=188
Cluster5_1_size=450
Cluster12_1_size=212
Cluster7_1_size=330
Cluster11_1_size=235
Cluster9_1_size=274
Cluster15_1_size=205
Cluster19_1_size=187
Cluster8_1_size=321
Cluster18_1_size=191
Cluster16_1_size=204
Cluster1_1_size=24322
Cluster6_1_size=372
Cluster10_1_size=249
Cluster17_1_size=204
Cluster14_1_size=210
Cluster4_1_size=676
Cluster13_1_size=213
Group I
Group II
Group III

(a)

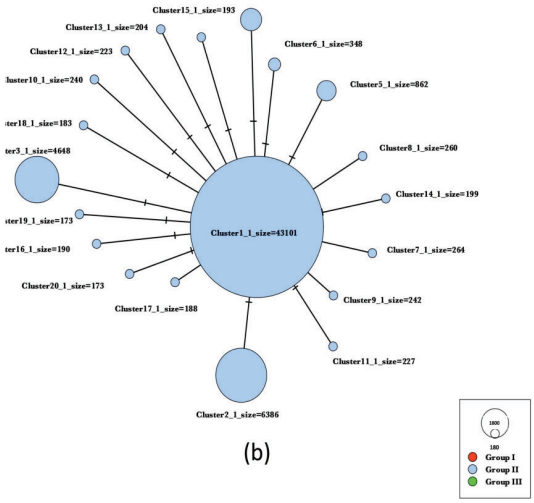
Cluster15_1_size=193
Cluster13_1_size=204
Cluster6_1_size=348
Cluster12_1_size=223
Cluster5_1_size=862
Cluster8_1_size=260
Cluster14_1_size=199
Cluster1_1_size=43101
Cluster7_1_size=264
Cluster9_1_size=242
Cluster11_1_size=227
Cluster2_1_size=6386
Cluster17_1_size=188
Cluster20_1_size=173
Group I
Group II
Group III

(b)

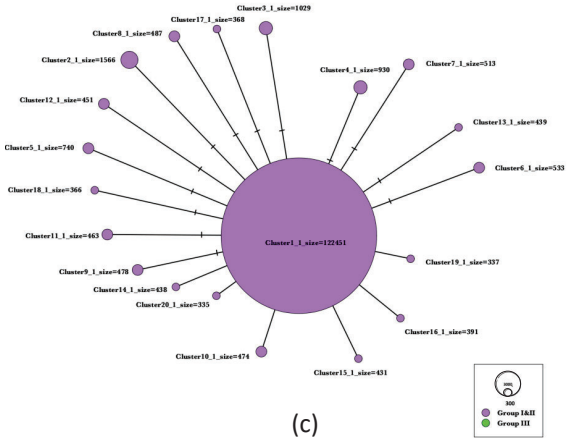
Cluster3_1_size=1029
Cluster17_1_size=368
Cluster8_1_size=487
Cluster2_1_size=1566
Cluster4_1_size=930
Cluster7_1_size=513
Cluster12_1_size=451
Cluster13_1_size=439
Cluster5_1_size=740
Cluster6_1_size=533
Cluster18_1_size=366
Cluster1_1_size=122451
Cluster11_1_size=463
Cluster19_1_size=337
Cluster9_1_size=478
Cluster14_1_size=438
Cluster20_1_size=335
Cluster16_1_size=391
Cluster10_1_size=474
Cluster15_1_size=431
Group I&II
Group III

(c)

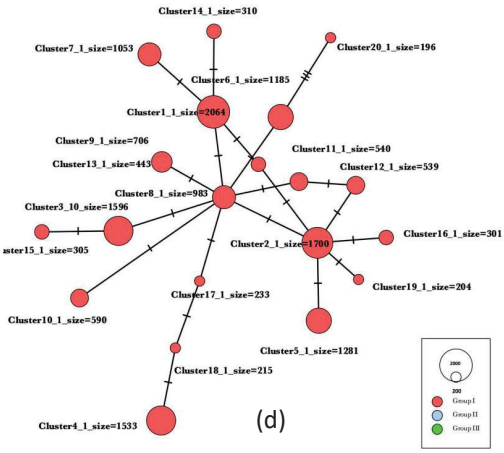
Cluster14_1_size=310
Cluster7_1_size=1053
Cluster20_1_size=196
Cluster6_1_size=1185
Cluster1_1_size=2064
Cluster9_1_size=706
Cluster11_1_size=540
Cluster13_1_size=443
Cluster12_1_size=539
Cluster8_1_size=983
Cluster3_10_size=1596
Cluster16_1_size=301
Cluster2_1_size=1700
Cluster19_1_size=204
Cluster10_1_size=590
Cluster17_1_size=233
Cluster5_1_size=1281
Cluster18_1_size=215
Cluster4_1_size=1533
Group I
Group II
Group III

(d)

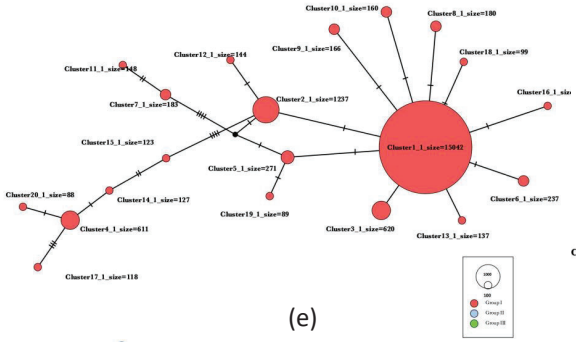
Cluster10_1_size=160
Cluster8_1_size=180
Cluster12_1_size=144
Cluster9_1_size=166
Cluster18_1_size=99
Cluster11_1_size=148
Cluster16_1_size
Cluster2_1_size=1237
Cluster7_1_size=183
Cluster1_1_size=15043
Cluster15_1_size=123
Cluster5_1_size=271
Cluster6_1_size=237
Cluster20_1_size=88
Cluster14_1_size=127
Cluster19_1_size=89
Cluster3_1_size=620
Cluster4_1_size=611
Cluster13_1_size=137
Cluster17_1_size=118
Group I
Group II
Group III

(e)

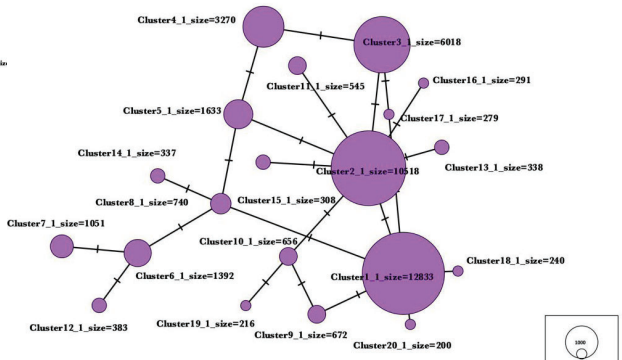
Cluster4_1_size=3270
Cluster3_1_size=6018
Cluster11_1_size=545
Cluster16_1_size=291
Cluster5_1_size=1633
Cluster17_1_size=279
Cluster14_1_size=337
Cluster2_1_size=10518
Cluster13_1_size=338
Cluster8_1_size=740
Cluster15_1_size=308
Cluster7_1_size=1051
Cluster10_1_size=656
Cluster18_1_size=240
Cluster6_1_size=1392
Cluster1_1_size=12833
Cluster12_1_size=383
Cluster19_1_size=216
Cluster9_1_size=672
Cluster20_1_size=200
100
Group I&II
Group III

(f)

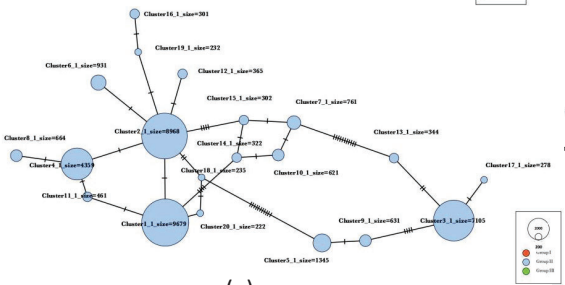
Cluster16_1_size=301
Cluster19_1_size=232
Cluster6_1_size=931
Cluster12_1_size=365
Cluster13_1_size=302
Cluster7_1_size=761
Cluster8_1_size=664
Cluster2_1_size=8968
Cluster14_1_size=322
Cluster13_1_size=344
Cluster4_1_size=4359
Cluster10_1_size=253
Cluster10_1_size=621
Cluster17_1_size=278
Cluster11_1_size=461
Cluster1_1_size=9679
Cluster20_1_size=222
Cluster9_1_size=631
Cluster3_1_size=7105
Cluster5_1_size=1345

(g)

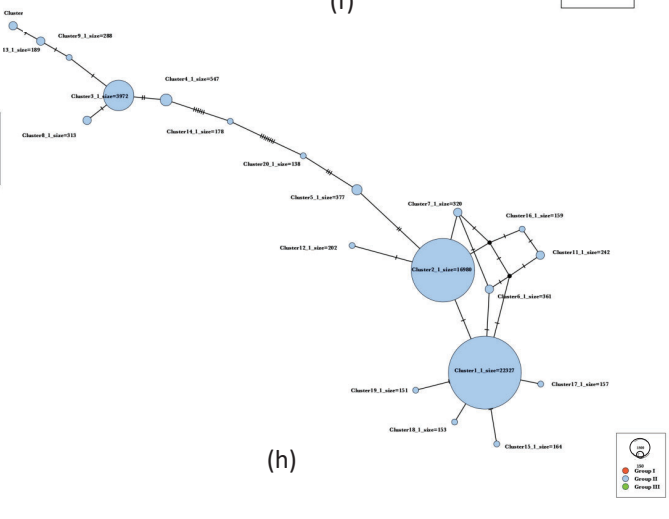
Cluster
Cluster9_1_size=288
Cluster3_1_size=3972
Cluster4_1_size=547
Cluster14_1_size=178
Cluster20_1_size=138
Cluster5_1_size=377
Cluster7_1_size=320
Cluster16_1_size=159
Cluster12_1_size=202
Cluster11_1_size=242
Cluster2_1_size=10980
Cluster6_1_size=361
Cluster1_1_size=22327
Cluster19_1_size=151
Cluster17_1_size=157
Cluster18_1_size=153
Cluster15_1_size=164
Group I
Group II
Group III

(h)

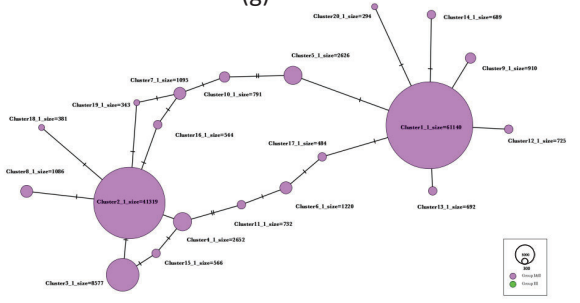
Cluster20_1_size=294
Cluster14_1_size=689
Cluster5_1_size=2626
Cluster9_1_size=910
Cluster7_1_size=1093
Cluster10_1_size=791
Cluster1_1_size=43140
Cluster19_1_size=343
Cluster18_1_size=381
Cluster16_1_size=544
Cluster12_1_size=725
Cluster17_1_size=404
Cluster8_1_size=1086
Cluster2_1_size=41319
Cluster6_1_size=1220
Cluster13_1_size=492
Cluster11_1_size=732
Cluster4_1_size=2652
Cluster15_1_size=566
Cluster3_1_size=8577

(i)

Figure 1. The intra-host diversity of coat protein (CP), movement protein (MP), and RNA-binding (RB) gene regions of grapevine virus A (GVA) in three grapevine samples, presented as median-joining haplotype networks (MJNs). Figure (a), (b), and (c), MJNs of the CP, MP, and RB gene, respectively, of the sample WIL3 which showed typical Shiraz disease symptoms from the Willunga site. Figure (d), (e), and (f), MJNs of the CP, MP, and RB genes, respectively, of the sample BV1 which showed mild leafroll disease symptoms from Barossa Valley. Figure (g), (h), and (i), MJNs of the CP, MP, and RB genes, respectively of the sample LC1 which showed typical SD symptoms for Langhorne Creek. Each of the red, blue, and green colours indicate the phylogenetic groups of each variant in each sample. GVA variants from phylogenetic groups I and II (GVA^{I} and GVA^{II}) of the RB gene were unable to be segregated (see explanation in Chapter 2) and labeled using purple named as $GVA^{I\&II}$. The size of the circle represents the copy numbers of the amplicon variant that it represents. The scale of each subfigure was individually assessed based on copy numbers of Cluster 20 in each data set. Only amplicon sequences of the largest 20 clusters of each sample were used to construct the figures. The 20 variant clusters with the largest number of amplicon sequences (Clusters 1 to 20) from each gene were chosen for analysis. The original copy numbers of each variant are given by "size=". The hatch mark indicates the number of mutations between each of the two variant clusters. The hypothetical median vectors (black dots) were implemented when the connection of two variant clusters was unknown.

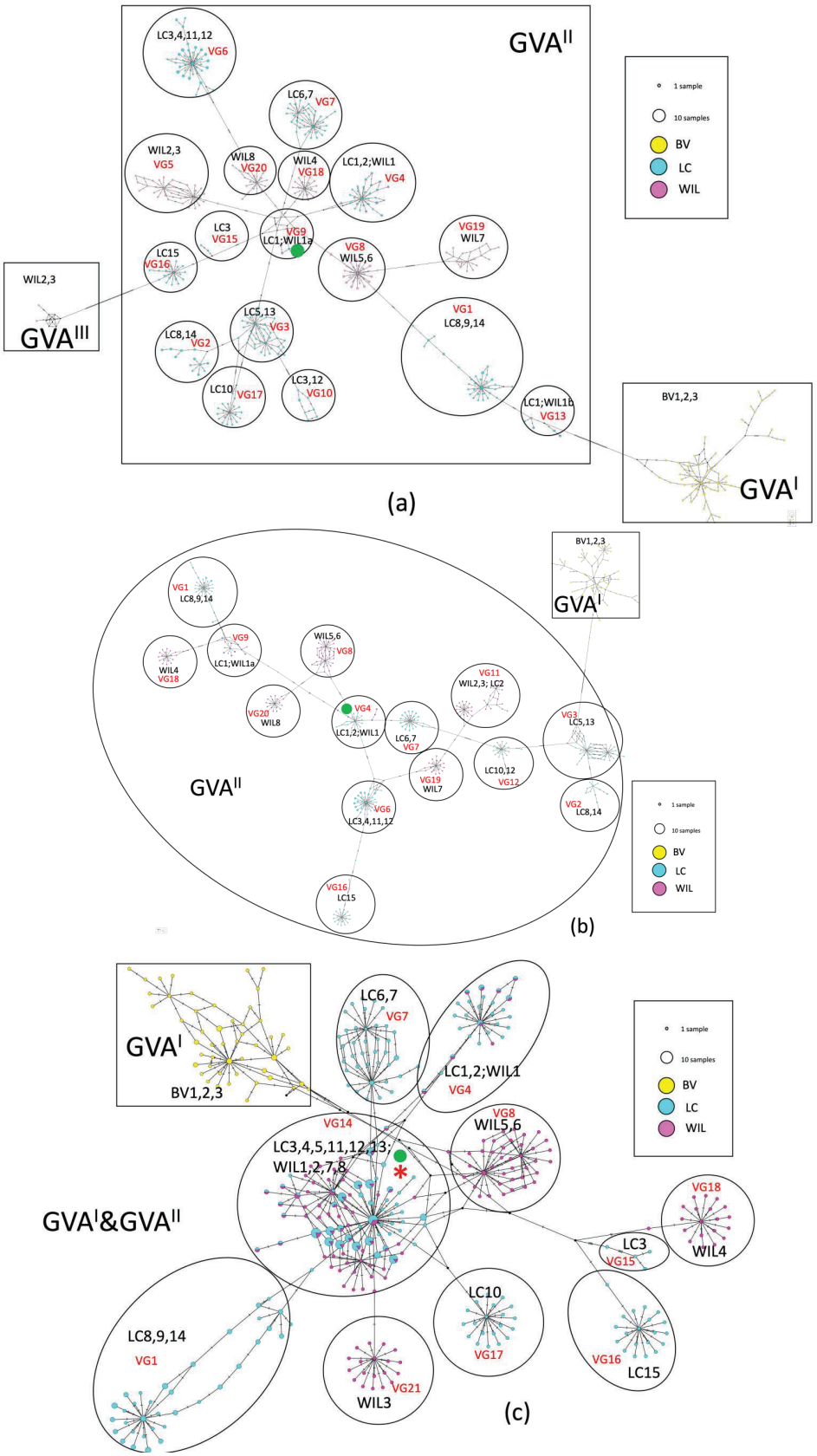

Figure 2. The intra-and inter- host diversity of coat protein (CP), movement protein (MP), and RNA-binding (RB) genes of grapevine virus A (GVA) within fifteen shiraz disease (SD) affected grapevines from Langhorne Creek (LC), eight SD affected grapevines from Willunga (WIL), and three leafroll disease affected grapevines from Barossa Valley (BV) were analyzed by phylogenetic median-joining haplotype networks (MJNs) clustering. Figures (a), (b), and (c) represent MJNs of the CP, MP, and RB genes, respectively. After amplicon sequence clustering, sequences that shared 100% nucleotide identity were merged into unique variants. The sequences of the 20 largest clusters of amplicon variants of each gene from each of the 26 grapevines from the three locations were used for analysis. Yellow, blue and purple colors represent variants from BV, LC and WIL, respectively. After MJNs were constructed, variants were grouped together to form variant groups, the original copy numbers of each variant are ignored. The size of the variant circles indicate number of samples in which the identical variant was found. The hatch mark indicates the number of mutations between each two variant clusters. The hypothetical median vectors (black dots) were implemented when the connection of two variant clusters was not known. The primary ancestral variant group of each gene is marked by a green dot in each subfigure. The super variant group VG14 of the RB gene is labeled by a red asterisk in Figure 3c. GVA variants from phylogenetic groups I, II and III are labeled as GVA^{I}, GVA^{II} and GVA^{III}. GVA^{I} and GVA^{II} variants of RB gene were together due to high similarity and labeled as $GVA^{I\&II}$. The number of hatch marks represent the number of mutations between each of the two variant clusters. The hypothetical median vectors (black dots) demonstrated hypothetical connection of two variant clusters when connections are missing. See supplementary Figures S1 for enlarged images of the GVA^{I} variants of Figure 2a, b and c.

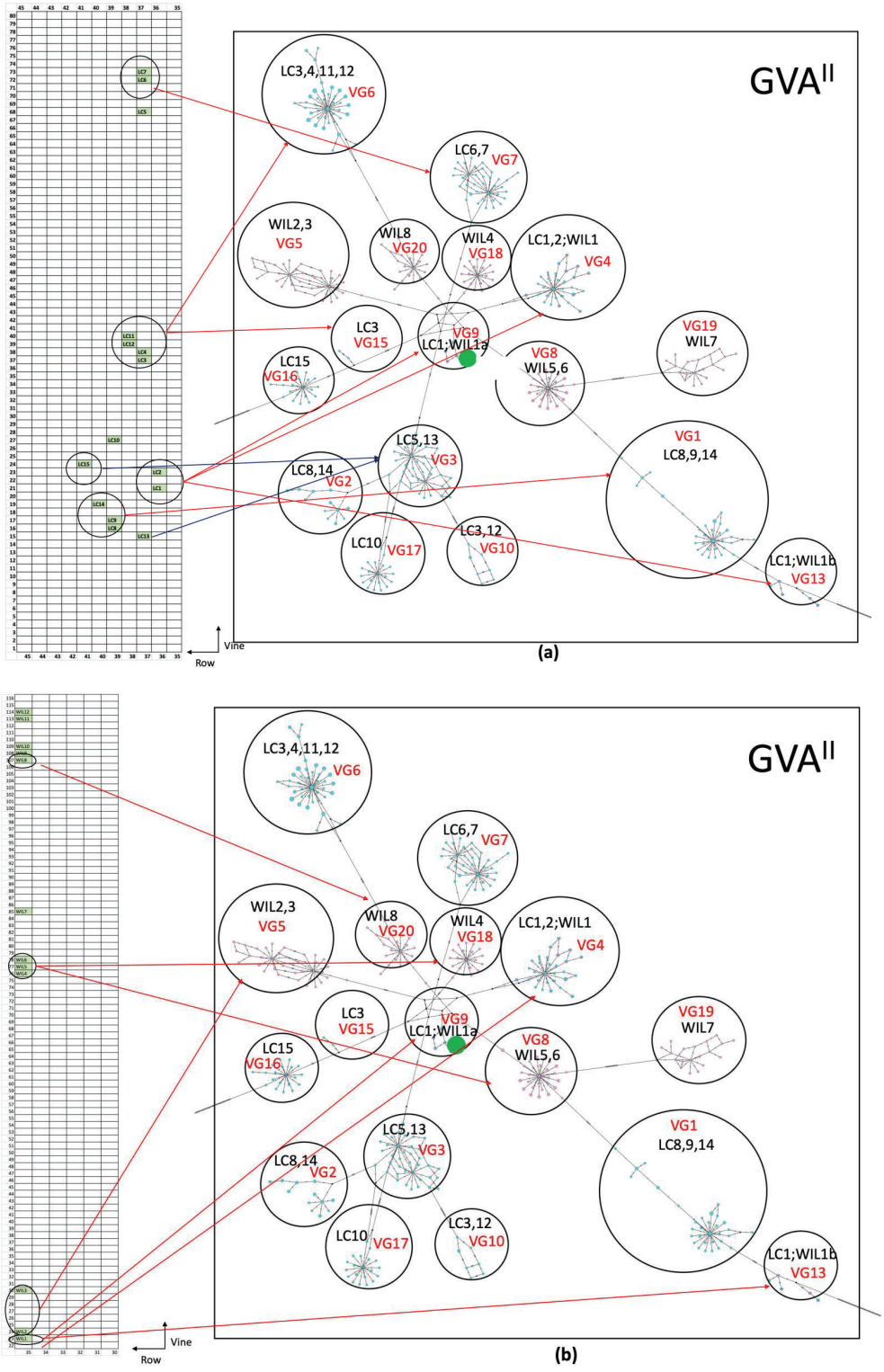

Figure 3. Median-joining haplotype networks of the coat protein (CP) gene versus relative geographical locations of grapevines from, (a) the Willunga vineyard (WIL1 to 8) and, (b) the Langhorne Creek vineyards (LC1 to 15). Relative geographical locations of each grapevine within the vineyard is shown on the left with row and grapevine numbers indicated and sampled grapevines shaded in green. Red arrows point to the multiple or single sample variant groups identified previously. Variant group IDs and symbols in the MJN are detailed in Table 4 and Figure 2a.

4. Discussion

This study used Amplicon-HTS of the MP, CP and RB genes of GVA to demonstrate the complexity of the genetic structure of a population of GVA variants in samples of individual grapevines expressing either SD or mild LRD symptoms in different vineyards. Plant virus populations can change with time in specific tissues due to genetic drift or selection [62,63] but this was not measured in this study. Instead, a single pooled sample (3 canes per grapevine) was collected from each of 26 grapevines across three different vineyards to provide a snapshot of GVA diversity in individual grapevines, within individual vineyards, and between vineyards at a single point in time. Even with this limitation, GVA diversity was observed and demonstrated the potential emergence of new variants within a population, but also demonstrated that most variants within a grapevine are likely to be related. This study also demonstrated relatedness between GVA populations in some grapevines within and between vineyards, which is likely to be associated with a combination of insect transmission and spread via propagation material.

4.1. Lowest pairwise identities

Diversity was found in all genes when assessing the largest genetic distance between GVA variants using lowest nt/aa identities and maximum nt/aa changes. It has been noted that the rate of mutation may differ between gene regions [64-66], however this was not observed in this study; for each GVA phylogroup, a similar depth of diversity was observed for each gene within individual samples (intra-host diversity) as was observed between samples (inter-host diversity). The largest genetic distance (up to ~12% and ~13.5% intra- and inter-host nucleotide diversity, respectively) was observed in the CP gene, however high levels of diversity were observed for the MP gene (up to ~9.6% and ~11.3% intra- and inter-host nucleotide diversity, respectively) and RB gene (up to ~9.9% and ~13.6% intra- and inter-host nucleotide diversity, respectively) in some samples. During data preprocessing and filtering amplicons were filtered to the same size and insertions and deletions were removed, therefore naturally occurring mutation events are the most likely explanation for the GVA diversity observed within and between grapevines in this study.

RNA viruses naturally have high mutation rates [20], which could lead to the high level of diversity observed in this study. Previous studies have suggested the mutation rate of RNA viruses is affected by virus species as well as the selection pressure imposed by the plant host, vector species and environment [20,67], which force adaptation. It is possible that these factors have contributed to the high level of diversity of GVA observed in many of the grapevines. However not all samples demonstrated a high level of diversity and the lowest level of diversity was ~1% for each of the three genes. The differences in the amount of diversity observed amongst the 26 grapevines could be associated with differences in selection pressures within and between the different vineyards. In potatoes it was found that vegetative propagation led to higher diversity, while insect transmission reduced diversity [68]. This could also explain the variability observed amongst the GVA populations of the 26 grapevines in this study, i.e. those with less diversity may have become infected through a more recent transmission event, since GVA is

transmitted by mealybug and scale species [4] , while those with higher level diversity may have been vegetatively propagated from an infected mother vine and/or had a much longer term infection. However, the fact that population diversity can be variable in different tissues within a single plant, even when collected at the same time point [62,63] cannot be excluded as possible explanation for the variation in diversity that was observed.

4.2. Intra-host diversity

This part of the study has been used to explore the evolutionary relationships between each of the distinct variant clusters as well as the population size of each cluster within three representative samples, each from a different location. The MJNs method used in this study detects single nucleotide variations within GVA populations, which provides an in-depth visualization of the population diversity. Similar to a previous study that analyzed diversity of prunus necrotic ringspot virus in *Prunus* trees by Amplicon-HTS [47], this study showed that for each of the CP, MP and RB genes, a GVA^{II} population within a host has at least one major variant cluster. Numerous unique variants of low copy number that are connected to but diverge from major clusters occur in a star-burst pattern. The major cluster usually represents the majority of the virus population in each grapevine, such as that observed for sample WIL3. This could represent a single, possibly recent, infection event followed by evolution and emergence of new strains. However, in some individual grapevines there was evidence of two or more distinct large copy number clusters of GVA^{I} and GVA^{II} variants in addition to the smaller low copy number variants, such as that observed for grapevine samples BV1 (GVA^{I}) and LC1 (GVA^{II}). GVA^{I} variants display a more dispersed distribution than GVA^{II} MJNs with no major variant cluster, and the size of clusters are similar. In these instances, there are some possible explanations: multiple infections have occurred either at the same time or at different times; a longer-term infection has given rise to multiple successful GVA variant clusters from a primary cluster through many generations; the three pooled canes were infected with one or more different variant clusters.

Both GVA^{II} and GVA^{III} variants were detected in three samples by Amplicon-HTS, although the presence of GVA^{III} was only seen for the CP gene. The lack of GVA^{III} detection for the MP and RB genes may have been due to a lack of amplification or inefficient amplification associated with poor primer specificity or low titre of GVA^{III}, or a combination of these two. Nevertheless, this detection of both phylogroups, based on the CP gene, supports the observations of multiple GVA infections possibly associated with different infection events. The evolutionary pathway of the GVA^{III} variants should be explored further by Amplicon-HTS using either group III variant specific primers or universal GVA primers.

GVA^{II} variants are often associated with SD [Chapter 2]. When this study was conceptualized the possibility that a dominant SD associated GVA^{II} variant might be observed amongst the SD affected grapevines was considered. However, no single dominant variant was observed, and further study is required to understand whether any linkage between the variant characteristics of GVA and SD exists.

Nonsense mutations naturally exist at a very low level of frequency and the population of nonsense mutants may be reduced during virus evolution, possibly by the nonsense-mediated mRNA decay in the host

[69,70]. Little is known about the impact of nonsense mutations within a virus population, however, it is known that nonsense mutations of the RdRp and MP gene attenuate the symptoms of tomato mosaic virus [71] and nonsense mutation affect virus transmissibility of a SARS-CoV-2 strain [72]. In this study, nonsense variants were found in 76/78 sequencing samples, but they were mostly low frequency variants and were not included in the analysis as they did not fall within the 20 largest variant clusters within any sample. Future research should investigate how nonsense mutations affect the severity of symptoms and transmission of GVA.

4.3. Evolutionary relationship between GVA phylogroups

MJNs of intra and inter-host diversity provides a snapshot of the evolutionary relationship of GVA phylogroups. Based on the CP gene, GVAI and GVAIII, which do not have an association with SD [Chapter 2], are more distant from each other than they are from GVAII and are linked to GVAII by a large number of hatch marks (Figure 3) indicating many mutational events have occurred during their evolution. Based on this observation, it is proposed that GVAII could be the ancestral phylogroup of GVAI and GVAIII. The direction of evolution of a virus towards milder or more virulent strains can be difficult to predict since many complicated factors such as virus and host interaction, environment adaptation and vector transmission lead to evolution [73-75]. However mild strains clearly benefit from escaping virus surveillance, improving the survival in a host and achieving a symbiotic relationship between coinfected viruses and hosts [76] and could have contributed to the emergence of GVAI and GVAIII. Evidence for this is that virulent strains were over taken by the mild strain of Omicron during the SARS-CoV-2 global pandemic [77]. The hypothesis of GVAII variants being the ancestral phylogroup needs to be tested by a larger scale study containing data from all three phylogroups and wider geographic locations in Australia and other countries.

4.4. Origin of GVA variants in vineyards

Two major modes of GVA transmission can occur: infected propagation material used for top working or planting, or transmission by insect vectors (mealybugs and scale) [78-80]. The haplotype analysis of this study demonstrates a common origin of GVAII variants within a vineyard, which is likely to be associated with spread via an insect vector. The first and second-instar nymphs are most efficient at transmitting viruses [79,81-83], which occurs as they crawl from vine to vine. This could explain the infection of adjacent grapevines at LC. Insects can also be carried on people's clothing and machinery and can be dispersed by wind or water [84,85] over short distances, which could explain the infection of grapevines with the same variant group in the same vineyard but that are not adjacent.

However, an alternate possibility for adjacent grapevines infected with the same variant group is the use of planting material or topworking grapevines already infected with the same GVA variant groups, originating from the same source. The first piece of evidence to support this hypothesis is the presence of the same CP, MP and RB variant groups in grapevines at LC (LC1, LC2) and WIL (WIL1) vineyards that are

approx. 70 kilometers apart. While the long distance movement of vectors by machinery is known and cannot be completely discounted [86], LC and WIL are not managed by the same growers and sharing of equipment is unlikely. Therefore, the distance between vineyards would make insect spread of GVA between these two locations unlikely. The second piece of evidence for spread by vegetative propagation is the presence of different GVA variant groups in adjacent grapevines within a vineyard, for example WIL4 was infected with a different variant group compared to WIL 5 and WIL 6, yet all three grapevines occurred in the same row. However, this study demonstrated variation within variant groups within a grapevine and its contribution to the variation in GVA variant groups between grapevines originating from the same original grapevine cannot be ruled out, since uneven distribution of variant groups in a grapevine might occur. Nor can insect transmission be disregarded; a proportion of GVA variants may have been selectively passed from the original source into a new host due to bottleneck events occurring in the vector [87,88], or by escaping plant defense and adapting to a new host [20]. More evidence supporting selective transmission of GVA variants is that Shiraz WIL9, WIL10 had only GVA^{III} variants, while WIL8 which was next to WIL9 had both GVA^{II} and GVA^{III} variants (Chapter 2).

4.5. Implementation of Amplicon-HTS in virus diversity studies

Conclusions arising from fine scale genomic epidemiology, intra-host genetic diversity and populations of genetic variants of viruses based on amplicon sequencing can be affected by PCR derived sequence errors associated with the fidelity of the Taq polymerase [89,90]. To minimize the risk we used Q5 Taq (280 x fidelity vs. Taq) for the initial RT-PCR amplification and for PCR-enrichment in the library preparation prior to sequencing on a MiSeq instrument. Nevertheless, a cut off value of 10 reads was used, as suggested by Kinoti *et al.* [44], who found that the variants with the copy number below 10 were often error prone. Using a Taq polymerase with a high fidelity in combination with the three filters that were used in the initial data processing to filter out any low-quality, short and unspecific reads prior to sequence clustering, provides a high level of confidence in the study of GVA variant groups enabling epidemiological conclusions.—However, size trimming resulted in a significant reduction of the number of reads in a few samples, possibly associated with the removal of a higher number of nonspecific reads from grapevine host or shorter viral reads that may have been a result of poor primer specificity for some GVA variants. This could result in loss of variants that are significant in SD epidemiology. Additionally, to minimize the impacts of sequencing error, this study used only the 20 largest groups of unique variants of each gene in each grapevine sample analysed. However, if all variants were analysed evidence may have emerged that more grapevines have been infected with two or more variant groups and those with at least two variant groups could have had three or more. Analysis of all valid variants, instead of just the 20 largest clusters of unique variants, could provide an even greater understanding of the intra and inter-host diversity that may reveal the emergence and spread of GVA in infected vineyards under this study.

5. Conclusion

This study demonstrated the utility of deep Amplicon-HTS as a tool for studying the epidemiology of SD, including transmission and the evolutionary pathway of GVA. A deeper insight was gained into the diversity of GVA in SD and LRD affected vineyards, and within infected grapevines. The MJN analysis connected variant groups to geographical locations of the grapevines demonstrating the expected pathway of GVA being transmitted to grapevines by insect vectors and by plant propagation, resulting in the spread of SD. Grapevines without SD but infected with GVA were not analyzed within SD vineyards due to a high level of diversity and lack of universal primers in different gene regions, thus no further information was derived from the study about the importance of specific GVA^{II} or GVA^{III} variants in association with disease. Greater diversity was observed using the CP gene compared to the MP and RB genes, making it more useful for fine scale genomic epidemiological studies using Amplicon-HTS. Future analysis could include deliberately inoculating Shiraz with specific GVA phylogroups, variant groups or unique variants and to observe disease development and emergence of GVA variants with time. This could be achieved by generating full-length infectious clones of the virus. In this study a small number of selected grapevines with SD or LRD that were sometimes clustered, but often randomly dispersed within a vineyard, were used to analyse GVA diversity. To better understand GVA and SD epidemiology using this fine scale Amplicon-HTS approach further studies, using the CP gene only, should include using a higher number of SD affected and unaffected grapevines which are planted together within a vineyard and several SD affected vineyards, planted with the same grapevine clone, should be analysed.

6. Supplementary Material

Table S1. The primers used to generate amplicons and the expected amplicon size (base pairs; bp) of the of the grapevine virus A coat protein, movement protein and RNA binding protein genes for amplicon sequencing.

Primer	Primer sequence (5′- 3′)	Gene/ORF	Amplicon size	Annealing temperature (C°)	Reference
GVACP565F	GATACCCTAGTTATGCCAGA	coat protein/ORF 4	565bp	56	This study
GVACP565R	CTGTATCACAGTAGCTTCTTG				
GVAMP404F	CATGGYAAGAATCTGCAAGG	movement protein/ORF 3	404bp	56	This study
GVAMP404R	TCTGGCATAACTAGGGTATC				
GVAH7038	AGGTCCACGTTTGCTAAG	RNA binding/ ORF 5	236bp	56	[91]
GVAC7273	CATCGTCTGAGGTTTCTACTAT				

Table S2. Number of amplicon sequencing reads generated for the three gene regions of grapevine virus A.

				Quality trimming		Size trimming		Primer trimming		Unique variants after cut-off[a]	Unique aa variants	Nonsense variants	Cluster 1[b]	Cluster 2	Cluster 3	Cluster 4	Cluster 5	Cluster 6	Cluster 7	Cluster 8	Cluster 9	Cluster 10	Cluster 11	Cluster 12	Cluster 13	Cluster 14	Cluster 15	Cluster 16	Cluster 17	Cluster 18	Cluster 19	Cluster 20
Gene[1]	Location[2]	Sample ID	Raw reads	Reads	% remaining	Reads	% remaining	Reads	% remaining																							
MP	LC	LC1	217,318	101,750	93.64%	84,046	77.35%	81,708	75.20%	524	161	7	22,327	16,980	3,972	547	377	361	320	313	288	285	242	202	189	178	164	159	157	153	151	138
		LC2	248,634	115,371	92.80%	90,658	72.92%	88,525	71.21%	590	381	17	51,254	2,516	757	509	451	438	420	395	275	262	261	247	240	237	236	230	226	213	211	203
		LC3	316,538	142,517	90.05%	114,899	72.60%	111,767	70.62%	607	186	10	20,717	8,894	7,121	1,363	1,009	725	621	569	458	416	359	354	339	339	305	304	302	290	280	274
		LC4	253,104	113456	89.65%	96,360	76.14%	93,972	74.26%	515	327	11	46,928	698	537	532	518	486	453	430	417	414	414	363	360	357	351	336	323	317	312	304
		LC5	298,918	139,639	93.43%	111,920	74.88%	109,288	73.12%	678	431	17	63,436	4,058	1,723	1,093	714	497	454	394	320	319	290	290	287	268	264	257	255	253	244	243
		LC6	294,096	137,754	93.68%	112,760	76.68%	110,383	75.07%	644	441	16	63,885	1,267	1,060	763	536	534	534	374	372	370	364	361	356	303	290	288	284	279	267	264
		LC7	250,288	114,222	91.27%	88,521	70.74%	86,495	69.12%	533	348	12	45,608	2,210	582	564	469	401	360	347	318	316	315	294	289	286	285	280	279	258	252	239
		LC8	280,678	125,720	89.58%	103,976	74.09%	100,755	71.79%	621	255	10	30,659	12,751	4,324	3,473	1,122	582	485	446	445	403	392	386	381	363	348	325	304	300	250	246
		LC9	264,532	107,201	81.05%	80,199	60.63%	77,364	58.49%	459	274	12	40,965	1,912	1,299	733	406	322	320	319	299	287	265	256	254	246	231	229	229	229	211	208
		LC10	228,504	99,513	87.10%	77,920	68.20%	75,329	65.93%	464	280	12	40,246	1,554	1,401	520	425	423	335	326	311	304	285	270	264	242	239	230	230	215	212	208
		LC11	233,492	97,875	83.84%	72,045	61.71%	70,079	60.03%	420	259	9	36,645	2,252	698	510	437	330	327	311	302	280	272	269	264	244	229	212	208	199	191	188
		LC12	211,318	88,706	83.95%	70,987	67.19%	69,080	65.38%	409	193	8	28,775	3,007	1,809	881	708	474	320	296	279	270	257	256	252	217	203	195	186	179	178	173
		LC13	246,956	116,953	94.72%	97,214	78.73%	95,120	77.03%	594	340	13	49,376	4,136	3,781	1,096	677	532	514	477	427	424	333	316	298	245	239	235	230	228	224	219
		LC14	252,652	120,654	95.51%	101,089	80.02%	97,904	77.50%	497	224	11	23,976	16,808	1,982	623	568	547	538	538	529	503	485	446	439	419	358	321	290	290	276	218

		LC15	276,306	131,937	95.50%	107,987	78.16%	105,134	76.10%	658	338	16	46,073	1,981	1,512	1,498	1,183	805	639	628	557	545	535	511	480	465	459	456	423	421	416	416
	WIL	WIL1	245,302	109,644	89.40%	91,812	74.86%	89,309	72.82%	596	196	13	25,479	15,350	3,968	530	455	455	440	360	319	271	235	231	222	212	199	195	187	187	179	172
		WIL2	206,068	89,292	86.66%	77,346	75.07%	75,213	73.00%	411	136	10	11,630	8,771	7,294	981	929	824	768	641	403	315	308	270	266	261	252	231	197	196	187	171
		WIL3	274,498	115,968	84.49%	92,163	67.15%	89,952	65.54%	591	325	14	43,101	6,386	4,648	1,116	862	348	264	260	242	240	227	223	204	199	193	190	188	183	173	173
		WIL4	102,720	39,416	76.74%	33,087	64.42%	32,188	62.67%	219	98	7	11,091	4,200	531	411	192	155	110	109	105	102	99	97	94	88	86	85	79	78	77	76
		WIL5	381,238	177,844	93.30%	149,167	78.25%	145,294	76.22%	975	445	29	59,226	2,494	1,821	1,523	1,457	912	892	837	789	772	735	704	670	652	633	617	613	589	572	553
		WIL6	267,442	128,102	95.80%	107,090	80.08%	104,860	78.42%	609	353	14	51,287	2,467	1,337	676	636	556	545	434	366	325	311	299	298	285	284	284	276	273	271	267
		WIL7	205,952	93,487	90.79%	71,846	69.77%	69,905	67.88%	418	218	8	32,063	2,199	1,074	467	465	433	357	346	287	282	253	252	251	241	239	238	238	235	223	220
		WIL8	259,524	124,432	95.89%	106,466	82.05%	104,284	80.37%	600	287	12	42,099	2,423	2,271	1,328	1,279	1,028	945	910	574	556	546	510	482	467	397	392	386	340	332	332
	BV	BV1*	258,588	118,116	91.35%	35,334	27.33%*	33,599	25.99%	238	73	5	15,042	1,237	620	611	271	237	183	180	166	160	148	144	137	127	123	118	118	99	89	88
		BV2*	191,480	82,850	86.54%	9,750	10.18%*	8,838	9.23%	88	15	0	1,252	800	457	244	200	109	91	90	85	73	71	68	63	61	50	47	45	43	40	38
		BV3*	199,966	86,706	86.72%	3,509	3.51%*	2,439	2.44%	25	9	0	348	224	222	130	83	48	45	28	26	26	25	24	21	16	16	16	16	14	13	12
CP	LC	LC1	452,700	207,485	91.67%	134,684	59.50%	131,106	57.92%	761	112	5	9,679	8,968	7,105	4,359	1,345	931	761	664	631	621	461	365	344	322	302	301	278	235	232	222
		LC2	319,480	148,895	93.21%	94,916	59.42%	92,369	57.82%	541	331	21	30,794	789	664	663	614	584	430	413	394	368	347	316	292	271	266	255	237	233	222	216
		LC3	230,566	97,618	84.68%	62,455	54.18%	60,478	52.46%	397	207	10	5,174	2,003	1,842	1,137	241	211	173	151	145	143	141	137	125	115	112	108	107	96	92	87
		LC4	202,170	91,462	90.48%	54,316	53.73%	52,658	52.09%	331	176	9	14,091	2,430	934	248	224	204	198	168	165	161	155	149	142	135	134	134	133	122	119	115
		LC5	315,062	138,800	88.11%	86,195	54.72%	83,575	53.05%	511	231	16	19,090	6,910	4,692	741	635	584	560	267	246	212	201	191	167	155	147	146	141	128	126	122
		LC6	272,106	125,897	92.54%	62,792	46.15%	61,131	44.93%	373	178	13	17,721	3,004	710	562	556	293	228	227	193	188	180	180	162	162	149	146	143	142	136	129
		LC7	350,856	163,058	92.95%	74,709	42.59%	72,494	41.32%	470	184	10	12,477	6,015	4,724	829	363	189	187	184	172	164	154	138	136	126	124	123	122	121	117	116
		LC8	223,674	97,547	87.22%	48,182	43.08%	46,688	41.75%	378	173	9	6,862	2,721	1,291	1,119	796	472	368	278	254	205	169	162	147	138	125	115	104	101	100	83
		LC9	331,944	139,221	83.88%	50,750	30.58%	49,052	29.55%	384	192	19	12,333	1,422	1,333	303	245	234	212	187	181	166	155	152	148	145	144	123	119	117	113	110
		LC10	226,406	98,317	86.85%	67,534	59.66%	65,420	57.79%	369	197	10	19,495	910	806	642	344	327	240	220	210	196	189	187	185	170	167	167	165	161	153	149
		LC11	299,072	127,148	85.03%	62,425	41.75%	60,653	40.56%	362	169	8	15,002	2,417	1,311	783	645	575	547	274	249	210	202	192	189	180	180	178	171	165	157	155
		LC12	321,830	147,381	91.59%	82,281	51.13%	79,772	49.57%	447	231	11	16,805	2,488	1,964	1,077	625	370	360	331	316	270	247	244	244	224	212	191	191	179	179	178
		LC13	332,664	149,085	89.63%	78,468	47.18%	75,308	45.28%	431	183	10	18,803	5,064	1,645	953	715	501	382	361	283	269	262	211	194	189	189	188	180	159	150	143
		LC14	319,244	145,564	91.19%	63,679	39.89%	61,617	38.60%	385	195	11	7,197	5,240	703	687	599	467	417	367	272	268	207	160	149	144	139	138	134	127	125	117

		LC15	378,102	174,410	92.26%	119,104	63.00%	115,705	61.20%	878	411	30	27,349	2,071	1,597	1,052	906	772	638	586	535	482	460	452	446	417	391	383	380	360	339	330
	WIL	WIL1	513,022	236,650	92.26%	157,580	61.43%	153,102	59.69%	876	144	8	10,069	9,490	7,673	4,392	1,359	847	751	671	658	597	472	432	355	347	323	267	257	232	230	204
		WIL2	362,178	166,958	92.20%	110,174	60.84%	107,339	59.27%	993	356	39	10,392	5,045	3,543	1,770	1,234	594	484	476	385	353	327	298	280	254	240	233	221	181	173	172
		WIL3	552,274	245,251	88.81%	88,337	31.99%	86,090	31.18%	507	281	12	24,322	2,361	1,040	676	450	372	330	321	274	249	235	212	211	210	205	204	204	191	187	180
		WIL4	499,358	230,096	92.16%	91,055	36.47%	88,443	35.42%	479	270	15	25,054	1,699	695	503	475	430	346	344	339	332	314	294	257	247	222	222	221	219	216	211
		WIL5	458,846	209,340	91.25%	102,437	44.65%	98,756	43.05%	730	349	35	21,997	540	513	440	419	377	375	372	351	345	327	320	319	305	283	274	271	263	263	255
		WIL6	363,750	157,266	86.47%	78,461	43.14%	76,091	41.84%	422	231	12	22,853	639	561	377	252	237	231	225	213	211	208	199	185	185	181	180	172	171	170	169
		WIL7*	309,620	121,091	78.22%	28,519	18.42%*	27,621	17.84%	271	127	6	2,250	1,380	1,149	937	659	500	414	288	192	187	166	165	117	96	94	92	81	69	67	66
		WIL8	359,502	164,959	91.77%	76,685	42.66%	74,146	41.25%	415	153	9	13,890	3,620	705	676	432	362	354	242	217	210	209	202	190	185	173	170	169	168	160	159
		BV1	274,456	100,920	73.54%	69,344	50.53%	67,264	49.02%	436	57	3	2,064	1,700	1,596	1,533	1,281	1,185	1053	983	706	590	540	539	443	310	305	301	233	215	204	196
	BV	BV2	165,704	56,636	68.36%	37,947	45.80%	35,226	42.52%	178	106	35	1,661	314	305	264	232	222	208	194	193	173	171	171	157	151	143	143	133	124	119	118
		BV3	349,700	136,115	77.85%	97,216	55.60%	93,016	53.20%	778	145	13	6,103	2,411	2,059	1,894	1,745	1,113	790	787	749	684	545	471	443	352	302	297	278	257	217	215
		LC1	383,012	177,332	92.60%	171,930	89.78%	156,691	81.82%	629	270	14	61,140	41,319	8,577	2,652	2,626	1,220	1095	1086	910	791	732	725	692	689	566	544	484	381	343	294
		LC2	308,528	141,902	91.99%	136,070	88.21%	123,590	80.12%	391	287	16	96,292	2,928	1,466	940	773	613	515	403	330	312	297	291	289	274	269	266	264	260	242	229
		LC3	260,144	114,146	87.76%	109,750	84.38%	97,387	74.87%	372	220	10	50,087	11,612	3,046	1,561	816	633	633	571	482	469	455	424	423	404	391	389	358	351	342	341
		LC4	234,768	100,467	85.59%	95,260	81.15%	85,266	72.64%	315	222	11	62,054	2,622	1,477	542	393	379	364	364	361	345	342	341	341	339	337	295	280	275	268	262
		LC5	272,524	107,010	78.53%	98,594	72.36%	90,409	66.35%	333	244	12	75,240	937	419	284	279	248	236	235	223	208	196	187	185	184	175	174	172	170	169	164
		LC6	79,678	29,403	73.80%	27,752	69.66%	25,238	63.35%	75	46	1	18,568	1,488	262	173	123	95	91	90	89	82	81	76	76	71	70	68	65	63	60	55
		LC7	290,598	106,667	73.41%	96,409	66.35%	87,173	60.00%	318	188	8	49,556	17,889	706	359	344	312	301	296	282	282	279	257	255	255	249	238	228	219	209	201
RB	LC	LC8	298,130	104,531	70.12%	95,350	63.97%	86,629	58.11%	289	184	11	36,096	30,127	621	617	599	573	419	326	313	297	297	288	268	239	228	204	193	189	188	178
		LC9	293,006	131,043	89.45%	118,079	80.60%	106,362	72.60%	384	256	16	72,162	9,395	1,630	775	597	495	406	402	382	371	368	359	359	323	314	298	293	287	284	268
		LC10	238,110	104,905	88.11%	94,395	79.29%	86,519	72.67%	332	245	13	67,547	661	608	589	492	336	307	290	278	272	269	263	259	247	245	240	236	232	229	228
		LC11	366,474	164,758	89.92%	151,290	82.57%	136,332	74.40%	469	318	21	95,322	6,843	4,077	1,802	1,235	725	542	538	510	459	456	454	435	427	402	400	361	330	329	328
		LC12	336,544	155,500	92.41%	145,008	86.17%	130,010	77.26%	425	248	16	92,100	5,303	2,225	977	724	575	553	546	543	524	518	513	505	500	491	482	477	449	442	427
		LC13	203,404	95,444	93.85%	88,809	87.32%	81,177	79.82%	315	223	12	58,680	2,312	1,227	1,111	839	799	787	785	578	317	293	240	217	211	180	178	172	172	171	157
		LC14	227,060	107,445	94.64%	100,394	88.43%	89,997	79.27%	322	202	9	37,446	25,135	974	916	723	708	679	439	423	372	369	322	304	294	274	266	264	255	242	241

	LC15	257,202	121,931	94.81%	117,084	91.04%	104,092	80.94%	406	271	15	71,000	1,860	1,239	1,100	971	704	672	666	643	602	560	550	535	529	528	517	515	487	484	472
WIL	WIL1	590,016	283,539	96.11%	275,497	93.39%	249,904	84.71%	898	335	19	92,490	66,582	13,020	4,356	4,247	1,918	1779	1457	1391	1359	1252	1244	1147	1035	991	901	888	851	739	666
	WIL2	432,906	206,852	95.56%	199,999	92.40%	176,931	81.74%	569	377	23	112,436	7,737	3,624	1,961	1,467	1,144	1051	1015	1001	964	927	912	903	853	852	831	830	808	777	725
	WIL3	426,814	197,090	92.35%	172,363	80.77%	154,382	72.34%	420	304	20	122,451	1,566	1,029	930	740	533	513	487	478	474	463	451	439	438	431	391	368	366	337	335
	WIL4	406216	193,012	95.03%	185,067	91.12%	144,054	70.92%	408	303	22	109,167	1,631	876	791	758	740	665	657	651	606	593	579	574	557	532	501	490	473	465	462
	WIL5	284,328	131,658	92.61%	126,101	88.70%	108,169	76.09%	456	283	17	68,656	2,414	2,185	1,688	1,151	895	893	888	855	772	764	754	741	668	629	593	563	546	533	525
	WIL6	280,500	131,380	93.68%	122,836	87.58%	112,001	79.86%	368	275	16	86,798	1,348	624	467	433	433	402	378	369	366	363	345	343	334	320	316	305	302	285	278
	WIL7	262,628	119,850	91.27%	108,352	82.51%	98,163	74.75%	398	245	12	57,561	10,414	4,668	1,861	1,006	614	489	436	366	361	349	307	295	293	259	257	250	245	238	235
	WIL8	223,044	97,899	87.78%	89,383	80.15%	80,615	72.29%	329	235	13	56,399	1,928	746	660	618	614	532	460	416	415	410	402	372	370	361	335	330	318	317	313
BV	BV1	154,174	71,287	92.48%	59,808	77.59%	53,314	69.16%	212	80	2	12,833	10,518	6,018	3,270	1,633	1,392	1051	740	672	656	545	383	338	337	308	291	279	240	216	200
	BV2	244,886	108,919	88.95%	88,650	72.40%	78,582	64.18%	313	141	6	25,081	12,471	5,671	2,411	2,077	2,041	1715	1570	1167	790	768	714	674	595	449	388	361	322	287	279
	BV3	213,784	95,242	89.10%	79,056	73.96%	71,659	67.04%	306	190	8	42,812	10,824	1,696	799	354	273	257	235	228	204	174	166	164	154	147	145	130	130	127	121

[1] MP = movement protein, CP = coat protein, RB = RNA- binding protein of grapevine virus A. [2] WIL = Willunga, LC = Langhorne Creek, BV = Barossa Valley. All grapevines listed are var. Shiraz.*Samples with a low percentage of remaining reads after the size trimming. [a] Amplicon reads with the frequency of less than 10 were excluded. [b] Original copy numbers of each amplicon variant before clustering.

Table S3. Number of trimmed reads, unique variants, and the lowest percentage pairwise identity within each sample.

Gene	Sample ID	Trimmed reads	Number of nucleotide (nt) variants	Number of amino acid (aa) variants	Lowest pairwise nt identity	Lowest aa identity	No. nt difference	No. aa difference	Phylogroup in this sample	Copy numbers of largest variant cluster	Phylo-group of the largest variant cluster
MP[1]	LC1	81,708	524	161	92.86	96.69	26	4	II	22,327	II
	LC2	88,525	590	381	93.96	96.69	22	4	II	51,254	II
	LC3	111,767	607	186	90.66	92.56	34	9	II	20,717	II
	LC4	93,972	515	327	91.48	94.21	31	7	II	46,928	II
	LC5	109,288	678	431	98.35	96.69	6	4	II	63,436	II
	LC6	110,383	644	441	98.9	97.52	4	3	II	63,885	II
	LC7	86,495	533	348	95.6	97.52	16	3	II	45,608	II
	LC8	100,755	621	255	90.11	92.56	36	9	II	30,659	II
	LC9	77,364	459	274	98.9	97.52	4	3	II	40,965	II
	LC10	75,329	464	280	98.63	97.52	5	3	II	40,246	II
	LC11	70,079	420	259	95.6	97.52	16	3	II	36,645	II
	LC12	69,080	409	193	91.21	93.39	32	8	II	28,775	II
	LC13	95,120	594	340	98.63	97.52	5	3	II	49,374	II
	LC14	97,904	497	224	90.38	92.56	35	9	II	23,976	II

	LC15	105,134	658	338	98.9	96.69	4	4	II	46,073	II
	WIL1	89,309	596	196	92.58	96.69	27	4	II	25,479	II
	WIL2	75,213	411	136	98.08	95.87	7	5	II	11,630	II
	WIL3	89,952	591	325	98.9	96.69	4	4	II	43,101	II
	WIL4	32,188	219	98	98.9	96.69	4	4	II	11,091	II
	WIL5	145,294	975	445	91.21	94.21	32	7	II	59,226	II
	WIL6	104,860	609	353	98.35	96.69	6	4	II	51,287	II
	WIL7	69,905	418	218	98.35	96.69	6	4	II	32,063	II
	WIL8	104,284	600	287	90.38	91.74	35	10	II	42,099	II
	BV1	33,599	238	73	96.15	96.69	14	4	I	15,042	I
	BV2	8,838	88	15	96.15	95.87	14	5	I	1,252	I
	BV3	2,439	25	9	96.43	95.87	13	5	I	348	I
CP[1]	LC1	131,106	761	112	95.27	98.15	23	3	II	9,679	II
	LC2	92,369	541	331	95.68	97.53	21	4	II	30,794	II
	LC3	60,478	397	207	94.24	96.3	28	6	II	5,174	II
	LC4	52,658	331	176	94.86	96.91	25	5	II	14,091	II
	LC5	83,575	511	231	98.77	97.53	6	4	II	19,090	II
	LC6	61,131	373	178	99.18	98.15	4	3	II	17,721	II
	LC7	72,494	470	184	97.94	96.91	10	5	II	12,477	II
	LC8	46,688	378	173	94.65	96.3	26	6	II	6,862	II
	LC9	49,052	384	192	98.35	96.3	8	6	II	12,333	II
	LC10	65,420	369	197	98.97	97.53	5	4	II	19,495	II
	LC11	60,653	362	169	98.97	96.91	5	5	II	15,002	II
	LC12	79,772	447	231	94.44	96.3	27	6	II	16,805	II
	LC13	75,308	431	183	98.97	98.15	5	3	II	18,803	II
	LC14	61,617	385	195	94.86	96.3	25	6	II	7,197	II
	LC15	115,705	878	411	95.47	96.3	22	6	II	27,349	II
	WIL1	153,102	876	144	95.27	97.53	23	4	II	10,069	II
	WIL2	107,339	993	356	$75.72^{II\&III*}$, 91.36^{II*}, 90.74^{III*}	$78.4^{II\&III}$, 88.82^{II}, 90.12^{III}	$118^{II\&III}$, 42^{II}, 45^{III}	$35^{II\&III}$, 18^{II}, 16^{III}	II&III	10,392	II
	WIL3	86,090	507	281	$76.13^{II\&III}$, 90.95^{II}, 88.07^{III}	$79.01^{II\&III}$, 98.77^{II}, 90.74^{III}	$116^{II\&III}$, 44^{II}, 58^{III}	$34^{II\&III}$, 2^{II}, 15^{III}	II&III	24,322	II
	WIL4	88,443	479	270	99.18	96.91	4	5	II	25,054	II
	WIL5	98,756	730	349	97.74	95.06	11	8	II	21,997	II
	WIL6	76,091	422	231	99.18	97.53	4	4	II	22,853	II
	WIL7	27,621	271	127	93.62	95.06	31	8	II	2,250	II
	WIL8	74,146	415	153	$76.13^{II\&III}$, 90.74^{II}, 90.95^{III}	$79.63^{II\&III}$, 89.51^{II}, 90.74^{III}	$116^{II\&III}$, 45^{II}, 44^{III}	$33^{II\&III}$, 17^{II}, 15^{III}	II&III	13,890	II

	BV1	67,264	436	57	97.53	98.15	12	3	I	2,064	I
	BV2	35,226	178	106	93	93.83	34	10	I	1,661	I
	BV3	93,016	778	145	97.12	97.53	14	4	I	6,103	I
RB[1]	LC1	156,691	629	270	94.95	93.94	10	4	I&II[2]	61,140	I&II
	LC2	123,590	391	287	96.46	93.94	7	4	I&II	96,292	I&II
	LC3	97,387	372	220	91.41	93.94	17	4	I&II	50,087	I&II
	LC4	85,266	315	222	97.98	93.94	4	4	I&II	62,054	I&II
	LC5	90,409	333	244	98.99	96.97	2	2	I&II	75,240	I&II
	LC6	25,238	75	46	97.98	95.45	4	3	I&II	18,568	I&II
	LC7	87,173	318	188	94.95	95.45	10	3	I&II	49,556	I&II
	LC8	86,629	289	184	94.44	93.94	11	4	I&II	36,096	I&II
	LC9	106,362	384	256	95.96	93.94	8	4	I&II	72,162	I&II
	LC10	86,519	332	245	94.95	95.45	10	3	I&II	67,547	I&II
	LC11	136,332	469	318	95.96	93.94	8	4	I&II	95,322	I&II
	LC12	130,010	425	258	97.98	95.45	4	3	I&II	92,100	I&II
	LC13	81,177	315	223	97.98	93.94	4	4	I&II	58,680	I&II
	LC14	89,997	322	202	95.45	92.42	9	5	I&II	37,446	I&II
	LC15	104,092	406	271	95.96	93.94	8	4	I&II	71,000	I&II
	WIL1	249,904	898	335	93.94	93.94	12	4	I&II	92,490	I&II
	WIL2	176,931	569	377	96.97	93.94	6	4	I&II	112,436	I&II
	WIL3	154,382	420	304	95.96	93.94	8	4	I&II	122,451	I&II
	WIL4	144,054	408	303	96.46	93.94	7	4	I&II	109,167	I&II
	WIL5	108,169	456	283	94.95	92.42	10	5	I&II	68,656	I&II
	WIL6	112,001	368	275	97.98	95.45	4	3	I&II	86,798	I&II
	WIL7	98,163	398	245	96.97	93.94	6	4	I&II	57,561	I&II
	WIL8	80,615	329	235	95.45	93.94	9	4	I&II	56,399	I&II
	BV1	53,314	212	80	94.44	93.94	11	4	I&II	12,833	I&II
	BV2	78,582	313	141	91.41	90.91	17	6	I&II	25,081	I&II
	BV3	71,659	306	190	95.45	93.94	9	4	I&II	42,812	I&II

[1] MP = movement protein, CP = coat protein, RB = RNA binding protein of grapevine virus A.[2] The Phylogenetic relationship of the phylo-group I and II of the RNA-binding gene cannot be differentiated, named "I&II", see details in Chapter 2. *[II&III] The lowest % nt identities, maximum nt or aa changes calculated using both GVA[II] and GVA[III] variants within the current sample, [II] The lowest % nt identities, maximum nt or aa changes by GVA[II] variants; [III] The lowest % nt identities, maximum nt or aa changes using only GVA[III] variants.

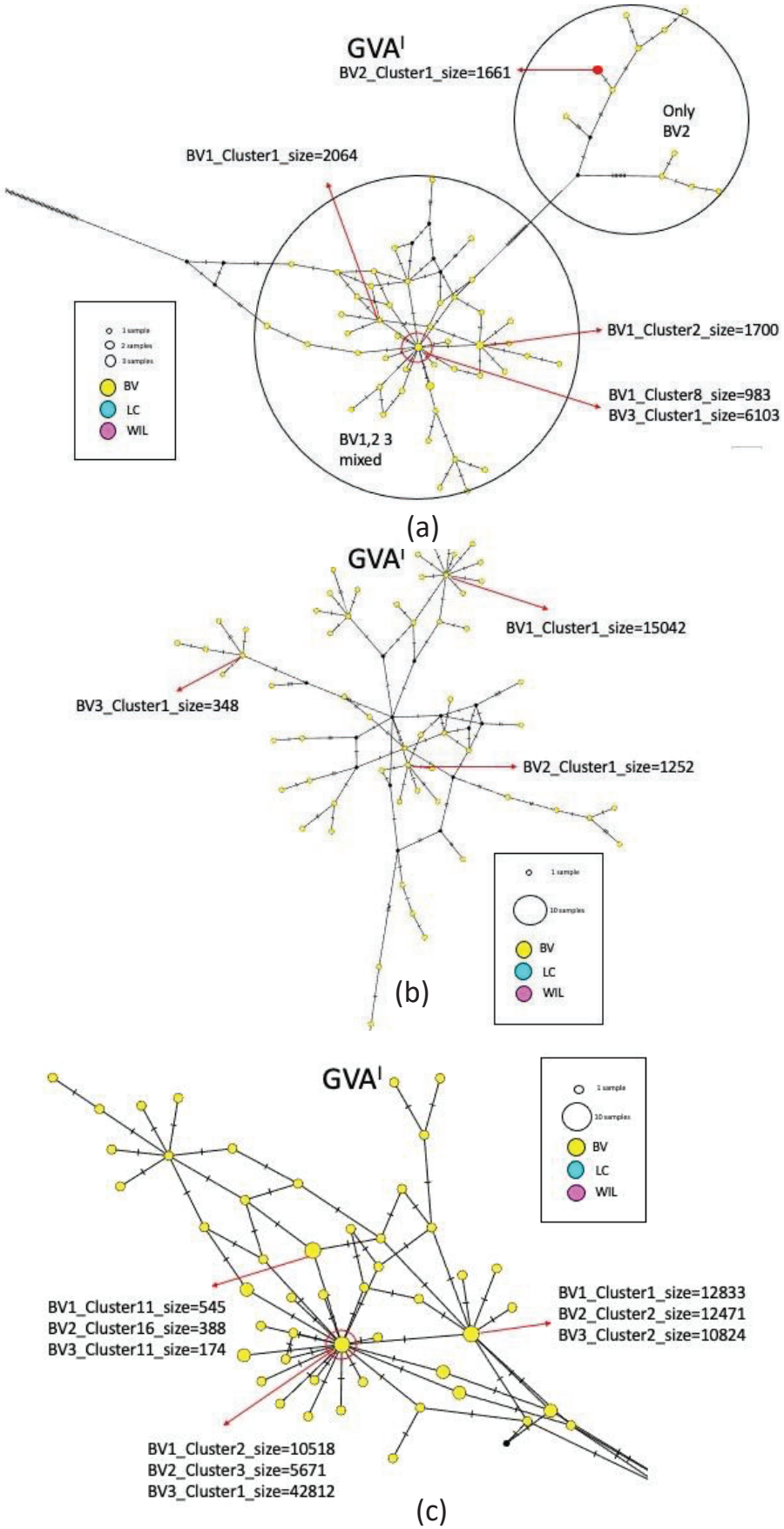

Figure S1. The intra-and inter- host diversity of a total of 23 samples affected by shiraz disease (SD) from Langhorne Creek (LC) and Willunga (WIL), and 3 samples affected by grapevine leafroll disease from Barossa Valley (BV) were analyzed by a phylogenetic median-joining haplotype networks (MJNs) clustering. GVA variants from phylogenetic groups I are labeled as GVAI. Figures (a), (b), and (c) are enlarged MJNs of the coat protein (CP), movement protein (MP) and RNA binding (RB) gene of GVAI variants in Figure 2a, 2b and 2c, respectively.

7. References (Chapter 3)

1. Corbett, M.K.; Wiid, J. Closterovirus-like particles in extracts from diseased grapevines. *Phytopathol. Mediterr.* **1985**, *24*, 91-100.
2. Habili, N.; Scliefert, L. The increasing threat of grapevine virus A and its association with restricted spring growth in Australia. *Aust. N.Z. Grapegrow. Winemak.* **2001**, *452*, 22-26.
3. Habili, N.; Wu, Q.; Pagay, V. Virus-associated Shiraz disease may lead Shiraz to become an endangered variety in Australia. *Wine and Viticulture J.* **2016**, *31*, 47-50.
4. Wu, Q.; Habili, N.; Constable, F.; Al Rwahnih, M.; Goszczynski, D.E.; Wang, Y.; Pagay, V. Virus pathogens in Australian vineyards with an emphasis on Shiraz disease. *Viruses* **2020**, *12*, 818, doi:10.3390/v12080818.
5. Habili, N.; Randles, J.W. Major yield loss in Shiraz vines infected with Australian Shiraz disease associated with grapevine virus A. In Proceedings of the 17th Meeting of the International Council for the Study of Viruses and Virus-like Diseases of the Grapevine, Davis, California, USA, 7–14 October 2012; pp. 164-165.
6. Habili, N.; Randles, J.W. Descriptors for grapevine virus A-associated syndrome in Shiraz, Merlot and Ruby Cabernet in Australia, and its similarity to Shiraz disease in South Africa. *Aust. N.Z. Grapegrow. Winemak.* **2004**, *488*, 71-74.
7. Adams, M.J.; Candresse, T.T.; Hammond, J.; Kreuze, J.F.; Martelli, G.P.; Namba, S.; Pearson, M.N.; Ryu, K.H.; Saldarelli, P.; Yoshikawa, N. Family -Betaflexiviridae. In *Virus Taxonomy: Ninth Report of the International Committee on Taxonomy of Viruses*, King, A.M.Q., Adams, M.J., Carstens, E.B., Lefkowitz, E.J., Eds.; Elsevier: Amsterdam: The Netherlands, 2012; pp. 920–941.
8. Minafra, A.; Saldarelli, P.; Grieco, F.; Martelli, G.P. Nucleotide sequence of the 3' terminal region of the RNA of two filamentous grapevine viruses. *Arch. Virol.* **1994**, *137*, 249-261.
9. Minafra, A.; Saldarelli, P.; Martelli, G.P. Grapevine virus A: nucleotide sequence, genome organization, and relationship in the Trichovirus genus. *Arch. Virol.* **1997**, *142*, 417-423.
10. Zhou, Z.S.; Dell'Orco, M.; Turturo, P.; Martelli, C.; Saldarelli, A.; Minafra, G.P.; Turturo, G.P. Identification of an RNA-silencing suppressor in the genome of grapevine virus A. *J. Gen. Virol.* **2006**, *87*, 2387-2395, doi:10.1099/vir.0.81893-0.
11. Galiakparov, N.; Tanne, E.; Mawassi, M.; Gafny, R.; Sela, I. ORF 5 of grapevine virus A encodes a nucleic acid-binding protein and affects pathogenesis. *Virus Genes* **2003**, *27*, 257-262, doi:10.1023/a:1026395815980.
12. Haviv, S.; Iddan, Y.; Goszczynski, D.E.; Mawassi, M. The ORF5 of grapevine virus A is involved in symptoms expression in Nicotiana benthamiana plants. *Ann. Appl. Biol.* **2012**, *160*, 181-190, doi:10.1111/j.1744-7348.2012.00531.x.
13. Goszczynski, D.E.; Du Preez, J.; Burger, J.T. Molecular divergence of grapevine virus A (GVA) variants associated with Shiraz disease in South Africa. *Virus Res.* **2008**, *138*, 105-110, doi:10.1016/j.virusres.2008.08.014.
14. Goszczynski, D.E.; Jooste, A.E.C. Identification of divergent variants of grapevine virus A. *Eur. J. Plant Pathol.* **2003**, *109*, 397-403, doi:10.1023/a:1023555018700.
15. Simon-Loriere, E.; Holmes, E.C. Why do RNA viruses recombine? *Nat. Rev. Microbiol.* **2011**, *9*, 617-626, doi:10.1038/nrmicro2614.
16. McDonald, S.M.; Nelson, M.I.; Turner, P.E.; Patton, J.T. Reassortment in segmented RNA viruses: mechanisms and outcomes. *Nat. Rev. Microbiol.* **2016**, *14*, 448-460, doi:10.1038/nrmicro.2016.46.
17. García-Arenal, F.; Fraile, A.; Malpica, J.M. Variability and genetic structure of plant virus populations. *Annu. Rev. Phytopathol.* **2001**, *39*, 157.

18. Harrison, B.D. Virus variation in relation to resistance-breaking in plants. *Euphytica* **2002**, *124*, 181-192.
19. Domingo, E. Quasispecies and the implications for virus persistence and escape. *Clin. Diagn. Virol.* **1998**, *10*, 97-101.
20. Elena, S.F.; Sanjuán, R. Adaptive value of high mutation rates of RNA viruses: separating causes from consequences. *J. Virol.* **2005**, *79*, 11555-11558.
21. Duffy, S. Why are RNA virus mutation rates so damn high? *PLoS Biol.* **2018**, *16*, e3000003, doi:10.1371/journal.pbio.3000003
22. Loewe, L.; Hill, W.G. The population genetics of mutations: good, bad and indifferent. *Phil. Trans. R. Soc. B* **2010**, *365*, 1153-1167, doi:10.1098/rstb.2009.0317.
23. Montoya, V.; Olmstead, A.; Tang, P.; Cook, D.; Janjua, N.; Grebely, J.; Jacka, B.; Poon, A.F.Y.; Krajden, M. Deep sequencing increases hepatitis C virus phylogenetic cluster detection compared to Sanger sequencing. *Infection, Genetics and Evolution* **2016**, *43*, 329-337, doi:10.1016/j.meegid.2016.06.015.
24. Liang, B.; Luo, M.; Scott-Herridge, J.; Semeniuk, C.; Mendoza, M.; Capina, R.; Sheardown, B.; Ji, H.; Kimani, J.; Ball, B.T. A comparison of parallel pyrosequencing and sanger clone-based sequencing and its impact on the characterization of the genetic diversity of HIV-1. *PLoS One* **2011**, *6*, e26745, doi:10.1371/journal.pone.0026745.
25. Telele, N.F.; Kalu, A.W.; Gebre-Selassie, S.; Fekade, D.; Abdurahman, S.; Marrone, G.; Neogi, U.; Tegbaru, B.; Sönnerborg, A. Pretreatment drug resistance in a large countrywide Ethiopian HIV-1C cohort: a comparison of Sanger and high-throughput sequencing. *Sci. Rep.* **2018**, *8*, 7556, doi:10.1038/s41598-018-25888-6.
26. Mohamed, S.; Penaranda, G.; Gonzalez, D.; Camus, C.; Khiri, H.; Boulmé, R.; Sayada, C.; Philibert, P.; Olive, D.; Halfon, P. Comparison of ultra-deep versus Sanger sequencing detection of minority mutations on the HIV-1 drug resistance interpretations after virological failure. *AIDS* **2014**, *28*, 1315-1324, doi:10.1097/QAD.0000000000000267.
27. Arias, A.; López, P.; Sánchez, R.; Yamamura, Y.; Rivera-Amill, V. Sanger and next generation sequencing approaches to evaluate HIV-1 virus in blood compartments. *Int. J. Environ. Res. Public Health* **2018**, *15*, 1697, doi:10.3390/ijerph15081697.
28. Knyazev, S.; Hughes, L.; Skums, P.; Zelikovsky, A. Epidemiological data analysis of viral quasispecies in the next-generation sequencing era. *Brief. Bioinform.* **2021**, *22*, 96-108, doi:10.1093/bib/bbaa101.
29. Harvala, H.; Wiman, Å.; Wallensten, A.; Zakikhany, K.; Englund, H.; Brytting, M. Role of sequencing the measles virus hemagglutinin gene and hypervariable region in the measles outbreak investigations in Sweden during 2013–2014. *J. Infect. Dis.* **2016**, *213*, 592-599.
30. Harismendy, O.; Ng, P.C.; Strausberg, R.L.; Wang, X.; Stockwell, T.B.; Beeson, K.Y.; Schork, N.J.; Murray, S.S.; Topol, E.J.; Levy, S. Evaluation of next generation sequencing platforms for population targeted sequencing studies. *Genome Biol.* **2009**, *10*, R32, doi:10.1186/gb-2009-10-3-r32.
31. Han, S.-W.; Kim, H.-P.; Shin, J.-Y.; Jeong, E.-G.; Lee, W.-C.; Lee, K.-H.; Won, J.-K.; Kim, T.-Y.; Oh, D.-Y.; Im, S.-A. Targeted sequencing of cancer-related genes in colorectal cancer using next-generation sequencing. *PLoS One* **2013**, *8*, e64271, doi:10.1371/journal.pone.0064271.
32. Ding, D.; Lou, X.; Hua, D.; Yu, W.; Li, L.; Wang, J.; Gao, F.; Zhao, N.; Ren, G.; Li, L. Recurrent targeted genes of hepatitis B virus in the liver cancer genomes identified by a next-generation sequencing–based approach. *PLoS Genet.* **2012**, *8*, e1003065.

33. Guerrero-Preston, R.; Godoy-Vitorino, F.; Jedlicka, A.; Rodríguez-Hilario, A.; González, H.; Bondy, J.; Lawson, F.; Folawiyo, O.; Michailidi, C.; Dziedzic, A. 16S rRNA amplicon sequencing identifies microbiota associated with oral cancer, human papilloma virus infection and surgical treatment. *Oncotarget* **2016**, *7*, 51320, doi:10.18632/oncotarget.9710.
34. Hugerth, L.W.; Andersson, A.F. Analysing microbial community composition through amplicon sequencing: from sampling to hypothesis testing. *Front. Microbiol.* **2017**, *8*, 1561, doi:10.3389/fmicb.2017.01561.
35. Schöler, A.; Jacquiod, S.; Vestergaard, G.; Schulz, S.; Schloter, M. Analysis of soil microbial communities based on amplicon sequencing of marker genes. *Biol. Fertil. Soils* **2017**, *53*, 485-489, doi:10.1007/s00374-017-1205-1.
36. Hata, A.; Kitajima, M.; Haramoto, E.; Lee, S.; Ihara, M.; Gerba, C.P.; Tanaka, H. Next-generation amplicon sequencing identifies genetically diverse human astroviruses, including recombinant strains, in environmental waters. *Sci. Rep.* **2018**, *8*, 1-9.
37. Taylor, D.L.; Walters, W.A.; Lennon, N.J.; Bochicchio, J.; Krohn, A.; Caporaso, J.G.; Pennanen, T. Accurate estimation of fungal diversity and abundance through improved lineage-specific primers optimized for Illumina amplicon sequencing. *Appl. Environ. Microbiol.* **2016**, *82*, 7217-7226, doi:10.1128/AEM.02576-16.
38. De Filippis, F.; Laiola, M.; Blaiotta, G.; Ercolini, D. Different amplicon targets for sequencing-based studies of fungal diversity. *Appl. Environ. Microbiol.* **2017**, *83*, e00905-00917, doi:10.1128/AEM.00905-17.
39. Ranjan, R.; Rani, A.; Metwally, A.; McGee, H.S.; Perkins, D.L. Analysis of the microbiome: Advantages of whole genome shotgun versus 16S amplicon sequencing. *Biochem. Biophys. Res. Commun.* **2016**, *469*, 967-977, doi:10.1016/j.bbrc.2015.12.083.
40. Kuczynski, J.; Lauber, C.L.; Walters, W.A.; Parfrey, L.W.; Clemente, J.C.; Gevers, D.; Knight, R. Experimental and analytical tools for studying the human microbiome. *Nat. Rev. Genet.* **2012**, *13*, 47-58.
41. Sabrià, A.; Pintó, R.M.; Bosch, A.; Quer, J.; Garcia-Cehic, D.; Gregori, J.; Dominguez, A.; Carol, M.; Sala-Farré, M.-R.; Guix, S. Characterization of intra-and inter-host norovirus P2 genetic variability in linked individuals by amplicon sequencing. *PLoS One* **2018**, *13*, e0201850, doi:10.1371/journal.pone.0209714.
42. Piry, S.; Wipf-Scheibel, C.; Martin, J.-F.; Galan, M.; Berthier, K. High throughput amplicon sequencing to assess within-and between-host genetic diversity in plant viruses. *bioRxiv* **2017**, 168773, doi:10.1101/168773.
43. Kinoti, W.M.; Constable, F.E.; Nancarrow, N.; Plummer, K.M.; Rodoni, B. Generic amplicon deep sequencing to determine Ilarvirus species diversity in Australian Prunus. *Front. Microbiol.* **2017**, *8*, doi:10.3389/fmicb.2017.01219.
44. Kinoti, W.M.; Constable, F.E.; Nancarrow, N.; Plummer, K.M.; Rodoni, B. Analysis of intra-host genetic diversity of Prunus necrotic ringspot virus (PNRSV) using amplicon next generation sequencing. *PLoS One* **2017**, *12*, e0179284, doi:10.1371journal.pone.0179284.
45. Kinoti, W.M.; Constable, F.E.; Nancarrow, N.; Plummer, K.M.; Rodoni, B. The incidence and genetic diversity of apple mosaic virus (ApMV) and prune dwarf virus (PDV) in Prunus species in Australia. *Viruses* **2018**, *10*, 136, doi:10.3390/v10030136.
46. Maina, S.; Zheng, L.; Rodoni, B.C. Targeted genome sequencing (TG-Seq) approaches to detect plant viruses. *Viruses* **2021**, *13*, 583, doi:10.3390/v13040583.
47. Bandelt, H.-J.; Forster, P.; Röhl, A. Median-joining networks for inferring intraspecific phylogenies. *Mol. Biol. Evol.* **1999**, *16*, 37-48.

48. Ramachandran, S.; Campo, D.S.; Dimitrova, Z.E.; Xia, G.-l.; Purdy, M.A.; Khudyakov, Y.E. Temporal variations in the hepatitis C virus intrahost population during chronic infection. *J. Virol.* **2011**, *85*, 6369-6380, doi:10.1128/JVI.02204-10.

49. Lee, D.-H.; Torchetti, M.K.; Killian, M.L.; Berhane, Y.; Swayne, D.E. Highly pathogenic avian influenza A (H7N9) virus, Tennessee, USA, March 2017. *Emerging Infect. Dis.* **2017**, *23*, 1860-1863, doi:10.3201/eid2311.171013.

50. Beerens, N.; Heutink, R.; Bergervoet, S.A.; Harders, F.; Bossers, A.; Koch, G. Multiple reassorted viruses as cause of highly pathogenic avian influenza A (H5N8) virus epidemic, the Netherlands, 2016. *Emerging Infect. Dis.* **2017**, *23*, 1974-1981, doi:10.3201/eid2312.171062.

51. Lundström, J.O.; Hesson, J.C.; Schäfer, M.L.; Östman, Ö.; Semmler, T.; Bekaert, M.; Weidmann, M.; Lundkvist, Å.; Pfeffer, M. Sindbis virus polyarthritis outbreak signalled by virus prevalence in the mosquito vectors. *PLoS Negl. Trop. Dis.* **2019**, *13*, e0007702, doi:10.1371/journal.pntd.0007702.

52. Saitou, N.; Nei, M. The neighbor-joining method: a new method for reconstructing phylogenetic trees. *Mol. Biol. Evol.* **1987**, *4*, 406-425.

53. Mihaescu, R.; Levy, D.; Pachter, L. Why neighbor-joining works. *Algorithmica* **2009**, *54*, 1-24, doi:10.1007/s00453-007-9116-4.

54. MacKenzie, D.J.; McLean, M.A.; Mukerji, S.; Green, M. Improved RNA extraction from woody plants for the detection of viral pathogens by reverse transcription-polymerase chain reaction. *Plant Dis.* **1997**, *81*, 222-226.

55. Schubert, M.; Lindgreen, S.; Orlando, L. AdapterRemoval v2: rapid adapter trimming, identification, and read merging. *BMC Res. Notes* **2016**, *9*, 1-7, doi:10.1186/s13104-016-1900-2.

56. Bushnell, B. *BBMap: a fast, accurate, splice-aware aligner*; LBNL Report LBNL-7065E; Lawrence Berkeley National Lab (LBNL), Berkeley, california, USA: 2014.

57. Altschul, S.F.; Madden, T.L.; Schäffer, A.A.; Zhang, J.; Zhang, Z.; Miller, W.; Lipman, D.J. Gapped BLAST and PSI-BLAST: a new generation of protein database search programs. *Nucleic Acids Res.* **1997**, *25*, 3389-3402.

58. Martin, M. Cutadapt removes adapter sequences from high-throughput sequencing reads. *EMBnet. J.* **2011**, *17*, 10-12.

59. Edgar, R.C. Search and clustering orders of magnitude faster than BLAST. *Bioinformatics* **2010**, *26*, 2460-2461, doi:10.1093/bioinformatics/btq461.

60. Kumar, S.; Stecher, G.; Tamura, K. MEGA7: molecular evolutionary genetics analysis version 7.0 for bigger datasets. *Mol. Biol. Evol.* **2016**, *33*, 1870-1874, doi:10.1093/molbev/msw054.

61. Muhire, B.M.; Varsani, A.; Martin, D.P. SDT: a virus classification tool based on pairwise sequence alignment and identity calculation. *PLoS One* **2014**, *9*, e108277, doi:10.1371/journal.pone.0108277.

62. Jridi, C.; Martin, J.-F.; Marie-Jeanne, V.; Labonne, G.; Blanc, S. Distinct viral populations differentiate and evolve independently in a single perennial host plant. *J. Virol.* **2006**, *80*, 2349-2357, doi:10.1128/JVI.80.5.2349–2357.2006.

63. Tamukong, Y.B.; Collum, T.D.; Stone, A.L.; Kappagantu, M.; Sherman, D.J.; Rogers, E.E.; Dardick, C.; Culver, J.N. Dynamic changes impact the plum pox virus population structure during leaf and bud development. *Virology* **2020**, *548*, 192-199, doi:10.1016/j.virol.2020.06.014.

64. Kearney, C.M.; Thomson, M.J.; Roland, K.E. Genome evolution of tobacco mosaic virus populations during long-term passaging in a diverse range of hosts. *Arch. Virol.* **1999**, *144*, 1513-1526.

65. Arthur, K.; Collins, N.C.; Randles, J.W. Mutation rate in Velvet tobacco mottle virus varies between genomic region and virus variant but is not influenced by obligatory mirid transmission. *Virus Genes* **2012**, *45*, 575-580.
66. Little, A.; Fazeli, C.F.; Rezaian, M.A. Hypervariable genes in grapevine leafroll associated virus 1. *Virus Res.* **2001**, *80*, 109-116.
67. Drake, J.W.; Holland, J.J. Mutation rates among RNA viruses. *Proc. Natl. Acad. Sci.* **1999**, *96*, 13910-13913, doi:10.1073/pnas.96.24.13910.
68. da Silva, W.; Kutnjak, D.; Xu, Y.; Xu, Y.; Giovannoni, J.; Elena, S.F.; Gray, S. Transmission modes affect the population structure of potato virus Y in potato. *PLoS Pathog.* **2020**, *16*, e1008608, doi:10.1371/journal.ppat.1008608.
69. Garcia, D.; Garcia, S.; Voinnet, O. Nonsense-mediated decay serves as a general viral restriction mechanism in plants. *Cell Host Microbe* **2014**, *16*, 391-402, doi:10.1016/j.chom.2014.08.001.
70. Nyikó, T.; Kerenyi, F.; Szabadkai, L.; Benkovics, A.H.; Major, P.; Sonkoly, B.; Merai, Z.; Barta, E.; Niemiec, E.; Kufel, J. Plant nonsense-mediated mRNA decay is controlled by different autoregulatory circuits and can be induced by an EJC-like complex. *Nucleic Acids Res.* **2013**, *41*, 6715-6728, doi:10.1093/nar/gkt366.
71. Yang, G.; Qiu, B.S.; Liu, X.G.; Li, Y.; Wang, X.F. Nonsense mutations of replicase and movement protein genes contribute to the attenuation of an avirulent tomato mosaic virus. *Virus Res.* **2002**, *87*, 119-128.
72. Pereira, F. SARS-CoV-2 variants combining spike mutations and the absence of ORF8 may be more transmissible and require close monitoring. *Biochem. Biophys. Res. Commun.* **2021**, *550*, 8-14, doi:10.1016/j.bbrc.2021.02.080.
73. Lefeuvre, P.; Martin, D.P.; Elena, S.F.; Shepherd, D.N.; Roumagnac, P.; Varsani, A. Evolution and ecology of plant viruses. *Nat. Rev. Microbiol.* **2019**, *17*, 632-644, doi:10.1038/ s41579-019-0232-3.
74. Mauck, K.E. Variation in virus effects on host plant phenotypes and insect vector behavior: what can it teach us about virus evolution? *Curr. Opin. Virol.* **2016**, *21*, 114-123, doi:10.1016/j.coviro.2016.09.002.
75. McCrone, J.T.; Lauring, A.S. Genetic bottlenecks in intraspecies virus transmission. *Curr. Opin. Virol.* **2018**, *28*, 20-25, doi:10.1016/j.coviro.2017.10.008.
76. Roossinck, M.J. Symbiosis versus competition in plant virus evolution. *Nat. Rev. Microbiol.* **2005**, *3*, 917-924, doi:10.1038/nrmicro1285.
77. Callaway, E. Beyond Omicron: what's next for COVID's viral evolution. *Nature* **2021**, *600*, 204-207.
78. Rosciglione, B.; Castellano, M.A.; Martelli, G.P.; Savino, V.; Cannizzaro, G. Mealybug transmission of grapevine virus A. *Vitis* **1983**, *22*, 331-347.
79. Hommay, G.; Komar, V.; Lemaire, O.; Herrbach, E. Grapevine virus A transmission by larvae of Parthenolecanium corni. *Eur. J. Plant Pathol.* **2008**, *121*, 185-188, doi:10.1007/s10658-007-9244-3.
80. Bertin, S.; Cavalieri, V.; Gribaudo, I.; Sacco, D.; Marzachì, C.; Bosco, D. Transmission of grapevine virus A and grapevine leafroll-associated virus 1 and 3 by Heliococcus bohemicus (Hemiptera: Pseudococcidae) nymphs from plants with mixed infection. *J. Econ. Entomol.* **2016**, *109*, 1504-1511, doi:10.1093/jee/tow120.
81. Tsai, C.-W.; Chau, J.; Fernandez, L.; Bosco, D.; Daane, K.; Almeida, R. Transmission of grapevine leafroll-associated virus 3 by the vine mealybug (Planococcus ficus). *Phytopathology* **2008**, *98*, 1093-1098, doi:10.1094 / PHYTO-98-10-1093.
82. Le Maguet, J.; Beuve, M.; Herrbach, E.; Lemaire, O. Transmission of six ampeloviruses and two vitiviruses to grapevine by Phenacoccus aceris. *Phytopathology* **2012**, *102*, 717-723, doi:10.1094 / PHYTO-10-11-0289.

83. Petersen, C.L.; Charles, J.G. Transmission of grapevine leafroll - associated closteroviruses by Pseudococcus longispinus and P. calceolariae. *Plant Pathol.* **1997**, *46*, 509-515.
84. Barrass, I.C.; Jerie, P.; Ward, S.A. Aerial dispersal of first-and second-instar longtailed mealybug, Pseudococcus longispinus (Targioni Tozzetti)(Pseudococcidae: Hemiptera). *Aust. J. Exp. Agric.* **1994**, *34*, 1205-1208.
85. Grasswitz, T.R.; James, D.G. Movement of grape mealybug, Pseudococcus maritimus, on and between host plants. *Entomol. Exp. Appl.* **2008**, *129*, 268-275, doi:10.1111/j.1570-7458.2008.00786.x.
86. Charleston, K.; Addison, S.; Miles, M.; Maas, S. The Solenopsis mealybug outbreak in Emerald. *Aust. Cottongrower* **2010**, *31*, 18-22.
87. Forrester, N.L.; Guerbois, M.; Seymour, R.L.; Spratt, H.; Weaver, S.C. Vector-borne transmission imposes a severe bottleneck on an RNA virus population. *PLoS Pathog.* **2012**, *8*, e1002897, doi:10.1371/journal.ppat.1002897.
88. Moury, B.; Fabre, F.; Senoussi, R. Estimation of the number of virus particles transmitted by an insect vector. *Proc. Natl. Acad. Sci.* **2007**, *104*, 17891-17896, doi:10.1073/pnas.0702739104.
89. Player, R.; Verratti, K.; Staab, A.; Bradburne, C.; Grady, S.; Goodwin, B.; Sozhamannan, S. Comparison of the performance of an amplicon sequencing assay based on Oxford Nanopore technology to real-time PCR assays for detecting bacterial biodefense pathogens. *BMC Genomics* **2020**, *21*, 1-21, doi:10.1186/s12864-020-6557-5.
90. Beerenwinkel, N.; Günthard, H.F.; Roth, V.; Metzner, K.J. Challenges and opportunities in estimating viral genetic diversity from next-generation sequencing data. *Front. Microbiol.* **2012**, *3*, 329, doi:10.3389/fmicb.2012.00329.
91. MacKenzie, D.J. A standard protocol for the detection of viruses and viroids using a reverse transcription-polymerase chain reaction technique. *Document CPHBT-RT PCR1. 00. The Canadian Food Inspection Agency* **1997**.

Chapter 4: Comparison of Physiology Performance and Berry Development of Shiraz Disease (SD), Leafroll Disease (LRD) and Asymptomatic (ASY) Grapevines

1. Introduction

Currently, there is very little understanding on the mechanisms of how grapevine viruses affect grapevine physiological performance. Various impacts of viruses have been reported including: changes to primary and secondary metabolism [1,2], modulation of flavonoids [3], overexpression of the gibberellic acid response pathway [4], altered carbohydrate homeostasis and cell wall composition [5], changes in gene expression [6], and reduced resistance to other pathogens by modulating genes associated with defense responses [7,8].

Numerous studies have measured the effect of viruses, including grapevine leafroll-associated virus 1 (GLRaV-1), grapevine leafroll-associated virus 3 (GLRaV-3), grapevine fanleaf virus (GFLV), grapevine fleck virus (GFkV) and grapevine red blotch virus (GRBV) on various aspects of grapevine physiology [5,9-24]. The impact of virus infection to various grapevine varieties were summarized in Chapter 1, including vegetative vigor, yield, photosynthesis, water potential of a grapevine, total soluble solids (TSS), titratable acidity (TA), anthocyanins, and tannins in berry and juice, anthocyanin and alcohol, colour density in wine (Chapter 1, Table 1). Some studies have evaluated the impact of grapevine virus A (GVA) mixed infected with either GLRaV-1 or GLRaV-3 in cv. Nebbiolo, which displayed typical leafroll disease symptoms (LRD) [9,12]. However, the physiological performance of Shiraz disease (SD) affected grapevines has not been measured in cv. Shiraz. Therefore, the aim of the research presented in this chapter was to examine the physiological effects of this disease on the most common Australian variety, Shiraz, under local climatic conditions, to identify the most sensitive physiological indicators that could be used to monitor this disease in the future.

2. Materials and Methods

2.1. Field trials and experimental approach

Shiraz grapevines for physiology performance were selected from the Willunga (WIL) (- 35° 15' 58.5468" S and 138° 29' 39.7464" E) and Langhorne Creek (LC) (- 35° 18' 50.8752" S, 139° 7' 30.9036" E) sites based on different symptom types described in Chapter 2. Shiraz clone BVRC12 has been established since 2004 in both of these two vineyards. The Shiraz grapevines at WIL are own-rooted. Shiraz grapevines at LC were grafted onto Chardonnay in 2015. The soil types of WIL and LC are black cracking clay and alluvial sandy loam, respectively. Grapevines from these two vineyards were regularly irrigated and managed by individual growers. Each SD or LRD grapevine was paired with an asymptomatic control grapevine (ASY) in the neighboring row. The virus status of each grapevine was determined by RT-PCR and metagenomics high-throughput sequencing (Meta-HTS) methods previously described [25]. Major viruses, grapevine virus A (GVA) and grapevine leafroll-associated virus 3 (GLRaV-3) in each grapevine can be found in Table S1. The basic descriptive information of each site and the comprehensive virus profile of each grapevine can be found in Tables S4 and S5 of Chapter 2. Decline and dead arms symptoms were first noticed in 2019-2020 season at WIL. As part of the measurement of health at WIL, the grapevines were also assessed for the presence of decline and dead arms symptoms that may be attributed to grapevine trunk diseases (GTDs). No further diagnostic test was done to confirm the presence of GTDs at both sites. The assumption of GTD presence at WIL are based on the symptom observation of vine decline and dead arms symptoms.

Physiological data were collected in three southern hemisphere growing seasons (Oct-Feb) during 2018-19, 2019-20, 2020-21 at the WIL site. Since the SD grapevines at the LC site were removed to prevent virus spread, data were collected only for one growing season (2018-19).

Rainfall and temperature data of the three growing seasons was gathered from the Noarlunga station (South Australia) from the Australian Government Bureau of Meteorology website (BoM; http://www.bom.gov.au/climate/data/), which was the closest weather station to both sites. The WIL site and LC site are approximately 16 km and 60 km away from the weather station, respectively. The mean January temperature, monthly mean growing season temperature (October-April), total rainfall, and growing degree days for the growing season (October-April) for each growing season are listed in Table 1.

Table 1. Mean January temperature, monthly mean growing season temperature, total rainfall, and growing degree days (GDD) of the growing season 2018-19, 2019-20 and 2020-21. Data were gathered from the Noarlunga station (South Australia) (http://www.bom.gov.au/climate/data/).

Climate conditions	2018-19	2019-20	2020-21
Mean January temperature (°C)[1]	24.9	22.25	22.25
Monthly mean growing season temperature (°C)[2]	20.86	19.79	19.81
Total growing season rainfall (mm)[3]	70.80	199.80	166.80

Growing degree days (GDD)[4]	2302.45	2089.20	2075.60

[1] Mean January temperature of 2019, 2020, and 2021were used for the 2018-2019, 2019-2020 and 2020-21 seasons. [2] Monthly mean growing season temperature of October to April of each growing season. [3] Total rainfall of the growing season from October to April. [4] Growing degree days = $[(T_{min}+T_{max})/2] - 10$ [26].

2.2. Vine health scores (VHS)

In addition to SD, decline and dead arm symptoms were recorded at WIL in 2019-20 and 2021-22, in SD affected grapevines. Similar symptoms were also observed in LRD or ASY grapevines at WIL, but not in SD and ASY affected grapevines at LC. To scientifically assess the effects of dead arms that may also affect canopy development apart from virus infection, the VHS system was engaged, in which the growth of shoots was assessed to provide an overall health pattern for this site.

Grapevines were double cordoned at WIL (four arms per vine) and each arm was scored. A completely healthy arm earnt a score of 2 (Figure 1a), a weaker arm gained a score of 1 (Figure 1b) and a completely dead arm received a score of 0 (Figure 1c). Therefore, each grapevine was given a total VHS ranging from 0 (all arms dead) to 8 (all arms healthy). VHS of each grapevine was assessed at E-L stage 27 (berry setting) in 2020 at WIL. The grapevines from LC site were removed after 2018-19 season, therefore, no VHS score was measured.

In this study the vine decline and dead arm symptoms that were used to measure VHS were assumed to be part of GTDs caused by fungal pathogens. This assessment was made on the basis of symptomology consistent with GTD. No further diagnostic test was done on fungal pathogens to determine the species of GTD.

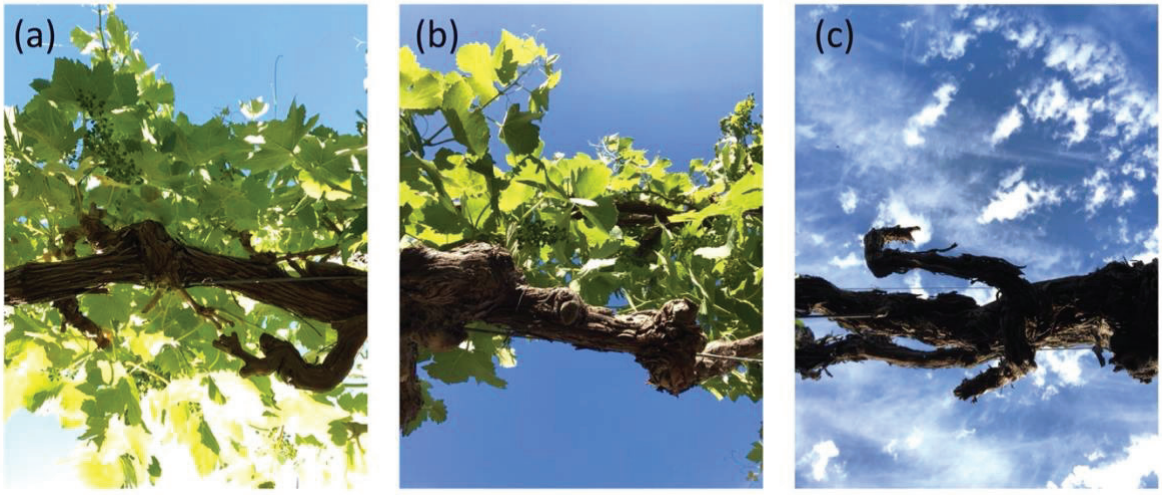

Figure 1. Vine health score (VHS) system at Willunga (WIL). (a) HVS = 2, a completely healthy arm (b) HVS = 1, a weaker arm (c) HVS = 0, a dead arm at the time when VHS score was assessed at E-L stage 27 (berry setting) in 2020 at WIL.

2.3. Plant area index (PAI) by Viticanopy

Plant area index (PAI) was defined as "area of leaves and woody materials per unit ground area" [27], which is one of the most important parameters used to assess grapevine canopy vigor. PAI in this study was calculated using the sum of leaves as well as any additional tissue visible in the images (shoots, fruits, berries) against canopy porosity and

corrected by clumping index [28]. PAI closely corresponds to the leaf area index (LAI) (https://viticanopy.com.au/faq). Selected grapevines were photographed from E-L stage 9 (2 to 3 leaves separated) until about E-L 35 (veraison) at both sites. The front camera of a smartphone was placed at the bottom of one side of the canopy approx. 15 cm above the ground (right above irrigation line) and about 30 cm away from the trunk to take an upward-looking image of the canopy. Each selected grapevine was photographed from both sides of the trunk along the row every two weeks, 8 times in total in the 2018-19 and 2020-21 seasons, and monthly at the WIL site for the 2019-20 season. Additional grapevines were selected from the Willunga site (WIL31 to WIL 81) for the 2020-21 season due to the removal of SD grapevines at the LC site. The PAI values were analysed within symptom type groups and plotted as timewise canopy development curves using GraphPad Prism 9 (v. 9.3.1).

2.4. Measurements of stomatal conductance and leaf chlorophyll

Stomatal conductance (g_s) and leaf chlorophyll (Chl) were measured about 60 days post-flowering between 11 am and 3 pm, at both sites in the 2018-19 season. Chl and g_s were measured using a SPAD leaf Chl meter and an AP4 type porometer (Delta-T Devices Ltd), respectively on sunlit leaves. The temperature and humidity of the porometer were calibrated to match the temperature and humidity on site prior to measurements according to manufacturer's instructions and re-calibrated when ambient temperature changed more than 2C° and humidity changed more than 5% relative humidity. The humidity range set in the instrument was taken as close as possible to ambient. Stomatal conductance and Chl were measured at approx. 50 days post-flowering at WIL in the 2020-21 season. Measurement of Chl was repeated once at 100 days post-flowering later in the 2020-21 season at WIL. Table 3 show the number of selected grapevines in each group measured. For all the parameters listed above, three to four leaves were measured for each of the grapevines.

2.5. Leaf photosynthesis parameters

An infrared gas analyser (IRGA) (LCpro-SD Portable Photosynthesis System, ADC BioScientific, Hoddeson, England) was used to measure key leaf photosynthesis parameters such as transpiration rate *(E)*, stomatal conductance (g_s), and net assimilation rate (*A*) about 50 days after flowering at WIL in the 2020-21 season. Since each *A* value has a corresponding *E* and g_s values, data of each leaf were analysed individually for all photosynthesis parameters.

2.6. Leaf and stem water potential

Leaf and stem water potential (ψ_{leaf} and ψ_{stem}) were measured about 100 days post-bloom in the 2020-21 season. They were measured using a pressure chamber (PMS Instrument Company, model 1005, Albany, OR, USA) [29]. Since a limited number of grapevines can be measured within the period of 11 am to 3 pm, one leaf was measured for either ψ_{stem} or ψ_{leaf} per grapevine. ψ_{leaf} was measured by cutting a fully expanded leaf from the petiole with a razor blade and sealing it into the pressure chamber immediately. The ψ_{leaf} was recorded as the negative of the pressure (MPa) required to make water just appear on the cut surface of the petiole [30]. For ψ_{stem} measurements, the leave on the same shoot below the one used to measure ψ_{leaf} was covered with a reflective bag 30 minutes prior to

measurement. The ψ_{stem} measurement was preformed immediately after the ψ_{leaf} measurement using the same procedure described above.

2.7. Trunk and cane carbohydrates

SD, LRD, and the paired ASY grapevines were sampled at E-L 42 right before leaf-fall on the 6th of May 2021. Trunk shavings were collected using an electric drill with a 5 mm diameter drill bit from approx. 40 cm above the ground. Two canes were sampled for each grapevine from the third node. Samples were sealed in a paper envelope and submerged into liquid nitrogen (LN2) immediately after being harvested and stored in LN2 until they could be freeze-dried in the laboratory. Envelopes with canes and trunk shaves were freeze-dried for at least 24 hours. Freeze-dried samples were ground into fine powder in a pulverising Mill (Essa®). Soluble carbohydrates and insoluble starch were extracted from five to six mg of freeze-dried tissue using the starch and anthrone assays which were previously described [31]. The concentration of extracted carbohydrates was measured by the absorbance of 505 nm and 600 nm for the starch assay and anthrone assay, respectively, by a plate reader (SPECTRO star® Nano). The final sugar concentrations were calculated against a glucose or fructose standard curve.

2.8. Fresh berry mass(FBM), total soluble solids (TSS) and juice pH

To monitor fresh berry mass (FBM), sugar accumulation and juice pH during berry ripening, berries were sampled every 7 to 10 days from E-L33 (Berries still hard and green) to E-L38 (harvest). Three berries from the top, middle and bottom part of each bunch and a total of 3 to 7 bunches were sampled from each selected grapevine. FBM was measured and recorded. The berries harvested from each grapevine were pooled and crushed in a plastic bag. Juice pH was measured by a pH meter and TSS were measured by a refractometer (Palette PR-101, Atago co., LTD.).

2.9. Statistical tests

Since standard deviations (SDevs) and sample sizes (n) are significantly different between the treatment groups for most of the physiology parameters, Welch's analysis of variance (ANOVA) was used for overall statistical analysis. The statistical power of Welch's F-test is less affected by unequal sample size and variations compared to ordinary ANOVA [32]. The pairwise comparison (post-hoc test) of each two groups was analysed using Dunnett's T3 multiple comparisons test to compare the significance of the mean between groups when there was unequal variance between each group [33]. When comparing only two groups, the unpaired T-test was applied. GraphPad Prism 9 (v. 9.3.1) was used to perform all statistical tests and for graphical presentation. As the overall data set of leaf photosynthesis parameters *A*, *E* and g_s roughly fit a normal distribution determined by the QQ plot and an equal sample size in each group (4 grapevines per group and 2 measurements per vine), the ordinary ANOVA test was performed to determine significance between means in all groups and Tukey's multiple comparison test was implemented to compare means of each two groups. The statistical tests used for each growth parameters can be found in Table 3.

2.9.1. Significance of linear regression

The "nonlin fit" function of Prism 9 was used to conduct analysis on each slope to study the correlation between PAI and VHS in Figure 5. The null hypothesis was set to 0, which means no correlation between the two factors. The results are provided in Table S4 along with the P and R-squared values for each slope while they were compared to the null hypothesis. A slope with $P \geq 0.05$ rejects the hypothesis of no correlation whereas a slope with $P < 0.05$ accept the hypothesis. Prism 9's "simple linear regression" analysis was used to determine the slopes' significant differences in Figure 5.

2.9.2. Kmeans clustering

PAI corrected for clumping for grapevines WIL1 to WIL30 from all three seasons as well as their VHS were combined for Kmeans clustering using the R (v. 4.1.1, R Core team, 2021) package "factoextra" (v. 1.0.7). The optimal number of groups was decided based on the results of the "elbow method" by the "fviz_nbclust" function [34]. Kmeans clustering was performed by "kmeans" function of the "stats" package in R (v. 4.1.1). The output of Kmeans clustering was visualized by ggplot2 (v. 3.3.5) R package [35].

2.10. Sample grouping systems

Two grouping systems were used in this study to evaluate the effect of viruses on grapevine physiology. The first was a liberal system which grouped grapevines for analysis by symptom type using three distinct symptoms described in Chapter 2 as follows: grapevines with typical Shiraz disease symptoms (SD), leafroll disease symptoms (LRD) and without any symptoms (ASY) (Table 2). This system was used for analyzing and comparing the time-dependent data between symptom groups for time courses of canopy and berry development.

The second more conservative grouping system was developed, based on the virus profile listed in Table 2. GVA^{II} is responsible for symptom development as it was detected only in SD grapevines [25]. In contrast, GVA^{III} was detected in SD, LRD and even ASY grapevines. However, it is possible that GVA^{III} may affect grapevine physiology that even if SD is not observed. Thus, the second group further divides the three symptom groups into 2 to 3 subgroups, to carefully study the differences that are likely to be associated with a particular GVA variant or with and without the presence of GLRaV-3. The virus profile of individual samples used in each experiment can be found in Table S1.

Table 2. Grouping system used in this study to evaluate the effect of disease status (symptom type) and viruses on grapevine physiology.

Groups	Symptom types	Subgroups	Virus profile	Site[1]
SD	Restricted spring growth (RSG), uneven lignification of canes (ULC), autumn leaf reddening	SD1	$GVA^{II\&III}$, GLRaV-3	WIL
		SD2	GVA^{II}, GLRaV-3	WIL
		SD3*	GVA^{II}	LC
LRD	Red leaf with green veins	LRD1	GVA^{III}, GLRaV-3	WIL

		LRD2	GLRaV-3	WIL
		ASY1	GVA^{III}	WIL
ASY	Asymptomatic	ASY2*	All negative	WIL, LC

*Grapevine leafroll associated virus 3 (GLRaV-3) was not detected at Langhorne Creek (LC), thus LC has only the SD1 and ASY2 groups.[1] WIL = Willunga, LC= Langhorne Creek.

3. Results

3.1. Vine health scores (VHS) and vine decline symptoms at WIL

The statistical comparison of VHS between the SD, LRD and ASY groups at WIL are shown in Figure 2 and the means and SDevs of each group are listed in Table 3. The mean VHS of the SD1 and SD2 groups were 2 and 1, respectively and the mean VHS of the LRD and ASY groups were above 6. In fact, 50% of VHS of the SD grapevines were below 2 whereas most of the LRD and ASY grapevines were above 5 (Figure 2 and Table 3).

Vine decline symptoms were observed on SD grapevines at WIL in the second season (2019-20) and two SD grapevines (25%) had no growth (VHS = 0). This percentage of dead grapevines increased to 47% in the 2020-21 season as five more SD grapevines had no growth (Table 4). In contrast, the LRD and ASY grapevines show less decline across the three growing seasons.

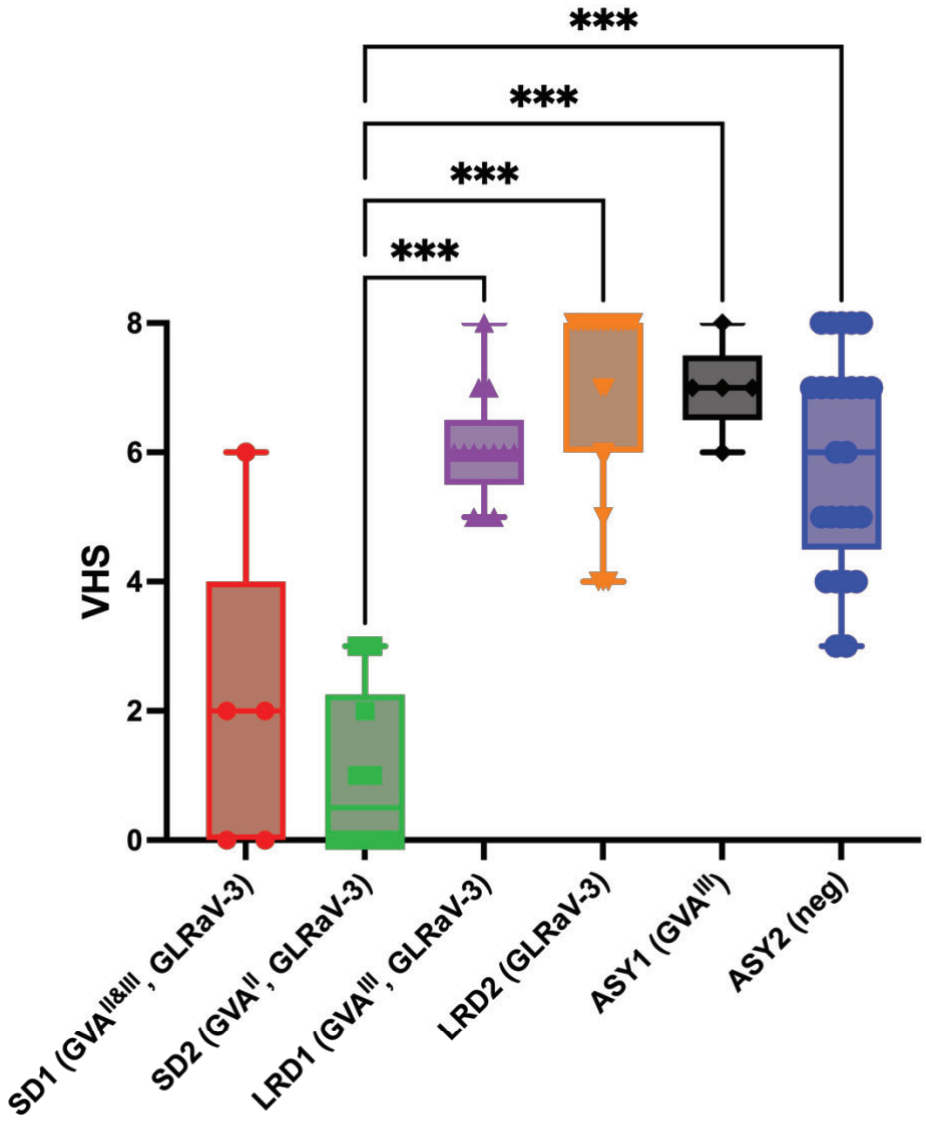

Figure 2. Vine health score (VHS) measured in 2020 of the groups of Willunga grapevines that had Shiraz disease (SD) and dead arm symptoms were infected with grapevine virus A (GVA) variants from phylogenetic groups II and/or III (GVA^{II}, GVA$^{II\&III}$; SD1, SD2); affected by leafroll disease (LRD) and infected grapevine leafroll associated virus -3 (GLRaV-3) and with or without GVA^{III} and (LRD1 and LRD2); and asymptomatic grapevines (ASY) that were infected with GVA^{III} or not (ASY1, ASY2). Individual values were shown as dot points. The top and bottom bars indicate the maximum and minimum values in each group. Dunnett's T3 test was used to examine the significance level between means of each two groups. The significance level is shown on top of the black line that connects each pair of significantly different groups. No line is shown when there is no significant difference between groups. * $P < 0.001$***, $P < 0.01$**, $P < 0.05$*

Table 3. Statistical analysis of physiology parameters of this study.

Parameters	Season	Site[1]	Stage of measurement	Time of measurement	No. of technical replicates	P	SD1 (GVA$^{II\&III}$, GLRaV-3) [a]	SD2 (GVA^{II}, GLRaV-3)	SD3(GVA^{II})	LRD1 (GVA^{III}, GLRaV-3)	LRD2 (GLRaV-3)	ASY1 (GVA^{III})	ASY 2 (Neg)	No. of groups	Total No. of grapevines	Significance of mean between groups	Statistical tests
Vine Health Scores (VHS)	2020-21	WIL	Mid-season	N/A	1	<.001 (***)	2±2.449(5)[b]	1±1.247(10)	N/A	6.077±0.8623(13)	7±1.517(21)	7±0.7071(5)	5.92±1.656(25)	6	79	SD2 vs. LRD1(***), SD2 vs. LRD2 (***), SD2 vs. ASY1 (***), SD2 vs. ASY2 (***)	Welch's, Dunnett's T3
leaf chlorophyll (µmol m^{-2})																	
leaf chlorophyll	2018-19	WIL	60 days post-flowering	N/A	4	0.431	14.13±2.602(3)	13.84±3.002(4)	N/A	11.23±1.626(2)	N/A	N/A	11.4±1.596(6)	4	15	No	Welch's, Dunnett's T3
leaf chlorophyll	2018-19	LC	60 days post-flowering	N/A	4	0.0881	N/A	N/A	12.84±1.458(5)	N/A	N/A	N/A	14.24±0.6889(5)	2	10	No	T-test
leaf chlorophyll	2020-21	WIL	50 days post-flowering	N/A	3	0.002 (**)	11.47±1.635(4)	11.42±2.854(7)	N/A	7.495±1.012(13)	8.278±1.348(21)	8.06±0.3876(5)	7.423±0.8094(10)	6	50	No	Welch's, Dunnett's T3
Carbohydrate (mg/g)																	
Cane starch	2020-21	WIL	E-L42	N/A	2	0.004 (**)	N/A	123±88.24(3)	N/A	220.7±12.09(4)	191.9±61.29(7)	N/A	118.1±19.01(3)	4	17	LRD1 vs. ASY2 (*)	Welch's, Dunnett's T3
Cane soluble sugar	2020-21	WIL	E-L42	N/A	2	0.668	N/A	59.89±14.84(3)	N/A	69.27±11.82(4)	62.91±8.262(7)	N/A	56.54±11.97(3)	4	17	No	Welch's, Dunnett's T3
Trunk starch	2020-21	WIL	E-L42	N/A	1	0.455	191.5±16.41(2)	141.9±74.06(3)	N/A	241.9±76.91(5)	180.4±54.05(7)	N/A	144.7±55.84(3)	5	18	No	Welch's, Dunnett's T3
Trunk soluble sugar	2020-21	WIL	E-L42	N/A	1	0.117	30.8±7.022(2)	35.95±5.649(3)	N/A	51.03±5.746(5)	43.12±5.248(7)	N/A	44.16±11.67(3)	5	18	No	Welch's, Dunnett's T3
Stomatal conductance (g_s) (mmol m^{-2} s^{-1})																	
Stomatal conductance	2018-19	WIL	60 days post-flowering	11 am to 3 pm	4	0.039 (*)	356.1±320.8(3)	336±124.6(4)	N/A	131.3±8.132(2)	N/A	N/A	165.9±17.51(6)	4	15	No	Welch's, Dunnett's T3
Stomatal conductance	2018-19	LC	60 days post-flowering	11 am to 3 pm	4	0.2514	N/A	N/A	391.2±110.5(10)	N/A	N/A	N/A	325.5±97.97(6)	2	16	No	T-test
Stomatal conductance	2020-21	WIL	50 days post-flowering	11 am to 3 pm	3	0.078	179.4±117(4)	166.1±87.05(8)	N/A	184.5±45.56(13)	214.5±43.24(21)	223.5±72.25(5)	194.8±64.31(10)	6	61	No	Welch's, Dunnett's T3
Stomatal conductance	2020-21	WIL	100 days post-flowering	11 am to 3 pm	4	0.471	313.5±135.9(4)	156.5±59.79(7)	N/A	169.7±61.57(13)	156.7±41.21(21)	209.5±31.58(5)	167.5±44.39(10)	6	60	No	Welch's, Dunnett's T3
Water potential (M Pa)																	
Stem water potential (ψ_{Stem})	2020-21	WIL	100 days post-flowering	8 to 12pm	1	0.081	-0.5053±0.06046(2)	N/A	N/A	-0.612±0.1267(10)	-0.5878±0.1008(9)	N/A	-0.6.95±0.05686(4)	4	25	No	Welch's, Dunnett's T3
Leaf water potential (ψ_{leaf})	2020-21	WIL	100 days post-flowering	8 to 12pm	1	0.143	-0.7625±0.003536(2)	N/A	N/A	-0.806±0.08822(10)	-0.7633±0.0923(9)	N/A	-0.865±0.08583(4)	4	25	No	Welch's, Dunnett's T3
Photosynthesis																	
Assimilation rate (A) (µmol m^{-2} s^{-1})	2020-21	WIL	100 days post-flowering	11 to 4pm	2	<.001 (***)	14.15±4.221(8)	11.82±3.047(8)	N/A	10.42±1.028(8)	8.004±0.9768(8)	11.31±1.998(8)	10.95±1.602(8)	6	48	SD1 vs.LRD1 (*), SD1 vs. LRD2(***), SD2 vs.LRD2 (*)	Ordinary ANOVA, Tukey's, Bartlett's test
Transpiration rate (E) (mmol m^{-2} s^{-1})	2020-2021	WIL	100 days post-flowering	11 to 4pm	2	<.001 (***)	2.656±0.7536(8)	2.478±0.7386(8)	N/A	2.024±0.3117(8)	1.356±0.2202(8)	2.266±0.4378(8)	2.153±0.4176(8)	6	48	SD1 vs.LRD2 (***), SD2 vs.LRD2 (**), LRD2 vs. ASY1 (*), LRD2 vs.ASY2 (*)	Ordinary ANOVA, Tukey's, Bartlett's test
Stomatal conductance (g_s) (mol m^{-2} s^{-1})	2020-2021	WIL	100 days post-flowering	11 to 4pm	2	0.004(**)	0.15±0.0699(8)	0.1163±0.05579(8)	N/A	0.0875±0.01753(8)	0.06375±0.01506(8)	0.1025±0.02252(8)	0.1025±0.0255(8)	6	48	SD1 vs.LRD1 (*), SD1 vs. LRD2 (**)	Ordinary ANOVA, Tukey's, Bartlett's test

Intrinsic water use efficiency (*WUEi* = A/g_s)	2020-2021	WIL	101 days post-flowering	8 to 12pm	2	0.161	103.9±25.26(8)	112.2±26.38(8)	N/A	121.7 ±15.61(8)	129.2±19.52(8)	112.3±16.87(8)	109.2±11.87(8)	6	48	No	Ordinary ANOVA, Tukey's, Bartlett's test

[1] WIL= Willunga, LC= Langhorne Creek, [a] SD = Shiraz disease, LRD = leafroll disease, ASY = asymptomatic, GVA^{II} and GVA^{III} = grapevine virus A variants from phylogenetic group II and III, GLRaV-3 = grapevine leafroll-associate virus 3, Neg = negative for both GVA and GLRaV-3. [b] The mean ± standard deviations (SDevs) and sample size (n) of each parameter. *Statistical significance level, P < 0.001***, P < 0.01**, P < 0.05*.

Table 4. Vine decline symptoms of the Shiraz disease (SD), leafroll disease (LRD), and asymptomatic (ASY) grapevines at the Willunga site.

Season	**SD (SD1& 2)[1]**		**LRD (LRD1&2)[1]**		**ASY (ASY1&2)[1]**	
	Number of grapevines with decline	Total number of grapevines observed	Number of grapevines with decline	Total number of grapevines observed	Number of grapevines with decline	Total number of grapevines observed
2018-2019	0	8	0	7	0	15
2019-2020	2	8	0	7	0	15
2020-2021	7	15	0	17	0	48

[1] See Table 2 for virus profile of each group.

3.2. Flowering time

The flowering curves of the LRD and ASY grapevines were identical to each other (Figure 3a) while the flowering time (100% caps-off) of the SD grapevines was delayed by about 7 days at WIL (Figure 3a) and 14 days at LC (Figure 3b). The small variance (indicated as SDev) of the LRD and ASY grapevines indicate that flowering stages of individual grapevines were uniform within these two groups (Figures 3a and b). The variance of the SD grapevines is larger than LRD and ASY grapevines, indicating that flowering of SD grapevines is more inconsistent.

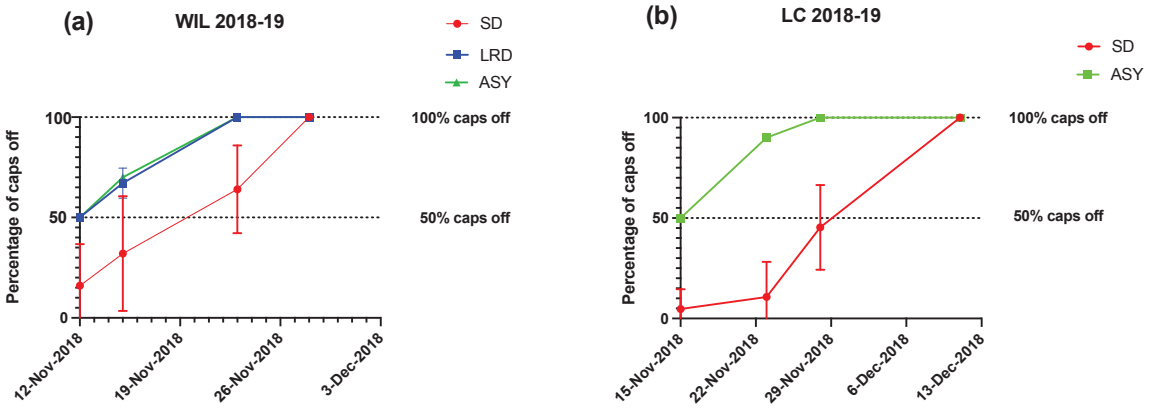

Figure 3. Comparison of the flowering period between grapevines with Shiraz disease (SD), leafroll disease (LRD) and asymptomatic (ASY) grapevines at (a) the Willunga (WIL) site, and (b) the Langhorne Creek (LC) site in the 2018-19 season. The horizontal dotted lines mark 50% caps off (E-L 23) and 100% caps off (E-L 26). Error bars represent the standard deviation (SDev) of each group.

3.3. Analysis of plant area index (PAI)

3.3.1. Grapevines grouped by symptom type

The means and SDevs of PAIs from each group of grapevines are listed in Table S2. A total of 30 (SD = 8, LRD = 7, ASY = 15), 28 (SD = 6, LRD = 7, ASY = 15) and 73 (SD = 8, LRD = 17, ASY = 48) grapevines measured at WIL in 2018-19, 2019-20, 2020-21, respectively. A total of 30 grapevines (SD = 15, ASY = 15) were measured at LC. PAI values of the grapevines with no growth were below 0.4 across the entire growing season and they were excluded for this analysis. The Shiraz grapevines were more vigorous at LC than WIL, since the maximum PAI was approximately 3 (Figure 4a), whereas PAI of WIL was 2.5 (Figure 4b) in the 2018-19 season. Comparing three years PAI data from WIL, the maximum PAI of 2019-20 and 2020-21 seasons were 1.8 (Figure 4c and d) indicating that they were less vigorous than 2018-19 season (PAI 2.5, Figure 4b). The greatest difference in PAI between individual grapevines, as reflected in the large variance (SDevs), was found in the SD affected group at WIL in all years (Figure 4).

At WIL in 2018-19 and 2020-21 (Figures 4b and d) ASY and LRD the growth curves are nearly identical. They diverge from and are represented by higher PAI values than SD grapevines throughout the season to E-L-35 (Verasion), suggesting that GVA may slow canopy growth, GLRaV-3 does not. In 2018-19 at LC (Figure 4a) and 2019-20 at WIL (Figure 4c), there was a similar divergence in the growth curve between the SD and the LRD and/or ASY grapevines, which have higher PAI values, and is observed earlier in the growing season but the curves and PAI values converge again just prior to E-L-35.

Based on the kinetics of canopy development at each site and in each year at WIL (Figure 4), it is proposed that the greatest differences between SD and ASY grapevines most likely occurs between late November to mid-January, roughly from bloom time to veraison. In 2018-19 at LC, no dead arm symptoms were observed, and no GLRaV-3 was detected Therefore the growth curve shown in Figure 4a is proposed to represent true canopy development in grapevines of SD vs. ASY grapevines.

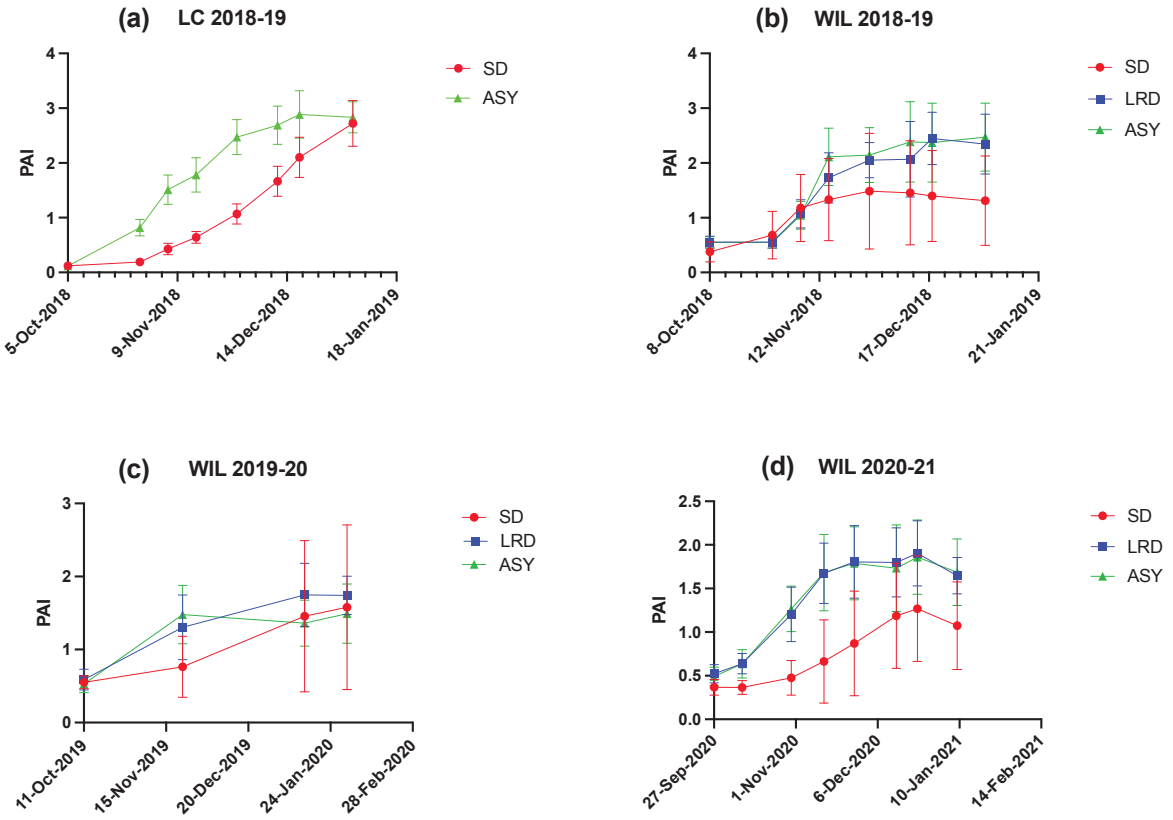

Figure 4. Analysis of plant area index (PAI) of grapevines with Shiraz disease (SD), leafroll disease (LRD) and asymptomatic controls (ASY) analysed over three seasons from 2018 to 2021 at Willunga (WIL) and in 2018-2019 at Langhorne Creek (LC). The time course PAI is shown for (a) 2018-19 LC, (b) 2018-19 WIL, (c) 2019-20 WIL, and (d) 2020-21 WIL. The vertical dotted lines indicated the time points when SD and ASY grapevines had the greatest differences in PAI. Standard deviations (SDevs) are shown by the error bars.

3.3.2. Correlations between vine health score (VHS) and plant area index (PAI)

To study the association between VHS and PAI, the PAI data set of 80 grapevines from WIL that were measured in the 2020-21 season were plotted against VHS (Figure 5). Given that 6/8 of R-squared (R^2) values are greater than 0.5, the association between VHS and PAI roughly fits segmental linear regression with an inflection point at VHS = 4 (Table S4). When VHS was ≤4, 8/8 P values were less than 0.05, demonstrating a substantial correlation between VHS and PAI when grapevines are significantly influenced by GTDs (Table S4). When VHS > 4, 6/8 of the P values were greater than 0.05 showing little correlation and hence indicating that the grapevines were less influenced by GTDs. (Figure 5 and Table S4).

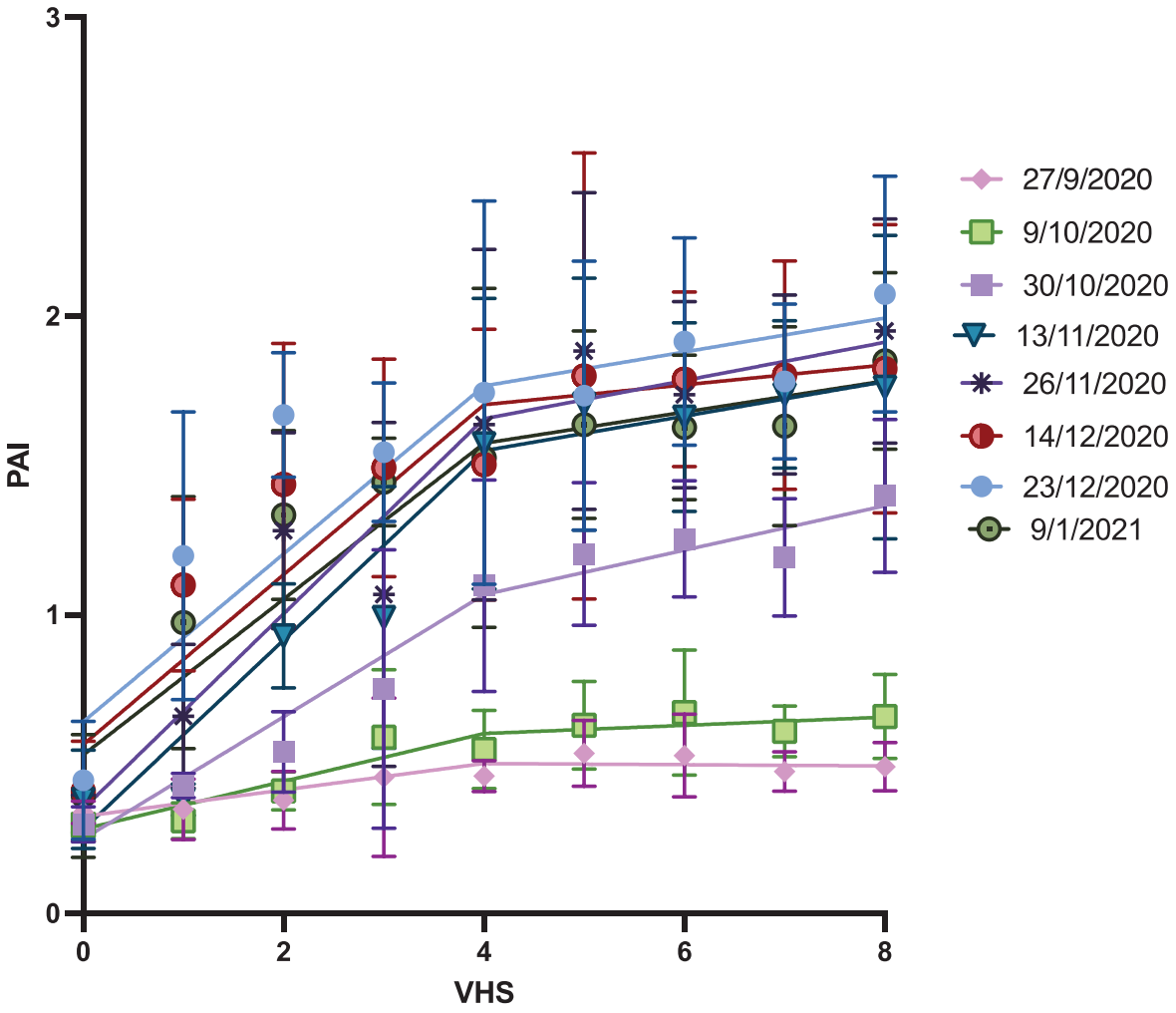

Figure 5. Plant area index (PAI) versus vine health score (VHS) for the Willunga site of the 2020-21 season. Each coloured line represents line of best fit for each date when PAI was measured. Error bars show the SDevs of the VHS at each measuring time.

3.3.3. Kmeans clustering of LC site

The optimal number of clusters was determined using the "elbow method" prior to Kmeans clustering. The elbow method uses total within sum of square (TWSS) to evaluate the variance within the data set. There will be less variation within the clusters as the number of clusters rises

and the optimal number of clusters is often indicated by the bend of the TWSS curve ("elbow") [34]. According to Figure S1a, the optimal number on the bend of the "elbow" is 2. Thus, the Kmeans clustering analysis for the LC site divided the grapevines into two clusters based on their PAI and VHS data. The first cluster contained all SD grapevines, which are infected with GVA^{II} variants (GLRaV-3 and GVA^{III} not detected), while the second cluster contained all ASY grapevines which are not infected with both viruses (Figure 6a).

3.3.4. Kmeans clustering of WIL site

The optimal number of clusters identified by the "elbow method" for the WIL site was three as indicated by the bend on the curve in Figure S1b. Since three symptom groups were identified previously, the Kmeans clustering of WIL was first performed using 3-cluster system, but this system cannot separate LRD and ASY grapevines (data not shown). Given that the PAI curves of the LRD and ASY grapevines were similar as previously described (Figure 3), it was assumed that the 2-cluster system is more closely related to physiological characteristics of SD than the 3-cluster system. Thus, the 2-cluster system was used. It can be seen from Figure 6b that most SD grapevines were in cluster 1 (red) and most of the LRD and ASY grapevines were in cluster 2 (blue). However, samples WIL 1, 2, and 5 were clustered with the LRD and ASY grapevines, and WIL25 was clustered with SD grapevines. When investigating the VHS scores of those outliers, the ASY grapevine WIL25 has a VHS of 4 which is below the average VHS of an ASY grapevine (Table 3, ASY2=5.92). WIL1, 2, and 5 have a VHS of 2, 6, and 2 respectively which are higher than most of the SD grapevines (Table 3).

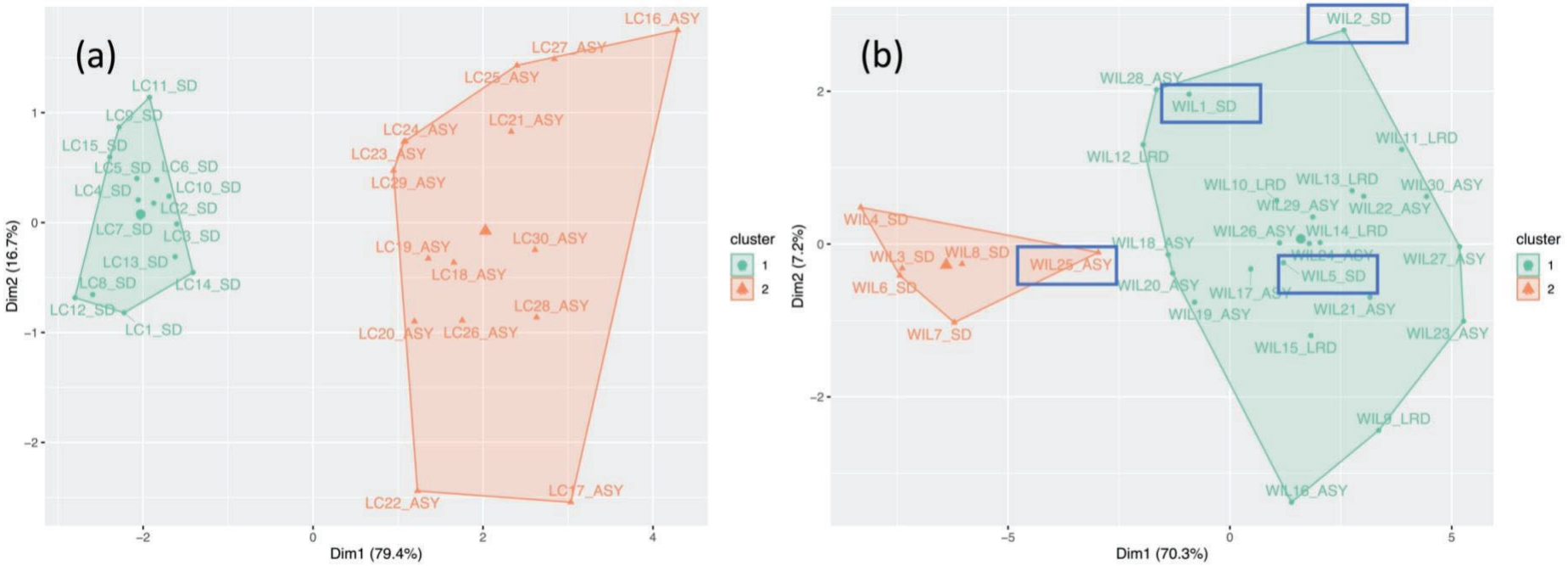

Figure 6. Kmeans clustering using plant area index (PAI) for grapevines affected by Shiraz Disease (SD), Leafroll disease (LRD) or which were asymptomatic (ASY) at. (a) Langhorne Creek (LC) (grapevines LC1 to LC30) using one year of data (2018-19) and (b) Willunga (WIL) (grapevines WIL1 to WIL30) using the three years of PAI data (2018-21) and combined with vine health score (VHS) data measured in 2020. The mean values of each cluster were indicated by a larger symbol in the center. Sample with squared in this figure have different symptom types than most members in this group. A detailed explanation of each symptom type can be found in Table 2. The symptom type of each grapevine is linked to the sample name in the figures.

3.4. Analysis of leaf chlorophyll

Total chlorophyll (Chl) of SD3 and ASY grapevines was measured at the LC site for the 2018-19 season. No statistical significance was found between SD and ASY grapevines of the 2018-19 season at the LC site (Table 3). The Mean Chl ± SDev of the SD3 and ASY2 grapevines are 12.84 ± 1.458 and 14.24 ± 0.6889 μmol m^{-2}, respectively (Table 3).

At the WIL site, leaf Chl was measured twice in the 2018-19 and 2020-21 seasons. In general, the means of Chl content was higher in SD grapevines than in LRD and ASY grapevines (Table 3 and Figure S2). Welch's ANOVA detected significant differences in the 2020-21 data set (P = 0.002) (Table 3). However, the Dunett's T3 test did not detect any statistical significance between any two groups (Table 3).

3.5. Analysis of stomatal conductance (g_s)

Stomatal conductance (g_s) was measured once 60 days post-flowering at both sites in the 2018-19 season, and twice at both 50 and 100 days post-flowering at WIL. No significance was found when comparing the mean g_s ± SDev of SD3 grapevines (391.2 ± 110.5 mmol m^{-2} s^{-1}) and ASY2 grapevines (325.5 ± 97.97 mmol m^{-2} s^{-1}) of the LC data set (with and without GVA^{II}) (Table 3).

A weak significant difference was found for the 2018-19 season by Welch's ANOVA (P = 0.039), but Dunnett's T3 test did not detect any significance between each of the two groups. ANOVA and post-hoc tests can provide different results since the test thresholds are different and post-hoc tests control familywise error rates and reduce the type one error rate [36]. The weak positive might be a type one error unless it is proved otherwise by more data.

Overall, no significant difference of g_s was found between groups at WIL and LC sites.

3.6. Analysis of leaf and stem water potentials

Welch's ANOVA and Dunnett's T3 tests indicated no statistical significance of leaf and stem water potential (ψ_{leaf} and ψ_{stem}) between all groups based on the current data set (Table 3). The ψ_{leaf} and $\psi_{stem,}$ ranged from -0.7 MPa to -0.9 MPa, and -0.5 MPa to -0.7 MPa, respectively (Table 3).

3.7. Analysis of carbohydrate accumulation

Typical symptoms of SD, RSG and delayed flowering, could be a consequence of insufficient carbohydrate accumulation during the previous season. To investigate this further, cane and trunk samples were harvested from SD, LRD and ASY WIL grapevines during the 2020-21 season at E-L42 right after leaf-fall. Storage sugar (starch) and soluble sugar in canes and trunks were extracted and analysed separately. The results show significantly higher starch content in canes of LRD1 grapevines (GVA^{III}, GLRaV-3) (220.7 ± 12.09 mg/g) compared to ASY2 grapevines (118.1 ± 19.01mg/g) (negative for GVA and GLRaV-3) (Table 3). None of the other two groups differ in their carbohydrate contents.

3.8. Analysis of photosynthesis parameters

In this study, the net photosynthesis rate (A) of individual leaves was measured between 11 am to 4 pm when the average leaf temperature was about 29.9°C. The individual value of g_s, A, E and intrinsic water use efficiency ($WUE_i = A/g_s$) and significance of means between each of the two groups are shown in Figure 7 and Table 3. Means and SDevs of A, E and g_s of individual leaves from the SD1 group ($GVA^{II\&III}$, GLRaV-3) are always the highest among all groups followed by SD2 (GVA^{II}, GLRaV-3) (Figures 7a, b and c). In the presence of GLRaV-3, the mean g_s of the grapevines infected with $GVA^{II\&III}$ variants (SD1) and GVA^{II} (SD2) were significantly different from the grapevines without GVA infection (LRD2) (Figure 7a and Table 3). This shows that GVA^{II} plays a central role in affecting g_s. Moreover, no significance was found when comparing the groups with and without GVA^{III} indicating that this variant may have no effect on g_s in these conditions. GVA^{II} and GLRaV-3 could affect E, since significances were found between SD1 and LRD2 (with and without $GVA^{II\&III}$), SD2 and LRD2 (with and without GVA^{II}), LRD2 and ASY2 (with and without GLRaV-3) (Figure 7b and Table 3). The E values of SD grapevines were higher than LRD and ASY grapevines (Table 3) suggesting GVA^{II} affects transpiration. GVA^{II} was the dominant factor in its effect on A, as A of SD grapevines are significantly higher than LRD grapevines, differences were found for SD1 and LRD1 (with and without GVA^{II}), SD2 and LRD2 (with and without GVA^{II}), SD1 and LRD2 (with and without $GVA^{II\&III}$) (Figure 7c and Table 3). No significance of A was found between SD and ASY, and between LRD and ASY groups (Figure 7c and Table 3).

A, E and g_s are more variable within the SD groups as illustrated by larger SDevs compared to those of the LRD and ASY groups (Table 3) and the data range (min to max) being much wider than any other groups (Figures 7a, b and c).

All groups have similar linear relationships between g_s vs. A and A vs. E (Figures 7d and e). No significant difference was found between these linear relationships by simple linear regression analysis. The slopes of intrinsic water use efficiency ($WUE_i = A/g_s$) of all groups are not significantly different from one another (Figure 7f).

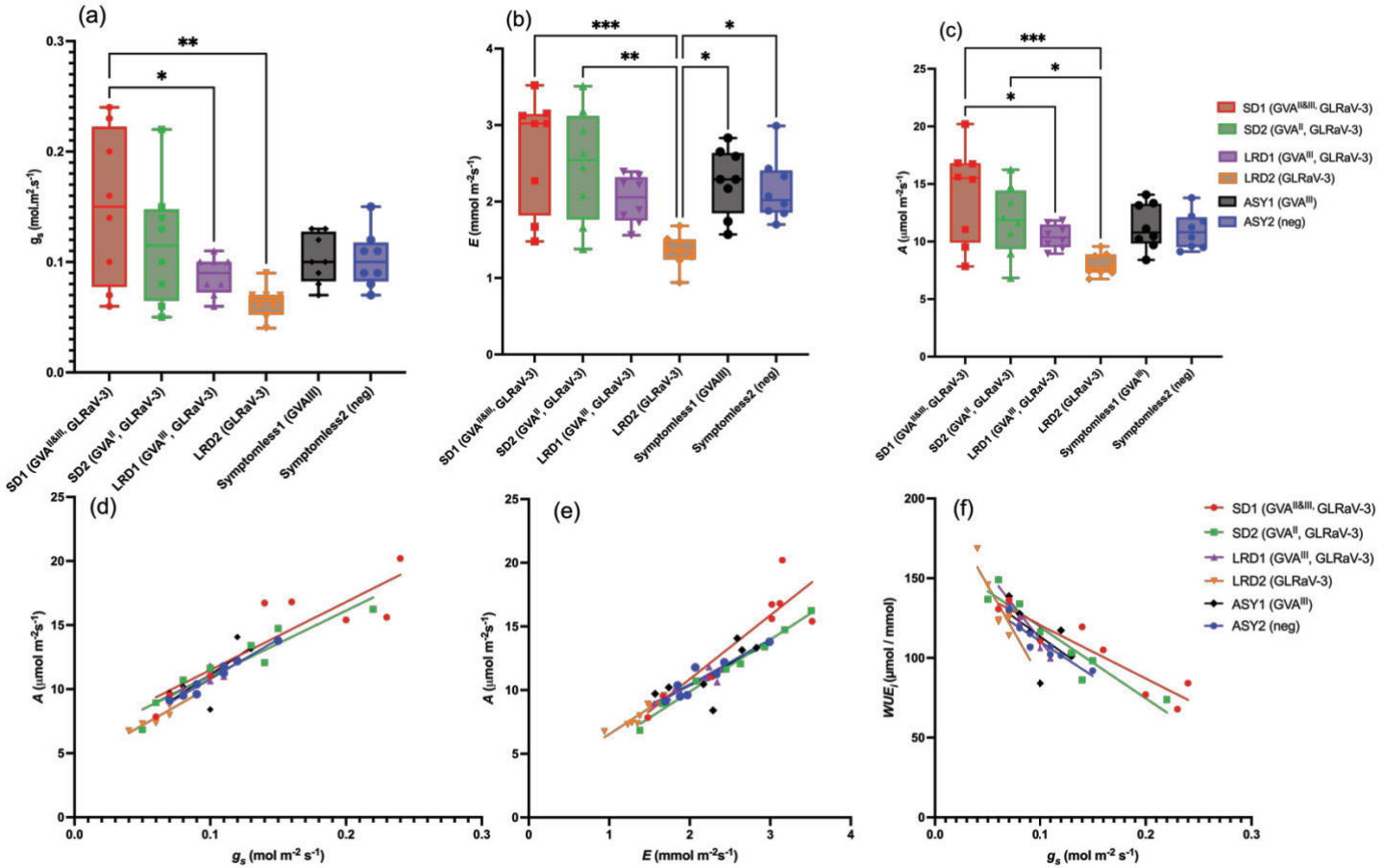

Figure 7. Leaf photosynthesis measurements of grapevines with and without Shiraz disease (SD) or leafroll disease (LRD) symptoms in the 2020-21 growing season at the Willunga site. Figure (a) stomatal conductance (g_s), (b) transpiration rate (E), (c) assimilation rate (A). Relationships between g_s vs. A (b), E vs. A (e), g_s vs. intrinsic water use efficiency ($WUE_i = A/g_s$) are also shown. Data was analysed by ordinary ANOVA. The XY box plots of the ANOVA significance of mean of each parameter were tested and compared individually by Tukey's test. The significance level s shown on top of the black line that connects each pair of significant groups. No line is shown for the groups without any significant differences. * Indicate significant level between of means, $P < 0.001$***, $P < 0.01$**, $P < 0.05$

3.9. Berry development

Timewise berry development curves of berry weight, sugar content, and pH were grouped by symptom type and analysed. Mean, SDev, and n of a particular sample and date can be found in Table S3.

3.9.1. Fresh berry mass (FBM)

The timewise development of fresh berry mass (FBM) is shown in Figure 8. In 2018-19 at LC and across all seasons at WIL, berry mass increased linearly from pea-size (early-January) until about veraison (mid-February) and then reduced towards the end of ripening starting from approximately 100 days post-flowering (Figures 8a, c, h). Comparison between the SD, LRD, and ASY symptom types showed slightly different trends across the three seasons. In 2018-19, the FBM curve of LRD grapevines in WIL was generally higher than ASY and SD grapevines (Figure 8c). The maximum FBM of the SD, LRD, and ASY grapevines were 1.13 ± 0.11, 1.27 ± 0.08 and 1.00 ± 0.18 g, respectively, measured on the 17th of February (Figure 8c and Table S3). In the 2019-20 season. The FBM curves of SD and ASY grapevines in WIL had almost no difference in FBM at the latest stage of berry ripening (Figure 8e). Berries of ASY and LRD grapevines reached their maximum berry weight earlier than the SD grapevines and the FBM curve of SD grapevines are generally above LRD and ASY grapevines for the 2020-21 season of the WIL site and 2018-19 season of the LC site (Figures 8h and a, Table S3).

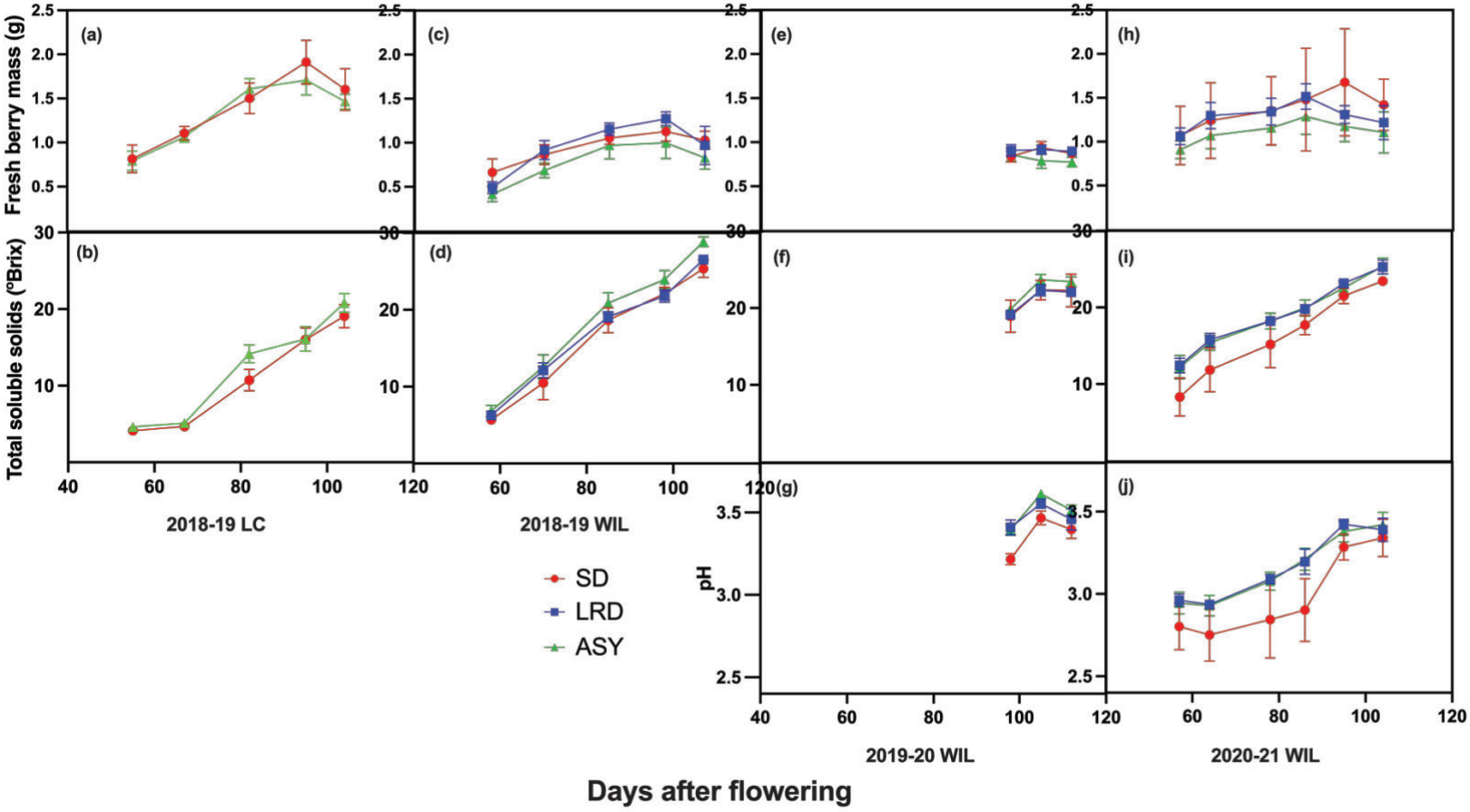

Figure 8. Berry maturation of the Shiraz Disease (SD), Leafroll disease (LRD), and asymptomatic grapevines (ASY) for three seasons from 2018 to 2021 at two sites Willunga (WIL) and Langhorne Creek (LC). The 2018-2019 data from the WIL site is shown in (a) fresh berry mass (FBM), and (b) total soluble solids (TSS), and in (c) FBM and (d) TSS for the LC site. The 2019-20 and 2020-21 data was only taken in the WIL vineyard and is shown in (e) FBM, (f) TSS and (g) pH for 2019-20 and, (h) FBM, (i) TSS and (j) pH for 2020-21. Data are shown as means ± standard deviations (SDevs) indicate by error bars, at each time point. Sample sizes (n) and the exact value of each group and grapevine are reported in Table S3.

3.9.2. Berry TSS

The reduced TSS in SD grapevines was observed at both study sites in 2018-19 at LC, and in 2018-19 and 2020-21 seasons at WIL when compared to accumulation in the ASY group of grapevines (Figure 8b, d, and i). TSS started to sharply increase about 60 days post flowering. An increase in sugar accumulation of the SD, LRD and ASY groups was similar (Figures 8b, d, f and i). The TSS of the LRD grapevines at WIL varied season to season. It was higher than the SD but lower than the ASY vines for the 2018-19 season (Figure 8d), similar to the SD grapevines for the 2019-20 season (Figure 8f), and identical to the ASY group in the 2020-21 season (Figure 8i).

3.9.3. Berry juice pH

The mean pH as it is shown by the curve in Figures 8g and j, the curve of SD grapevines was always below the other two groups during the whole monitoring period for the seasons 2019-20 and 2020-21. The pH at the latest berry ripening stage was around 3.6 at 108 days post-flowering and 3.4 at 105 days for the season 2019-20 (Figures 8g) and 2020-21 (Figure 8j), respectively. The large SDevs of the SD curve indicate the extremely variable pH within the SD grapevines.

4. Discussion

The purpose of this study was to investigate the effects of SD on the physiological performance of *V. vinifera* cv. Shiraz, one of the most widely grown varieties in Australia, in two South Australian vineyards. It is the first comprehensive study done in Australia to measure effects of viruses on grapevine physiological performance. Considering all parameters measured in this study, the reduction of PAI and delayed berry maturation are most likely to be affected in SD grapevines at WIL and LC, which suggests that SD may delay canopy development and fruit ripening. However, dead arms symptoms were also observed in the SD affected grapevines as well as in ASY grapevines at WIL, which are likely to have contributed to poor physiological performance. Thus, other parameters such as Chl, A, E, g_s, carbohydrate, water potentials, were highly variable depending on measuring time and season and were not an accurate measure of impact of SD.

Determining the impacts of a particular grapevine virus on vine performance and berry composition can be complicated and challenging for the following reasons. A field grapevine is frequently infected with two or more viruses, or even multiple variants of a virus, each with distinct biological properties. Both GVA^{II} and GVA^{III} were isolated from SD grapevines [25], however only GVA^{II} variants were associated with SD. Moreover, the degree of biotic and abiotic stress on each grapevine within a vineyard is never equal and difficult to manage in the field. Abiotic conditions that may interact with biotic stress associated with a virus infection include soil type (nutrient deficiencies, compaction, aeration, salinity, pH etc.), irrigation regime (periodic water stress), geographical location of the vineyards, micro-climate (heat stress, frost) and the annual variation of weather conditions affecting dormancy, bud burst, and ripening period. More critically, there might be other organisms that affect the growth parameters of a field grapevine, like

fungal pathogens associated with GTDs [37-39] that exacerbate the effects of a virus infection, including the impacts of SD associated GVA variants.

4.1. Impacts on canopy vigor

A balanced vegetative growth of the canopy and reproductive growth of the berry is essential to obtain high quality grapes for wine. The direct method used to assesses canopy vigor via LAI can be destructive and labor intensive [40]. A previous study demonstrated that a balanced canopy architecture partly indicated by PAI, which is similar to LAI but is non-destructive and less labor intensive, can be an indicator of favourable berry quality for wine [41]. Therefore, the Viticanopy method, which measures PAI, was used to estimate canopy vigor at the WIL and LC vineyards. Figure 5 illustrates that when VHS, which was only measured at WIL, is less than 4 (grapevines with poor growth), there is a substantial association between PAI and VHS, and when VHS is greater than 4 (relatively healthy), there is no correlation. This illustrates that the PAI value effectively measured the detrimental impact of grapevines with SD and GTDs. Moreover, Figure 5 suggests that the association between VHS and PAI should be examined primarily in the late season, specifically after the 13th of November. This time period showed a stronger correlation between VHS and PAI compared to the early stages of the growing season.

Because SD and GTDs occurred together on grapevines at WIL in 2019-20 and 2020-21, the impact of SD alone on grapevine health could not be measured. It should also be noted that RSG symptoms occurring in grapevines with SD at WIL and LC in 2018-19 may be attributable to GTDs instead of SD. However, the fact that there is a significant difference in PAI between SD grapevines with GTD and ASY grapevines at WIL, but essentially no difference between LRD and ASY grapevines, suggests that SD and/or GTD are key factors in delayed canopy growth. If the RSG observed in SD affected grapevines was only associated with SD at WIL and LC in 2018-19, the low PAIs observed at both sites in that year, compared to ASY, would provide further support for the hypothesis that SD and therefore GVA^{II} impacts canopy growth. The biggest difference in canopy vigor between ASY and SD affected grapevines, as measured by PAI, was found between late November to mid-January (bloom to veraison). This finding is helpful to distinguish SD/GTD affected grapevines from ASY grapevines within the same block using the Viticanopy app or area photography.

When PAI was estimated via Viticanopy, the following constraints were also shown to influence the PAI value. When photographing a grapevine from the bottom of a double cordon grapevine, even though one tier was poorly grown, the Viticanopy method only measures an overall PAI value of the top and bottom tier of the canopy and from the same side of the grapevine. Furthermore, the bottom tier of the canopy affects the PAI more than the top tier as the image of the top tier may be covered by the bottom tier of the canopy towards the mid-late measuring period. When vine decline and dead arms partially affect the grapevine (VHS > 4), the remaining arms have the potential to obtain nutrient and water from the entire root system, and they have the potential to grow more leaves and compensate for the loss of the dead arms. Therefore, since GTDs were also present in those grapevines measured, the analysis of PAI (Figure 4) might have revealed fewer variances between SD and ASY grapevines than using direct LAI approaches.

4.2. Impacts on leaf chlorophyll

Based on the data collected in this study the impact that SD may have on Chl is unclear. Statistically significant differences between the SD and ASY groups were only found in one out of three data sets for Chl (WIL, 2020-21), although SD affected grapevine group had higher total Chl content compared to the LRD and ASY groups (Table 3). Higher leaf Chl levels corresponds to higher leaf nitrogen [42] and higher photosynthetic capacity of a leaf [43] and this accounts for the higher assimilation rate (*A*) of SD grapevines compared to other groups (Table 3). The likely reason of higher *A* in SD grapevines will be discussed in the following photosynthesis section.

In this study there was no significant difference between the Chl levels in LRD only and ASY grapevines. This supports a previous study that concluded there was no difference in leaf Chl between the GLRaV-3 infected and control grapevines (cv. Cabernet Sauvignon) under *in vitro* conditions [44]. However, it differs to another study in which Chl content was lower in GLRaV-3 infected field-grown grapevines (cv. Lagrein) compared to heat-treated virus-free grapevines [45]. Different results could be due to the differences in biological characteristics of GLRaV-3 variants, grapevine varieties, rootstocks and experimental conditions.

4.3. Impacts on carbohydrate

Carbohydrate reserve dynamics can have a significant impact on vegetative growth of the grapevine canopy and reproduction of berries [46-48]. A previous study showed that carbohydrates were mainly stored as starch at a maximum of about 13% of dry mass in trunks and about 17% in shoots between harvest and leaf fall in cv. Chasselas [47]. In the same study, the soluble sugars in canes and trunks were usually less than 7% across the growing season and sharply increased from about 2% of dry mass (veraison) to 7% (leaf-fall) [47]. The percentage of carbohydrate in trunks and canes measured in this study, is within the range of the seasonal evolution kinetics between leaf-fall and budburst previously reported by Zufferey *et al.* [47] but slightly below the mean values of cv. Chardonnay on Ramsey rootstock reported by De Bei *et al.* [49]. The results in this study are in contrast to a recent study that demonstrated significantly increase sucrose and starch content in leaves of cv. Merlot and starch in cv. Shiraz that were infected by GRBV [5]. In another study, grapevine fanleaf virus (GFLV) caused overexpression of the genes involved in carbohydrate metabolism, which could also impact sucrose accumulation [50]. Although no statistical significance was found between SD and ASY grapevines in this study, because SD and GTD occurred together, the true effect of GVA^{II} on carbohydrate accumulation and metabolism could not be effectively measured and needs to be investigated further.

4.4. Impacts on stomatal conductance

Stomatal conductance (g_s) is sensitive to environmental conditions like temperature, air humidity and soil water content [51-53], as well as being influenced by grapevine and rootstock varieties [54,55]. The maximum stomatal conductance of Shiraz estimated by Winkel and Rambal [56] was 360 mmol m^{-2} s^{-1} which is the lowest compared to varieties Merlot and Carignane when in a Mediterranean environment.

Several previous studies conducted in the Barossa Valley in South Australia, reported the average g_s of own-rooted Shiraz ranging from 200 to 300 mmol m^{-2} s^{-1} under local conditions [53,57]. The g_s of the LC grapevines tested in this study roughly fits this range, and it is higher than g_s of WIL grapevines at the same measuring time. The rootstock could have affected g_s at LC since the LC Shiraz grapevines were grafted onto Chardonnay rootstocks. No statistical significance of g_s between SD and ASY grapevines at LC may indicate that SD does not affect g_s at LC. Only one data set (WIL, 2020-2021) supports there might be some difference between SD1 and the two LRD groups, with and without the combination of GVA^{II} and GVA^{III} (Table 3).

4.5. Impacts on water potentials

There is evidence that the function of aquaporins, which regulate water transport across cell membranes, can be affected by plant-pathogens [58] and might lead to changes in water potential in infected plants. However, there were no significant different of ψ_{leaf} and ψ_{stem} between any groups measured by this study. The ψ_{leaf} and ψ_{stem} values between SD, ASY and LRD affected grapevines in this study would indicate that grapevines were not water stressed at the time they were measured. Furthermore, the gradients between ψ_{leaf} and ψ_{stem} in all disease groups are similar to those previously reported for Shiraz at a similar time after bloom indicating that water potential was not impacted [26,59,60]. Similar studies reported no difference in water status in virus infected grapevines and controls for GRBV [61], GVB [62] and GLRaV-1 and 3 [14]. Interestingly, a recent study found GFLV infected grapevines performed better than the healthy grapevines under mild water stress [24].

4.6. Impacts on photosynthesis parameters

Across all disease groups examined in this study, the values of A were similar to those previously reported for Shiraz at a similar stage after bloom and at a similar leaf temperature [26,63] although E and g_s were somewhat lower. Lower g_s and similar A lead to a greater WUE_i (A/g_s), similar to the response when grapevines infected with GLRaV-1 and 3 [64]. However, apart from the reduction of g_s and E, several previous studies found that A also significantly reduced when grapevines were infected with GLRaV-1 and 3 [15,45,65] and GRBV [66]. In this study, the mean of g_s, A and E of the SD grapevines were higher than the LRD and ASY grapevines. A likely reason is that when canopy growth is negatively affected by biotic stress (virus or GTDs), the total photosynthetic rate of a grapevine is reduced [67,68], and the grapevine compensates by increasing A of individual leaves. This is similar to the effect of leaf removal and shoot-thinning [69]. Since A and g_s are strongly associated with other abiotic conditions and time of measurement, and SD affected grapevines at WIL may also affected by GTDs, the true impact of GVA^{II} and SD on these parameters needs to be investigated further.

4.7. Impacts on berry maturation

A reduction in berry mass towards the end of berry ripening could be a consequence of berry shrivel. Berry cell death in Shiraz normally begins around 87 days post flowering and mass reduction occurs at about 100 days [70,71]. Little is known about the cause of Shiraz berry shrivel, it may be linked to elevated temperature [70], hypoxia within berries

[72,73], and inhibition of the *VvBAP1* gene under drought stress [74]. The characteristics of Shiraz berry maturation including preharvest FBW reduction, sugar accumulation and pH elevation agree with what has been previously described [26,75]. However, the exact value of maximum FBM is highly variable from season to season due to different environmental conditions [76]. GLRaV-1, GLRaV-3 and GRBV infection often reduce FBM, TSS and pH in berries [10,14]. However, in other studies, TSS remained unaffected [11,12]. This is likely due to the differences in virus, grapevine variety studied and the biotic and abiotic conditions where the experiments were conducted. The mean TSS and pH of the SD grapevines were often lower than LRD and ASY grapevines in this study likely due to their delay in ripening response to delayed canopy growth and flowering time.

4.8. Growth cycle variations in SD affected grapevines

At WIL, SD grapevines had greater variance in flowering time (Figure 3), canopy development (Figure 4), berry maturation (Figure 8), VHS, Chl, g_s and A (Table 3) as shown by large error bars and SDevs in most of the analyses. Since these differences, except VHS which was not measured, were also detected in the LC data set (Figures 3b, 4c, and 8a), and if it is assumed that GTDs did not affect grapevines at LC, the variations may be attributed to SD. Higher variance within physiological parameters of the SD grapevines could indicate that each grapevine was under a different level of stress or at different stages of disease status. The level of stress may depend on the duration of infection, virus status, rootstocks, GTDs severity, and any abiotic condition in the field.

5. Conclusions

This study has shown that SD can affect the physiological performance of affected Shiraz, especially in grapevines that were also affected by GTDs. There were significant delays in SD grapevines compared to ASY and LRD in terms of flowering pattern, canopy development, and berry ripening at both study sites and almost no difference between LRD and ASY grapevines at WIL. This may suggest GVA, in particular GVA^{II}, is more likely to be associated with those changes than GLRaV-3. Since almost no significance was found between subgroups with the same symptom type, and it appeared that GVA^{III} had no effect in almost any parameter measured in this study. This agrees with the earlier finding of Goszczynski [77] that GVA^{III} induces mild symptoms on *Nicotiana benthamiana* and did not induce SD symptoms on Shiraz. However, as this study was done in a grower managed vineyard where other biotic and abiotic factors that can also affect physiological performance were also present, further research in controlled conditions is required to study the effects of SD and GVA^{II} in isolation.

This study touched on several basic grapevine health indicators in an attempt to understand which physiological parameters are likely to be associated with virus infection and decline. Since GTDs and several abiotic factors could interfere with field measurements and cannot be disregarded, the conclusion of this study are proposed as a confidence level in Table 5. The factors with a higher confidence level are more likely to be SD-related. Any factors with medium to low confidence levels require further investigation.

This study identified the best period to monitor SD using a model based on PAI and statistical grouping. For future SD surveillance, it is possible to monitor SD on a large-scale using aerial photography rather than test grapevine viruses by RT-PCR year to year. Also, stomatal conductance variability would suggest that remote infrared thermography would be better to indicate differences between SD and ASY grapevines for future exploration.

Table 5. The confidence level of grapevine physiological parameters which may link to grapevine virus A infection.

Health indicators	**Impacts on SD vines**	**Confidence level**	**Evidence**
Flowering time	Delayed flowering time	High	Figure 3
Canopy size	Delayed canopy development	High	Figure 4
Leaf chlorophyll	Higher Leaf chlorophyll	Low	Table 3
Photosynthesis	Higher photosynthesis rate per unit of leaf	Medium	Table 3
Carbohydrate	Unaffected	Low	Table 3
Stomatal conductance	Unaffected	Low	Table 3
Water potential	Unaffected	Low	Table 3
Berry size	Larger berries	Medium	Figure 8
Berry TSS and pH	Lower TSS and pH	High	Figure 8

6. Supplementary Material

Table S1. Major viruses and symptom type and vine health score (VHS) of individual vines.

Sample ID[1]	Groups[2]	Symptom type [3]	Major viruses[4]	VHS	Plant area index (PAI) (2018-19)	PAI (2019-20)	PAI (2020-21)	Stomatal conductance (g_s) (2018-19)	g_s (2020-21a)	g_s (2020-21b)	leaf chlorophyll (2018-19)	leaf chlorophyll (2020-21)	Water potential (2020-21)	Photosynthesis (2020-21)	Carbohydrate (2020-21)	Berry (2018-19)	Berry (2019-20)	Berry 2020-21
WIL1	SD1	SD	$GVA^{II\&III}$, GLRaV-3	2	Yes#	Yes	Yes	Yes	Yes	Yes	No	Yes	Yes	Yes	Yes	Yes	Yes	Yes
WIL2	SD1	SD	$GVA^{II\&III}$, GLRaV-3	6	Yes	Yes	Yes	Yes	Yes	Yes	No	Yes	Yes	Yes	No	Yes	Yes	Yes
WIL3*	SD1	SD	$GVA^{II\&III}$, GLRaV-3	0	Yes	Yes	No	Yes	No	No	No	No	No	No	No	Yes	No	No
WIL4*	SD2	SD	GVA^{II}, GLRaV-3	0	Yes	No#	No	Yes	No	No	Yes	No	No	No	Yes	Yes	No	No
WIL5	SD2	SD	GVA^{II}, GLRaV-3	2	Yes	Yes	Yes	Yes	Yes	Yes	Yes	Yes	Yes	Yes	No	Yes	Yes	No
WIL6*	SD2	SD	GVA^{II}, GLRaV-3	0	Yes	No	No	Yes	No	No	Yes	No	No	No	No	Yes	No	No
WIL7*	SD2	SD	GVA^{II}, GLRaV-3	0	Yes	Yes	No	Yes	Yes	Yes	No	Yes	No	Yes	No	Yes	No	No
WIL8*	SD1	SD	$GVA^{II\&III}$, GLRaV-3	0	Yes	Yes	No	No	Yes	Yes	No	Yes	No	Yes	Yes	No	No	No
WIL9	LRD1	LRD	GVA^{III}, GLRaV-3	5	Yes	Yes	Yes	No	Yes	Yes	No	Yes	Yes	Yes	No	No	Yes	Yes
WIL10	LRD1	LRD	GVA^{III}, GLRaV-3	6	Yes	Yes	Yes	Yes	Yes	Yes	Yes	Yes	Yes	Yes	No	Yes	Yes	Yes
WIL11	LRD1	LRD	GVA^{III}, GLRaV-3	5	Yes	Yes	Yes	Yes	Yes	Yes	Yes	Yes	Yes	Yes	Yes	Yes	Yes	Yes
WIL12	LRD1	LRD	GVA^{III}, GLRaV-3	5	Yes	Yes	Yes	No	Yes	Yes	No	Yes	Yes	Yes	Yes	No	Yes	Yes
WIL13	LRD1	LRD	GVA^{III}, GLRaV-3	6	Yes	Yes	Yes	No	Yes	Yes	No	Yes	Yes	No	Yes	No	Yes	Yes
WIL14	LRD2	LRD	GLRaV-3	7	Yes	Yes	Yes	Yes	Yes	Yes	Yes	Yes	Yes	Yes	No	Yes	Yes	Yes
WIL15	LRD2	LRD	GLRaV-3	6	Yes	Yes	Yes	No	Yes	Yes	No	Yes	Yes	Yes	Yes	No	Yes	Yes
WIL16	ASY2	ASY	Neg	3	Yes	Yes	Yes	Yes	No	No	Yes	No	No	No	No	Yes	Yes	No
WIL17	ASY2	ASY	Neg	3	Yes	Yes	Yes	Yes	No	No	Yes	No	No	No	No	Yes	Yes	Yes
WIL18	ASY2	ASY	Neg	4	Yes	Yes	Yes	No	No	No	No	No	No	No	No	No	No	No
WIL19	ASY2	ASY	Neg	5	Yes	Yes	Yes	Yes	No	No	Yes	No	No	No	No	Yes	Yes	Yes
WIL20	ASY2	ASY	Neg	5	Yes	Yes	Yes	No	No	No	No	No	No	No	No	No	No	No
WIL21	ASY2	ASY	Neg	7	Yes	Yes	Yes	No	No	No	No	No	No	No	No	No	No	No
WIL22	ASY2	ASY	Neg	5	Yes	Yes	Yes	Yes	No	No	Yes	No	No	No	No	Yes	Yes	Yes
WIL23	ASY2	ASY	Neg	8	Yes	Yes	Yes	No	No	No	No	No	No	No	No	No	No	No

WIL24	ASY2	ASY	Neg	6	Yes	Yes	Yes	Yes	No	No	Yes	No	No	No	No	Yes	Yes	Yes
WIL25	ASY2	ASY	Neg	4	Yes	Yes	Yes	No	No	No	No	No	No	No	No	No	No	No
WIL26	ASY2	ASY	Neg	7	Yes	Yes	Yes	No	No	No	No	No	No	No	No	No	No	No
WIL27	ASY2	ASY	Neg	5	Yes	Yes	Yes	No	No	No	No	No	No	No	No	No	No	No
WIL28	ASY2	ASY	Neg	4	Yes	Yes	Yes	No	No	No	No	No	No	No	No	No	No	No
WIL29	ASY2	ASY	Neg	7	Yes	Yes	Yes	No	No	No	No	No	No	No	No	No	No	No
WIL30	ASY2	ASY	Neg	4	Yes	Yes	Yes	Yes	No	No	Yes	No	No	No	No	Yes	Yes	Yes
WIL31	ASY1	ASY	GVA^{III}	6	No	No	Yes	No	Yes	Yes	No	Yes	No	Yes	No	No	No	No
WIL32	N/A	SD	GVA$^{II\&III}$	1	No	No	Yes	No	Yes	Yes	No	Yes	Yes	No	No	No	No	No
WIL33	LRD1	LRD	GVA^{III}, GLRaV-3	8	No	No	Yes	No	Yes	Yes	No	Yes	No	No	No	No	No	No
WIL34	ASY1	ASY	GVA^{III}	7	No	No	Yes	No	Yes	Yes	No	Yes	No	Yes	No	No	No	No
WIL35	LRD1	LRD	GVA^{III}, GLRaV-3	6	No	No	Yes	No	Yes	Yes	No	Yes	No	No	No	No	No	No
WIL36	LRD2	LRD	GLRaV-3	5	No	No	Yes	No	Yes	Yes	No	Yes	No	No	No	No	No	No
WIL37	LRD2	LRD	GLRaV-3	4	No	No	Yes	No	Yes	Yes	No	Yes	No	No	No	No	No	No
WIL38	LRD1	LRD	GVA^{III}, GLRaV-3	7	No	No	Yes	No	Yes	Yes	No	Yes	Yes	No	No	No	No	No
WIL39	ASY1	ASY	GVA^{III}	7	No	No	Yes	No	Yes	Yes	No	Yes	No	Yes	No	No	No	No
WIL40	LRD1	LRD	GVA^{III}, GLRaV-3	6	No	No	Yes	No	Yes	Yes	No	Yes	Yes	No	No	No	No	No
WIL41	LRD2	LRD	GLRaV-3	8	No	No	Yes	No	Yes	Yes	No	Yes	Yes	No	No	No	No	No
WIL42	LRD2	LRD	GLRaV-3	4	No	No	Yes	No	Yes	Yes	No	Yes	No	No	No	No	No	No
WIL43	LRD1	LRD	GVA^{III}, GLRaV-3	6	No	No	Yes	No	Yes	Yes	No	Yes	No	No	No	No	No	No
WIL44	ASY2	ASY	Neg	7	No	No	Yes	No	Yes	Yes	No	Yes	No	Yes	No	No	No	No
WIL45	ASY1	ASY	GVA^{III}	7	No	No	Yes	No	Yes	Yes	No	Yes	No	Yes	No	No	No	No
WIL47	SD1	SD	GVA$^{II\&III}$, GLRaV-3	2	No	No	Yes	No	Yes	Yes	No	Yes	No	Yes	No	No	No	Yes
WIL48	SD2	SD	GVA^{II}, GLRaV-3	1	No	No	Yes	No	Yes	Yes	No	Yes	No	Yes	No	No	No	No
WIL49	SD2	SD	GVA^{II}, GLRaV-3	3	No	No	Yes	No	No	Yes	No	Yes	No	Yes	No	No	No	No
WIL50	SD2	SD	GVA^{II}, GLRaV-3	3	No	No	Yes	No	Yes	Yes	No	Yes	No	No	Yes	No	No	Yes
WIL51*	SD2	SD	GVA^{II}, GLRaV-3	0	No	No	No	No	Yes	Yes	No	Yes	No	No	Yes	No	No	No
WIL52*	SD2	SD	GVA^{II}, GLRaV-3	0	No	No	No	No	No	Yes	No	No	No	No	No	No	No	No

WIL53	SD2	SD	GVA^{II}, GLRaV-3	1	No	No	Yes	No	Yes	Yes	No	Yes	No	No	No	No	No	Yes
WIL54	LRD2	LRD	GLRaV-3	8	No	No	Yes	No	Yes	Yes	No	Yes	Yes	No	Yes	No	No	Yes
WIL55	LRD2	LRD	GLRaV-3	8	No	No	Yes	No	Yes	Yes	No	Yes	Yes	No	Yes	No	No	Yes
WIL56	ASY1	ASY	GVA^{III}	8	No	No	Yes	No	Yes	Yes	No	Yes	Yes	No	No	No	No	No
WIL57	ASY2	ASY	Neg	8	No	No	Yes	No	Yes	Yes	No	Yes	No	No	No	No	No	No
WIL58	ASY2	ASY	Neg	8	No	No	Yes	No	Yes	Yes	No	Yes	No	No	No	No	No	No
WIL59	ASY2	ASY	Neg	7	No	No	Yes	No	Yes	Yes	No	Yes	No	No	No	No	No	No
WIL60	LRD2	LRD	GLRaV-3	8	No	No	Yes	No	Yes	Yes	No	Yes	No	No	No	No	No	No
WIL61	LRD2	LRD	GLRaV-3	6	No	No	Yes	No	Yes	Yes	No	Yes	No	No	Yes	No	No	Yes
WIL62	LRD1	LRD	GVA^{III}, GLRaV-3	7	No	No	Yes	No	Yes	Yes	No	Yes	Yes	No	No	No	No	No
WIL63	LRD2	LRD	GLRaV-3	8	No	No	Yes	No	Yes	Yes	No	Yes	No	No	No	No	No	Yes
WIL64	LRD2	LRD	GLRaV-3	8	No	No	Yes	No	Yes	Yes	No	Yes	No	No	No	No	No	No
WIL65	LRD2	LRD	GLRaV-3	8	No	No	Yes	No	Yes	Yes	No	Yes	Yes	No	No	No	No	No
WIL66	LRD2	LRD	GLRaV-3	7	No	No	Yes	No	Yes	Yes	No	Yes	Yes	No	No	No	No	No
WIL67	LRD1	LRD	GVA^{III}, GLRaV-3	6	No	No	Yes	No	Yes	Yes	No	Yes	Yes	No	Yes	No	No	Yes
WIL68	LRD1	LRD	GVA^{III}, GLRaV-3	6	No	No	Yes	No	Yes	Yes	No	Yes	Yes	No	No	No	No	Yes
WIL69	ASY2	ASY	Neg	8	No	No	Yes	No	Yes	Yes	No	Yes	Yes	No	Yes	No	No	Yes
WIL70	LRD2	LRD	GLRaV-3	8	No	No	Yes	No	Yes	Yes	No	Yes	Yes	Yes	Yes	No	No	No
WIL71	ASY2	ASY	Neg	5	No	No	Yes	No	Yes	Yes	No	Yes	Yes	Yes	Yes	No	No	Yes
WIL72	ASY2	ASY	Neg	8	No	No	Yes	No	Yes	Yes	No	Yes	Yes	No	No	No	No	No
WIL73	LRD2	LRD	GLRaV-3	4	No	No	Yes	No	Yes	Yes	No	Yes	Yes	Yes	No	No	No	Yes
WIL74	ASY2	ASY	Neg	7	No	No	Yes	No	Yes	Yes	No	Yes	Yes	No	Yes	No	No	Yes
WIL75	ASY2	ASY	Neg	7	No	No	Yes	No	Yes	Yes	No	Yes	No	Yes	No	No	No	No
WIL76	ASY2	ASY	Neg	6	No	No	Yes	No	Yes	Yes	No	Yes	No	Yes	No	No	No	No
WIL77	LRD2	LRD	GLRaV-3	8	No	No	Yes	No	Yes	Yes	No	Yes	No	No	Yes	No	No	Yes
WIL78	LRD2	LRD	GLRaV-3	8	No	No	Yes	No	Yes	Yes	No	Yes	No	No	Yes	No	No	Yes
WIL79	LRD2	LRD	GLRaV-3	8	No	No	Yes	No	Yes	Yes	No	Yes	No	No	No	No	No	Yes
WIL80	LRD2	LRD	GLRaV-3	8	No	No	Yes	No	Yes	Yes	No	Yes	No	No	No	No	No	Yes
WIL81	LRD2	LRD	GLRaV-3	8	No	No	Yes	No	Yes	Yes	No	Yes	No	No	No	No	No	Yes
LC1	SD3	SD	GVA^{II}	No	Yes	No		No		No		No				No	No	
LC2	SD3	SD	GVA^{II}		Yes	No		No		No		No				No	No	
LC3	SD3	SD	GVA^{II}		Yes	No		No		No		No				No	No	
LC4	SD3	SD	GVA^{II}		Yes	Yes		Yes		Yes		Yes				Yes	Yes	
LC5	SD3	SD	GVA^{II}		Yes	Yes		Yes		Yes		Yes				Yes	Yes	

LC6	SD3	SD	GVA^{II}	Yes	Yes	Yes	Yes
LC7	SD3	SD	GVA^{II}	Yes	Yes	Yes	Yes
LC8	SD3	SD	GVA^{II}	Yes	Yes	No	No
LC9	SD3	SD	GVA^{II}	Yes	Yes	Yes	Yes
LC10	SD3	SD	GVA^{II}	Yes	Yes	Yes	Yes
LC11	SD3	SD	GVA^{II}	Yes	Yes	Yes	Yes
LC12	SD3	SD	GVA^{II}	Yes	Yes	Yes	Yes
LC13	SD3	SD	GVA^{II}	Yes	Yes	Yes	Yes
LC14	SD3	SD	GVA^{II}	Yes	Yes	Yes	Yes
LC15	SD3	SD	GVA^{II}	Yes	No	No	No
LC16	ASY2	ASY	Neg	Yes	Yes	Yes	Yes
LC17	ASY2	ASY	Neg	Yes	No	No	No
LC18	ASY2	ASY	Neg	Yes	Yes	Yes	Yes
LC19	ASY2	ASY	Neg	Yes	No	No	No
LC20	ASY2	ASY	Neg	Yes	Yes	Yes	Yes
LC21	ASY2	ASY	Neg	Yes	No	No	No
LC22	ASY2	ASY	Neg	Yes	No	No	No
LC23	ASY2	ASY	Neg	Yes	No	No	No
LC24	ASY2	ASY	Neg	Yes	Yes	Yes	Yes
LC25	ASY2	ASY	Neg	Yes	No	No	No
LC26	ASY2	ASY	Neg	Yes	No	No	No
LC27	ASY2	ASY	Neg	Yes	Yes	Yes	Yes
LC28	ASY2	ASY	Neg	Yes	No	No	No
LC29	ASY2	ASY	Neg	Yes	No	No	No
LC30	ASY2	ASY	Neg	Yes	Yes	Yes	Yes

* Grapevines with vine decline symptoms. # Yes = data included, No = data not collected. [1] WIL1 to 81, grapevines from Willunga, WIL 46 was removed by the vineyard manager, LC 1 to 30, grapevines from Langhorne Creek. [2] Grouping system refer to Table 2. [3] SD = Shiraz disease, LRD = leafroll disease, ASY = asymptomatic. [4] GVA^{II} and GVA^{III} = grapevine virus A variants from phylogenetic group II and III, GLRaV-3 = grapevine leafroll-associate virus 3, Neg = negative for both GVA and GLRaV-3.

Table S2. Plant area index (PAI) measured by the Viticanopy app at Langhorne creek (LC) in 2018-19 and Willunga (WIL) from 2019-2021. Date of measurements with matching mean and standard deviations (SDevs) of PAI readings of grapevines in Shiraz disease (SD), Leafroll disease (LRD) and asymptomatic (ASY) groups.

Season, location and Figures	SD[1]				LRD[1]			ASY[1]		
	Date	**Mean**	**SDev**	**n**[2]	**Mean**	**SDev**	**n**	**Mean**	**SDev**	**n**
2018-2019 Langhorne Creek (Figure 4a)	5-Oct-18	0.122301867	0.028280047	15	N/A			0.1177	0.063554001	15
	28-Oct-18	0.191713333	0.05052465	15				0.818126933	0.151658296	15
	6-Nov-18	0.428280567	0.104353897	15				1.511054	0.266993746	15

	15-Nov-18	0.640218	0.107743052	15				1.7828589	0.315785292	15
	28-Nov-18	1.066903767	0.184851877	15				2.470288633	0.32037179	15
	11-Dec-18	1.664929733	0.272558628	15				2.6892885	0.352566927	15
	18-Dec-18	2.1005458	0.368739891	15				2.886383033	0.435595653	15
	4-Jan-19	2.7213147	0.418168378	15				2.8303245	0.283599256	15
2018-2019 Willunga (Figure 4b)	8-Oct-18	0.378538563	0.182192173	8	0.555103714	0.106118273	7	0.548975133	0.102589553	15
	28-Oct-18	0.680279375	0.436341808	8	0.555103714	0.106118273	7	0.548975133	0.102589553	15
	6-Nov-18	1.179351125	0.614552972	8	1.070782357	0.256279113	7	1.046175533	0.255384597	15
	15-Nov-18	1.33054025	0.751376739	8	1.727462214	0.457052996	7	2.1108461	0.522892685	15
	28-Nov-18	1.485832438	1.057338281	8	2.051605214	0.321555103	7	2.1459342	0.501872059	15
	11-Dec-18	1.4538905	0.951389828	8	2.06971	0.690056262	7	2.3844548	0.734111899	15
	18-Dec-18	1.398854813	0.830481465	8	2.447821929	0.476712293	7	2.372756267	0.7213298	15
	4-Jan-19	1.3101825	0.816865094	8	2.343768714	0.547755705	7	2.4701226	0.620164116	15
2019-2020 Willunga (Figure 4c)	11-Oct-19	0.550793583	0.086839046	6	0.587935286	0.142168121	7	0.527676667	0.11851785	15
	22-Nov-19	0.763497	0.416756243	6	1.302710929	0.444216644	7	1.4792422	0.400618008	15
	13-Jan-20	1.45588325	1.035816655	6	1.749906643	0.434551042	7	1.361918533	0.316346961	15
	31-Jan-20	1.578327417	1.127034424	6	1.740311214	0.263762108	7	1.491033033	0.404400835	15
2020-2021 Willunga (Figure 4d)	27-Sep-20	0.368708455	0.091214991	8	0.521535441	0.105296709	17	0.490547052	0.107176677	48
	9-Oct-20	0.365087318	0.079044715	8	0.638632529	0.115737334	17	0.637017698	0.162457259	48
	30-Oct-20	0.476254227	0.197979481	8	1.2021985	0.31340078	17	1.265062	0.260069939	48
	13-Nov-20	0.662605545	0.477727856	8	1.674037971	0.346423194	17	1.682353406	0.438355745	48
	26-Nov-20	0.870757364	0.600288232	8	1.805031088	0.416421092	17	1.787508281	0.420153573	48
	14-Dec-20	1.1868815	0.602991679	8	1.798006971	0.39616026	17	1.73252024	0.49572617	48
	23-Dec-20	1.267276864	0.604354536	8	1.903202235	0.373841226	17	1.860412552	0.425917977	48
	9-Jan-21	1.074128091	0.503029962	8	1.645967588	0.209977683	17	1.685688667	0.38197688	48

[1] SD = Shiraz disease, LRD = leafroll disease, ASY = asymptomatic.

Table S3. Berry development of fresh berry weight, sugar, and pH measured from 2018 to 2021 at the Willunga and Langhorne Creek sites. The highest value in each data set is highlighted in bold. Mean, standard deviation (SDev) and sample size (n) are shown.

			SD[1]			LRD[1]			ASY[1]		
	Season, location and Figures		**Mean**	**SDev**	**n**	**Mean**	**SDev**	**n**	**Mean**	**SDev**	**n**
Berry size (g)	2018-19 Willunga (Figure 8c)	9-Jan-2019	0.66	0.15	5	0.49	0.07	3	0.42	0.08	6
		21-Jan-2019	0.87	0.11	5	0.92	0.11	3	0.69	0.08	6
		5-Feb-2019	1.05	0.07	5	1.15	0.07	3	0.97	0.15	6
		17-Feb-2019	1.13	0.11	5	1.27	0.08	3	1.00	0.18	6
		27-Feb-2019	1.03	0.10	5	0.97	0.22	3	0.83	0.13	6
	2019-20 Willunga (Figure 8e)	18-Feb-2020	0.84	0.06	3	0.91	0.07	7	0.86	0.07	6
		25-Feb-2020	0.94	0.07	3	0.92	0.05	7	0.79	0.09	6
		3-Mar-2020	0.87	0.02	3	0.90	0.04	7	0.78	0.05	6
	2020-21Willunga (Figure 8h)	8-Jan-2021	1.07	0.33	5	1.06	0.10	6	0.91	0.10	15
		15-Jan-2021	1.24	0.43	5	1.30	0.15	6	1.07	0.15	15
		29-Jan-2021	1.35	0.39	5	1.34	0.15	6	1.16	0.20	15
		6-Feb-2021	1.48	0.58	5	1.52	0.15	6	1.29	0.20	15
		15-Feb-2021	1.68	0.61	2	1.31	0.10	6	1.17	0.18	15
		24-Feb-2021	1.42	0.29	2	1.22	0.19	6	1.11	0.23	15
	2018-19 Langhorne Creek (Figure 8a)	9-Jan-2019	0.82	0.16	10	N/A			0.79	0.11	6

		21-Jan-2019	1.11	0.08	10				1.06	0.06	6
		5-Feb-2019	1.50	0.17	10				1.61	0.12	6
		17-Feb-2019	1.91	0.25	10				1.71	0.17	6
		27-Feb-2019	1.60	0.24	10				1.46	0.08	6
Berry TSS (Brix°)	2018-19 Willunga (Figure 8d)	9-Jan-2019	5.70	0.38	5	6.27	0.32	3	6.83	0.75	6
		21-Jan-2019	10.48	2.18	5	12.13	0.98	3	12.58	1.58	6
		5-Feb-2019	18.64	1.62	5	19.10	0.66	3	20.88	1.36	6
		17-Feb-2019	22.12	0.85	5	21.80	0.79	3	23.95	1.18	6
		27-Feb-2019	25.36	1.14	5	26.53	0.38	3	28.85	0.65	6
	2019-20 Willunga (Figure 8f)	18-Feb-2020	18.93	2.10	3	19.14	0.41	7	19.85	0.60	6
		25-Feb-2020	22.33	1.27	3	22.33	0.71	7	23.67	0.72	6
		3-Mar-2020	22.30	2.13	3	22.09	0.46	7	23.43	0.63	6
	2020-21Willunga (Figure 8i)	8-Jan-2021	8.30	2.50	5	12.42	0.95	6	12.21	1.52	15
		15-Jan-2021	11.84	2.85	5	15.77	0.84	6	15.38	0.96	15
		29-Jan-2021	15.18	3.05	5	18.23	0.54	6	18.22	1.02	15
		6-Feb-2021	17.72	1.27	5	19.80	0.54	6	19.95	1.07	15
		15-Feb-2021	21.50	0.99	2	23.15	0.41	6	22.53	0.89	15
		24-Feb-2021	23.45	0.49	2	25.28	0.92	6	25.39	1.05	15
	2018-19 Langhorne Creek (Figure 8b)	9-Jan-2019	4.12	0.29	10				4.63	0.18	6
		21-Jan-2019	4.67	0.49	10				5.13	0.60	6
		5-Feb-2019	10.73	1.38	10				14.17	1.16	6
		17-Feb-2019	16.01	1.53	10				16.10	1.60	6
		27-Feb-2019	19.10	1.52	10	N/A			20.82	1.22	6
	2019-20 Willunga (Figure 8g)	18-Feb-2020	3.22	0.04	3	3.41	0.05	7	3.40	0.03	6
		25-Feb-2020	3.47	0.04	3	3.55	0.03	7	3.61	0.03	6
		3-Mar-2020	3.40	0.06	3	3.46	0.06	7	3.51	0.03	6
	2020-21Willunga (Figure 8j)	8-Jan-2021	2.80	0.14	5	2.96	0.04	6	2.94	0.07	15
		15-Jan-2021	2.75	0.16	5	2.94	0.02	6	2.93	0.06	15
		29-Jan-2021	2.84	0.23	5	3.09	0.03	6	3.08	0.05	15
		6-Feb-2021	2.90	0.19	5	3.20	0.08	6	3.21	0.07	15
		15-Feb-2021	3.29	0.08	2	3.42	0.03	6	3.38	0.06	15
		24-Feb-2021	3.34	0.11	2	3.39	0.07	6	3.42	0.08	15

[1] SD = Shiraz disease, LRD = leafroll disease, ASY = asymptomatic. [2] n = sample size.

Table S4. The P and R-squared values (R^2) of Figure 5. P values were obtained using the null hypothesis value of 0.

Date	27/9/2020	9/10/2020	30/10/2020	13/11/2020	26/11/2020	14/12/2020	23/12/2020	9/1/2021
P value (VHS 0-4)	0.0303	0.0001	<0.0001	<0.0001	<0.0001	<0.0001	<0.0001	<0.0001
P value (VHS 4-8)	0.6908	0.2421	0.0071	0.2973	0.1372	0.2378	0.0359	0.0218
R^2	0.219	0.406	0.6747	0.6028	0.6119	0.4467	0.5315	0.5892

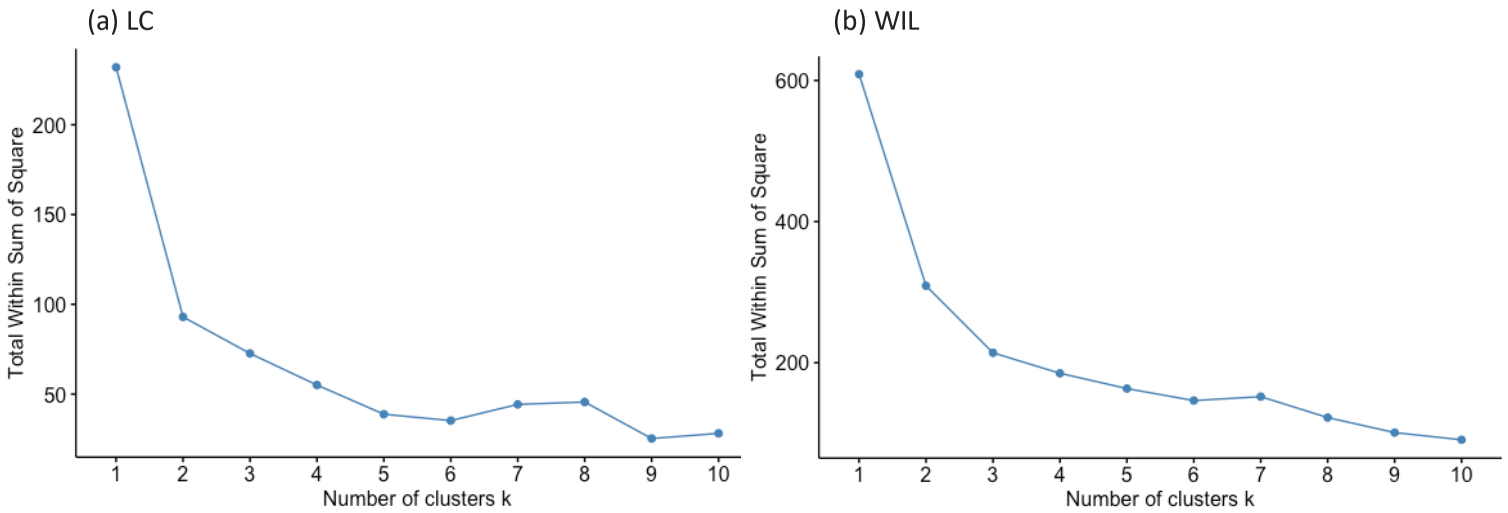

Figure S1. Elbow method for identifying the optional number of clusters to be used in Kmeans clustering. Plots of total within sum of square vs. number of clusters for the (a) Langhorne Creek (LC) and (b) Willunga (WIL) data sets.

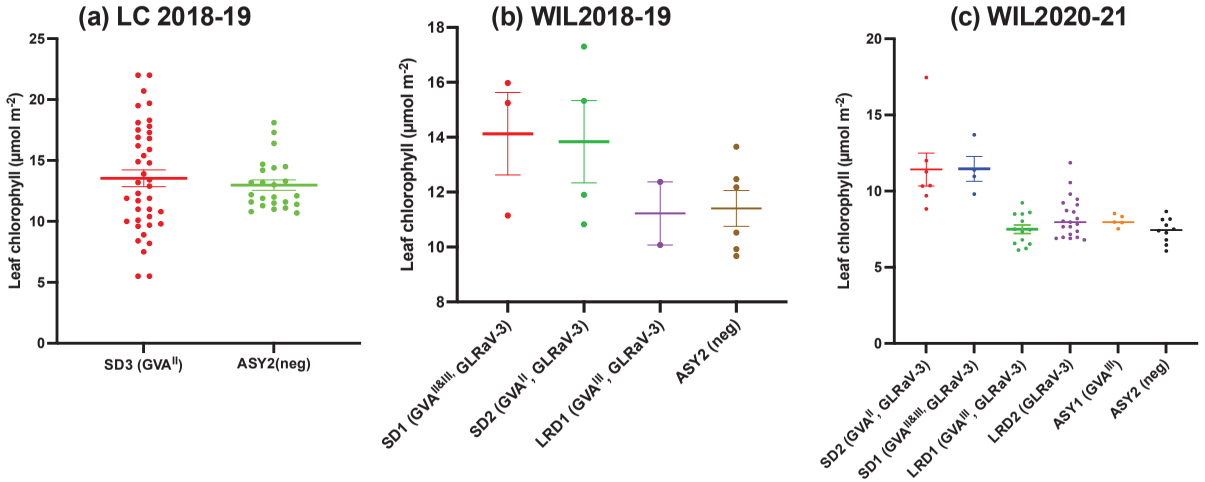

Figure S2. Leaf chlorophyll (Chl) of grapevines with Shiraz disease (SD1, 2 and 3), leafroll disease (LRD 1and 2) symptoms and asymptomatic grapevines (ASY1 and 2) in the 2018-19 and 2020-21 growing seasons at the Willunga (WIL) and Langhorne Creek (LC) sites. Leaf Chl of (a) LC grapevines in the 2018-19 season, (b) WIL grapevines in the 2018-19 season, and (c) WIL grapevines in the 2020-21 season. Data was analysed by the Welch's ANOVA and Dunett's T3 tests (Table 3). The line and error bars represent the mean and standard deviations (SDevs) of each group, respectively.

7. References (Chapter 4)

1. Espinoza, C.; Vega, A.; Medina, C.; Schlauch, K.; Cramer, G.; Arce-Johnson, P. Gene expression associated with compatible viral diseases in grapevine cultivars. *Funct. Integr. Genomics* **2007**, *7*, 95-110, doi:10.1007/s10142-006-0031-6.
2. Gambino, G.; Cuozzo, D.; Fasoli, M.; Pagliarani, C.; Vitali, M.; Boccacci, P.; Pezzotti, M.; Mannini, F. Co-evolution between grapevine rupestris stem pitting-associated virus and Vitis vinifera L. leads to decreased defence responses and increased transcription of genes related to photosynthesis. *J. Exp. Bot.* **2012**, *63*, 5919-5933, doi:10.1093/jxb/ers244.
3. Gutha, L.R.; Casassa, L.F.; Harbertson, J.F.; Naidu, R.A. Modulation of flavonoid biosynthetic pathway genes and anthocyanins due to virus infection in grapevine (Vitis vinifera L.) leaves. *BMC Plant Biol.* **2010**, *10*, 187.
4. Tobar, M.; Fiore, N.; Pérez-Donoso, A.G.; León, R.; Rosales, I.M.; Gambardella, M. Divergent molecular and growth responses of young "Cabernet Sauvignon"(Vitis vinifera) plants to simple and mixed infections with grapevine rupestris stem pitting-associated virus. *Hortic. Res.* **2020**, *7*, 1-14, doi:10.1038/s41438-019-0224-5.
5. Swamy, P.; Pattathil, S.; Unda, F.; Mansfield, S.D. Grapevine red blotch disease affects carbohydrate homeostasis and cell call characteristics in Vitis vinifera L. *Res. Sq. Prepr.* **2021**, doi:10.21203/rs.3.rs-428067/v1.
6. Song, Y.; Hanner, R.H.; Meng, B. Probing into the effects of grapevine leafroll-associated viruses on the physiology, fruit quality and gene expression of grapes. *Viruses* **2021**, *13*, 593, doi:10.3390/v13040593.
7. Vondras, A.M.; Lerno, L.; Massonnet, M.; Minio, A.; Rowhani, A.; Liang, D.; Garcia, J.; Quiroz, D.; Figueroa-Balderas, R.; Golino, D.A. Rootstock influences the effect of grapevine leafroll-associated viruses on berry development and metabolism via abscisic acid signalling. *Mol. Plant Pathol.* **2021**, *22*, 984-1005, doi:10.1111/mpp.13077.
8. Wallis, C.M.; Sudarshana, M.R. Effects of grapevine red blotch-associated virus (GRBaV) infection on foliar metabolism of grapevines. *Can. J. Plant Pathol.* **2016**, *38*, 358-366, doi:10.1080/07060661.2016.1227374.
9. Guidoni, S.; Mannini, F.; Ferrandino, A.; Argamante, N.; Di Stefano, R. The effect of grapevine leafroll and rugose wood sanitation on agronomic performance and berry and leaf phenolic content of a Nebbiolo clone (Vitis vinifera L.). *Am. J. Enol. Vitic.* **1997**, *48*, 438-442.
10. Cabaleiro, C.; Segura, A.; Garcia-Berrios, J.J. Effects of grapevine leafroll-associated virus 3 on the physiology and must of Vitis vinifera L. cv. Albarino following contamination in the field. *Am. J. Enol. Vitic.* **1999**, *50*, 40-44.
11. Komar, V.; Vigne, E.; Demangeat, G.; Fuchs, M. Beneficial effect of selective virus elimination on the performance of Vitis vinifera cv. Chardonnay. *Am. J. Enol. Vitic.* **2007**, *58*, 202-210.
12. Giribaldi, M.; Purrotti, M.; Pacifico, D.; Santini, D.; Mannini, F.; Caciagli, P.; Rolle, L.; Cavallarin, L.; Giuffrida, M.G.; Marzachì, C. A multidisciplinary study on the effects of phloem-limited viruses on the agronomical performance and berry quality of Vitis vinifera cv. Nebbiolo. *J. Proteomics* **2011**, *75*, 306-315, doi:10.1016/j.jprot.2011.08.006.
13. Mannini, F.; Mollo, A.; Credi, R. Field performance and wine quality modification in a clone of Vitis vinifera cv. Dolcetto after GLRaV-3 elimination. *Am. J. Enol. Vitic.* **2012**, *63*, 144-147, doi:10.5344/ajev.2011.11020.
14. Moutinho-Pereira, J.; Correia, C.M.; Gonçalves, B.; Bacelar, E.A.; Coutinho, J.F.; Ferreira, H.F.; Lousada, J.L.; Cortez, M.I. Impacts of leafroll-associated viruses (GLRaV-1 and-3) on the physiology of the Portuguese grapevine cultivar 'Touriga Nacional'growing under field conditions. *Ann. Appl. Biol.* **2012**, *160*, 237-249, doi:10.1111/j.1744-7348.2012.00536.x.
15. Endeshaw, S.T.; Sabbatini, P.; Romanazzi, G.; Schilder, A.C.; Neri, D. Effects of grapevine leafroll associated virus 3 infection on growth, leaf gas exchange, yield and basic fruit chemistry of Vitis vinifera L. cv. Cabernet Franc. *Sci. Hortic.* **2014**, *170*, 228-236, doi:10.1016/j.scienta.2014.03.021.
16. Bota, J.; Cretazzo, E.; Montero, R.; Rosselló, J.; Cifre, J. Grapevine fleck virus (GFkV) elimination in a selected clone of Vitis vinifera L. cv. Manto negro and its effects on photosynthesis. *J. Int. Sci. Vigne Vin* **2014**, *48*, 11-19.
17. El Aou-ouad, H.; Montero, R.; Medrano, H.; Bota, J. Interactive effects of grapevine leafroll-associated virus 3 (GLRaV-3) and water stress on the physiology of Vitis vinifera L. cv. Malvasia de Banyalbufar and Giro-Ros. *J. Plant Physiol.* **2016**, *196*, 106-115, doi:10.1016/j.jplph.2016.04.003.

18. El Aou-ouad, H.; Pou, A.; Tomás, M.; Montero, R.; Ribas-Carbo, M.; Medrano, H.; Bota, J. Combined effect of virus infection and water stress on water flow and water economy in grapevines. *Physiol. Plant.* **2017**, *160*, 171-184, doi:10.1111/ppl.12541.
19. Reynard, J.-S.; Brodard, J.; Dubuis, N.; Zufferey, V.; Schumpp, O.; Schaerer, S.; Gugerli, P. Grapevine red blotch virus: Absence in Swiss vineyards and analysis of potential detrimental effect on viticultural performance. *Plant Dis.* **2018**, *102*, 651-655, doi:10.1094/PDIS-07-17-1069-RE.
20. Halldorson, M.M.; Keller, M. Grapevine leafroll disease alters leaf physiology but has little effect on plant cold hardiness. *Planta* **2018**, *248*, 1201-1211, doi:10.1007/s00425-018-2967-x.
21. Girardello, R.C.; Cooper, M.L.; Smith, R.J.; Lerno, L.A.; Bruce, R.C.; Eridon, S.; Oberholster, A. Impact of grapevine red blotch disease on grape composition of Vitis vinifera Cabernet Sauvignon, Merlot, and Chardonnay. *J. Agric. Food Chem.* **2019**, *67*, 5496-5511, doi:10.1021/acs.jafc.9b01125.
22. Bowen, P.; Bogdanoff, C.; Poojari, S.; Usher, K.; Lowery, T.; Úrbez-Torres, J.R. Effects of grapevine red blotch disease on Cabernet franc vine physiology, bud hardiness, and fruit and wine quality. *Am. J. Enol. Vitic.* **2020**, *71*, 308-318, doi:10.5344/ajev.2020.20011.
23. Copp, C.R.; Levin, A.D. Irrigation improves vine physiology and fruit composition in grapevine red blotch virus-infected Vitis vinifera L. *Am. J. Enol. Vitic.* **2021**, *72*, 307-317, doi:10.5344/ajev.2021.21007.
24. Jež-Krebelj, A.; Rupnik-Cigoj, M.; Stele, M.; Chersicola, M.; Pompe-Novak, M.; Sivilotti, P. The physiological impact of GFLV virus infection on grapevine water status: First observations. *Plants* **2022**, *11*, 161, doi:10.3390/plants11020161.
25. Wu, Q.; Habili, N.; Kinoti, W.M.; Tyerman, S.D.; Rinaldo, A.; Zheng, L.; Constable, F.E. A Metagenomic Investigation of the Viruses Associated with Shiraz Disease in Australia. *Viruses* **2023**, *15*, 1-21, doi:10.3390/v15030774.
26. Caravia, L.; Collins, C.; Petrie, P.R.; Tyerman, S.D. Application of shade treatments during Shiraz berry ripening to reduce the impact of high temperature. *Aust. J. Grape Wine Res.* **2016**, *22*, 422-437, doi:10.1111/ajgw.12248.
27. Chen, J.M.; Black, T.A.; Adams, R.S. Evaluation of hemispherical photography for determining plant area index and geometry of a forest stand. *Agric. For. Meteorol.* **1991**, *56*, 129-143.
28. De Bei, R.; Fuentes, S.; Gilliham, M.; Tyerman, S.; Edwards, E.; Bianchini, N.; Smith, J.; Collins, C. VitiCanopy: A free computer App to estimate canopy vigor and porosity for grapevine. *Sensors* **2016**, *16*, 585, doi:10.3390/s16040585.
29. Turner, N.C. Measurement of plant water status by the pressure chamber technique. *Irrig. Sci.* **1988**, *9*, 289-308.
30. Boyer, J.S. Leaf water potentials measured with a pressure chamber. *Plant Physiol.* **1967**, *42*, 133-137.
31. Edwards, E.J.; Downie, A.F.; Clingeleffer, P.R. A simple microplate assay to quantify nonstructural carbohydrates of grapevine tissues. *Am. J. Enol. Vitic.* **2011**, *62*, 133-137, doi:10.5344/ajev.2010.10051.
32. Tomarken, A.J.; Serlin, R.C. Comparison of ANOVA alternatives under variance heterogeneity and specific noncentrality structures. *Psychol. Bull.* **1986**, *99*, 90-99.
33. Dunnett, C.W. Pairwise multiple comparisons in the unequal variance case. *J. Amer. Statistical Assoc.* **1980**, *75*, 796-800.
34. Kassambara, A. *Practical guide to cluster analysis in R: Unsupervised machine learning*, 1st ed.; Statistical Tools for High-throughput Data Analysis (STHDA): 2017.
35. Wickham, H. *ggplot2: elegant graphics for data analysis*, 2nd ed.; Wickham, H., Ed.; Springer: 2016.
36. Kim, H.-Y. Statistical notes for clinical researchers: post-hoc multiple comparisons. *Restor. Dent. Endod.* **2015**, *40*, 172-176, doi:10.5395/rde.2015.40.2.172.
37. Hrycan, J.; Hart, M.; Bowen, P.; Forge, T.; Urbez-Torres, J.R. Grapevine trunk disease fungi: their roles as latent pathogens and stress factors that favour disease develop-ment and symptom expression. *Phytopathol. Mediterr.* **2020**, *59*, 395-424, doi:10.14601/Phyto-11275.
38. Baumgartner, K.; Hillis, V.; Lubell, M.; Norton, M.; Kaplan, J. Managing grapevine trunk diseases in California's southern San Joaquin Valley. *Am. J. Enol. Vitic.* **2019**, *70*, 267-276, doi:10.5344/ajev.2019.18075.
39. Fontaine, F.; Pinto, C.; Vallet, J.; Clément, C.; Gomes, A.C.; Spagnolo, A. The effects of grapevine trunk diseases (GTDs) on vine physiology. *Eur. J. Plant Pathol.* **2016**, *144*, 707-721, doi:10.1007/s10658-015-0770-0.
40. Fang, H.; Baret, F.; Plummer, S.; Schaepman-Strub, G. An overview of global leaf area index (LAI): Methods, products, validation, and applications. *Reviews of Geophysics* **2019**, *57*, 739-799, doi:10.1029/2018RG000608.
41. De Bei, R.; Kidman, C.; Wotton, C.; Shepherd, J.; Fuentes, S.; Gilliham, M.; Tyerman, S.; Collins, C. Canopy architecture is linked to grape and wine quality in Australian Shiraz. Wine Australia. Available

online: https://www.wineaustralia.com/news/articles/canopy-management-to-optimise-performance (accessed on 20 July 2022).
42. Taskos, D.G.; Koundouras, S.; Stamatiadis, S.; Zioziou, E.; Nikolaou, N.; Karakioulakis, K.; Theodorou, N. Using active canopy sensors and chlorophyll meters to estimate grapevine nitrogen status and productivity. *Precis. Agric.* **2015**, *16*, 77-98, doi:10.1007/s11119-014-9363-8.
43. Croft, H.; Chen, J.M.; Luo, X.; Bartlett, P.; Chen, B.; Staebler, R.M. Leaf chlorophyll content as a proxy for leaf photosynthetic capacity. *Glob. Chang. Biol.* **2017**, *23*, 3513-3524, doi:10.1111/gcb.13599.
44. Christov, I.; Stefanov, D.; Velinov, T.; Goltsev, V.; Georgieva, K.; Abracheva, P.; Genova, Y.; Christov, N. The symptomless leaf infection with grapevine leafroll associated virus 3 in grown in vitro plants as a simple model system for investigation of viral effects on photosynthesis. *J. Plant Physiol.* **2007**, *164*, 1124-1133, doi:10.1016/j.jplph.2005.11.016.
45. Bertamini, M.; Muthuchelian, K.; Nedunchezhian, N. Effect of grapevine leafroll on the photosynthesis of field grown grapevine plants (Vitis vinifera L. cv. Lagrein). *J. Phytopathol.* **2004**, *152*, 145-152.
46. Bennett, J.; Jarvis, P.; Creasy, G.L.; Trought, M.C.T. Influence of defoliation on overwintering carbohydrate reserves, return bloom, and yield of mature Chardonnay grapevines. *Am. J. Enol. Vitic.* **2005**, *56*, 386-393.
47. Zufferey, V.; Murisier, F.; Vivin, P.; Belcher, S.; Lorenzini, F.; Spring, J.-L.; Viret, O. Carbohydrate reserves in grapevine (Vitis vinifera L.'Chasselas'): the influence of the leaf to fruit ratio. *Vitis* **2012**, *51*, 103-110.
48. Field, S.K.; Smith, J.P.; Holzapfel, B.P.; Hardie, W.J.; Emery, R.J.N. Grapevine response to soil temperature: xylem cytokinins and carbohydrate reserve mobilization from budbreak to anthesis. *Am. J. Enol. Vitic.* **2009**, *60*, 164-172.
49. De Bei, R.; Fuentes, S.; Sullivan, W.; Edwards, E.J.; Tyerman, S.; Cozzolino, D. Rapid measurement of total non-structural carbohydrate concentration in grapevine trunk and leaf tissues using near infrared spectroscopy. *Comput. Electron. Agric.* **2017**, *136*, 176-183, doi:10.1016/j.compag.2017.03.007.
50. Gilardi, G.; Chitarra, W.; Moine, A.; Mezzalama, M.; Boccacci, P.; Pugliese, M.; Gullino, M.L.; Gambino, G. Biological and molecular interplay between two viruses and powdery and downy mildews in two grapevine cultivars. *Hortic. Res.* **2020**, *7*, 188, doi:10.1038/s41438-020-00413-x.
51. Dry, P.; Loveys, B. Grapevine shoot growth and stomatal conductance are reduced when part of the root system is dried. **1999**.
52. Sadras, V.; Montoro, A.; Moran, M.; Aphalo, P. Elevated temperature altered the reaction norms of stomatal conductance in field-grown grapevine. *Agric. For. Meteorol.* **2012**, *165*, 35-42.
53. Soar, C.J.; Collins, M.J.; Sadras, V.O. Irrigated Shiraz vines (Vitis vinifera) upregulate gas exchange and maintain berry growth in response to short spells of high maximum temperature in the field. *Funct. Plant Biol.* **2009**, *36*, 801-814.
54. Soar, C.J.; Speirs, J.; Maffei, S.; Penrose, A.; McCarthy, M.G.; Loveys, B. Grape vine varieties Shiraz and Grenache differ in their stomatal response to VPD: apparent links with ABA physiology and gene expression in leaf tissue. *Aust. J. Grape Wine Res.* **2006**, *12*, 2-12.
55. Soar, C.J.; Dry, P.R.; Loveys, B.R. Scion photosynthesis and leaf gas exchange in Vitis vinifera L. cv. Shiraz: mediation of rootstock effects via xylem sap ABA. *Aust. J. Grape Wine Res.* **2006**, *12*, 82-96.
56. Winkel, T.; Rambal, S. Stomatal conductance of some grapevines growing in the field under a Mediterranean environment. *Agric. For. Meteorol.* **1990**, *51*, 107-121.
57. Bonada, M.; Buesa, I.; Moran, M.A.; Sadras, V.O. Interactive effects of warming and water deficit on Shiraz vine transpiration in the Barossa Valley, Australia. *OENO one* **2018**, *52*, 189-202, doi:10.20870/oeno-one.2018.52.2.2141.
58. Li, G.; Chen, T.; Zhang, Z.; Li, B.; Tian, S. Roles of aquaporins in plant-pathogen interaction. *Plants* **2020**, *9*, 1134, doi:10.3390/plants9091134.
59. Coupel-Ledru, A.; Lebon, É.; Christophe, A.; Doligez, A.; Cabrera-Bosquet, L.; Péchier, P.; Hamard, P.; This, P.; Simonneau, T. Genetic variation in a grapevine progeny (Vitis vinifera L. cvs Grenache× Syrah) reveals inconsistencies between maintenance of daytime leaf water potential and response of transpiration rate under drought. *J. Exp. Bot.* **2014**, *65*, 6205-6218, doi:10.1093/jxb/eru228.
60. De Bei, R.; Cozzolino, D.; Sullivan, W.; Cynkar, W.; Fuentes, S.; Dambergs, R.; Pech, J.; Tyerman, S. Non-destructive measurement of grapevine water potential using near infrared spectroscopy. *Aust. J. Grape Wine Res.* **2011**, *17*, 62-71, doi:10.1111/j.1755-0238.2010.00117.x.
61. Calvi, B.L. Effects of red-leaf disease on Cabernet Sauvignon at the Oakville experimental vineyard and mitigation by harvest delay and crop adjustment. University of California, Davis, 2011.

62. Chitarra, W.; Cuozzo, D.; Ferrandino, A.; Secchi, F.; Palmano, S.; Perrone, I.; Boccacci, P.; Pagliarani, C.; Gribaudo, I.; Mannini, F. Dissecting interplays between Vitis vinifera L. and grapevine virus B (GVB) under field conditions. *Mol. Plant Pathol.* **2018**, *19*, 2651-2666, doi:10.1111/mpp.12735.
63. Poni, S.; Casalini, L.; Bernizzoni, F.; Civardi, S.; Intrieri, C. Effects of early defoliation on shoot photosynthesis, yield components, and grape composition. *Am. J. Enol. Vitic.* **2006**, *57*, 397-407.
64. Moutinho-Pereira, J.; Correia, C.; Gonçalves, B.; Bacelar, E.; Coutinho, J.; Ferreira, H.; Lousada, J.; Cortez, M. Impacts of leafroll-associated viruses (GLRaV-1 and-3) on the physiology of the P ortuguese grapevine cultivar 'T ouriga N acional'growing under field conditions. *Ann. Appl. Biol.* **2012**, *160*, 237-249.
65. Moutinho-Pereira, J.; Correia, C.M.; Gonçalves, B.; Bacelar, E.A.; Coutinho, J.F.; Ferreira, H.F.; Lousada, J.L.; Cortez, M.I. Impacts of leafroll-associated viruses (GLRaV-1 and-3) on the physiology of the P ortuguese grapevine cultivar 'T ouriga N acional'growing under field conditions. *Ann. Appl. Biol.* **2012**, *160*, 237-249, doi:10.1111/j.1744-7348.2012.00536.x.
66. Martínez-Lüscher, J.; Plank, C.M.; Brillante, L.; Cooper, M.L.; Smith, R.J.; Al-Rwahnih, M.; Yu, R.; Oberholster, A.; Girardello, R.; Kurtural, S.K. Grapevine red blotch virus may reduce carbon translocation leading to impaired grape berry ripening. *J. Agric. Food Chem.* **2019**, *67*, 2437-2448, doi:10.1021/acs.jafc.8b05555.
67. Ashraf, M.; Harris, P.J.C. Photosynthesis under stressful environments: an overview. *Photosynthetica* **2013**, *51*, 163-190, doi:10.1007/s11099-013-0021-6.
68. Balachandran, S.; Hurry, V.M.; Kelley, S.E.; Osmond, C.B.; Robinson, S.A.; Rohozinski, J.; Seaton, G.G.R.; Sims, D.A. Concepts of plant biotic stress. Some insights into the stress physiology of virus-infected plants, from the perspective of photosynthesis. *Physiol. Plant.* **1997**, *100*, 203-213.
69. Iannini, C.; Mattii, G.B.; Rivelli, A.R.; Rotundo, A. Leaf removal and cluster thinning trials in Aglianico grapevine. *Acta Hortic.* **2005**, *754*, 241–248.
70. Bonada, M.; Sadras, V.O.; Fuentes, S. Effect of elevated temperature on the onset and rate of mesocarp cell death in berries of Shiraz and Chardonnay and its relationship with berry shrivel. *Aust. J. Grape Wine Res.* **2013**, *19*, 87-94, doi:10.1111/ajgw.12010.
71. Tilbrook, J.; Tyerman, S.D. Cell death in grape berries: varietal differences linked to xylem pressure and berry weight loss. *Funct. Plant Biol.* **2008**, *35*, 173-184, doi:10.1071/FP07278.
72. Xiao, Z.; Rogiers, S.Y.; Sadras, V.O.; Tyerman, S.D. Hypoxia in grape berries: the role of seed respiration and lenticels on the berry pedicel and the possible link to cell death. *J. Exp. Bot.* **2018**, *69*, 2071-2083, doi:10.1093/jxb/ery039.
73. Xiao, Z.; Liao, S.; Rogiers, S.Y.; Sadras, V.O.; Tyerman, S.D. Berry Cell death: Are berries suffocating to death under high temperature and water stress? *Wine and Viticulture J.* **2019**, *34*, 42-45, doi:10.1007/s00271-010-0252-2.
74. Cao, S.; Xiao, Z.; Jiranek, V.; Tyerman, S.D. The VvBAP1 gene is identified as a potential inhibitor of cell death in grape berries. *Funct. Plant Biol.* **2019**, *46*, 428-442, doi:10.1071/FP18272.
75. Walker, R.R.; Read, P.E.; Blackmore, D.H. Rootstock and salinity effects on rates of berry maturation, ion accumulation and colour development in Shiraz grapes. *Aust. J. Grape Wine Res.* **2000**, *6*, 227-239.
76. Kuhn, N.; Guan, L.; Dai, Z.W.; Wu, B.-H.; Lauvergeat, V.; Gomès, E.; Li, S.-H.; Godoy, F.; Arce-Johnson, P.; Delrot, S. Berry ripening: recently heard through the grapevine. *J. Exp. Bot.* **2013**, *65*, 4543-4559, doi:10.1093/jxb/ert395.
77. Goszczynski, D.E. Single-strand conformation polymorphism (SSCP), cloning and sequencing reveal a close association between related molecular variants of Grapevine virus A (GVA) and Shiraz disease in South Africa. *Plant Pathol.* **2007**, *56*, 755-762, doi:10.1111/j.1365-3059.2007.01624.x.

Chapter 5: Evaluating the Impact of Shiraz Disease on Wine Composition and Fermentation Products

1. Introduction

The previous chapters described Shiraz disease (SD) and leafroll disease (LRD) in two South Australian vineyards, Willunga (WIL) and Langhorne Creek (LC) including disease symptoms, the virome of the vineyards with focus on the phylogenetic groups of the core pathogen, grapevine virus A (GVA), and analysis on how SD affects the physiological performance of a grapevine. Chapter 4 presents research aimed to understand how SD affects the physiological performance of a grapevine. This chapter provides a preliminary insight on how GVA infection may affect wine quality since no research on wine composition of SD-affected berries is available in the literature. Previous research has focused on grapevine leafroll associated viruses (GLRaVs) [1-3] and grapevine red blotch virus (GRBV) [4-6] that are thought to be economically important grapevine viruses worldwide. Virus infection can result in less vigorous and low yielding grapevines [7], and reduced total soluble solids (TSS) and colour density in berries likely translating to reduced alcohol and colour intensity, as well as changing sensory characteristics of the wine [6]. However, the consequences of a virus infection highly depend on cultivars, genetic differences of the viruses, the growing conditions of the grapevines, when measurements were conducted, and how wines were made. In a GLRaV-3 study, reduced yield and field performance were observed, however almost no effect of virus infection was reported on wine sensory profiles [7]. In contrast, multiple virus infections (GLRaV-1, GVA and GRSPaV) of *Vitis vinifera* cv. Nebbiolo did not affect yield but had a significant impact on berry quality [8]. Grapevines are frequently infected with multiple viruses, and in the present research, distinct GVA variants were detected on the same grapevine (Chapter 2) adding complexity to the analysis. While performing physiological measurements and wine analysis, most earlier studies used PCR or ELISA-based virus detection methods, which did not provide comprehensive genetic information of the viruses studied. In contrast, the present research aims to examine which variations in wine composition and fermentation products were likely caused by SD or even distinct variants of SD-associated GVA.

2. Materials and Methods

2.1. Grapevine selection

The grapevines selected for this study (Table 1) were located in a vineyard affected by both SD and grapevine trunk diseases (GTDs) at Willunga (-35° 15' 58.5468" S and 138° 29' 39.7464" E) (Chapter 4). Information on the rainfall, temperature, soil type, and irrigation conditions of this vineyard can be found in Chapter 4. SD-affected grapevines were selected based on the SD symptoms described in Chapter 2, and were compared to grapevines that were SD unaffected (NSD) to measure the effect of SD on wine quality.

To minimised the impact of abiotic conditions and management practices, NSD grapevines that were geographically close (neighbouring row) to the SD grapevines were selected. Grapevines in the three NSD groups (i.e. NSD1, NSD2, and NSD3) are all paired control grapevines randomly selected from the neighbouring row of the SD grapevines (Table 1). It is worth noting that this experiment has only one biological replicate for the SD group due to poor yields of the SD grapevines. Berries

of grapevines from the same group were pooled together and 4 ferments (technical replicates) were conducted per group, resulting in a total of 16 wine ferments. Table 1 provides the names of wine groups and replicates, yield composition (berry weight) from each grapevine and its corresponding grapevine virus profiles. The virus status of the grapevines was determined by metagenomics high throughput sequencing (Meta-HTS) and/or RT-PCR as described in Chapter 2.

2.2. Berry harvesting

Berries were harvested between E-L stage 38 (berries harvest-ripe) to 39 (berries over-ripe) from the WIL site on the 24th of February 2021 when predicted Brix was about 26 using weekly berry monitoring data (Chapter 4, Table S3). A total of 4.3 kg of berries were harvested for each group aiming for 16 ferments, 4 replicates per group with 900 g of berries each ferment. They sampled bunches were stored at 4°C overnight.

2.3. Ferment preparation

Ferments were prepared using the method described by Holt, *et al.* [9] with minor modifications as follows: the second day after harvest, bunch and berry stems were carefully removed, and 300 berries were randomly sampled to measure 100-berries weights. Each 900 g of berries was weighed in a 1.5-liter glass jar, and 20 ppm of SO_2 (as potassium metabisulphite) was added to the berries before crushing with a potato masher. After crushing, 25 ml of juice was used for measuring TSS, pH, and titratable acidity (TA) prior to fermentation. On the third day after crushing (must stored at 4°C.), the jars were placed in a laminar flow for at least one hour prior to inoculation to allow ferments to warn up to room temperature. Prior to yeast inoculation, 200 ppm of diammonium phosphate (DAP) was added to each ferment.

2.4. Yeast culturing and inoculation

The yeast *Saccharomyces cerevisiae* strain AWRI-838 (a robust industrial strain) was kindly provided by the Australian Wine Research Institute (AWRI) microorganism culture collection. Yeast was cultured at 28°C in yeast extract peptone dextrose (YPD) for 24 hours with agitation and then grown in a sterile 50% Chardonnay juice for 48 hours. The concentration of the yeast was determined using a hemocytometer and predicted based on the formula described by Holt, Iland and Ristic [9]. Ferments were inoculated to a final concentration of $1x\ 10^6$ yeast cells per ml and incubated in a 17C° room for 14 days.

2.5. Fermentation monitoring

Ferments were plunged with a potato masher at least twice daily, and the total weight and total soluble solids (TSS) of each ferment were measured and recorded daily. TSS was measured using a refractometer. Remaining sugars was monitored with AimTab™ tablets when TSS was less than 5%, following the manufacturer's instruction.

2.6. Grape pressing

After 14 days of fermentation, ferments were pressed and racked into fresh Schott bottles. A mini grape press was cleaned and rinsed with hot water prior to use (Figure 1, step 1). An electric drill was connected to facilitate even pressing (Figure 1, step 2). The Schott bottles were

autoclaved and prefilled with a small amount of dry ice and connected to the grape press with a plastic pipe (Figure 1, step 3). Wine juice flowed, into the bottle when the drill was operating (Figure 1, step 4). After pressing a small amount of dry ice was added to the top of each ferment to displace air. The bottles were sealed with a fermenting lid and a U-shape gas trap containing sterile water (Figure 1, step 5). The ferments were stored in a 17C° incubation room until the fermentation was completed which was determined by TSS being less than 0.25%.

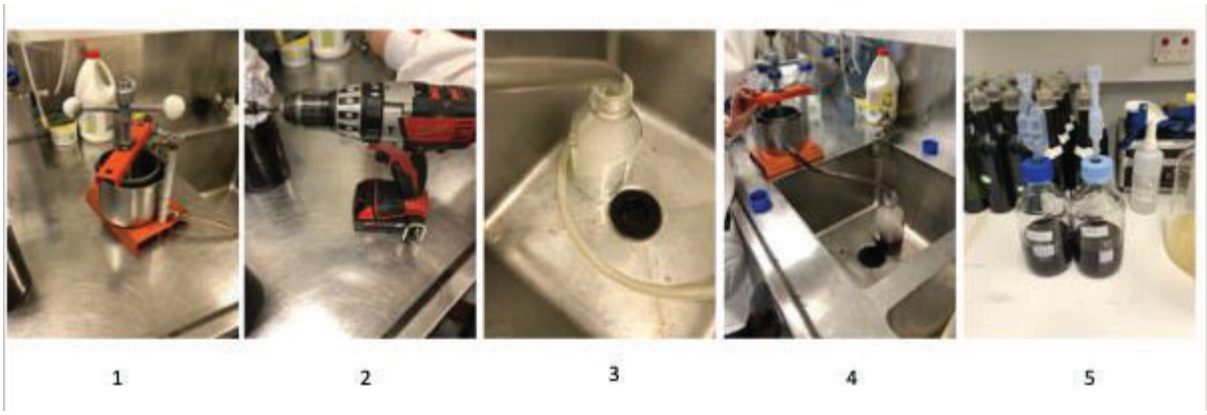

Figure 1. Process of pressing the berries using a grape press with an electric drill.

2.7. Cold settling and wine ranking

Finished wines were sealed and placed in a 4°C cold room for 14 days to cold settle. Subsequently 50 mL of the clear wine from the top of the bottles was poured into test tubes and sent to The Australian Wine Research Institute (AWRI) for red wine colour profiles by modified spectroscopic analysis [10,11] and wine tannin measured by the ethylcellulose precipitation method [12]. Residual sugars, ethanol, and acids were analysed using high-performance liquid chromatography (HPLC) [13]. Wines were also sent to AWRI Metabolomics for wine fermentation product analysis using a method based on headspace solid-phase microextraction coupled with gas chromatography mass spectrometry (HS-SPME-GC-MS) [14]. The remaining wine was bottled into 330 ml dark glass bottles and stored in a 15°C room for future analysis.

2.8. Statistical tests and principal component analysis (PCA) methods

Since this study is a preliminary trial to gain some basic understanding of how SD could affect wine characteristics, and due to the lack of biological replicates, analysis of variance (ANOVA) could not be performed with biological replication. However, ANOVA was done using the wine technical replications to enable a limited principal component analysis (PCA) to compare wine quality. Therefore, the P and F values of the ANOVA tests were not considered as the true significance between any SD and NSD groups. Ordinary one-way ANOVA and Tukey's multiple comparison test were implemented to detect significant difference between means of the four technical replicates using GraphPad Prism 9 (v. 9.3.1). A total of 48 wine metrics were analysed by the ANOVA

test, 34 compounds which have a significant difference of mean by ANOVA test ($P < 0.05$) (Table 2). Any wine metrics which were significant by the initial ANOVA test were combined to conduct a PCA. The PCA was conducted by R (v. 4.1.1, R Core team, 2021) using the build-in function "prcomp" from the default package "Datasets". PCA plots were generated using packages "FactoMineR" and "factoextra" [15].

3. Results

3.1 Bunch stem necrosis (BSN) symptoms on berries

Bunch Stem Necrosis (BSN) was the main reason preventing a larger scale of wine making, as both SD and LRD grapevines were affected, and BSN was worse for the SD grapevines when berries were harvested. Symptoms of BSN were noted directly after veraison in January 2021. A pinkish colour first appeared on the bunch stem (Figure 2a) and berry stem (Figure 2b). After 2 weeks, the bunch stem went brown, and berries senesced and detached from bunches (Figure 2c). Only two SD grapevines were harvested since berries from most SD grapevines had dropped before harvesting while NSD groups had sufficient berries from six grapevines. Field observations suggest that the yield of SD grapevines was reduced more significantly compared to the LRD and asymptomatic grapevines.

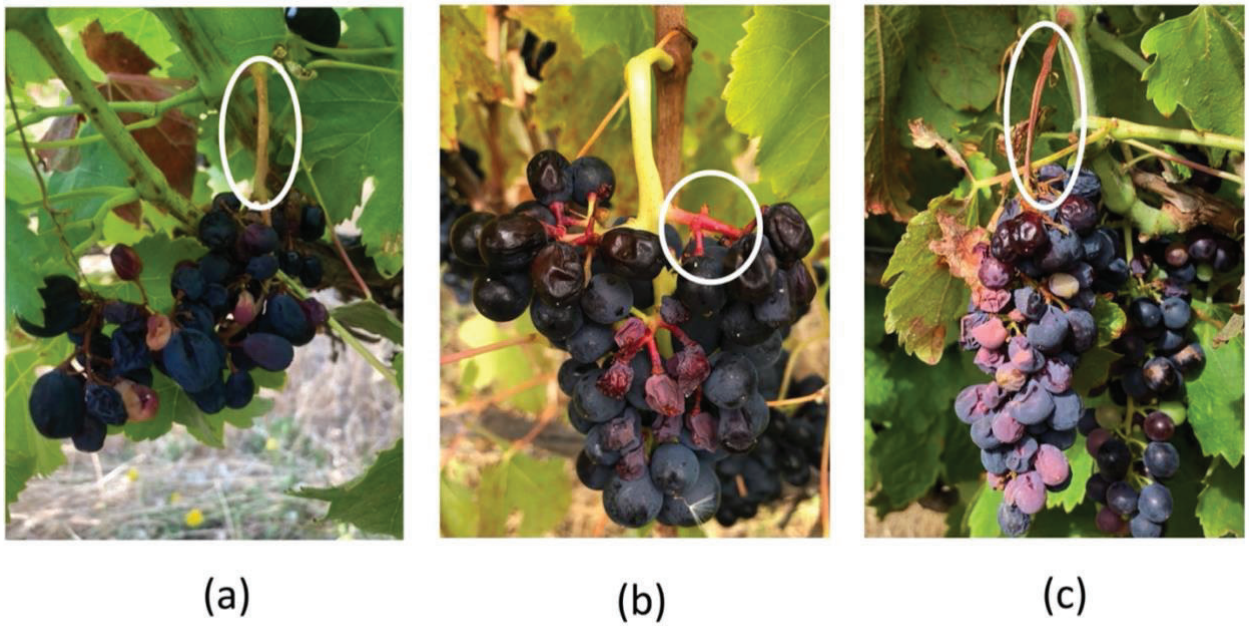

Figure 2. Symptoms of bunch stem necrosis (BSN; circled). (a) An early sign of BSN on bunch stem, (b) berry stem necrosis, (c) late symptoms of stem browning.

3.2. Wine grouping and virus status

The difference between the three NSD groups is that GLRaV-3 was only detected in 4/6 grapevines, most grapevines in NSD2 and NSD3 contain berries collected from grapevines infected with the GVA variants from phylogenetic group III (GVA^{III}) and grapevine leafroll-associated virus 4 strain 6 (GLRaV-4/6), which had no noticeable symptoms and

grapevine physiology performance was unaffected (see Chapter 4). Since the wines were made before the discovery of GVA^{III} variants by the Meta-HTS study (Chapter 2, section 3.2), NSD2 and 3 contain different proportions of GVA^{III} berries as shown in Table 1. The mean and SDevs of basic wine metrics, colour, tannins, and fermentation products are listed in Table 2.

Table 1. Virus status, field symptoms, berry weight of the selected grapevines for small-scale wine making.

Group ID	No. of grapevines in this group	Sample ID	Berry weight (kg)	Symptoms[1]	Virus profile[2]	Total berry weight (kg)
SD	2	WIL-1	2.1	SD	$GVA^{II\&III}$, GLRaV-3, GLRaV-4/9	4.3
		WIL-2	2.2	SD	$GVA^{II\&III}$, GLRaV-3, GLRaV-4/9	
NSD1	6	WIL-54	0.255	LRD	GLRaV-3, GLRaV-4/9	4.27
		WIL-55	0.545	LRD	GLRaV-3, GLRaV-4/9	
		WIL-56	1.07	ASY	GVA^{III}, GLRaV-4/9	
		WIL-58	0.9	ASY	GLRaV-4/9	
		WIL-61	0.7	LRD	GLRaV-3, GLRaV-4/9	
		WIL-63	0.8	LRD	GLRaV-3, GLRaV-4/9	
NSD2	6	WIL-9	0.67	LRD	GVA^{III}, GLRaV-3, GLRaV-4/6, GLRaV-4/9,	4.376
		WIL-10	0.7	LRD	GVA^{III}, GLRaV-3, GLRaV-4/6, GLRaV-4/9,	
		WIL-11	0.666	LRD	GVA^{III}, GLRaV-3, GLRaV-4/6, GLRaV-4/9,	
		WIL-13	0.89	LRD	GVA^{III}, GLRaV-3, GLRaV-4/5, GLRaV-4/9	
		WIL-14	0.25	LRD	GLRaV-3, GLRaV-4/5, GLRaV-4/6, GLRaV-4/9	
		WIL-15	1.2	LRD	GLRaV-3, GLRaV-4/5, GLRaV-4/6	
NSD3	6	WIL-67	0.75	LRD	GVA^{III}, GLRaV-3, GLRaV-4/6, GLRaV-4/9	4.28
		WIL-68	0.55	LRD	GVA^{III}, GLRaV-3, GLRaV-4/6, GLRaV-4/9	
		WIL-69	0.94	LRD	GLRaV-3, GLRaV-4/6, GLRaV-4/9	
		WIL-71	0.34	ASY	GLRaV-4/6, GLRaV-4/9	
		WIL-73	0.8	LRD	GLRaV-3, GLRaV-4/6	
		WIL-74	0.9	ASY	GLRaV-4/6	

[1] SD = Shiraz disease, LRD = leafroll disease (LRD), ASY = asymptomatic. [2] GLRaV -3 = grapevine leafroll-associated virus 3, GLRaV-4/5, -4/6, -4/9 = grapevine leafroll-associated virus 4 strains 5, 6, and 9, GVA = grapevine virus A. GVA^{II} and GVA^{III} = GVA variants from phylogenetic group II and III. Grapevine rupestris stem pitting-associated virus and grapevine rupestris vein feathering virus were also present in almost all the samples listed in this table. See details in Table S4 and S5 of Chapter 2.

Table 2. Composition of wines made from Shiraz disease (SD) affected and non-affected grapevines (cv. Shiraz).

Analyte	**F value[1]**	**P value[1]**	**SD**		**NSD1**		**NSD2**		**NSD3**	
Basic wine metrics			**Mean**	**Standard deviation (SDev)**	**Mean**	**SDev**	**Mean**	**SDev**	**Mean**	**SDev**
pH	99.89	***	3.325	0.02082	3.423	0.04717	3.585	0.01732	3.63	0.01633
TSS	271.2	***	24.1	0.2944	24.4	0.1414	26.5	0.08165	26.95	0.1
Titratable acidity	1343	***	6.228	0.1333	3.038	0.09639	3.545	0.01915	2.99	0.02828
compounds measured by HPLC (g/L)										
Citric acid	5.964	**	1.245	0.1047	1.443	0.07632	1.363	0.05377	1.278	0.03862
Tartaric acid	2.099	No	0.4675	0.02217	0.645	0.1618	0.735	0.2146	0.6975	0.1848
Glucose	0	N/A	0	0	0	0	0	0	0	0

Malic acid	2.055	No	2.715	0.09713	2.853	0.2128	2.58	0.0469	2.6	0.256
Fructose	13.94	***	0.6475	0.09912	0.8925	0.05123	0.905	0.124	1.053	0.06702
Succinic acid	2.154	No	1.845	0.2565	1.918	0.1676	2.168	0.1522	2.038	0.1778
Lactic acid	0.4444	No	0.01	0.008165	0.0075	0.005	0.0075	0.005	0.005	0.005774
Glycerol	12.64	***	9.128	0.3225	8.97	0.2837	9.97	0.4485	10.33	0.3944
Acetic acid	0	N/A	0	0	0	0	0	0	0	0
Ethanol	31.85	***	103.4	3.687	107	1.472	116.6	0.8657	119.6	3.643
Anthocyanin_and_tannin										
% Pigmented tannin	27.8	***	4.913	0.6412	5.793	0.325	8.385	0.8605	7.933	0.5895
Chemical Age 1	22.5	***	0.2	0.02449	0.2125	0.005	0.2775	0.02217	0.2725	0.005
Chemical Age 2	23.69	***	0.0475	0.005	0.0575	0.005	0.085	0.01	0.08	0.008165
Colour Density (a.u.)	243.3	***	9.425	0.5909	14.58	0.3594	16.3	0.216	16.9	0.483
Free Anthocyanins (mg/L)	12.28	***	464.3	51.5	632.8	30.35	592.8	41.15	631.3	54.49
Hue	29.9	***	0.5325	0.02217	0.5375	0.009574	0.5825	0.005	0.6075	0.009574
Pigmented Tannin (a.u.)	207.3	***	1.23	0.07257	2.028	0.06238	2.878	0.1919	2.87	0.04546
Total phenolics (a.u.)	48.87	***	36	2.944	52.25	2.062	55.25	2.63	59.25	3.775
Total pigment (g/L)	20.47	***	25.25	2.526	35.01	1.505	34.42	1.954	36.35	2.757
Total tannin%	62.47	***	0.4725	0.09743	1.093	0.0789	1.245	0.09983	1.383	0.125
Fermentation products (µg/L)										
Ethyl acetate	31.85	***	103.4	3.687	107	1.472	116.6	0.8657	119.6	3.643
2-methylpropanol	1.618	No	36243	2173	32009	1215	34813	3952	33033	3618
Acetic acid	5.201	*	208730	9116	234546	12781	252033	25448	247613	16505
Ethyl propanoate	11.82	***	115	5.164	141.3	3.202	155.5	12.61	154.3	16.82
3-methylbutanol	2.53	No	251514	6842	229773	11643	243906	5111	239975	17592
2-methylbutanol	9.089	**	72561	2922	66802	4084	79847	2733	76764	4846
Propanoic acid	11.91	***	2263	112.8	1955	63.05	2114	63.97	2120	21.59
2-methylpropyl acetate	5.143	*	18	1.155	14.5	1.291	14.5	3.109	13	1.155
Ethyl butanoate	2.744	No	126.8	5.62	133.5	7.767	128.5	18.06	152	19.03
2-methylpropanoic acid	7.175	**	1519	57.38	1399	32.69	1401	85.45	1337	35.11
Ethyl-3-methylbutanoate	4.368	*	4.75	0.5	5	0	6	0.8165	6	0.8165
Butanoic acid	4.143	*	1148	102.4	1108	25.94	1026	64.33	1188	56.8
3-methylbutyl acetate	0.6993	No	495.8	53.8	450	43.04	442.3	64.77	451.8	67.01
2-methylbutyl acetate	3.079	No	26.25	4.573	25.5	4.655	35.5	7.55	32.25	4.573
Hexanol	17.64	***	3914	177.6	2964	336.9	2814	114.2	2857	298
3-methylbutanoic acid	7.65	**	1226	43.52	1074	64.47	1162	49.24	1117	18.16
2-methylbutanoic acid	6.724	**	1112	55.75	1118	64.57	1272	79.42	1216	28.46
Ethyl hexanoate	1.285	No	493.8	89.41	558.3	12.04	484	67.69	551	74.39
Hexyl acetate	12.38	***	23	4.83	15	0.8165	10.25	2.5	12.5	3.109

Hexanoic acid	12.23	***	2514	216	2009	124.2	1963	130	2016	98.02
2-phenylethanol	2.771	No	71153	4374	72126	3002	78965	2406	75633	6271
Ethyl octanoate	2.663	No	442	54.71	381.3	12.28	384.8	41.82	432.5	33.23
Octanoic acid	8.811	**	1779	61.35	1648	209.4	1370	130	1412	64.23
2-phenylethyl acetate	6.312	**	70	7.165	86.25	7.5	86.75	3.686	82.75	5.852
Ethyl decanoate	3.365	No	137.5	38.83	99.25	6.994	96.25	8.5	113.8	7.544

[1] P and F values were not considered as the true significance between groups, due to the lack of biological replicates of this study. They were used to determine the metrics for the preliminary principal component analysis only. * Indicates significant level between means, $P < 0.001$***, $P < 0.01$**, $P < 0.05$

3.3. Wine composition differences between SD and NSD groups

A simultaneous comparison was conducted of the whole panel of the wine including all SD and NSD groups as well as pairwise comparisons of SD and NSD1.

3.3.1. Differences in Basic wine metrics

When comparing the means with the SD wines, NSD2 and NSD3 are high in pH and Brix, but low in titratable acidity (TA) (Table 2). The mean TSS of the SD and NSD1 groups were similar (SD = 24.1, NSD = 24.4) which were lower than the mean of NSD2 and NSD3 groups (NSD2 = 26.5, NSD3 = 26.95) (Table 2). The mean TA of SD is almost twice that of NSD1, but the mean pH of SD berry juice, 3.3, is just a fraction lower than 3.4 of the NSD1 juice (Table 2). However, when comparing only NSD2 and NSD3 that both had GLRaV-3 and GVA^{III} variants, pH and TSS of these two groups were similar, but the TA of NSD2 is higher than NSD3.

3.3.2. Differences in organic acids, ethanol and residual sugars

All 16 wine replicates completed fermentation to dryness as they contained 0 g/L glucose (Table 2). The residual fructose concentration in SD wines was lower than in NSD wines. The mean fructose in SD wines is 0.65 g/L whereas the NSD wines ranged from 0.89 to 1.1 g/L (Table 2). The wines from all four groups resulted in wines with 10% to 12% alcohol. SD wines contain lower citric acid concentrations of 1.245 g/L compared to NSD1 wines with 1.443g/L and were similar to NSD3 wines (1.278 g/L). When comparing concentrations of organic acids and glycerol, no major differences was found between SD and NSD1 (Table 2).

3.3.3 Difference in red wine colour profiles and tannins

The colour profiles of wine was strongly affected, as free anthocyanins, pigmented tannin, total phenolics, total pigment and total tannin were all lower in the SD wines compared to NSD1 (Table 2). The results of anthocyanin and tannin assays suggest, in general, colour and tannin in SD wine is half of a NSD wine (Table 2).

3.3.4. Differences in fermentation products

Major differences were found when comparing means of aroma compounds of wines made from all four groups. In general, SD wines had lower pleasant aromas compared to NSD grapevines, like ethyl acetate (floral, rose) and ethyl propanoate (fruity), but had higher undesirable compounds like 2-methylbutanol (nail polish), 2-methylpropanoic acid (cheese, rancid), hexanol (herbaceous, grassy) (Table 2). When comparing only SD and NSD1 wines, fewer differences were found. The SD wines have a lower mean ethyl propanoate (fruity), 2-phenylethyl acetate (floral, rose) contents, but higher mean propanoic acid (vinegar), hexanol, 3-methylbutanoic acid (blue cheese), hexyl acetate (sweet, perfume), hexanoic acid (cheese, sweaty) concentration (Table 2).

3.4. Principal component analysis (PCA)

In order to compare the wine composition data between the four virus profile groups, it was decided to conduct a preliminary PCA. It is

important to note that while this analysis may provide an indication as to how the different viruses affect wine composition, it was only conducted on technical replicates and the ANOVA statistical analysis that was used was not robust. The first and second component dimensions (PC1 and 2) explained 72.5% of the correlations of the overall data set of this study (Figure 3). This PCA indicates that SD wines have different characteristics compared to NSD wines since they cluster independently of the NSD groups in Figure 3. The ellipse at 95% confidence level of the NSD2 and NSD3 wines by PCA are almost identical to each other and this indicates that they may have a similar sensory profile. The PCA positions of SD1 and NSD1 wines are distinctly apart, this may suggest they have a distinct sensory profile.

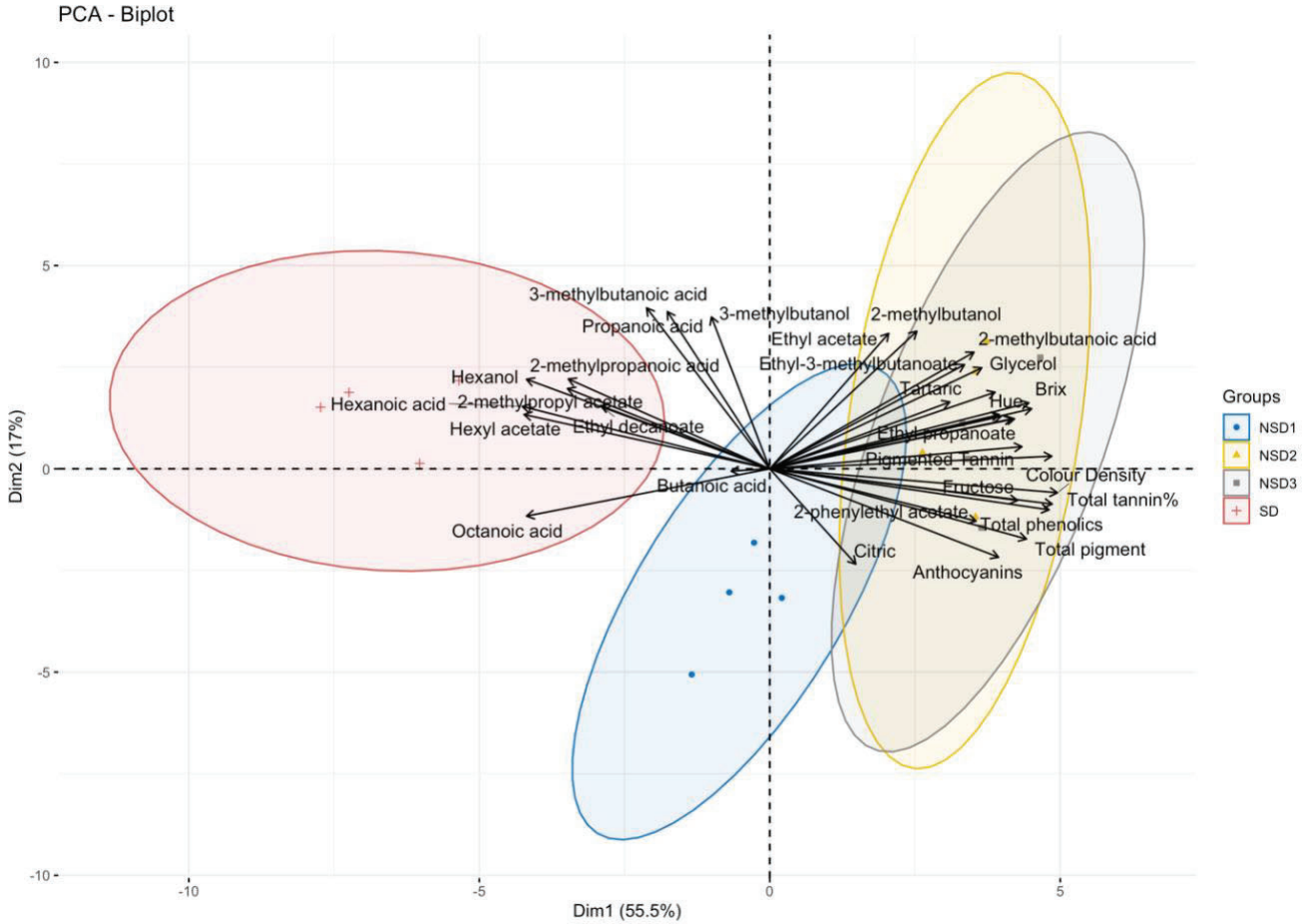

Figure 3. The preliminary principal component analysis (PCA) of wine analytes of the Shiraz disease (SD) and None-Shiraz Disease (NSD) wines. Each wine replicate is represented by dots. Red dots represent wine replicates from the SD group (2 grapevines with pooled berries). NSD1 to 3 are three control groups for the SD group. Each of the red, blue, yellow, and grey ellipses represent 95% confidence level of the SD, NSD1, NSD2, and NSD3 groups, respectively. The length of the errors indicates the contribution of this factor in this PCA.

4. Discussion

This study, although preliminary, provides an indication of the effect that SD may have on wine composition and aroma profiles. It indicates wine metrics that could be further examined in the future. It should be noted that the comparison of GVA variants is subject to the presence of GLRaV-3, since it was widespread in the WIL site and most grapevines near the SD grapevines were infected with GLRaV-3. The wine produced from SD-affected grapevine berries could have low ethanol, high acidity and aromas associated with unripened berries even though the TSS of the fruit was similar. As described earlier, this preliminary study was limited by lack of biological replication of SD grapevines. Prior to the small-lot wine making of this study, it was observed that berries of SD grapevines matured late and ripened unevenly compared to NSD grapevines, which could significantly affect wine composition. The statistical tests were done on technical replicates rather than biological replicates, which is not ideal for this type of analysis. Therefore, the limitations of this study are discussed in the following sections and conclusions made with these limitations in mind.

4.1. Bunch stem necrosis (BSN) symptoms on berries

The BSN symptoms were observed right after veraison in the 2020-21 season in SD and LRD affected grapevines. The causes of the symptom remain unclear, but it is more likely to be associated with mineral nutrients or light [16], GTDs, or other abiotic stress rather than virus infection, since BSN was not observed in previous years while monitoring berry maturation. The TSS of SD berries reached as high as 27 in the 2018-19 season (Chapter 4, Figure 7d).

4.2. Berry harvesting

Chapter 4 described delayed ripening in SD grapevines, it was anticipated that SD berries would be at an earlier stage of ripening than NSD berries and their TSS and pH would be lower. (Chapter 4, Figure 8). It was decided to harvest the berries from all groups at the same time, a practice that growers and most international studies usually follow [6,7]. It is understood that the differences in wine composition are likely caused by the difference in ripeness of SD and NSD berries. However, harvesting SD and NSD berries at different times but at the same level of ripeness may also impact the validity of comparisons, since environmental conditions when berries were harvested, and storage procedures may also impact berry composition. Moreover, berries in SD grapevines may never fully ripen. In 2012 at McLaren Vale, berries of a Shiraz block which had over 50% of SD grapevines remained unripened throughout winter (Habili, unpublished). Thus, the differences between SD and NSD groups are carefully compared in conditions of uneven ripeness between the groups, with the presence GLRaV-3, GLRaV–4 and GTDs (Chapter 5, Table 1; Chapter 4) and which may reflect the impact of GVA infection.

4.3. Effects on basic wine metrics, anthocyanins and tannins

During berry ripening, TSS increases and TA decreases, therefore late harvest results in higher TSS and pH but lower TA [17,18]. Sugars (glucose and fructose) start to accumulate approximately 60 days post flowering and anthocyanin mainly accumulates towards the end of ripening about

90 days post-flowering [19]. Based on the previous results in Chapter 4, it is likely that the delayed canopy growth (Chapter 4, Figure 4) and flowering time (Chapter 4, Figure 3) of SD grapevines both contribute to late fruit ripening (lower TSS and higher TA content) compared to NSD grapevines. However, high TA did not result in lower pH when comparing mean of SD and NSD1 (with and without $GVA^{II\&III}$ variants) (Table 2).The same situation was reported for grapevine red blotch virus (GRBV) in various varieties [4,6].

Anthocyanins and tannins play an important role in red wine quality. These may change the sensorial properties of wine due to anthocyanin-tannin reactions [20,21]. If any sensory evaluation research were to be undertaken, it is most likely that the mouth feel of SD wine would be significantly lighter, more bitter and astringent, than that of NSD wine since total anthocyanins and total tannins in SD wines were only half of those in NSD wines (Table 2). However, the relevance of these two groups of compounds can decrease because of either delayed berry ripening on its own or as a result of both SD and delayed berry ripening. Since reduced anthocyanin and tannin were also reported for GLRaVs [1-3] and GRBV [6,22], this should be investigated by future sensory studies to evaluate how these differences affect the taste of the SD and NSD wines.

The importance of tannins in grapevines also cannot be ignored as they are used as a protection against pest and pathogens [23,24]. Lower tannin levels may result in a weaker defense system making them more vulnerable to pests and diseases. Moreover, pests, including viruses, can alter secondary metabolites that are used for plant defence mechanisms against other pests [23]. It is possible that virus infection alters defense systems by making SD grapevines more susceptible to other pests. It might explain the prevalence of GTDs amongst the SD affected grapevines at WIL.

4.4. Effects on aroma compounds

Studying how virus infection may affect the aroma of wine can be challenging, since hundreds of compounds contribute to the aroma profile with complex interactions between them [25]. Yeast and other microorganisms in fermentations [25-27], the variety of the grapevine, and harvesting time are the core factors impacting aroma profile of a wine [28]. This study aimed to identify the most likely compounds that are altered in SD affected grapevines, and which could affect the wine aromas of small-scale wines, made from berries of SD and SD affected grapevines that were picked at the same timepoint, using a single yeast strain.

According to data in Table 2, SD wines contain high hexanol content that contribute to vegetal characters and less flavour compounds that contribute to pleasant aromas than NSD wines. This is not surprising since SD berries are at an earlier stage of ripening as compared to NSD berries. Towards the end of ripening, flavour compounds like terpeneoids, which may be related to pleasant aroma, accumulate, while undesirable compounds of several methoxypyrazines tend to decrease [19]. Therefore, this could be more of a direct impact of unripeness of SD berries than the disease per se, since fewer differences in aroma compounds are observed when comparing only SD1 and NSD1 (similar berry ripening stage) than when all groups were compared. It is uncertain if the differences between SD and NSD wines are SD-related, since SD wines were made from only two SD affected grapevines and no additional biological replicates, however the study provides an indication that some aroma compounds

are affected which could lower wine quality. More experiments must be conducted if possible, using more biological replication to investigate whether the differences in Table 2 is SD-related or a result from delayed ripening, or a combination of both.

4.5. Wine PCA

PCA was implemented to visualize potential positive or negative correlations of the wine metrics and how they might be linked to grapevine virus profiles, since it can detect correlations of variables regardless of test methods and unit of measurements of each variable [29].

The PCA in Figure 3 shows that SD and NSD1 wines are separate, indicating that they had unique compositions. The PCA also indicated differences in composition between SD wines and NSD2 and NSD3 wines. While this provides some indication that GVA^{II} affects wine quality, in this study SD affected grapevines also had GTDs, so it is difficult to determine if GVA^{II} was a primary contributing factor to the differences in wine composition.

Based on the PCA, NSD wines generally had a higher TSS, ethanol, color, and tannins whereas SD wines may have a stronger herbaceous, grassy flavor due to high hexanol content. Differences of volatile organic compounds in grapevines could be due to pathogen infection, abiotic stress, or unripeness of the berries [30-32]. The differences between NSD1 wines and NSD2 and NSD3 (with and without GVA^{III} and GLRaV-4/6) wines may indicate that GVA^{III} and GLRaV-4/6 may affect wine composition or it is also possible that the difference is due to different berry ripening stage of NSD1 and other NSD groups since the mean TSS of NSD1 is lower than TSS of NSD2 and NSD3 (Table 2).

5. Conclusion

Although this study was limited by the lack of biological and technical replicates to support statistically based conclusions, it does provide a preliminary insight to the potential impact of SD, GTDs and other viruses on wine composition in Australian grown Shiraz. It suggests that GVA^{II} and GVA^{III} variants may affect wine composition differently. It also implies that GLRaV-4/6, in combination with GVA^{III} may affect wine composition. The differences in wine composition, such as lower ethanol and color, more of vegetal characters compared to NSD wines, can be due to the impact of delayed ripening of the SD berries. The biological properties of two distinct virus variants (phylogroup) of the same virus (GVA^{II} and GVA^{III}) may differ in how they impact the aromatic composition of wine based on the results of PCA. Future studies should be performed using a larger number of biological and technical replicates, ideally in the vineyards that have both SD and NSD grapevines with less confounding factors (GTDs, other GLRaVs) and more controllable experimental conditions. Wines should be made using more berries and in multiple years to identify the sole wine metrics that are associated with virus infection.

6. References (Chapter 5)

1. Alabi, O.J.; Casassa, L.F.; Gutha, L.R.; Larsen, R.C.; Henick-Kling, T.; Harbertson, J.F.; Naidu, R.A. Impacts of grapevine leafroll disease on fruit yield and grape and wine chemistry in a wine grape (Vitis vinifera L.) cultivar. *PLoS One* **2016**, *11*, e0149666, doi:10.1371/journal.pone.0149666.
2. Lee, J.; Martin, R.R. Influence of grapevine leafroll associated viruses (GLRaV-2 and-3) on the fruit composition of Oregon Vitis vinifera L. cv. Pinot noir: Phenolics. *Food Chem.* **2009**, *112*, 889-896, doi:10.1016/j.foodchem.2008.06.065.
3. Alabi, O.J.; Gutha, L.R.; Casassa, L.F.; Harbertson, J.; Mirales, M.; Beaver, C.W.; Naidu, R.A. Impacts of grapevine leafroll disease on own-rooted wine grape cultivar in cool climate viticulture. In Proceedings of the 17th Meeting of the International Council for the Study of Viruses and Virus-like Diseases of the Grapevine, Davis, California, USA, 7–14 October, 2012; pp. 170-171.
4. Rumbaugh, A.C.; Sudarshana, M.R.; Oberholster, A. Grapevine red blotch disease etiology and its Impact on grapevine physiology and berry and wine composition. *Horticulturae* **2021**, *7*, 552, doi:10.3390/horticulturae7120552.
5. Girardello, R.C.; Cooper, M.L.; Smith, R.J.; Lerno, L.A.; Bruce, R.C.; Eridon, S.; Oberholster, A. Impact of grapevine red blotch disease on grape composition of Vitis vinifera Cabernet Sauvignon, Merlot, and Chardonnay. *J. Agric. Food Chem.* **2019**, *67*, 5496-5511, doi:10.1021/acs.jafc.9b01125.
6. Bowen, P.; Bogdanoff, C.; Poojari, S.; Usher, K.; Lowery, T.; Úrbez-Torres, J.R. Effects of grapevine red blotch disease on Cabernet franc vine physiology, bud hardiness, and fruit and wine quality. *Am. J. Enol. Vitic.* **2020**, *71*, 308-318, doi:10.5344/ajev.2020.20011.
7. Mannini, F.; Mollo, A.; Credi, R. Field performance and wine quality modification in a clone of Vitis vinifera cv. Dolcetto after GLRaV-3 elimination. *Am. J. Enol. Vitic.* **2012**, *63*, 144-147, doi:10.5344/ajev.2011.11020.
8. Giribaldi, M.; Purrotti, M.; Pacifico, D.; Santini, D.; Mannini, F.; Caciagli, P.; Rolle, L.; Cavallarin, L.; Giuffrida, M.G.; Marzachì, C. A multidisciplinary study on the effects of phloem-limited viruses on the agronomical performance and berry quality of Vitis vinifera cv. Nebbiolo. *J. Proteomics* **2011**, *75*, 306-315, doi:10.1016/j.jprot.2011.08.006.
9. Holt, H.E.; Iland, P.; Ristic, R. A method for mini-lot fermentation for use in research and commercial viticultural and winemaking trials. *Aust. N.Z. Grapegrow. Winemak.* **2006**, *509a*, 74-81.
10. Somers, T.C.; Evans, M.E. Spectral evaluation of young red wines: Anthocyanin equilibria, total phenolics, free and molecular SO2,"chemical age". *J. Sci. Food Agric.* **1977**, *28*, 279-287.
11. Somers, T.C.; Evans, M.E. Wine quality: Correlations with colour density and anthocyanin equilibria in a group of young red wines. *J. Sci. Food Agric.* **1974**, *25*, 1369-1379.
12. Sarneckis, C.J.; Dambergs, R.G.; Jones, P.; Mercurio, M.; Herderich, M.J.; Smith, P.A. Quantification of condensed tannins by precipitation with methyl cellulose: development and validation of an optimised tool for grape and wine analysis. *Aust. J. Grape Wine Res.* **2006**, *12*, 39-49.
13. Varela, C.; Bartel, C.; Nandorfy, D.E.; Borneman, A.; Schmidt, S.; Curtin, C. Identification of flocculant wine yeast strains with improved filtration-related phenotypes through application of high-throughput sedimentation rate assays. *Sci. Rep.* **2020**, *10*, 1-13, doi:10.1038/s41598-020-59579-y.
14. Siebert, T.E.; Smyth, H.E.; Capone, D.L.; Neuwöhner, C.; Pardon, K.H.; Skouroumounis, G.K.; Herderich, M.J.; Sefton, M.A.; Pollnitz, A.P. Stable isotope dilution analysis of wine fermentation products by HS-SPME-GC-MS. *Analytical and bioanalytical chemistry* **2005**, *381*, 937-947, doi:10.1007/s00216-004-2992-4.
15. Yao, Z. Principal Component Methods in R: Practical Guide Principal Component Methods in R: Practical Guide. Available online: http://www.sthda.com/english/articles/31-principal-component-methods-in-r-practical-guide/ (accessed on 7 May 2022).
16. Krasnow, M.; Matthews, M.; Smith, R.; Benz, J.; Weber, E.; Shackel, K. Distinctive symptoms differentiate four common types of berry shrivel disorder in grape. *Calif. Agric.* **2010**, *64*, 155-159.
17. Jančářová, I.; Jančář, L.; Náplavová, A.; Kubáň, V. Changes of organic acids and phenolic compounds contents in grapevine berries during their ripening. *Cent. Eur. J. Chem.* **2013**, *11*, 1575-1582, doi:10.2478/s11532-013-0288-2.
18. Luna, L.H.M.; Reynolds, A.G.; Di Profio, F. Crop level and harvest date impact composition of four Ontario winegrape cultivars. I. Yield, fruit, and wine composition. *Am. J. Enol. Vitic.* **2017**, *68*, 431-446, doi:10.5344/ajev.2017.17019.
19. Kennedy, J. Understanding grape berry development. *Pract. Winery Vineyard* **2002**, *4*, 1-5.
20. Cheynier, V.; Duenas-Paton, M.; Salas, E.; Maury, C.; Souquet, J.-M.; Sarni-Manchado, P.; Fulcrand, H. Structure and properties of wine pigments and tannins. *Am. J. Enol. Vitic.* **2006**, *57*, 298-305.

21. Vidal, S.; Francis, L.; Noble, A.; Kwiatkowski, M.; Cheynier, V.; Waters, E. Taste and mouth-feel properties of different types of tannin-like polyphenolic compounds and anthocyanins in wine. *Anal. Chim. Acta* **2004**, *513*, 57-65, doi:10.1016/j.aca.2003.10.017.
22. Martínez-Lüscher, J.; Plank, C.M.; Brillante, L.; Cooper, M.L.; Smith, R.J.; Al-Rwahnih, M.; Yu, R.; Oberholster, A.; Girardello, R.; Kurtural, S.K. Grapevine red blotch virus may reduce carbon translocation leading to impaired grape berry ripening. *J. Agric. Food Chem.* **2019**, *67*, 2437-2448, doi:10.5344/ajev.2020.20011.
23. Bennett, R.N.; Wallsgrove, R.M. Secondary metabolites in plant defence mechanisms. *New Phytol.* **1994**, *127*, 617-633.
24. War, A.R.; Taggar, G.K.; Hussain, B.; Taggar, M.S.; Nair, R.M.; Sharma, H.C. Plant defence against herbivory and insect adaptations. *AoB plants* **2018**, *10*, ply037, doi:10.1093/aobpla/ply037.
25. Lambrechts, M.G.; Pretorius, I.S. Yeast and its importance to wine aroma-a review. *South African J. Enol. Vitic.* **2000**, *21*, 97-129.
26. Liu, D.; Legras, J.-L.; Zhang, P.; Chen, D.; Howell, K. Diversity and dynamics of fungi during spontaneous fermentations and association with unique aroma profiles in wine. *Int. J. Food Microbiol.* **2021**, *338*, 108983, doi:10.1016/j.ijfoodmicro.2020.108983.
27. Swiegers, J.H.; Bartowsky, E.J.; Henschke, P.A.; Pretorius, I.S. Yeast and bacterial modulation of wine aroma and flavour. *Aust. J. Grape Wine Res.* **2005**, *11*, 139-173.
28. González-Barreiro, C.; Rial-Otero, R.; Cancho-Grande, B.; Simal-Gándara, J. Wine aroma compounds in grapes: A critical review. *Crit. Rev. Food Sci. Nutr.* **2015**, *55*, 202-218, doi:10.1080/10408398.2011.650336.
29. Bro, R.; Smilde, A.K. Principal component analysis. *Anal. Methods* **2014**, *6*, 2812-2831, doi:10.1039/C3AY41907J.
30. Lazazzara, V.; Avesani, S.; Robatscher, P.; Oberhuber, M.; Pertot, I.; Schuhmacher, R.; Perazzolli, M. Biogenic volatile organic compounds in the grapevine response to pathogens, beneficial microorganisms, resistance inducers, and abiotic factors. *J. Exp. Bot.* **2022**, *73*, 529-554, doi:10.1093/jxb/erab367.
31. Algarra Alarcon, A.; Lazazzara, V.; Cappellin, L.; Bianchedi, P.L.; Schuhmacher, R.; Wohlfahrt, G.; Pertot, I.; Biasioli, F.; Perazzolli, M. Emission of volatile sesquiterpenes and monoterpenes in grapevine genotypes following Plasmopara viticola inoculation in vitro. *J. Mass Spectrom.* **2015**, *50*, 1013-1022, doi:10.1002/jms.3615.
32. Rienth, M.; Vigneron, N.; Darriet, P.; Sweetman, C.; Burbidge, C.; Bonghi, C.; Walker, R.P.; Famiani, F.; Castellarin, S.D. Grape berry secondary metabolites and their modulation by abiotic factors in a climate change scenario–a review. *Front. Plant Sci.* **2021**, *12*, 262, doi:10.3389/fpls.2021.643258.

Chapter 6: First Report of Grapevine Rupestris Vein Feathering Virus in Grapevine in Australia

Wu, Q.; Kehoe, M.; Kinoti, W.M.; Wang, C.; Rinaldo, A.; Tyerman, S.; Habili, N.; Constable, F.E. First Report of Grapevine Rupestris Vein Feathering Virus in Grapevine in Australia. Plant Dis. 2020, 105, 515, doi:10.1094/PDIS-06-20-1240-PDN.

Statement of Authorship

Title of Paper	First report of grapevine rupestris vein feathering virus in grapevine in Australia
Publication Status	☒ Published ☐ Accepted for Publication ☐ Submitted for Publication ☐ Unpublished and Unsubmitted work written in manuscript style
Publication Details	Journal: Plant Disease Year 2021,volume: 105, issue 2, page 515

Principal Author

Name of Principal Author (Candidate)	Qi Wu		
Contribution to the Paper	original draft preparation, review and editing, data analysis		
Overall percentage (%)	30%		
Certification:	This paper reports on original research I conducted during the period of my Higher Degree by Research candidature and is not subject to any obligations or contractual agreements with a third party that would constrain its inclusion in this thesis. I am the primary author of this paper.		
Signature		Date	16/01/2023

Co-Author Contributions

By signing the Statement of Authorship, each author certifies that:

i. the candidate's stated contribution to the publication is accurate (as detailed above);

ii. permission is granted for the candidate in include the publication in the thesis; and

iii. the sum of all co-author contributions is equal to 100% less the candidate's stated contribution.

Name of Co-Author	Monica Kehoe		
Contribution to the Paper	original draft preparation, review and editing, data analysis		
Signature		Date	24/11/22

Name of Co-Author	Wycliff Kinoti		
Contribution to the Paper	review and editing, data analysis		
Signature		Date	23/11/2022

Name of Co-Author	Cuiping Wang		
Contribution to the Paper	data analysis		
Signature		Date	12/12/2022

Name of Co-Author	Amy Rinaldo		
Contribution to the Paper	review and editing		
Signature		Date	19/10/22

Name of Co-Author	Stephen Tyerman		
Contribution to the Paper	review and editing		
Signature		Date	

Name of Co-Author	Nuredin Habili		
Contribution to the Paper	review and editing		
Signature		Date	11/1/2023

Name of Co-Author	Fiona Constable		
Contribution to the Paper	original draft preparation, review and editing		
Signature		Date	21/10/2022

Disease Notes

Diseases Caused by Viruses

First Report of Grapevine Rupestris Vein Feathering Virus in Grapevine in Australia

Q. Wu,[1,2,†] M. A. Kehoe,[3] W. M. Kinoti,[4] C. P. Wang,[3] A. Rinaldo,[2] S. Tyerman,[1] N. Habili,[2] and F. E. Constable[4]

[1] School of Agriculture, Food and Wine, University of Adelaide, Glen Osmond, SA 5064, Australia
[2] The Australian Wine Research Institute, Glen Osmond, SA 5064, Australia
[3] Department of Primary Industries and Regional Development, Diagnostic Laboratory Services, South Perth, WA 6151, Australia
[4] Agriculture Victoria Research, Department of Jobs, Precincts and Regions, AgriBio, Bundoora, VIC 3083, Australia

Funding: Funding was provided by Department of Agriculture, the University of Adelaide, Wine Australia, and Pawsey Supercomputing Centre, with funding from the Government of Western Australia and the Australian Government. Plant Dis. 105:515, 2021; published online as https://doi.org/10.1094/PDIS-06-20-1240-PDN. Accepted for publication 8 September 2020.

Grapevine rupestris vein feathering virus (GRVFV; tentative genus *Marafivirus*; family *Tymoviridae*) was first detected from a Greek grapevine (*Vitis vinifera*) with asteroid mosaic-like symptoms (El Beaino et al. 2001; Ghanem-Sabanadzovic et al. 2003) and was also infected with grapevine fleck virus. GRVFV has been detected in the United States, South Africa, Canada, Spain, China, New Zealand, Brazil, Germany, Korea, Slovakia, Hungary, and Pakistan (Cho et al. 2018; Mahmood et al. 2019). Transmission vectors are currently unknown. In 2018, nine grapevine samples were collected between May and July in South Australia (SA) and Western Australia (WA) and were analyzed by high-throughput sequencing (HTS) to characterize grapevine viruses in Australian vineyards. Total RNA or double-stranded RNA was extracted from grapevine canes using an RNeasy 96 QIAcube HT kit (Qiagen) with MacKenzie buffer (MacKenzie et al. 1997) or using CF-11 (Balijja et al. 2008). Libraries were prepared using the NEBNext Ultra II RNA library Prep Kit (NEB) or TruSeq Stranded mRNA Prep kit (Illumina) with Ribo-Zero gold plant kit for ribosomal depletion (Illumina, San Diego, CA). Libraries were sequenced using Illumina MiSeq (SA) or HiSeq (WA) technology with 2 × 300 (SA) or 2 × 100 (WA) paired-end reads, which were trimmed using Trim Galore! (0.4.0) or BBmap (38.20), respectively. De novo assembly, using the SPAdes (version 3.12.0) genome assembler with default settings, resulted in 12 near-full-length GRVFV genomes (6,713 to 6,737 nt), eight sequences from the WA samples and four from the SA samples. WA samples 171 and 178 and SA sample BV each had two distinct GRVFV molecular variants. Variants 171-1 and 171-2 (GenBank accessions MT084811 and MT084812) from sample 171 shared 83.39% nucleotide (nt) identity. Variants 178-1 and 178-2 (MT084813 and MT084814) from sample 178 shared 83.54% nt identity. Variants BV6799 and BV8822 (MN974274 and MN974275) from sample BV shared 82.85% nt identity. Only one GRVFV sequence was obtained from all other samples. The genome of SA isolate LC1 (MN974273) was confirmed by RT-PCR amplification and Sanger sequencing of overlapping genome regions. Tissue from the infected LC1 isolate has been deposited into the Victorian plant pathogen reference collection (VPRI accession no. 43698). When the genomes of all Australian isolates were compared, they had 78.94 to 94.37% nt identity with each other. The SA isolates LC1, BV8822, BV6799, and SEL-L (MN974276) and the WA isolates 172 (MT084807), 179 (MT084808), 180 (MT084809), and 182 (MT084810) were most closely related to the Swiss isolate CHASS (KY513702; 82.87 to 85.46% nt identity). The WA isolates 171-1, 171-2, 178-1, and 178-2 were most closely related to the New Zealand isolate Ch8021 (MF000325; 83.21 to 93.87%). Grapevine leafroll-associated virus 1 (GLRaV-1), GLRaV-3, GLRaV-4 (strain 6 and 9), grapevine virus A, grapevine rupestris stem pitting associated virus, grapevine yellow speckle viroid 1, and hop stunt viroid were also identified in the sequencing data. This is the first report of GRVFV in Australia. All WA samples were collected during dormancy, and symptoms were not observed. Sample LC1 from SA had Shiraz disease, the other SA samples were asymptomatic, and none had asteroid mosaic-like symptoms. Further research is required to determine its distribution and association with disease in Australia.

References:

Balijja, A., et al. 2008. J. Virol. Methods 152:32.
Cho, I., et al. 2018. Plant Dis. 102:1471.
El Beaino, T., et al. 2001. Vitis 40:65.
Ghanem-Sabanadzovic, N. A., et al. 2003. Virus Genes 27:11.
MacKenzie, D. J., et al. 1997. Plant Dis. 81:222.
Mahmood, M., et al. 2019. J. Plant Pathol. 101:1261.

The author(s) declare no conflict of interest.

e-Xtra

Keywords: *Marafivirus*, vein feathering, Australia

[†]Indicates the corresponding author.
E-mail: Q. Wu; qi.wu@adelaide.edu.au

Supplementary materials

Table S1. NGS sample Information including the GenBank accession number, isolate name, grapevine variety, Australian location, the percentage (%) nucleotide (nt) identity to the grapevine rupestris vein feathering virus (GRVFV) isolate LC1, and the % nt identity of each Australian isolate to the most closely matched international isolates with sequences publicly available on GenBank.

Isolate name	Variety	Location	GenBank Accession No.	Genome sequence length of Australian isolates (nt)	Pairwise % nt identity with GRVFV isolate LC1	International GRVFV isolates with highest % nt identity	Pairwise % nt identity with the international isolate
LC1	Shiraz	Langhorne Creek,SA	MN974273	6715	100%	CHASS (KY513702)	82.87%
BV8822	Shiraz	Barossa Valley,SA	MN974274	6737	94.37%	CHASS	82.95%
BV6799	Shiraz	Barossa Valley,SA	MN974275	6730	82.93%	CHASS	84.68%
SEL-L	Semillon	Loxton,SA	MN974276	6720	82.68%	CHASS	84.00%
171-1	Viognier	Harvey,WA	MT084811	6723	79.31%	NZ Ch8021 (MF000325)	93.73%
171-2	Viognier	Harvey,WA	MT084812	6725	79.00%	NZ Ch8021	83.21%
172	Chardonnay	Hamelin Bay,WA	MT084807	6725	81.90	CHASS	85.44%
178-1	Viognier	Harvey,WA	MT084813	6722	78.94%	NZ Ch8021	83.38%
178-2	Viognier	Harvey,WA	MT084814	6718	79.25%	NZ Ch8021	93.87%
179	Chardonnay	Harvey,WA	MT084808	6713	81.89%	CHASS	85.46%
180	Frontignac	Caversham,WA	MT084809	6716	81.83%	CHASS	85.38%
182	Gamay	Harvey,WA	MT084810	6715	82.05%	CHASS	84.43%

Table S2. Summarising the total number of raw sequence and trimmed reads obtained by high throughput sequencing, average coverage of contigs, and whether confirmation by RT-PCR was completed for each sequenced isolate.

Accession No.	Isolate name	Total raw reads	No. trimmed reads	Av. coverage of contigs	RT-PCR confirmed
MN974273[1]	LC1	2,446,079	2,392,319	68×	Yes
MN974274[1]	BV8822	2,349,058	2,300,420	47×	Yes
MN974275[1]	BV6799			12×	Yes
MN974276	SEL-L	2,179,406	2,119,216	35×	Not tested, no sample left
MT084811[2]	171-1	11,478,448	11,469,048	51×	Yes
MT084812[2]	171-2			51×	Yes

MT084807	172	10,205,761	10,203,413	56×	Not tested, no sample left
MT084813[2]	178-1	9,110,583	9,108,785	46×	Yes
MT084814[2]	178-2			57×	Yes
MT084808[2]	179	11,350,393	11,346,960	41×	Yes
MT084809[2]	180	11,416,303	11,413,413	41×	Yes
MT084810[2]	182	9,735,769	9,733,911	18×	Yes

[1] RT-PCR confirmed by gene specific primers (GRVFV237F 5′-ACTGAGCTACAAGGTGAATTGC-3′ and GRVFV237R 5′-AGCAACCCACTGGAAGGGGATGG-3′)

[2] RT-PCR confirmed by primers published by Reynard et al. 2017 (https://apsjournals.apsnet.org/doi/10.1094/PDIS-01-17-0140-PDN)

Chapter 7: General Discussion

This thesis provides a deeper understanding of Shiraz disease (SD) in Australia at the level of the genetics and biology of distinct grapevine virus A (GVA) variants, and their impact on grapevine growth, physiology, berry development and resulting wine composition. It provides compelling evidence for GVA phylogroup II (GVA^{II}) as the most likely aetiological agent of SD (Chapter 2). The metagenomic investigation study indicated that grapevine rupestris stem pitting-associated virus (GRSPaV), grapevine rupestris vein feathering virus (GRVFV), and grapevine leafroll-associated virus 4 (GLRaV-4) strain 5, 6 and 9 were detected in SD, leafroll disease (LRD), and asymptomatic grapevines and were not associated with SD [1]. This is consistent with other studies that also indicate that GRSPaV, GRVFV and GLRaV-4 can remain asymptomatic in grapevines [2-6]. Some isolates of virulent viruses like grapevine leafroll-associated virus 1 (GLRaV-1) (isolates 80PL1, 82PL1[3]), grapevine leafroll-associated virus 2 (GLRaV-2) (isolates GLRaV-2-SG [7]; 1/PL2 and 2PL2 [3]) and GLRaV-3 (3m-139 [8,9]) were reported to be asymptomatic in some grapevines and is similar to findings of this study in which GVA variants from phylogenetic group I and III (GVA^{I} and GVA^{III}) were not associated with SD (Chapter 2). The lack of an association between GVA^{I} and GVA^{III} strains is also consistent with previous studies [10].

An essential step in understanding plant disease aetiology is to identify pest species that are consistently present in affected plants but are not or inconsistently present in unaffected plants. This study used two popular investigative approaches, RT-PCR and metagenomics high-throughput sequencing (Meta-HTS) with each complementing the other, to obtain the most accurate association between viruses and SD. Detecting viruses by a single RT-PCR assay can often provide false-negative results due to sequence variation in the primer binding site [11-13]. Thus, three sets of primers–were used to detect all GVA variants in SD grapevines. Meta-HTS, which does not require any previous knowledge of candidate viruses [14], clearly shows its power in detecting novel viruses or new strains of known viruses as well as obtaining complete genome sequences. Two genetically distinct GVA isolates, GVA^{II} and GVA^{III} were identified together in samples of a few grapevines with SD from the Willunga (WIL) study site using Meta-HTS.

SD has been reported from both Australia and South Africa [15,16] and in this thesis and previous studies GVA^{II} was identified as the core pathogen of SD [10,15], whereas GVA^{III} and GVA^{I} were not associated with SD. The high incidence of SD in Australia and South Africa as compared to other countries could be due to the high prevalence of GVA^{II} in these countries and a low prevalence of GVA^{II} in other countries. Supporting this hypothesis, 20/251 (7.97%) GVA sequences available in GenBank were from countries other than Australia and South Africa where SD has not been reported, contrasting to 231/251 (92.03%) sequences that were either GVA^{I} or GVA^{III} (Chapter 2, Table 7S). Another possibility could be due to the unique variety and clone composition of Australian viticulture. SD-sensitive grapevine varieties such as Shiraz, Merlot, Malbec and Ruby Cabernet are among the top ten red berry varieties grown in Australia and with the highest crush in 2021 and 2022 [17,18]. Furthermore, a commonly planted clone of Cabernet Sauvignon

(SA125) (Chapter 2) and several Chardonnay clones [19] carry virulent GVA^{II} variants and have been widely distributed across Australia. They could be potential sources of SD spread by insect vectors when planted next to a SD sensitive variety or when used as a rootstock or interstock for grafting. Future research should explore the prevalence of the varieties containing SD associated GVA^{II} variants in different grape-growing regions in Australia and investigating their role in SD spread through grafting, propagating, and insect transmission. This could provide valuable insights for developing effective management strategies to reduce the impact of SD on berry production of SD-sensitive varieties.

After identifying different GVA populations in SD grapevines by Meta-HTS, Chapter 3 describes amplicon high-throughput sequencing (Amplicon-HTS) utilized to study the intra-host diversity and potential evolutionary path of GVA. A single sample and a combination of 26 sample MJNs displayed evolution of a virus population that was derived from one or two major variants or a centralized variant group to satellite variants with much lower copy numbers (Chapter 3, Figures 1 and 2). The major variants in each sample and variant group could be the ancestor variant that first adapted to the host [20]. Alternatively, the major variant could be the existing variants in the original virus population or it may have generated from the original variants by virus mutation [21]. Previous studies demonstrated the potential use of MJNs to trace the infectious source of a virus disease [22-24]. MJNs studies in Chapter 3 demonstrated that GVA from the WIL and Langhorne Creek (LC) sites may share the same source of infection. Chapter 2 provides evidence that the spread may have occurred between the Cabernet Sauvignon (SA 125) and the neighbouring WIL block of Shiraz based on sequence similarity. This could be investigated further by studying intra host diversity of GVA of the Cabernet Sauvignon at WIL, and inter host diversity among Cabernet Sauvignon at WIL, Shiraz at WIL and Shiraz at LC. This may not only reveal the evolutionary relationship of GVA variants between the LC and WIL sites, but also explore the potential evolutionary path between GVA^{II} and GVA^{III} variants.

No GVA^{III} amplicons were obtained using the MP and RB RT-PCR assays mainly due to sequence variation on the primer binding site (Chapter 3). It was known from Chapter 2, that the RB primer pairs for amplicon-HTS, H7038/C7273 detected GVA variants from all phylogroups in South Africa [25], but not the GVA^{III} variants from Australia. For a future study of diversity of different GVA populations, new universal primers should be used and longer amplicons from additional genes would be preferrable.

Field grapevines are often under various abiotic and biotic stresses such as water stress [26], salinity stress [27], heat stress [28], viral and fungal diseases and insect damage [29]. The degree of stress and growing conditions are variable season to season, which could significantly affect the outcome of physiology and wine studies that were undertaken for this thesis. Also affecting vine performance are factors such as vine age, rootstock, the variety and clone of the grapevine and management practices in each season at different vineyards.

Chapter 4 outlined that Shiraz grapevines at the LC site were only affected by SD whereas SD grapevines at the WIL site may be under stress from both SD and grapevine trunk diseases (GTDs), possibly in combination with other biotic and abiotic stresses. A previous study reported that *Diplodia serratia*, one of the GTD species, was present on

grapevines that showed both SD and vine decline symptoms in warmer viticultural regions, Riverland, SA [16]. This study proposed that the combination of SD and GTD may result in more severe disease than when SD occurs alone. This could explain the increasing number of vines declining each year at the WIL site (Chapter 4). A similar trend was previously reported for SD in the Riverland [16]. Because the SD affected grapevines that were monitored for physiological performance also had GTDs, the effect of SD alone could not be determined. It is likely that GTDs also contributed to changes in vine physiological parameters measured at WIL, compared to unaffected grapevines, including photosynthetic rate, stomatal conductance, leaf chlorophyll, carbohydrate stores, water potentials, berry maturation and berry quality [30,31].

With this in mind, the 2018/19 data set from the WIL site (with dead arms and vine decline symptoms) were carefully compared with the LC site data sets (without dead arms symptoms) from the same year. At the LC site, although the canopy growth of SD grapevines was lower (represented by plant area index PAI) than asymptomatic (ASY) grapevines at earlier growing stages, SD caught up with ASY grapevines around veraison. When grapevines are affected by both SD and GTDs (WIL), the PAI of SD grapevines was always below the ASY grapevines and never caught up with ASY grapevines. Previous studies addressing the responses to both abiotic stress and GTDs showed that it can be difficult to decouple their effects since it is highly dependent on the biology of the pathogens, variety and clone of the grapevine, variety of rootstock and intensity of the stress [32]. Combined abiotic and biotic stress like water deficiency, winter damage or spring frost, nematode and insect damage can contribute to symptom expression of GTDs [33]. However, there appears to be no in-depth study available on how viruses interact with GTDs with and without other abiotic stresses. A previous study suggested a potential association between the presence of grapevine-associated cogu-like virus 4 and the occurrence of esca syndrome of GTDs in grapevines [34]. The threat of GTDs to the viticulture industry world-wide and in Australia has been increasing [35-38]. This could be due to climate change leading to more abiotic stress or to increasing occurrence of nematode, insect or viral associated diseases, like SD. Assessing the impact of SD in combination with other biotic and abiotic stresses is essential. Further research could focus on understanding the complex interaction between viral infections and GTDs. This could involve studying the effects of different viruses on GTD symptom expression, disease progression, and overall grapevine health. This should be conducted under controlled conditions to reveal the true correlation between SD and GTDs. Furthermore, it is important to investigate grapevine responses to the combined effects of SD and other abiotic and biotic stresses, conducting experiments to assess the impact of various combinations of stresses on SD expression and severity, and identifying potential synergistic or antagonistic interactions.

In Chapter 4, the physiological parameters were measured on the same Shiraz clone BVRC12, but at the LC site, Shiraz grapevines were grafted on to Chardonnay rootstock, in contrast to the WIL site where Shiraz were self-rooted (Chapter 2, Table 1). Rootstocks may have various impacts on scion characteristic as they may improve the resistance of a grapevine to diseases and abiotic stress and increase or reduce vine vigor [39-42]. Previous studies found that the impact of a viral disease on grapevines is dependent on the combination of rootstock and scion

[41,43,44]. The LC site used Chardonnay as rootstock, which may have lessened the impact of SD on Shiraz, since Chardonnay never displays SD symptoms [16]. Further research could investigate the impact of different rootstock-scion combinations on symptom expression of SD and physiological performance of SD grapevines. This could be achieved by a long-term study of grafting SD-affected, SD-sensitive grapevine varieties onto various rootstocks in controlled experimental conditions, and then monitoring physiological parameters and symptom progression.

SD grapevines at both WIL and LC sites showed delayed canopy growth, and berry maturation (Chapter 4) that resulted in berries with lower pH and lower total soluble solids (TSS) as compared to Non-SD (NSD) juice (Chapter 5). Typically, during fruit ripening, TSS, anthocyanin, total phenol content, total tannin, and pH tend to increase, while TA decreases [45,46]. The lower pH and TSS in SD berries confirm the finding of delayed berry maturation in SD-affected grapevines. Similarly, delayed berry maturity was also found in grapevine leafroll associated-viruses 1, 2 and 3 (GLRaV-1, 2 and 3), GVA, GRSPaV, grapevine fleck virus (GFkV) infected Cabernet Franc [47], as well as GVA and GLRaV-3 infected Nebbiolo [48]. Furthermore, the small-scale wines made from berries harvested from SD-affected grapevines (Chapter 5) gave undesirable aromas and low ethanol content, and low anthocyanins in wine not dissimilar to wines produced from unripe berries. Evidence suggests that GRBV may interfere with primary metabolism, transcriptional machinery, and carbon translocation, resulting in uneven berry ripening [49-53] and it is possible that GVA^{II} variants also interfere in the same way. Further functional analysis is needed to explore how GVA influences primary and secondary metabolism and hormonal regulation during berry ripening in the future.

Due to the low yield caused by bunch stem necrosis (BSN) symptoms especially on SD-affected grapevines, only one group of SD wines could be studied, with no biological replication. As has been discussed in Chapter 5, BSN could be associated with mineral nutrients deficiency, light or GTDs. Future studies would require biological replicates across more than one season to ensure that the differences are SD-related rather than variations between seasons. Furthermore, to determine which differences are specifically linked to unripeness and which are SD-related, additional experiments should be conducted using berries harvested at the same level of ripeness and compared with those harvested at the same time. Moreover, the differences between SD and NSD wines by statistical analysis should be confirmed with wine sensory analyses to identify the real differences in wine taste between SD and NSD wines.

Over 150 near full-length viral contigs including sequences of GRSPaV, GVA, GLRaV-1, GLRaV-3, GLRaV-4 strains 5, 6 and 9, grapevine syrah virus 1 (GSyV-1), GRVFV, grapevine Cabernet Sauvignon reovirus (GCSV), grapevine red globe virus (GRGV) and grapevine virus F (GVF) were obtained by Meta-HTS (Table 1), providing valuable insights into the presence and diversity of viruses and variants in Australia and their associations to viral diseases (Chapter 2). Wu et al. [16] describes the viruses that were known to occur in Australia at the time of publication (2020). Table 1 below, provides information on viruses that were subsequently found including those found in this thesis. The Meta-HTS detected a total of six viruses that are exotic to Australia [54,55]. The vector, symptoms and associated disease of these viruses are unknown. Table 1 also includes grapevine red blotch virus (GRBV) that was reported

from three states of Australia in 2022 [56]. Following the discovery of grapevine Pinot gris virus (GPGV) in 2017 [57], an increasing number of exotic viruses have been reported from Australia, raising concerns about which of these may pose a threat to the local wine industry and how to manage virus diseases under local conditions. Although most of these exotic viruses were detected in asymptomatic grapevines, the potential economic importance on sensitive varieties should not be disregarded.

Despite its utility, Meta-HTS also has inherent limitations. Literature suggests that a low proportion of viral reads in relation to total reads could result in false negatives, posing a significant challenge when employing this method as a routine diagnostic tool for plant virus detection [14,58]. Additionally, the lack of standardized national protocols for bioinformatic workflows and data interpretation in the context of Meta-HTS for diagnostic purposes may give rise to inconsistent diagnoses across different laboratories, potentially leading to misleading results. Therefore, in this study it is possible that other viruses that might infect grapevines in Australia were not detected.

Table 1. Additional grapevine viruses occurring in Australia, their associated disease, and vectors (update to Table 1 in Wu et al. 2020 [16]).

Family/Genome	Genus	Species[1]	Associated Disease	Vector
Geminiviridae circular ssDNA	*Grablovirus*	grapevine red blotch virus (GRBV)[1]	Red leaf disease on red varieties, leaf irregular chlorotic and necrotic on white varieties	Three-cornered alfalfa hopper (*Spissistilus festinus*)
	Maldovirus	grapevine geminivirus A (GGVA)[2]	Unknown	Unknown
Tymoviridae Monopartite, linear ssRNA (+)	*Maculavirus*	grapevine red globe virus (GRGV)[2]	Unknown	Unknown
	Marafivirus	grapevine syrah virus 1 (GSyV-1)[2]	Unknown	Unknown
Reoviridae Monopartite, liner dsRNA	Unassigned	grapevine Cabernet Sauvignon reovirus (GCSV)[2]	Unknown	Unknown
Betaflexiviridae Monopartite linear ssRNA (+)	*Vitivirus*	grapevine virus F (GVF)[2]	Unknown	Unknown

[1] GRBV has been detected in Australia, but currently under quarantine [2] These viruses have been detected in Australia by this study [54].

References (Chapter 7)

1. Wu, Q.; Habili, N.; Kinoti, W.M.; Tyerman, S.D.; Rinaldo, A.; Zheng, L.; Constable, F.E. A Metagenomic Investigation of the Viruses Associated with Shiraz Disease in Australia. *Viruses* **2023**, *15*, 774, doi:10.3390/v15030774.
2. Fiore, N.; Zamorano, A.; Sanchez-Diana, N.; González, X.; Pallas, V.; Sanchez-Navarro, J. First detection of grapevine rupestris stem pitting-associated virus and grapevine rupestris vein feathering virus, and new phylogenetic groups for grapevine fleck virus and Hop stunt viroid isolates, revealed from grapevine field surveys in Spain. *Phytopathol. Mediterr.* **2016**, *55*, 225-238, doi:10.14601 / Phytopathol_Mediterr-15875.
3. Komorowska, B.; Berniak, H.; Golis, T. Detection of grapevine viruses in Poland. *J. Phytopathol.* **2014**, *162*, 326-331, doi:10.1111/jph.12186.
4. Meng, B.; Li, C.; Wang, W.; Goszczynski, D.; Gonsalves, D. Complete genome sequences of two new variants of Grapevine rupestris stem pitting-associated virus and comparative analyses. *J. Gen. Virol.* **2005**, *86*, 1555-1560, doi:10.1099/vir.0.80815-0.
5. Beuve, M.; Moury, B.; Spilmont, A.-S.; Sempé-Ignatovic, L.; Hemmer, C.; Lemaire, O. Viral sanitary status of declining grapevine Syrah clones and genetic diversity of grapevine Rupestris stem pitting-associated virus. *Eur. J. Plant Pathol.* **2013**, *135*, 439-452, doi:10.1007/s10658-012-0101-7.
6. Eichmeier, A.; Pieczonka, K.; Peňázová, E.; Pečenka, J.; Gajewski, Z. Occurrence of Grapevine Pinot gris virus in Poland and description of asymptomatic exhibitions in grapevines. *J. Plant Dis. Prot.* **2017**, *124*, 407-411, doi:10.1007/s41348-017-0076-x.
7. Poojari, S.; Alabi, O.J.; Naidu, R.A. Molecular characterization and impacts of a strain of Grapevine leafroll-associated virus 2 causing asymptomatic infection in a wine grape cultivar. *Virol J.* **2013**, *10*, 324.
8. Rast, H.E.; James, D.; Habili, N.; Masri, S.A. Genome organisation and characterization of a novel variant of grapevine leafroll-associated virus 3. In Proceedings of the 17th Meeting of the International Council for the Study of Virus and Virus-like Diseases of the Grapevine, Davis, California, USA, 7–14 October 2012; pp. 61-63.
9. Habili, N.; Cameron, I.; Randles, J. A mild strain of grapevine leafroll-associated virus 3 is present in desirable clones of Crimson seedless table grapes in Western Australia. In Proceedings of the 16th Meeting of the International Council for the Study of Virus and Virus-like Diseases of the Grapevine, Dijon, France, 31 August–4 September, 2009; pp. 237–238.
10. Goszczynski, D.E.; Du Preez, J.; Burger, J.T. Molecular divergence of grapevine virus A (GVA) variants associated with Shiraz disease in South Africa. *Virus Res.* **2008**, *138*, 105-110, doi:10.1016/j.virusres.2008.08.014.
11. Mollaei, H.R.; Afshar, A.A.; Kalantar-Neyestanaki, D.; Fazlalipour, M.; Aflatoonian, B. Comparison five primer sets from different genome region of COVID-19 for detection of virus infection by conventional RT-PCR. *Iran. J. Microbiol.* **2020**, *12*, 185-193.
12. Tahamtan, A.; Ardebili, A. Real-time RT-PCR in COVID-19 detection: issues affecting the results. *Expert Rev. Mol. Diagn.* **2020**, *20*, 453-454, doi:10.1080/14737159.2020.1757437.
13. Whiley, D.M.; Bialasiewicz, S.; Bletchly, C.; Faux, C.E.; Harrower, B.; Gould, A.R.; Lambert, S.B.; Nimmo, G.R.; Nissen, M.D.; Sloots, T.P. Detection of novel influenza A (H1N1) virus by real-time RT-PCR. *J. Clin. Virol.* **2009**, *45*, 203-204, doi:10.1016/j.jcv.2009.05.032.
14. Adams, I.P.; Glover, R.H.; Monger, W.A.; Mumford, R.; Jackeviciene, E.; Navalinskiene, M.; Samuitiene, M.; Boonham, N. Next - generation sequencing and metagenomic analysis: a universal diagnostic tool in plant virology. *Mol. Plant Pathol.* **2009**, *10*, 537-545, doi:10.1111/J.1364-3703.2009.00545.X.
15. Goszczynski, D.E.; Habili, N. Grapevine virus A variants of group II associated with Shiraz disease in South Africa are present in plants affected by Australian Shiraz disease, and have also been detected in the USA. *Plant Pathol.* **2012**, *61*, 205-214, doi:10.1111/j.1365-3059.2011.02499.x.
16. Wu, Q.; Habili, N.; Constable, F.; Al Rwahnih, M.; Goszczynski, D.E.; Wang, Y.; Pagay, V. Virus pathogens in Australian vineyards with an emphasis on Shiraz disease. *Viruses* **2020**, *12*, 818, doi:10.3390/v12080818.
17. Wine Australia. National vintage report 2021. Available online: https://www.wineaustralia.com/getmedia/1195b141-323e-4a8d-8f99-9ae3005e40fd/MI_VintageReport2021.pdf (accessed on 7 February 2022).
18. Australia, W. National vintage report 2022. Available online: https://www.wineaustralia.com/getmedia/374e13f5-a4a9-4d13-8d3c-aeef30b84fd4/MI_VintageReport2022_summary.pdf (accessed on 13 February 2023).
19. Habili, N.; Wu, Q.; Pagay, V. Virus-associated Shiraz disease may lead Shiraz to become an endangered variety in Australia. *Wine and Viticulture J.* **2016**, *31*, 47-50.

20. Yarwood, C.E. Host passage effects with plant viruses. *Adv. Virus Res.* **1979**, *25*, 169-190, doi:10.1016/S0065-3527(08)60570-9.
21. García-Arenal, F.; Fraile, A.; Malpica, J.M. Variation and evolution of plant virus populations. *Int. Microbiol.* **2003**, *6*, 225-232, doi:10.1007/s10123-003-0142-z.
22. Forbi, J.C.; Vaughan, G.; Purdy, M.A.; Campo, D.S.; Xia, G.-l.; Ganova-Raeva, L.M.; Ramachandran, S.; Thai, H.; Khudyakov, Y.E. Epidemic history and evolutionary dynamics of hepatitis B virus infection in two remote communities in rural Nigeria. *PLoS One* **2010**, *5*, e11615, doi:10.1371/journal.pone.0011615.
23. Nituch, L.A.; Bowman, J.; Wilson, P.; Schulte‐Hostedde, A.I. Molecular epidemiology of Aleutian disease virus in free‐ranging domestic, hybrid, and wild mink. *Evol. Appl.* **2012**, *5*, 330-340, doi:10.1111/j.1752-4571.2011.00224.x.
24. Forster, P.; Forster, L.; Renfrew, C.; Forster, M. Phylogenetic network analysis of SARS-CoV-2 genomes. *Proc. Natl. Acad. Sci.* **2020**, *117*, 9241-9243, doi:10.1073/pnas.2004999117.
25. Goszczynski, D.E.; Jooste, A.E.C. Identification of grapevines infected with divergent variants of grapevine virus A using variant-specific RT-PCR. *J. Virol. Methods* **2003**, *112*, 157-164, doi:10.1016/s0166-0934(03)00198-8.
26. Phogat, V.; Cox, J.W.; Šimůnek, J. Identifying the future water and salinity risks to irrigated viticulture in the Murray-Darling Basin, South Australia. *Agric. Water Manage.* **2018**, *201*, 107-117, doi:10.1016/j.agwat.2018.01.025.
27. Cramer, G.R.; Ergül, A.; Grimplet, J.; Tillett, R.L.; Tattersall, E.A.R.; Bohlman, M.C.; Vincent, D.; Sonderegger, J.; Evans, J.; Osborne, C. Water and salinity stress in grapevines: early and late changes in transcript and metabolite profiles. *Funct. Integr. Genomics* **2007**, *7*, 111-134, doi:10.1007/s10142-006-0039-y.
28. Webb, L.; Whiting, J.; Watt, A.; Hill, T.; Wigg, F.; Dunn, G.; Needs, S.; Barlow, E.W.R. Managing grapevines through severe heat: A survey of growers after the 2009 summer heatwave in south-eastern Australia. *J. Wine Res.* **2010**, *21*, 147-165, doi:10.1080/09571264.2010.530106.
29. Corrie, A.M.; Crozier, R.H.; Van Heeswijck, R.; Hoffmann, A.A. Clonal reproduction and population genetic structure of grape phylloxera, Daktulosphaira vitifoliae, in Australia. *Heredity* **2002**, *88*, 203-211, doi:10.1038/sj/hdy/6800028.
30. Fontaine, F.; Pinto, C.; Vallet, J.; Clément, C.; Gomes, A.C.; Spagnolo, A. The effects of grapevine trunk diseases (GTDs) on vine physiology. *Eur. J. Plant Pathol.* **2016**, *144*, 707-721, doi:10.1007/s10658-015-0770-0.
31. Bertsch, C.; Ramírez‐Suero, M.; Magnin‐Robert, M.; Larignon, P.; Chong, J.; Abou‐Mansour, E.; Spagnolo, A.; Clément, C.; Fontaine, F. Grapevine trunk diseases: complex and still poorly understood. *Plant Pathol.* **2013**, *62*, 243-265.
32. Songy, A.; Fernandez, O.; Clément, C.; Larignon, P.; Fontaine, F. Grapevine trunk diseases under thermal and water stresses. *Planta* **2019**, *249*, 1655-1679, doi:10.1007/s00425-019-03111-8.
33. Hrycan, J.; Hart, M.; Bowen, P.; Forge, T.; Urbez-Torres, J.R. Grapevine trunk disease fungi: Their roles as latent pathogens and stress factors that favour disease development and symptom expression. *Phytopathol. Mediterr.* **2020**, *59*, 395-424, doi:10.14601/Phyto-11275.
34. Bertazzon, N.; Chitarra, W.; Angelini, E.; Nerva, L. Two new putative plant viruses from wood metagenomics analysis of an esca diseased vineyard. *Plants* **2020**, *9*, 835, doi:10.3390/plants9070835.
35. Cottral, E.; Pascoe, I. Developments in grapevine trunk diseases research in Australia. *Phytopathol. Mediterr.* **2000**, *39*, 68-75.
36. Bruez, E.; Lecomte, P.; Grosman, J.; Doublet, B.; Bertsch, C.; Fontaine, F.; Ugaglia, A.; Teissedre, P.-L.; Da Costa, J.-P.; Guerin-Dubrana, L. Overview of grapevine trunk diseases in France in the 2000s. *Phytopathol. Mediterr.* **2013**, *52*, 262-275.
37. Billones-Baaijens, R.; Savocchia, S. A review of Botryosphaeriaceae species associated with grapevine trunk diseases in Australia and New Zealand. *Australas. Plant Pathol.* **2019**, *48*, 3-18, doi:10.1007/s13313-018-0585-5.
38. Guerin-Dubrana, L.; Fontaine, F.; Mugnai, L. Grapevine trunk disease in European and Mediterranean vineyards: occurrence, distribution and associated disease-affecting cultural factors. *Phytopathol. Mediterr.* **2019**, *58*, 49-71, doi:10.13128/Phytopathol_Mediterr-25153.
39. Cookson, S.J.; Ollat, N. Grafting with rootstocks induces extensive transcriptional re-programming in the shoot apical meristem of grapevine. *BMC Plant Biol.* **2013**, *13*, 1-14.
40. Wallis, C.M.; Wallingford, A.K.; Chen, J. Grapevine rootstock effects on scion sap phenolic levels, resistance to Xylella fastidiosa infection, and progression of Pierce's disease. *Front. Plant Sci.* **2013**, *4*, 502.
41. Lee, J.; Martin, R.R. Influence of grapevine leafroll associated viruses (GLRaV-2 and-3) on the fruit composition of Oregon Vitis vinifera L. cv. Pinot noir: Phenolics. *Food Chem.* **2009**, *112*, 889-896, doi:10.1016/j.foodchem.2008.06.065.

42. Edwards, E.J.; Betts, A.; Clingeleffer, P.R.; Walker, R.R. Rootstock - conferred traits affect the water use efficiency of fruit production in Shiraz. *Aust. J. Grape Wine Res.* **2022**, *28*, 316-327, doi:10.1111/ajgw.12553.
43. Lee, J.; Keller, K.E.; Rennaker, C.; Martin, R.R. Influence of grapevine leafroll associated viruses (GLRaV-2 and-3) on the fruit composition of Oregon Vitis vinifera L. cv. Pinot noir: Free amino acids, sugars, and organic acids. *Food Chem.* **2009**, *117*, 99-105, doi:10.1016/j.foodchem.2009.03.082.
44. Komar, V.; Vigne, E.; Demangeat, G.; Lemaire, O.; Fuchs, M. Comparative performance of virus-infected Vitis vinifera cv. Savagnin rose grafted onto three rootstocks. *Am. J. Enol. Vitic.* **2010**, *61*, 68-73.
45. Hellman, E. How to judge grape ripeness before harvest. In Proceedings of the Southwest regional vine & wine conference, Albuquerque, New Mexico, 27-28 February, 2004.
46. Nadal, M.; Hunter, K. Different wine styles as related to ripeness level of Syrah/R99 grapes. In Proceedings of the 59th Intervitis Interfructa Congress, Stuttgart, Germany, 22–26 April, 2007; pp. 139-148.
47. Komar, V.; Vigne, E.; Demangeat, G.; Fuchs, M. Beneficial effect of selective virus elimination on the performance of Vitis vinifera cv. Chardonnay. *Am. J. Enol. Vitic.* **2007**, *58*, 202-210.
48. Guidoni, S.; Mannini, F.; Ferrandino, A.; Argamante, N.; Di Stefano, R. The effect of grapevine leafroll and rugose wood sanitation on agronomic performance and berry and leaf phenolic content of a Nebbiolo clone (Vitis vinifera L.). *Am. J. Enol. Vitic.* **1997**, *48*, 438-442.
49. Girardello, R.C.; Cooper, M.L.; Smith, R.J.; Lerno, L.A.; Bruce, R.C.; Eridon, S.; Oberholster, A. Impact of grapevine red blotch disease on grape composition of Vitis vinifera Cabernet Sauvignon, Merlot, and Chardonnay. *J. Agric. Food Chem.* **2019**, *67*, 5496-5511, doi:10.1021/acs.jafc.9b01125.
50. Bowen, P.; Bogdanoff, C.; Poojari, S.; Usher, K.; Lowery, T.; Úrbez-Torres, J.R. Effects of grapevine red blotch disease on Cabernet franc vine physiology, bud hardiness, and fruit and wine quality. *Am. J. Enol. Vitic.* **2020**, *71*, 308-318, doi:10.5344/ajev.2020.20011.
51. Alabi, O.J.; Casassa, L.F.; Gutha, L.R.; Larsen, R.C.; Henick-Kling, T.; Harbertson, J.F.; Naidu, R.A. Impacts of grapevine leafroll disease on fruit yield and grape and wine chemistry in a wine grape (Vitis vinifera L.) cultivar. *PLoS One* **2016**, *11*, e0149666, doi:10.1371/journal.pone.0149666.
52. Martínez-Lüscher, J.; Plank, C.M.; Brillante, L.; Cooper, M.L.; Smith, R.J.; Al-Rwahnih, M.; Yu, R.; Oberholster, A.; Girardello, R.; Kurtural, S.K. Grapevine red blotch virus may reduce carbon translocation leading to impaired grape berry ripening. *J. Agric. Food Chem.* **2019**, *67*, 2437-2448, doi:10.1021/acs.jafc.8b05555.
53. Blanco-Ulate, B.; Hopfer, H.; Figueroa-Balderas, R.; Ye, Z.; Rivero, R.M.; Albacete, A.; Pérez-Alfocea, F.; Koyama, R.; Anderson, M.M.; Smith, R.J. Red blotch disease alters grape berry development and metabolism by interfering with the transcriptional and hormonal regulation of ripening. *J. Exp. Bot.* **2017**, *68*, 1225-1238, doi:10.1093/jxb/erw506.
54. Wu, Q.; Habili, N.; Tyerman, S.; Rinaldo, A.; Constable, F. First detection of five exotic grapevine viruses with minimal economic importance in Australia. In Proceedings of the 14th Australasian Plant Virology Workshop, Melbourne, Australia, 5-7 December, 2022.
55. Wu, Q.; Kehoe, M.; Kinoti, W.M.; Wang, C.; Rinaldo, A.; Tyerman, S.; Habili, N.; Constable, F.E. First report of grapevine rupestris vein feathering virus in grapevine in Australia. *Plant Dis.* **2020**, *105*, 515, doi:10.1094/PDIS-06-20-1240-PDN.
56. Vine Health Australia. Grapevine red blotch virus detections: your questions answered. Available online: https://vinehealth.com.au/2022/09/grapevine-red-blotch-virus-detections-in-australia-your-questions-answered/ (accessed on 12 November 2022).
57. Wu, Q.; Habili, N. The recent importation of Grapevine Pinot gris virus into Australia. *Virus Genes* **2017**, *53*, 935-938.
58. Huson, D.H.; Auch, A.F.; Qi, J.; Schuster, S.C. MEGAN analysis of metagenomic data. *Genome Res.* **2007**, *17*, 377-386, doi:10.1101/gr.5969107.